



INTERNATIONAL DOCTORAL
SCHOOL OF THE USC

Marta Carolina
Afonso Lages

PhD Thesis

Characterization of the High-Pathogenicity Island encoding the siderophore piscibactin in *Vibrio anguillarum*: effects on bacterial virulence and implications for the control of vibriosis in fish

Santiago de Compostela, 2022

Doctoral Programme in Advances in Microbial and Parasitic Biology



DOCTORAL THESIS

**CHARACTERIZATION OF THE HIGH-PATHOGENICITY ISLAND ENCODING THE
SIDEROPHORE PISCIBACTIN IN *VIBRIO ANGUILLARUM*: EFFECTS ON BACTERIAL
VIRULENCE AND IMPLICATIONS FOR THE CONTROL OF VIBRIOSIS IN FISH**

Marta Carolina Afonso Lages

INTERNATIONAL PHD SCHOOL OF THE UNIVERSITY OF SANTIAGO DE COMPOSTELA

PHD PROGRAMME IN ADVANCES IN MICROBIAL AND PARASITIC BIOLOGY

SANTIAGO DE COMPOSTELA

2022



D./Dña. **Marta Carolina Afonso Lages**

Título da tese: **Characterization of the High-Pathogenicity Island encoding the siderophore piscibactin in *Vibrio anguillarum*: effects on bacterial virulence and implications for the control of vibriosis in fish**

Presento mi tesis, siguiendo el procedimiento adecuado al Reglamento y declaro que:

- 1) La tesis abarca los resultados de la elaboración de mi trabajo.
- 2) De ser el caso, en la tesis se hace referencia a las colaboraciones que tuvo este trabajo.
- 3) Confirmando que la tesis no incurre en ningún tipo de plagio de otros autores ni de trabajos presentados por mí para la obtención de otros títulos.
- 4) La tesis es la versión definitiva presentada para su defensa y coincide la versión impresa con la presentada en formato electrónico.

Y me comprometo a presentar el Compromiso Documental de Supervisión en el caso que el original no esté depositado en la Escuela.

En **Santiago de Compostela, 27 de diciembre de 2021.**

AUTORIZACIÓN DEL DIRECTOR / TUTOR DE LA TESIS

Characterization of the High-Pathogenicity Island encoding the siderophore piscibactin in *Vibrio anguillarum*: effects on bacterial virulence and implications for the control of vibriosis in fish

D./D^a. **Manuel Luis Lemos Ramos** (Tutor y Director)

D./D^a. **Miguel Balado Dacosta** (Director)

INFORMAN:

Que la presente tesis, se corresponde con el trabajo realizado por D/D^a. **Marta Carolina Afonso Lages**, bajo nuestra dirección/tutorización, y autorizamos su presentación, considerando que reúne los requisitos exigidos en el Reglamento de Estudios de Doctorado de la USC, y que como directores de esta no incurrir en las causas de abstención establecidas en la Ley 40/2015.

De acuerdo con lo indicado en el Reglamento de Estudios de Doctorado, declaran también que la presente tesis doctoral es idónea para ser defendida en base a la modalidad Monográfica con reproducción de publicaciones, en los que la participación de la doctoranda fue decisiva para su elaboración y las publicaciones se ajustan al Plan de Investigación.

This work was supported by grants AGL2015-63740-C2-1-R, RTI2018-093634-B-C21 from the State Agency for Research (AEI) of Spain, both cofunded by the FEDER Programme (“A way to make Europe”) from the European Union, and by grant PID2019-103891RJ-100 from MCIN/AEI (Spain) (MCIN/AEI/10.13039/501100011033/FEDER). The work was also supported by grants GRC-2014/007 and GRC2018/018 from Xunta de Galicia. The stay in University of Porto (Portugal) was supported by the FEMS fellowship, FEMS-GO-2019-600.



ACKNOWLEDGMENTS

When I started my PhD studies, I thought that hard work, strong commitment, and passion for my project would make this journey unforgettable. I never thought about the emotional journey I would go through, the changes in social life and relationships.

This journey would never be completed if it was not for the people that I met over the years.

To my supervisor, Prof. Manuel Lemos, a sincere thank you for the opportunity, the help, the insightful suggestions and for the patience.

To Dr. Miguel Balado, thank you for the help to accomplish every milestone and for always having time to talk. Thank you for sharing your knowledge and experience.

A special thank you to the Organic Chemistry Group at the University of A Coruña for actively contributing for the development of this thesis.

To Dr. Ana do Vale and the members of the research group for kindly welcoming to the group during the research visit at the i3S. Thank you for your support and for the initiation in the world of protein purification.

To my colleagues. Dr. Diego Rey, thank you for always being there for me and for your constant support (sorry for invading your bench... but I needed the space!). Diego, Fabián and Pilar, thank you for making a pleasant, lively, and stimulating work environment.

To my fellow department colleagues. Sol, thank you for all the help over the years and for the explanations on fish anatomy. To the

virologists, thank you for the help every time I needed it. Ana, Lucía, Alba, Laura, Mateus y Xosé, thank you for always being there and for the great moments mostly outside the lab!

To Prof. Alicia Estévez, Prof. Beatriz Magariños, Prof. Juan Barja and Celsa, thank you for the help and the kind words.

To my family. Thank you for giving the best education possible, for the constant support, love and for letting me pursue my dreams. I hope I made you proud. Gabriel, thank you for being my partner in this journey. You are always there for me, you supported every step of the way, and you made sure I could see the best side in everything.

To all that have contributed to where I am today:

Thank you

Gracias

Grazas

Obrigada

PUBLICATIONS DERIVED FROM THE PRESENT THESIS

1. Balado, M., **Lages, M. A.**, Fuentes-Monteverde, J. C., Martínez-Matamoros, D., Rodríguez, J., Jiménez, C., et al. (2018). The siderophore piscibactin is a relevant virulence factor for *Vibrio anguillarum* favored at low temperatures. *Front. Microbiol.* 9: 1766.

DOI: [10.3389/fmicb.2018.01766](https://doi.org/10.3389/fmicb.2018.01766)

- Contributions: Marta A. Lages performed the lab experiments.
- Impact factor (2018): 4.259 (Q1, Microbiology).
- Authorisation from the journal: Papers published in *Frontiers in Microbiology* are under an open access license, Creative Commons CC BY license, which permits unrestricted use, distribution, and reproduction.
- This paper is reproduced in the Material and Methods and Results and Discussion chapters of this thesis.

2. **Lages, M. A.**, Balado, M., and Lemos, M. L. (2019). The expression of virulence factors in *Vibrio anguillarum* is dually regulated by iron levels and temperature. *Front. Microbiol.* 10: 2335.

DOI: [10.3389/fmicb.2019.02335](https://doi.org/10.3389/fmicb.2019.02335)

- Contributions: Marta A. Lages contributed to the design of the study, performed the lab experiments, analysed the data, and contribute to the writing of the manuscript.
- Impact factor (2019): 4.236 (Q1, Microbiology).
- Authorisation from the journal: Papers published in *Frontiers in Microbiology* are under an open access license, Creative Commons CC BY license, which permits unrestricted use, distribution, and reproduction.
- This paper is reproduced in the Material and Methods and Results and Discussion chapters of this thesis.

3. **Lages, M. A.,** Balado, M., and Lemos, M. L. (2021). The Temperature-Dependent Expression of the High-Pathogenicity Island Encoding Piscibactin in *Vibrionaceae* Results From the Combined Effect of the AraC-Like Transcriptional Activator PbtA and Regulatory Factors From the Recipient Genome. *Front. Microbiol.* 12: 748147.

DOI: [10.3389/fmicb.2021.748147](https://doi.org/10.3389/fmicb.2021.748147)

- Contributions: Marta A. Lages contributed to the design of the study, performed the lab experiments, analysed the data, and contribute to the writing of the manuscript.
- Impact factor (2020): 5.64 (Q1, Microbiology).
- Authorisation from the journal: Papers published in *Frontiers in Microbiology* are under an open access license, Creative Commons CC BY license, which permits unrestricted use, distribution, and reproduction.
- This paper is reproduced in the Material and Methods and Results and Discussion chapters of this thesis.

4. **Lages, M. A.,** de la Fuente, M. C., Ageitos, L., Martínez-Matamoros, D., Rodríguez, J., Balado, M., Jiménez, C., Lemos, M. L. (2022). FrpA is the outer membrane piscibactin transporter in *Vibrio anguillarum*: structural elements in synthetic piscibactin analogues required for transport. *J. Biol. Inorg. Chem.* 27(1): 133-142.

DOI: [10.1007/s00775-021-01916-1](https://doi.org/10.1007/s00775-021-01916-1)

- Contributions: Marta A. Lages contributed to the design of the study, performed the lab experiments, analysed the data, and contribute to the writing of the manuscript.
- Impact factor (2020): 3.358 (Q2, Chemistry).
- Authorisation from the journal: This paper was published in *Journal of Biological Inorganic Chemistry* and is under an open

access license, Creative Commons CC BY license, which permits unrestricted use, distribution, and reproduction.

- This paper is reproduced in the Material and Methods and Results and Discussion chapters of this thesis.

ABSTRACT

Vibrio anguillarum is one of the most important pathogens for aquacultured fish, causing vibriosis, a haemorrhagic septicaemia that affects fish species living at different temperatures. Besides, *V. anguillarum* is an inhabitant of marine and estuarine environments, so it must be able to adapt its physiology to the changing levels of salinity, nutrients, and temperature. Although water temperature raising is usually associated with a higher incidence of vibriosis, 15 °C is considered enough for the occurrence of vibriosis outbreaks.

In this work, we analyzed the physiological adaptations of *V. anguillarum* to low-iron availability and temperature changes that enable it to cause vibriosis in a wide diversity of fish species. Some of these adaptations include the expression of virulence factors that will lead to the disease. We used the serotype O2a pathogenic strain RV22 as a model of study. The faster growth shown by *V. anguillarum* RV22 at 25 °C compared to growth at 15 °C, contrasts with its higher virulence at 15 °C. Temperature and iron levels usually act as signals during host colonization. Therefore, first we analyzed by RNAseq the effect of iron levels and temperature changes on the transcriptome of *V. anguillarum* RV22. The comparative analysis revealed that under iron deficiency deep changes in the metabolism appear and virulence factors are induced. Metabolic routes requiring iron such as TCA cycle and cytochromes were down-regulated, while genes related to the glycolytic and pentose phosphate pathways were up-regulated. Some components of amino acids and carbohydrate metabolism were down-regulated at 15 °C, which suggests a slower nutrient import rate at 15 °C. Interestingly, *V. anguillarum* expresses different virulence factors at 15 °C or 25 °C. At warm temperature, *V. anguillarum* induces chemotaxis, motility, exopolysaccharide biosynthesis, haemolysin Vah1, T6SS, and the outer membrane components OmpA and OmpV. Conversely, the haemolysin RTX, T6SS2, OmpC, and genes related to

exopolysaccharide transport and assembly, were induced preferentially at 15 °C. Regarding iron uptake systems, ferrous iron uptake *feoB*, the vanchrobactin siderophore system and haem utilization were preferentially expressed at 25 °C whereas the piscibactin siderophore system was strongly up-regulated at 15 °C. The differential expression of virulence factors in relation to temperature indicates that their relevance may vary between hosts, enabling *V. anguillarum* to infect fish species living at cold and warm waters.

Siderophores are key virulence factors in most pathogens. In *V. anguillarum*, two siderophore systems have been described: the pJM1 plasmid-encoded anguibactin, which is restricted to serotype O1 strains, and the chromosomally encoded vanchrobactin, which is widespread among pathogenic and environmental isolates. In addition, the genome of *V. anguillarum* RV22 contains a genomic island that is homologous to the pathogenicity island *irp*-HPI harbored in plasmid pPHDP70 of *Photobacterium damsela* subsp. *piscicida* (*Pdp*). This island encodes the siderophore piscibactin and it is likely spread among bacteria through HGT. An *in silico* analysis revealed that *irp*-HPI is present in several highly virulent *V. anguillarum* strains that have an active vanchrobactin system. In fact, the 4'-phosphopantetheinyl transferase activity needed for piscibactin synthesis is only encoded by *vabD*, which is part of the vanchrobactin gene cluster. The chemical analysis clearly demonstrated that *V. anguillarum* synthesizes piscibactin in addition to vanchrobactin. *In vitro* growth ability and virulence assays performed with single and combined mutants, suggest that vanchrobactin could be more related to environmental survival, while piscibactin is a key virulence factor for *V. anguillarum* pathogenesis.

The *irp*-HPI island putatively encodes synthesis and transport of piscibactin and their regulation. The construction of mutants by allelic exchange allowed the elucidation of the role of Irp1, Irp4, Irp8 and FrpABC in piscibactin biosynthesis and utilization. Irp1 is the main NRPS/PKS essential for piscibactin synthesis. The type II thioesterase Irp4 is required for the biosynthesis final steps. Piscibactin is secreted out of the cell through the MFS protein Irp8 located at the plasma membrane. The ferri-piscibactin complex reaches the periplasm through FrpA, a TonB-dependent outer membrane transporter, and it is

transported through the inner membrane by the ABC-type transporter FrpBC. To identify the key structural elements of piscibactin necessary for its transport through FrpA, piscibactin analogues were synthesized and their ability to act as iron source was investigated. The growth promotion assays identified the configuration of C-13 as crucial for iron chelation and recognition by FrpA. The widespread distribution of FrpA suggests that piscibactin analogues carrying antimicrobials could be used in novel therapies against a wide range of pathogens.

The transcriptional analysis of *irp*-HPI showed that piscibactin promoters *PpbtA*, *PfrpA* and *PfrpBC* respond to iron levels and temperature. The measure of transcriptional activity revealed that piscibactin regulatory (*PpbtA*) and transport genes (*PfrpA* and *PfrpBC*) are preferentially expressed under iron deficiency at 15 °C. *irp*-HPI putatively encodes two AraC-like transcriptional regulators, PbtA and PbtB. In addition, the global regulators H-NS and ToxR-S are also present in *V. anguillarum*. To analyze the regulation of *irp*-HPI expression, in-frame deletion mutants of *pbtA*, *pbtB* and the global regulators *h-ns* and *toxR-S* were constructed and their relevance for growth under iron deficiency and *irp*-HPI gene expression was analyzed at 15 and 25 °C. The results showed that whereas *pbtA* is required for the expression of piscibactin biosynthetic and transport genes, *pbtB* is not. The inactivation of H-NS resulted in a decreased growth under iron deficiency and a low activity of *PfrpA* at 15 and 25 °C. Inactivation of ToxR-S increased the transcriptional activity of *PfrpA* and *PpbtA* at 25 °C. Notably, the inactivation of PbtA and H-NS resulted in a marked decrease of virulence for fish, which corroborates the importance of piscibactin for the virulence of *V. anguillarum*. The results suggest that PbtA is the main modulator of *irp*-HPI gene expression, and that H-NS is indirectly required for the maximum production of piscibactin. ToxR-S could be involved in the repression of piscibactin genes at 25 °C.

Several versions of the promoters *PpbtA* and *PfrpA* were identified in different bacteria harbouring *irp*-HPI. *PfrpA* showed the highest variability, which indicates that different expression patterns might be present. For instance, the shorter version of *PfrpA* present in *Pdp* does not act as transcription start and, in contrast to *V. anguillarum*, *irp*-HPI

from *Pdp* did not show a temperature dependent expression. However, when *PfrpA* and *PpbtA* promoters of *irp*-HPI from *Pdp* were cloned into *V. anguillarum*, they also showed a temperature-dependent expression pattern. This indicates that the temperature-dependent expression of *irp*-HPI depends on activator(s) present in *V. anguillarum* and absent in *Pdp*.

Since siderophore systems are expressed during the infection process, we finally evaluated the use of the siderophore outer membrane transporters FrpA and FvtA as subunit vaccines against vibriosis. Fish were immunized with the recombinant proteins rFrpA or rFvtA, a RV22 or *Pdp* bacterin and the antibody levels were measured by ELISA. Both FrpA and FvtA are immunogenic proteins, but they confer limited protection against *V. anguillarum* infection. However, it is noteworthy that *V. anguillarum* FrpA conferred cross protection against *Pdp*. This result indicates that the widespread distribution of FrpA could be used to formulate subunit vaccines against *irp*-HPI-harbouring pathogens.

In summary, in this thesis we demonstrated that *V. anguillarum* expresses a specific cocktail of virulence factors depending on the environmental temperature, which enables it to infect fish living at cold and warm waters. In addition, *V. anguillarum* produces the siderophore piscibactin as a key virulence factor, whose expression is regulated by iron levels and favoured at low temperatures.

RESUMO

A acuicultura é un sector en constante expansión e nas últimas décadas medrou de maneira exponencial, superando á pesca como principal fonte de produtos acuáticos. Con todo, a alta densidade de individuos nos sistemas de cultivo promoven a aparición e transmisión de patóxenos. Este ambiente favorece fenómenos de evolución das poboacións bacterianas onde a adquisición de factores de virulencia a través da transferencia horizontal de xenes conduce á aparición de novos patóxenos nas plantas de cultivo. *Vibrio anguillarum* é un dos patóxenos de peixes máis importantes na acuicultura, sendo o axente causal da vibriose, unha septicemia hemorráxica que afecta a especies de peixes que viven nun amplo rango de temperaturas. Así mesmo, *V. anguillarum* é unha bacteria que habita tanto ambientes mariños como en esteiros, polo que debe de ser capaz de adaptar a súa fisioloxía aos constantes cambios nos niveis de salinidade, nutrientes e temperatura. Aínda que o aumento da temperatura da auga adoita estar asociado coa proliferación de especies de *Vibrio* e, en consecuencia, cunha maior incidencia de vibriose, *V. anguillarum* é capaz de causar gromos a temperaturas baixas (5 - 18 °C), sendo unha temperatura de 15 °C suficiente como para permitir a aparición de gromos. A vibriose é unha enfermidade de evolución rápida na que a morte do hóspede pode ocorrer sen mostrar ningún síntoma externo de enfermidade. Neste tipo de infeccións é de suma importancia o estudo das interaccións hóspede-patóxeno e dos mecanismos implicados na virulencia.

En bacterias patóxenas a temperatura e os niveis de ferro adoitan actuar como sinais para iniciar a colonización do hóspede. Neste traballo, analizamos as adaptacións fisiolóxicas de *V. anguillarum* en condicións de baixa dispoñibilidade de ferro e a diferentes temperaturas, factores que permiten á bacteria provocar gromos de vibriose nun amplo rango de especies de peixes. Algunhas das devanditas adaptacións inclúen a expresión de factores de virulencia que contribúen de forma significativa ao desenvolvemento da enfermidade. Nesta tese utilizouse como modelo a cepa patóxena RV22

que pertence ao serotipo O2a de *V. anguillarum*. Nesta bacteria observouse unha maior taxa de crecemento a 25 °C en comparación a 15 °C, o cal contrasta coa súa maior virulencia a esta última temperatura. Para estudar estes dous factores de virulencia, primeiro analizouse por medio da técnica de RNAseq o efecto dos niveis de ferro e dos cambios de temperatura no transcriptoma de *V. anguillarum* RV22. Para iso cultivouse a bacteria en medio mínimo CM9 suplementado co quelante de ferro 2,2'- dipiridilo a 15 °C e 25 °C. Esta redución da dispoñibilidade de ferro intenta simular as condicións que atopan os patóxenos bacterianos cando infectan a un hóspede. Como control utilizouse a condición de exceso de ferro para identificar especificamente aqueles xenes regulados polos niveis de ferro. A análise comparativa revelou que en déficit de ferro danse cambios profundos no metabolismo celular da bacteria e indúcese a transcripción de factores de virulencia. Así mesmo, verificouse unha redución na expresión dos xenes relacionados cas rutas metabólicas con altos requirimentos de ferro para o seu funcionamento, como o ciclo do ácido tricarbóxico (TCA) e os citocromos, mentres que os xenes relacionados coas vías glucolítica e das pentosas fosfato aumentaron a súa expresión. O crecemento baixo condicións de limitación de ferro induce tamén cambios nos requirimentos de aminoácidos. Demostrouse que existe unha diminución na expresión de xenes relacionados coa degradación de valina, leucina e isoleucina e co metabolismo da histidina. Pola contra, houbo un aumento na expresión de xenes implicados na síntese dos aminoácidos aromáticos fenilalanina, tirosina e triptófano. En particular, existe unha activación da ruta de síntese da arxinina, un aminoácido necesario para a síntese do sideróforo vancrobactina. Ademais, algúns dos compoñentes do metabolismo de aminoácidos e carbohidratos reduciron a súa expresión a 15 °C, o que suxire unha taxa de captación de nutrientes máis lenta a esta temperatura. Esta diminución dos nutrientes correlacionase de maneira directa coa taxa de crecemento máis lenta observada a temperatura baixa. Ademais, a 15 °C observouse unha diminución na expresión de xenes relacionados coa síntese das subunidades maiores e menores que conforman os ribosomas e coa bióxénese de tARN.

A deficiencia de ferro induciu a expresión de factores de virulencia, pero curiosamente, *V. anguillarum* expresa distintos factores de virulencia a 15 °C e a 25 °C. A temperatura alta indúcese a biosíntese do lipopolisacárido, hemolisina Vah1, T6SS-1 e compoñentes da membrana externa OmpA e OmpV. Pola contra, a hemolisina RTX, T6SS-2, OmpC e xenes relacionados co transporte e ensamblaxe de exopolisacáridos, inducíronse preferentemente a 15 °C. En xeral, os xenes relacionados coa virulencia inducíronse en condicións de limitación de ferro, con todo, atopáronse dúas excepcións a este feito. Os xenes relacionados coa quimiotaxe e a motilidade sufriron unha redución da súa expresión baixo limitación de ferro. En canto aos sistemas de captación de ferro, o sistema de internalización do ión ferroso *feoB*, o sistema do sideróforo vancrobactina e a utilización de hemo expresáronse preferentemente a 25 °C, mentres que a síntese do sideróforo piscibactina incrementouse de maneira significativa a 15 °C. Con respecto ao sistema do sideróforo piscibactina, os xenes para o posible regulador transcricional *araC1* e o posible transportador de membrana externa *frpA* encóntranse entre os xenes máis inducidos a 15 °C. A virulencia é un trazo multifactorial e a expresión diferencial dos factores de virulencia en relación coa temperatura indica que a relevancia destes factores pode variar entre hóspedes, o que permite a *V. anguillarum* infectar especies de peixes que viven tanto en augas frías como cálidas.

A restrición de ferro é un mecanismo de defensa do hóspede, polo tanto, para establecer unha infección exitosa, os patóxenos deben posuír mecanismos para adquirir ferro das fontes do hóspede. Os sideróforos como método de captación de ferro son factores clave para a virulencia na maioría dos patóxenos. En *V. anguillarum*, describíronse dous sistemas de sideróforos: a anguibactina codificada polo plásmido pJM1, que está restrinxida ás cepas do serotipo O1, e a vancrobactina que está codificada cromosómicamente. A vancrobactina considérase o sideróforo ancestral da especie xa que está moi estendida entre illados patóxenos e ambientais. Este sistema de sideróforo inactivase nas cepas que albergan o plásmido pJM1. Ademais, no xenoma de *V. anguillarum* RV22 atópase unha illa xenómica homóloga á illa de patoxenicidade *irp*-HPI localizada no plásmido conxugativo pPHDP70 de

Photobacterium damsela subsp. *piscicida*. Esta illa codifica o sideróforo piscibactina e é probable que se propague entre as bacterias a través de fenómenos de transferencia horizontal de xenes. Unha análise *in silico* revelou que a illa *irp*-HPI está presente en varias cepas de *V. anguillarum* altamente virulentas que portan o sistema da vancrobactina activo. De feito, a actividade da 4'-fosfopanteteinil transferasa, requirida para a síntese da piscibactina, só está codificada polo xene *vabD* o cal está localizado no sistema de xenes da vancrobactina. Polo tanto, a interacción entre os sistemas de sideróforos da vancrobactina e da piscibactina é esencial para a síntese deste último sideróforo. A análise química dos sobrenadantes dos cultivos da bacteria demostrou inequivocamente que *V. anguillarum* é capaz de sintetizar piscibactina ademais de vancrobactina. Os ensaios de capacidade de crecemento *in vitro* e de virulencia realizados con mutantes simples e combinados suxiren que a vancrobactina podería estar máis relacionada coa supervivencia ambiental, mentres que a piscibactina sería un factor de virulencia clave para a patoxénese de *V. anguillarum*, xa que a súa inactivación non afectou en gran medida a capacidade de *V. anguillarum* para crecer en condicións limitantes de ferro.

A illa *irp*-HPI codificaría funcións relacionadas coa síntese, transporte e regulación da piscibactina. A construción de mutantes por intercambio alélico dos xenes desta illa permitiu dilucidar o papel das proteínas Irp1, Irp4, Irp8 e FrpABC na biosíntese e utilización de este sideróforo. Irp1 (NRPS/PKS) é a principal encima da ruta, sendo esencial para a síntese do sideróforo. A inactivación do xene *irp1* nunha cepa produtora de piscibactina afectou de maneira significativa á capacidade de crecemento en condicións de limitación de ferro resultando nunha diminución na produción de sideróforos. A tioesterasa tipo II Irp4 é necesaria para os pasos finais da biosíntese, xa que libera o sideróforo do complexo multienzimático. A inactivación de *irp4* resultou tamén nunha diminución do crecemento en déficit de ferro, e, ademais, non se detectou piscibactina en sobrenadantes dos cultivos desta cepa mutante. A secreción de metabolitos por parte da célula debe ocorrer de maneira secuencial. A piscibactina transportase ao periplasma a través da proteína Irp8, pertencente á superfamilia maior

de facilitadores situada na membrana plasmática, xa que o mutante para este transportador non puido promover o crecemento dunha cepa incapaz de producir sideróforos. Con todo, non se definiron todos os compoñentes que interveñen no proceso de secreción. O complexo de ferri-piscibactina internalízase a través de transportadores de membrana externa específicos. A enerxía para o devandito transporte é subministrada pola forza protón-motriz da membrana interna. Logo, o complexo ferri-piscibactina é transportado ao periplasma a través de FrpA, un transportador de membrana externa dependente de TonB, para finalmente ser transportado a través da membrana interna polo transportador de tipo ABC dimérico FrpBC. As deleccións simples para ambos transportadores deron como resultado unha diminución drástica da capacidade de crecemento en condicións de déficit de ferro, ademais de que ningunha das cepas mutantes puido utilizar a piscibactina como fonte de ferro en ensaios de alimentación cruzada. Co obxectivo de identificar os elementos estruturais clave do sideróforo piscibactina necesarios para o recoñecemento por parte do transportador FrpA, sintetizáronse químicamente análogos deste sideróforo e determinouse a súa capacidade para actuar como fonte de ferro. Os ensaios de actividade dos análogos identificaron a configuración do C-13 do sideróforo como crucial para quelar o ferro e para ser recoñecido por parte do transportador FrpA. Curiosamente, tamén se demostrou que estes análogos da piscibactina poden ser internalizados eficientemente a través de diferentes versións de FrpA (*V. anguillarum* e *P. damselae* subsp. *piscicida*). A ampla distribución de FrpA suxire que a utilización de análogos de piscibactina como vectores para axentes antimicrobianos podería abrir a porta ao desenvolvemento de novas terapias contra unha ampla gama de patóxenos.

A activación de factores de virulencia debe estar estritamente regulada a nivel transcricional para que estes se activen cando sexa necesario. A análise transcricional de *irp*-HPI mostrou que o grupo de xenes da piscibactina transcribíase nun único mARN policistrónico que inclúe os xenes *pbtA*, *pbtB*, *frpA*, *irp1-5*, *irp8* e *irp9*. Así mesmo, os xenes da piscibactina relacionados coa súa síntese, transporte e regulación cotranscribíase dende o promotor situado augas arriba de *pbtA*. Con todo, a análise dos niveis transcricionais revelou que existen

rexións interxénicas que actúan como promotores. Ademais, os promotores *PpbtA*, *PfrpA* e *PfrpBC* responden aos niveis de ferro e a temperatura. O estudo da actividade transcricional revelou que os xenes reguladores (*PpbtA*) e de transporte (*PfrpA* e *PfrpBC*) da piscibactina exprésanse preferentemente en déficit de ferro a 15 °C, é dicir posúen un dobre requisito para poder expresarse de forma significativa. A adquisición da illa *irp*-HPI por parte de *V. anguillarum* mellora a súa flexibilidade de nicho e permite que o patóxeno infecte unha ampla gama de hóspedes. O ADN adquirido a través da transferencia horizontal adoita codificar factores que regulan a súa propia expresión. Pola contra, elementos codificados no xenoma bacteriano receptor poderían estar implicados na regulación dos xenes adquiridos. Por tanto, son necesarios mecanismos de regulación estritos para modular a expresión do ADN adquirido. *irp*-HPI probablemente codifica dous reguladores transcricionais similares a AraC nomeados como PbtA e PbtB. Os activadores transcricionais do tipo AraC están involucrados nunha variedade de funcións reguladoras relacionadas con procesos celulares: modulación do metabolismo do carbono, resposta ao estrés e virulencia. PbtA e PbtB teñen a característica organización de dous dominios, un dominio C-terminal conservado e un dominio N-terminal variable. Ademais, *V. anguillarum* porta os reguladores xerais H-NS e ToxR-S. H-NS participa na represión de xenes adquiridos mediante transferencia horizontal, mentres que ToxR-S media na activación transcricional de factores de virulencia relevantes en *Vibrios* patóxenos en resposta a sinais ambientais. Para analizar a regulación da expresión de *irp*-HPI, construíronse mutantes por delección *in-frame* de *pbtA*, *pbtB* e dos reguladores globais *h-ns* e *toxR-S* e analizouse a súa relevancia para o crecemento baixo deficiencia de ferro e para a expresión dos xenes da illa *irp*-HPI a 15 e 25 °C. Os resultados mostraron que *pbtA* é necesario para o crecemento en condicións de limitación de ferro e para a expresión dos xenes biosintéticos e de transporte da piscibactina. Polo contrario, a inactivación de *pbtB* non produciu ningún cambio fenotípico nin de expresión xénica. Ademais, PbtA non induce a expresión do seu propio promotor (*PpbtA*). A inactivación de H-NS produciu unha diminución do crecemento en déficit de ferro e unha redución da actividade transcricional de *PfrpA*

tanto a 15 como a 25 °C. A inactivación de ToxR-S aumentou a actividade transcricional de *PfrpA* e *PpbtA* a 25 °C. Ademais, o silenciamento de *pbtA* e *h-ns* resultou nunha marcada diminución da virulencia en peixes, o que corrobora a importancia da piscibactina para a patoxénese de *V. anguillarum*. Os resultados suxiren que PbtA é o principal regulador da expresión dos xenes da illa *irp*-HPI, e que H-NS é necesario indirectamente para acadar a produción máxima de piscibactina, con todo, non tería ningún efecto regulador sobre a expresión de PbtA. ToxR-S podería estar implicado na represión dos xenes da piscibactina a 25 °C.

En base aos resultados anteriores PbtA sería o activador transcricional esencial para a expresión do sistema sideróforos da piscibactina, polo que se realizou un Ensaio de Cambio de Mobilidade Electroforética (EMSA) para avaliar a interacción da proteína completa PbtA e os seus dominios C- e N-terminal co ADN obxectivo. Realizáronse varias tentativas para obter PbtA purificada, pero a proteína estaba presente en cantidades moi baixas e en presenza doutros produtos proteicos. Por tanto, non se puido utilizar a proteína completa nestes ensaios. Os dominios C- e N-terminal de PbtA purificáronse con éxito e usáronse para avaliar as interaccións proteína-ADN e determinar a función de cada dominio. Os ensaios EMSA revelaron que o dominio C-terminal está implicado na unión ao ADN, e únese directamente a secuencias situadas ao redor de 100 pb augas arriba do codón de inicio ATG de *frpA* e *frpBC*. Confirmando os resultados da actividade transcricional, o dominio C-terminal de PbtA non interactúa co seu propio promotor *PpbtA*. A función do dominio N-terminal non está relacionada coa unión ao ADN; con todo, a imposibilidade de usar a proteína total PbtA non permitiu analizar o seu papel como sensor ambiental.

A illa *irp*-HPI está moi estendida na familia *Vibrionaceae* e poidéronse identificar varias versións dos promotores *PpbtA* e *PfrpA* en diferentes bacterias. O aliñamento de *irp*-HPI entre as diferentes especies revelou que a rexión augas arriba do codón de inicio ATG de *pbtA* e a rexión interxénica *pbtB*-*frpA* teñen grandes diferenzas. Así mesmo, a rexión augas abaixo de *pbtB* mostrou tamén grandes diferenzas. Para rematar, unha secuencia conservada de

aproximadamente 100 pb augas arriba do codón de inicio de *frpA* está presente en todas as secuencias analizadas. En base á lonxitude da secuencia establecéronse diferentes tipos de rexións promotoras. Unha versión máis longa da rexión interxénica *pbtB-frpA* de preto de 360 pb atopouse en *V. anguillarum*, *V. ordalii* e *V. qinghaiensis*. Pola contra, unha versión intermedia de esta zona está presente en *V. neptunius* e *V. mimicus*. Finalmente, unha versión máis curta entre 100 e 140 pb atópase en *P. damsela* subsp. *piscicida*, *V. ostreicida*, *V. sonorensis* e *V. cholerae*. Sorprendentemente, a rexión de *PfrpA* mostrou a maior variabilidade, o que podería desembocar en diferentes patróns de expresión. A versión máis curta de *PfrpA*, presente en *P. damsela* subsp. *piscicida*, non actúa como promotor e, ao contrario do que se verifica en *V. anguillarum*, a illa *irp*-HPI de *P. damsela* subsp. *piscicida* non mostrou unha expresión dependente da temperatura. Con todo, cando os promotores *PfrpA* e *PpbtA* de *irp*-HPI de *P. damsela* subsp. *piscicida* foron clonados en *V. anguillarum*, mostraron un patrón de expresión dependente da temperatura. Isto indica que a expresión dependente da temperatura de *irp*-HPI depende de activadores presentes en *V. anguillarum* e ausentes en *P. damsela* subsp. *piscicida* que inducirían a transcrición de *PpbtA* cando a temperatura diminúe.

Dado que os sistemas de sideróforos exprésanse durante a infección, avaliamos o uso dos transportadores de membrana externa dos sideróforos piscibactina e vancrobactina FrpA e FvtA, respectivamente, como vacinas de subunidades fronte a vibriose. Os peixes inmunizáronse coas proteínas recombinantes rFrpA, rFvtA ou con unha bacterina formulada a partir de células inactivadas de *V. anguillarum* RV22 ou de *P. damsela* subsp. *piscicida*. Os niveis de anticorpos producidos por cada un dos tratamentos cuantificáronse mediante un ensaio ELISA. Tanto rFrpA como rFvtA son proteínas inmuno-xénicas, non obstante, os peixes inmunizados con estas proteínas posuían niveis baixos de anticorpos contra RV22 e *P. damsela* subsp. *piscicida* en comparación coas bacterinas. Isto suxire que as proteínas non están presentes en niveis significativos na membrana externa das células completas. Para determinar a protección conferida polos tratamentos, os alevíns de linguado foron infectados experimentalmente con *V. anguillarum* ou *P. damsela* subsp.

piscicida. Dado que os sistemas de sideróforos exprésanse preferentemente a diferentes temperaturas, avalíouse a protección conferida por FrpA nunha infección experimental a 18 °C para *V. anguillarum* e a 22 °C para *P. damsela* subsp. *piscicida*. Doutra banda, a protección conferida por FvtA avalíouse nunha infección experimental con *V. anguillarum* a 24 °C. Os resultados mostraron que a inmunoxenicidade das proteínas non se correlacionou coa protección contra a infección por *V. anguillarum*. Con todo, cabe destacar que FrpA de *V. anguillarum* conferiu protección cruzada fronte a *P. damsela* subsp. *piscicida*. Este resultado indica que, dada a distribución xeneralizada de FrpA, esta podería usarse para formular vacinas de subunidades contra diversos patóxenos que alberguen a illa *irp*-HPI.

En resumo, nesta tese demostramos que *V. anguillarum* expresa un cóctel específico de factores de virulencia en función da temperatura ambiental o que lle permite infectar a peixes tanto de augas frías como cálidas. Ademais, *V. anguillarum* produce o sideróforo piscibactina como factor esencial de virulencia, cuxa expresión está regulada polos niveis de ferro e vese favorecida a baixas temperaturas.

ABBREVIATIONS

A

A₄₅₀ – Absorbance measured at the wavelength of 450 nm

A₅₇₀ – Absorbance measured at the wavelength of 570 nm

A₆₃₀ – Absorbance measured at the wavelength of 630 nm

ABC – ATP-Binding Cassette

Amp – Ampicillin

Amp^r – Ampicillin resistance

ASK cells – Atlantic Salmon Kidney cells

ATP – Adenosine Triphosphate

C

C-9 – Carbon 9

C-10 – Carbon 10

C-13 – Carbon 13

ca. – circa, about

CAS – Chrome Azurol-S

cDNA – Complementary Deoxyribonucleic Acid

CFU – Colony Forming Units

CM9 – Minimal Medium 9

COG – Clusters of Orthologous Genes

CP – Carrier Protein

CTD – C-terminal Domain

D

DEGs – Differentially Expressed Genes

DHBA – 2,3-Dihydroxybenzoic acid

DNase – Deoxyribonuclease

dNTP – Deoxynucleoside Triphosphate

E

E100 – Elution 100 mM imidazole

E200 – Elution 200 mM imidazole

E400 – Elution 400 mM imidazole

EDDHA – etilendiamine-di(*o*-hidroxifenil-acetic) acid

ELISA – *Enzyme-Linked ImmunoSorbent Assay*

EmpA – extracellular zinc metalloprotease
EMSA – Electrophoretic Mobility Shift Assay
EPS – Exopolysaccharide

F

FPKM – Fragments Per kilobase of transcripts per Million mapped reads

G

Gm – Gentamycin
Gm^r – Gentamycin resistance

H

HGT – Horizontal gene transfer
HMWP1 – High Molecular Weight Protein 1
H-NS – Histone-like Nucleoid Structuring Protein
HPI – High-Pathogenicity Island
HRP – Horseradish Peroxidase

I

IPTG – Isopropyl β -D-1-thiogalactopyranoside
IS – Insertion Sequence

K

Kan – Kanamycin
Kan^r – Kanamycin resistance
KEGG – Kyoto Encyclopedia of Genes and Genomes

L

LB – Luria Bertani
LC-MS – Liquid Chromatography-Mass Spectrometry
LPS – Lipopolysaccharide

M

MARTX – Multifunctional Autoprocessing Repeat in Toxin
MFS – Major Facilitator Superfamily

N

NADH – Nicotinamide Adenine Dinucleotide
NADPH – Nicotinamide Adenine Dinucleotide Phosphate
NRPS – Non-ribosomal peptide synthetase
NTD – N-terminal Domain

O

OD₆₀₀ – Optical Density at 600 nm

OMP – Outer Membrane Proteins

ORF – Open Reading Frame

P

PBS – Phosphate-buffered Saline

Pcb – Piscibactin

PCP – Peptidyl Carrier Protein

PCR – Polymerase Chain Reaction

Pdp – *Photobacterium damsela* subsp. *piscicida*

PKS – Polyketide Synthase

PVDF – Polyvinylidene Fluoride

R

Rif – Rifampicin

Rif^r – Rifampicin resistance

RNAseq – Whole mRNA Sequencing

RND – Resistance-nodulation-cell division

RT-PCR – Reverse Transcription Polymerase Chain Reaction

RTX – Repeat in Toxin

S

SDS-PAGE – Sodium Dodecyl Sulphate-Polyacrylamide Gel Electrophoresis

T

T1SS – Type I Secretion System

T6SS – Type VI Secretion System

TAE – Tris, acetic acid and EDTA buffer

TBDT – TonB Dependent Transporter

TBE – Tris, boric acid and EDTA buffer

TBO – Temperature Below Optimal

TBS – Tris-buffered Saline

TBST – Tris-buffered Saline with Tween

TCA – Tricarboxylic acid cycle

TE – Thioesterase

TE I – Type I Thioesterase

TE II – Type II Thioesterase

TSA-1 – Tryptic Soy Agar supplemented until 1% of NaCl

TSB-1 – Tryptic Soy Broth supplemented until 1% of NaCl

TTBS – Tween Tris-buffered Saline

V

Vah – *V. anguillarum* haemolysin

Vang – *V. anguillarum*

W

wgs – whole-genome shotgun

INDEX

I. INTRODUCTION	1
1. AQUACULTURE: PAST, PRESENT AND FUTURE PERSPECTIVES	3
1.1. Infectious diseases and vaccines in aquaculture	5
2. <i>VIBRIO ANGUILLARUM</i> AS A FISH PATHOGEN	8
2.1. General characteristics of <i>V. anguillarum</i>	9
2.2. Host colonization and vibriosis.....	10
2.3. Virulence factors described in <i>Vibrio anguillarum</i>	12
2.3.1. Chemotactic motility and adhesion.....	12
2.3.2. Metalloproteases and haemolysins	13
2.3.3. Outer membrane components – LPS and OMPs	14
2.3.4. Type VI Secretion System - T6SS	15
2.3.5. Iron uptake mechanisms	16
3. IRON UPTAKE MEDIATED BY SIDEROPHORES IN <i>V. ANGUILLARUM</i>	19
3.1. The vanchrobactin siderophore system.....	21
3.2. Evidence for a third siderophore in <i>V. anguillarum</i>	25
4. KEY SIGNALS IN VIRULENCE FACTORS REGULATION	28
II. OBJECTIVES.....	33
III. MATERIAL AND METHODS	37
1. BACTERIAL STRAINS, PLASMIDS AND GROWTH CONDITIONS.....	39
2. DNA MANIPULATION AND CLONING.....	42
2.1. Genomic and plasmidic DNA extraction.....	42
2.2. Polymerase chain reactions (PCR).....	42
2.3. Cloning of DNA fragments.....	42
2.4. Construction of mutant strains by allelic exchange	43
2.5. Complementation of mutant strains	47
3. RNA ANALYSIS.....	51
3.1. RNA purification and RT-PCR.....	51
3.2. RNA sequencing	51
3.2.1. Growth conditions and total RNA extraction	51
3.2.2. cDNA library construction and sequencing.....	52
3.2.3. Bioinformatic analysis and gene expression quantification	52
4. LACZ TRANSCRIPTIONAL FUSIONS AND β -GALACTOSIDASE ASSAYS... ..	53
5. PHENOTYPIC CHARACTERIZATION	55
5.1. Growth promotion assays and siderophore production.....	55
5.2. Cross-feeding assays.....	55
5.3. Motility	56
5.4. Biofilm formation	56

5.5. Haemolytic activity	56
6. WESTERN BLOT ANALYSIS.....	57
6.1. Antibody anti-FrpA design.....	58
7. BIOLOGICAL ACTIVITY OF PISCIBACTIN ANALOGUES	58
8. ELECTROPHORETIC MOBILITY SHIFT ASSAY	59
8.1. Cloning.....	59
8.2. Expression tests	61
8.3. Protein purification.....	61
8.4. Electrophoretic Mobility Shift Assay (EMSA)	63
9. EXPERIMENTAL INFECTIONS	65
10. VACCINATION ASSAYS.....	65
10.1. Immunization	65
10.2. Determination of antibody levels by ELISA	67
11. BIOINFORMATIC ANALYSIS	69
11.1. <i>irp</i> -HPI structure and distribution	69
11.2. Promoter sequence analysis and phylogenetic reconstitution ...	69
11.3. FrpA phylogenetic analysis.....	70
IV. RESULTS AND DISCUSSION	71
1. ADAPTATIONS OF <i>V. ANGUILLARUM</i> THAT ENABLE IT TO CAUSE VIBRIOSIS IN WARM-AND COLD-WATER FISH SPECIES.....	73
1.1. EFFECT OF TEMPERATURE IN THE GROWTH KINETICS AND VIRULENCE OF <i>V. ANGUILLARUM</i>	73
1.2. TRANSCRIPTOMIC ADAPTATIONS OF <i>V. ANGUILLARUM</i> TO GROWTH UNDER LOW IRON AVAILABILITY AT COLD OR WARM TEMPERATURE	75
1.3. METABOLIC ADAPTATIONS TO GROWTH UNDER IRON STARVATION	78
1.4. EXPRESSION OF VIRULENCE FACTORS AT WARM- AND COLD- WATER TEMPERATURE UNDER IRON STARVATION	82
1.4.1. Lipopolysaccharide and exopolysaccharide related genes..	83
1.4.2. Type VI Secretion System and outer membrane proteins ...	86
1.4.3. Haemolysins.....	89
1.4.4. Chemotaxis and Motility	92
1.4.5. Iron uptake systems.....	95
1.5. SUMMARY OF CHAPTER 1	98
2. CHARACTERIZATION OF THE PISCIBACTIN GENOMIC ISLAND (<i>irp</i> -HPI) AND IDENTIFICATION OF ELEMENTS REQUIRED FOR PISCIBACTIN PRODUCTION AND UTILIZATION.....	99
2.1. <i>V. ANGUILLARUM irp</i> -HPI GENOMIC ISLAND (<i>irp</i> -HPI _{VANG}).....	99
2.2. PRODUCTION OF PISCIBACTIN BY <i>V. ANGUILLARUM</i> RV22	102

2.3. CHARACTERIZATION OF FUNCTIONS REQUIRED FOR PISCIBACTIN PRODUCTION	105
2.3.1. Deletion of <i>irp1</i> impairs piscibactin synthesis	106
2.3.2. <i>Irp4</i> is required for piscibactin synthesis	108
2.3.3. <i>Irp8</i> is involved in piscibactin export.....	112
2.4. PISCIBACTIN CONTRIBUTES SIGNIFICANTLY TO <i>V. ANGUILLARUM</i> VIRULENCE.....	116
2.5. CHARACTERIZATION OF FERRI-PISCIBACTIN UPTAKE	117
2.5.1. <i>FrpA</i> and <i>FrpBC</i> are involved in ferri-piscibactin uptake	118
2.5.2. Distribution of <i>frpA</i> in different bacteria and phylogenetic analysis	121
2.5.3. Structural requirements in piscibactin analogues to be transported through <i>FrpA</i>	122
2.6. SUMMARY OF CHAPTER 2	128
3. IDENTIFICATION OF REGULATORS INVOLVED IN <i>IRP</i> -HPI GENE EXPRESSION	131
3.1. <i>IRP</i> -HPI IS PREFERENTIALLY EXPRESSED AT COLD TEMPERATURES	131
3.2. REGULATORS INVOLVED IN <i>IRP</i> -HPI GENE EXPRESSION MODULATION	133
3.2.1. <i>araC1</i> (<i>pbtA</i>) deletion impairs growth under iron limited conditions.....	134
3.2.2. The global regulators <i>ToxR-S</i> and <i>H-NS</i> play indirect roles in the regulation of the <i>irp</i> -HPI _{<i>vang</i>} gene expression.....	136
3.2.3. <i>PbtA</i> and <i>H-NS</i> are needed for full virulence of <i>V. anguillarum</i>	136
3.2.4. <i>PbtA</i> is the main expression modulator of genes encoding piscibactin synthesis and transport	138
3.2.5. Purification of <i>PbtA</i> and its N- and C-terminal domains..	143
3.2.6. <i>PbtA</i> interacts directly with the piscibactin promoters <i>PfrpA</i> and <i>PfrpBC</i>	145
3.2.7. <i>irp</i> -HPI is widespread in <i>Vibrionaceae</i> and contains several versions of <i>frpA</i> and <i>pbtA</i> promoters	148
3.2.8. <i>irp</i> -HPI expression pattern results from the interaction of the type of promoter and other elements in the genome.....	152
3.3. SUMMARY OF CHAPTER 3	154
4. UTILITY OF THE SIDEROPHORES OUTER MEMBRANE TRANSPORTERS TO DEVELOP NEW VACCINES AGAINST VIBRIOSIS.....	157
4.1. USE OF SIDEROPHORE TRANSPORTERS <i>FVTA</i> AND <i>FRPA</i> TO DEVELOP VACCINES AGAINST VIBRIOSIS.....	157

4.1.1. Fish immunization assay	157
4.1.2. FrpA and FvtA are immunogenic proteins.....	159
4.1.3. Evaluation of protection in experimental infections	163
4.2. SUMMARY OF CHAPTER 4	169
V. CONCLUSIONS	171
VI. REFERENCES.....	175
VII. APPENDIX.....	205

I. INTRODUCTION

I. INTRODUCTION

1. AQUACULTURE: PAST, PRESENT AND FUTURE PERSPECTIVES

Fish is an extraordinarily nutritious and healthy food product that responds to the constant consumer demand for fresh, sustainable, and less processed food. There is a wide variety of aquatic products available for human consumption, therefore their nutritional composition also differs significantly depending not only in the species but also in the way the product is processed before consumption. Fish are a source of protein, fatty acids, and nutrients essential for the human health. Although the caloric content of fish and fish products is relatively low, they are a vital source of long chain omega-3 fatty acids, amino acids, vitamins A, B and D and micronutrients such as iron, calcium zinc and selenium. Nowadays, humanity is consuming record-breaking levels (Figure I.1) of aquatic products and this demand can only be met by the additional efforts of the aquaculture sector to the extractive fisheries (FAO, 2020).

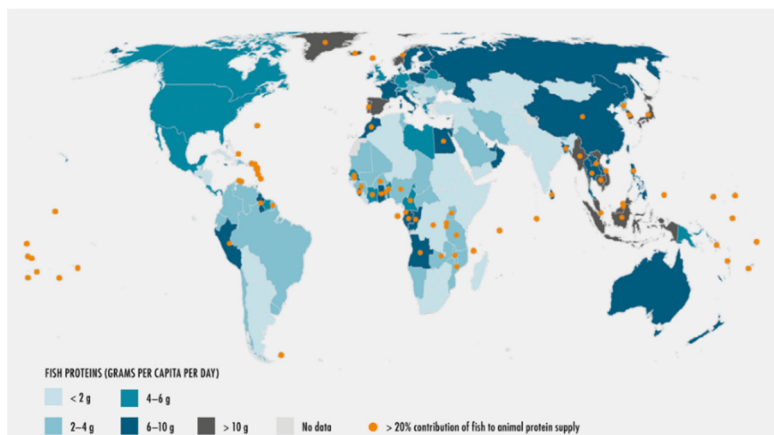


Figure I.1. Fish consumption in the globe (FAO, 2020).
Authorization to reproduce in appendix 1.

In 2017, fish consumption represented 17% of the total animal protein intake of the world population and this fact represents a challenge to produce high-quality aquatic goods. To deal with this increasing demand, innovative solutions must be taken as the extractive fisheries cannot sustainably cover the total requirement of aquatic products. In fact, the capture fishing industry has declined as well as the wild stocks (FAO, 2020). Therefore, aquaculture has become a reliable source of fish, crustaceans, and molluscs (Sommerset *et al.*, 2005). Aquaculture has demonstrated a decisive role in global food security and the sector has been growing consistently over the past decades, at a 7.5% per year since 1970 (FAO, 2020). For the sixth consecutive year aquaculture has surpassed fisheries production, specifically in 2018 aquaculture produced 17.1 million tonnes more than fisheries (114.5 million tonnes) (Figure I.2) (FAO, 2020).

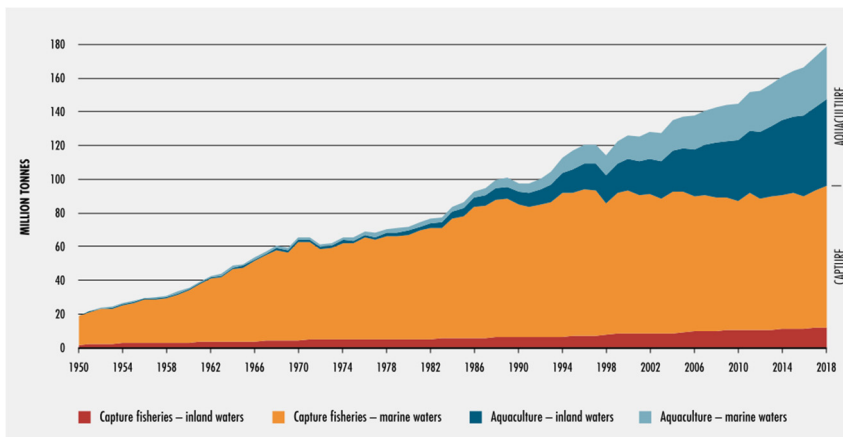


Figure I.2. Contribution in millions of tones of capture fishing and aquaculture to the global fish consumption (FAO, 2020). Authorization to reproduce in appendix 1.

In 2018, finfish dominated the farmed aquatic animals (54.3 million tonnes) followed by molluscs (17.7 million tonnes), crustaceans (9.4 million tonnes), marine invertebrates (435.400 tonnes), aquatic turtles (370.000 tonnes) and frogs (131.300 tonnes) (FAO, 2020). Spain was the leading country of the European Union in the production of aquacultured products in 2018 (25.5%) however this prominent place was not reflected in terms of value (11%) (APROMAR, 2020). In 2018,

in Spain the most relevant aquacultured products were mussels (273.600 tonnes), sea bass (22.460 tonnes), rainbow trout (18.955 tonnes) and sea bream (14.930 tonnes) (APROMAR, 2020). Galicia is a relevant producing area of turbot and sole fish in Spain and Europe. Turbot produced in Galician waters corresponded to 76.9% of the total harvested in Europe in 2018. In the case of sole, 818 tonnes were produced in Spain in 2019, mainly in Galicia and Andalusia (APROMAR, 2020).

1.1. Infectious diseases and vaccines in aquaculture

Fish and aquatic products are some of the most traded commodities in the world. However, the intensive production of aquatic animals at high densities, leads to an increasing number of infectious diseases outbreaks reported, because pathogens can easily be transmitted in these environments (Sommerset *et al.*, 2005). Thus, one of the main bottlenecks that is limiting aquaculture from achieving maximal yield are infectious diseases. Overall, it is estimated that 10% of the aquacultured animals are discarded due to infectious diseases (Adams, 2019). Reports suggest that disease outbreaks in aquaculture are mainly caused by bacteria (54.9%), viruses (22.6%), parasites (19.4%) and mycotic agents (3.1%) (Dadar *et al.*, 2017). Bacteria from *Vibrio* spp. are autochthonous of the aquatic environment and ubiquitous in aquaculture production systems. However, some *Vibrio* species are pathogenic leading to a variety of “vibriosis” diseases. The most important bacterial pathogens in fish culture are listed in Table I.1 (Toranzo *et al.*, 2005).

The aquatic environment creates a constant risk for the host-pathogen contact and frequently leads to the emergence of novel or the persistence of known pathogens. This environment favours the genomic plasticity where the acquisition of virulence factors through horizontal gene transfer (HGT) has a great impact (Le Roux and Blokesch, 2018). This mechanism includes the gene flux in mobile elements as conjugative plasmids, bacteriophages, transposons, insertion elements and genomic islands (Schmidt and Hensel, 2004).

Table I.1. Bacterial pathogens and infectious diseases that affect aquaculture marine fish (Toranzo *et al.*, 2005).

Infectious Agent	Disease	Main marine hosts
<i>Vibrio anguillarum</i>	Vibriosis	Salmonids, turbot, seabass, striped bass, eel, ayu, cod, red seabream
<i>Vibrio ordalii</i>	Vibriosis	Salmonids
<i>Vibrio salmonicida</i>	Vibriosis	Atlantic salmon, cod
<i>Vibrio vulnificus</i>	Vibriosis	Eels
<i>Moritella viscosa</i>	“Winter ulcer”	Atlantic salmon
<i>Photobacterium damselae</i> subsp. <i>piscicida</i>	Photobacteriosis	Seabream, seabass, sole, striped bass, yellowtail
<i>Pasteurella skyensis</i>	Pasteurellosis	Atlantic salmon
<i>Aeromonas salmonicida</i> subsp. <i>salmonicida</i>	Furunculosis	Salmonids, turbot
<i>Tenacibaculum maritimum</i>	Flexibacteriosis	Turbot, salmonids, sole, seabass, gilthead seabream, red seabream, flounder
<i>Pseudomonas anguilliseptica</i>	Pseudomonadiasis “Winter disease”	Seabream, eel, turbot, ayu
<i>Lactococcus garvieae</i>	Streptococcosis or lactococcosis	Yellowtail, eel
<i>Streptococcus iniae</i>	Streptococcosis	Yellowtail, flounder, seabass, barramundi
<i>Streptococcus parauberis</i>	Streptococcosis	Turbot
<i>Streptococcus phocae</i>	Streptococcosis	Atlantic salmon
<i>Renibacterium salmoninarum</i>	Bacterial kidney disease	Salmonids
<i>Mycobacterium marinum</i>	Mycobacteriosis	Seabass, turbot, Atlantic salmon
<i>Piscirickettsia salmonis</i>	Piscirickettsiosis	Salmonids

Efforts must be taken to prevent infections and the primary choice to tackle disease outbreaks was the use of antibiotics. However, their excessive use led to the emergence of resistant pathogens which could evolve to their dispersion in the environment and/or food chain. Therefore, vaccination arose as the best option to mitigate pathogens affecting finfish (Stentiford *et al.*, 2017). Aquaculture and vaccination have an intrinsic development path. The development and use of

vaccines based on formalin inactivated whole cells, proved to be very effective to prevent infectious diseases, and their progressive use instead of antibiotics resulted in a significant increase in fish production (Somerset *et al.*, 2005).

The first licensed and commercially available vaccines against the enteric red mouth disease and vibriosis, were reported in the 1970s in the USA and were based on formalin inactivated cells administered by immersion. Immersion vaccines are not effective against all bacterial pathogens. The development of injectable vaccines containing adjuvants soon became the product of choice and led to an exponential increase in fish production. These vaccines can contain different antigen combinations (Somerset *et al.*, 2005). However, the immunological response of fish not only depends on the vaccines used, but it is considerably influenced by temperature, stress, and diet (Le Morvan *et al.*, 1998).

Nowadays, high value fish species are being inoculated with vaccines that confer protection against more than one pathogen. Multivalent vaccines contain antigens from several pathogens alleviating the use of different vaccines and the induced stress from fish manipulation (Brudeseth *et al.*, 2013). Several vaccine types have been developed for use in aquaculture: inactivated, live attenuated, subunit, and nucleic acids vaccines. The most used vaccines in aquaculture are inactivated vaccines, bacterins. Whole cells are inactivated through physical (temperature) or chemical methods (formalin) (Toranzo *et al.*, 2009). The subunit vaccines are based on the application of molecular biology techniques to obtain and produce highly immunogenic antigens. The production of vaccines through recombinant vectors requires previous work to identify the pathogen component that promotes a significant immunogenic reaction (Dadar *et al.*, 2017). In the case of bacterial pathogens, the outer membrane proteins are natural candidates for this vaccine formulation due to its external localization and immunogenicity (Valderrama *et al.*, 2019).

Vaccine design is time consuming and expensive, and it cannot be developed for all known pathogens. Therefore, a promising strategy is to develop vaccines against a specific pathogen (autogenous) of a concrete aquaculture plant (Brudeseth *et al.*, 2013). However, the

selective pressure exerted in the aquaculture environment leads to rapidly evolving pathogens thus vaccines must be constantly renewed and improved.

2. *VIBRIO ANGUILLARUM* AS A FISH PATHOGEN

Vibrios are marine bacteria that include both symbiotic and pathogenic species. They are generally widespread in coastal and estuarine environments and on the surface and/or in the intestinal tract of aquatic animals. Several *Vibrio* spp. comprise a high risk for human health through ingestion of contaminated water or food or via skin wounds. *V. cholerae*, the causative agent of cholera (Morris, 2003) and *V. parahaemolyticus* and *V. vulnificus*, responsible for foodborne diseases related to the ingestion of contaminated fish and shellfish (Drake *et al.*, 2007), represent the most relevant pathogens to humans (Austin, 2010). In addition, *Vibrio* infections are common in animals (Ben-Haim *et al.*, 2003) and are a major threat for the aquaculture industry. In nature, the virulence of pathogenic bacteria is restrained due to the constant stress imposed by the environmental variations as well as the climate changes. In the aquaculture environment, where animals are found at high densities and in a controlled environment to maximize growth rate, the prevalence of pathogens tends to increase (Toranzo *et al.*, 2005).

Among Vibrios, one of the most relevant pathogens for the aquaculture industry is *V. anguillarum*. It is the causative agent of vibriosis, a fatal haemorrhagic septicaemia, that leads to high morbidity and mortality rates in over 50 species of fresh and salt-water fish, molluscs, and crustaceans in different geographic locations (Frans *et al.*, 2011). From the economic point of view, it leads to relevant losses in the culture of cold- and warm-water adapted fish species of high economic importance including cod (*Gadus morhua*), salmon (*Salmo salar*), rainbow trout (*Oncorhynchus mykiss*), turbot (*Scophthalmus maximus*), sole (*Solea senegalensis*), sea bass (*Dicentrarchus labrax*), sea bream (*Sparus aurata*), eel (*Anguilla japonica* and *Anguilla anguilla*) and ayu (*Plecoglossus altivelis*) (Buller, 2004; Toranzo *et al.*, 2005).

2.1. General characteristics of *V. anguillarum*

V. anguillarum is a bacterium with global distribution which was firstly described as the causative agent of the red disease in eel with reports dating from 1893 (Canestrini, 1893). It is a Gram-negative rod-shaped bacterium, 0.5-0.8 μm in width and 1.4-2.6 μm in length that belongs to the *Vibrionaceae* family (Figure I.3) (Holt *et al.*, 1994).

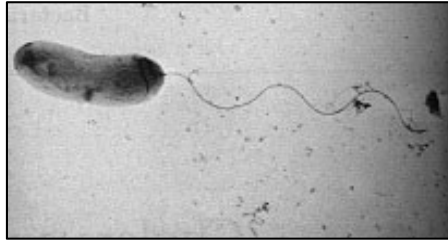


Figure I.3. *V. anguillarum* observed by electron microscopy.

V. anguillarum is a facultative anaerobe with a fermentative and respiratory metabolism, and it can ferment D-glucose with no gas production. Additionally, it can use D-fructose, maltose, and glycerol as carbon sources. It is oxidase positive and sensitive to the vibriostatic agent O/129. *V. anguillarum* is highly motile by means of one polar flagellum, and motility is enhanced by salinity. As a halophilic bacterium it requires NaCl between 1 and 2% for optimal growth. It is an eurythermal organism as it can grow in a wide range of temperatures, from 10 to 42 $^{\circ}\text{C}$, being 25 $^{\circ}\text{C}$ considered the optimal growth temperature (Holt *et al.*, 1994; Guérin-Faublée *et al.*, 1995).

Twenty-three serotypes (O1-O23) have been established based on the detection of O antigens by side agglutination (Sørensen and Larsen, 1986; Pedersen *et al.*, 1999). Nonetheless, only certain serotypes are associated with disease as each one shows different pathogenicity and host specificity. The pathogenic strains, those that can successfully establish an infection, belong to serotypes O1, O2 and to a lesser extent O3. Serotype O2 was divided in sub-groups O2a, O2b and O2c, which differ in the host organism. The same division has been recognized in serotype O3, where O3a groups pathogenic strains and O3b clusters environmental isolates (Toranzo *et al.*, 2005). To the remaining serotypes belong environmental isolates from seawater, animals, or

sediments (Frans *et al.*, 2011; Toranzo *et al.*, 2017). In northern Europe, the most common isolated serotype of *V. anguillarum* from non-salmonid outbreaks is serotype O2a. Serotype O1 is frequently isolated from salmonid fish species in Norway, and from European seabass and gilthead seabream in the Mediterranean (Mohamad *et al.*, 2019).

Like other *Vibrio* species, the genome of *V. anguillarum* is formed by two chromosomes and several plasmids, depending on the strain. Many *V. anguillarum* genomes from strains of serotypes O1, O2 and O3 have been sequenced (Naka *et al.*, 2011; Li *et al.*, 2013; Busschaert *et al.*, 2015) and depending on the strain (mainly serotype O1) they can contain small or large plasmids, including virulence related plasmids (Skov *et al.*, 1995). Most of the genes related to essential metabolic functions are located in chromosome I. In contrast, chromosome II has a less conserved structure as it generally contains a larger proportion of hypothetical proteins. Moreover, both chromosomes harbour genomic islands potentially encoding virulence factors (Naka *et al.*, 2011). The size of the genome varies from ca 4 Mbp to 5.6 Mbp, showing a total number of genes from ca. 4,500 to 6,500. The total GC content is generally below 45% (Hansen *et al.*, 2020). Most of the isolates from serotype O1 contain a plasmid pJM1-like (Naka *et al.*, 2011). Interestingly, virulent strains can be classified based on the geographical location and special features of the pJM1 plasmid. Strains isolated in the Pacific coast of the USA and Japan harbour the classical pJM1, whereas isolates from the Atlantic coast of the USA, Spain, Scotland, and North European countries, harbour a pJM1-like plasmid that contains insertion elements and a specific mutation (Naka *et al.*, 2011).

2.2. Host colonization and vibriosis

Vibriosis is a haemorrhagic septicaemia (Figure I.4) characterized by weight loss, lethargy, circulatory haemorrhage, internal and external ulcerated lesions, eye lesions that evolved sequentially from opacity to ulceration and exophthalmia, and eventually death. Nevertheless, in some acute cases the infection spreads rapidly, and the hosts die without showing external signs of disease. Two days after the first contact with the pathogen, the infection is established, and three days later the host

can already be dead (Frans, *et al.*, 2011). In rapidly evolving diseases such as vibriosis, host-pathogen studies are of particularly importance. Two modes of infection have been reported for *V. anguillarum*: internalization through the skin and/or ingestion of contaminated water or food (Grisez *et al.*, 1996; Svendsen and Bogwald, 1997).



Figure I.4. Turbot with signs of vibriosis characterized by the appearance of haemorrhagic spots.

In the early stages of infection attachment and colonization of the host surface is key. Although the skin is a difficult barrier to cross due to the presence of the mucus layer, a discontinuity on the skin through injuries or damaged mucus can constitute a colonization site for *V. anguillarum* from where it can initiate the invasion of the host. The mucus layer is one of the main components of the fish innate immune system, but it is the first barrier that bacteria must cross for the establishment of a successful infection. It contains substances such as lysozyme, proteases and antimicrobial peptides that avoid the adhesion of bacteria (Ellis, 2001). However, *V. anguillarum* was shown to be resistant to rainbow trout skin mucus and even can use it as a source of nutrients (O'Toole *et al.*, 1996; O'Toole *et al.*, 1999). The attachment to the epithelial cells must occur very quickly before the antimicrobial nature of the mucus and its continuous renewal detaches the pathogenic bacteria. In the first 24 hours of infection, *V. anguillarum* colonizes both the skin and the intestines (Croxatto *et al.*, 2007; Weber *et al.*, 2010). However, the numbers differ significantly, existing a higher number of bacteria on the skin, indicating that this is an important colonization site and additionally, it suggests that the intestines are more difficult to access and/or that they constitute a more inhospitable

environment for the growth of this bacterium (Weber *et al.*, 2010). After the attachment to the epithelia, *V. anguillarum* moves gradually from the surface until reaching the blood stream and organs (Weber *et al.*, 2010; Schmidt *et al.*, 2017).

2.3. Virulence factors described in *Vibrio anguillarum*

Virulence is a measure of pathogenicity and virulence factors are properties of each pathogen that may cause disease in a susceptible host in a concrete environment. These factors allow the adherence, colonization, growth, and persistence within a susceptible host. They may also cause tissue damages and evasion of the host immune system. Although the virulence mechanisms of *V. anguillarum* are not completely known, several virulence factors have been identified such as motility, chemotaxis, lipopolysaccharide, extracellular products with proteolytic and haemolytic activity, and iron uptake mechanisms.

2.3.1. Chemotactic motility and adhesion

The chemotactic response and motility are tightly coupled. Chemotactic motility is a requirement for *V. anguillarum* virulence. Fish skin and gut are covered by a protective mucus layer that pathogens must invade to disseminate a successful infection. Chemotactic motility towards chemoattractants present in the mucus is used in the initial steps of infection (O'Toole *et al.*, 1996). In fact, a mutation in the *cheR* gene that encodes a cytoplasmic methyl transferase, leads to a decrease in virulence for rainbow trout. However, the chemotactic response is important for the movement towards the host but not in the persistence within the host (O'Toole *et al.*, 1996). Additionally, the flagellum plays an essential role in pathogenesis. *V. anguillarum* possess five flagellin proteins encoded by *flaABCDE*. FlaA, FlaD and FlaE contribute directly to virulence since non-motile mutants showed a decrease in virulence in experimental infections by bath, a method that mimics the natural infection route (McGee *et al.*, 1996; Milton *et al.*, 1996). During the first steps of infection, the flagellum may serve as a motility component involved in the penetration of epithelial mucosa. Nonetheless, it can also be involved in the adhesion process by carrying adhesins (Frans *et al.*, 2011).

2.3.2. Metalloproteases and haemolysins

After adhesion to the skin or gut mucus, *V. anguillarum* must penetrate the epithelial cells. The secretion of the extracellular zinc metalloprotease EmpA, with mucinase activity, degrades the mucus. This tissue damage enables the pathogen to colonize and penetrate the host tissues and consequently cause the infection that at the final stages can reach internal organs such as the liver and spleen (Denkin and Nelson, 1999; Denkin and Nelson, 2004; Croxatto *et al.*, 2007). This metalloprotease is expressed as an inactive proenzyme and only when *V. anguillarum* is in contact with the intestinal mucus an enzyme with metalloproteolytic function cleaves the propeptide allowing the EmpA to function (Varina *et al.*, 2008).

The haemolytic activity of *V. anguillarum* greatly contributes to the characteristic haemorrhagic septicaemia of vibriosis and the haemolysis directly kills host cells. The lysis of erythrocytes releases the intracellular haem. In *V. anguillarum* several extracellular haemolysins have been described, Vah 1-5 and a repeat in toxin, RTX (Hirono *et al.*, 1996; Rodkhum *et al.*, 2005; Li *et al.*, 2008). The sequence analysis of Vah 1-5 reveals that they are different types of haemolysins. Additionally, single haemolysin deletion revealed a haemolytic phenotype but in a lesser degree than that observed for the parental strain, indicating that more than one haemolysin contributes to the haemolytic activity of *V. anguillarum* (Rodkhum *et al.*, 2005). The *rtx* gene cluster, *rtxACHBDE*, is comprised of *rtxA* that encodes the toxin, *rtxC* encoding the activator, *rtxH* encoding a conserved hypothetical protein and *rtxBDE* encoding the transporters. RTX toxins are a diverse group of proteins which include toxins with cytolytic activity, metalloproteases, lipases and adenylate cyclases (Li *et al.*, 2008). Vah1 and RtxA are both exotoxins that work synergistically, however their cytotoxicity leads to different effects in ASK cells. Vah1 causes cell vacuolation and RtxA causes cell rounding. RTX proteins are secreted via the T1SS and in *V. anguillarum* the *rtx* operon shows a high degree of amino acid similarity with homologous systems of *V. vulnificus* and *V. cholerae* El Tor N16961 (Li *et al.*, 2008).

2.3.3. Outer membrane components – LPS and OMPs

The complement system in fish plays a crucial role in host defence against pathogens as it generates a specific immune response. Although it is usually in an inactive state, it can be activated by the interaction of its components with antibody-antigen complexes or by a direct contact with the pathogen (Holland and Lambris, 2002). Some Gram-negative bacteria can evade the host immune system by resisting the bactericidal effect of the fish serum. In *V. anguillarum* the long polysaccharide side chains (O antigen) of their lipopolysaccharide (LPS) are essential for this resistance and there is a correlation between the length of the LPS O-antigen and the ability to evade the complement system. The O-antigen protects the bacteria by restraining the complement components to access the cytoplasmic membrane. Serotype O1 and O2 strains of *V. anguillarum* have been described as resistant to rainbow trout serum and these same strains were reported as pathogenic for Atlantic salmon. Thus, serum resistance mediated by the O-antigen contributes to the survival of bacteria within the host and to the infection process (Boesen *et al.*, 1999).

The outer membrane of Gram-negative bacteria is a complex structure composed of phospholipids, LPS, lipoproteins and porins (Henderson *et al.*, 2016). Outer membrane porins are transmembrane pore-forming proteins (OMP) that allow the passive transport of hydrophilic compounds. Besides this transport function, porins are involved in the maintenance of the cell integrity and antibiotic resistance (Choi and Lee, 2019). OmpA and OmpC have been described as essential for the maintenance of membrane integrity whereas the role of OmpF is mainly the transport of antibiotics (Choi and Lee, 2019). Moreover, OmpA is a relevant virulence factor because it is involved in bacterial adhesion, invasion, intracellular survival, serum resistance and evasion of the host immune system (Confer and Ayalew, 2013). OmpA and OmpA-like proteins are found in high numbers in pathogens outer membranes and this surface exposure activates both the innate and the adaptative immune system, making them good candidates for the development of new antimicrobials (Confer and Alyalew, 2013). Additionally, *V. anguillarum* OMPs confer resistance to bile and induce biofilm formation (Wang *et al.*, 2003). Resistance to bile allows the

pathogen to survive within the host and biofilm formation is an advantage for colonization and survival. Some OMPs such as Omp26La, OmpW and OmpU, are not directly involved in virulence, in fact they are salt-responsive and allow the adaptation of *V. anguillarum* to different salt concentrations (Kao *et al.*, 2009).

2.3.4. Type VI Secretion System - T6SS

Secreted proteins contribute not only to virulence but also to environmental adaptation. The secretion systems are classified according to their structural components, the secreted proteins, and the mechanism of transport. The Type VI Secretion System (T6SS) was firstly described in *Vibrio cholerae* (Pukatzki *et al.*, 2006) and its contribution to virulence has been characterized. It is a contact-dependent system that allows the translocation of effector proteins directly into eukaryotic or prokaryotic cells. The translocation event occurs through the contraction of the structure that propels the end spike of the system into other cells. The T6SS of Gram-negative bacteria share core elements (Joshi *et al.*, 2017). The assembly of the T6SS begins with the formation of the membrane complex which is composed by three proteins (VasDFK in *V. cholerae*) that are the structural support of the whole system. Then, the proteins that form the baseplate complex (HsiF, VasABE and VgrG1-3 in *V. cholerae*) are recruited and anchored to the inner membrane. The tip of the apparatus is formed by VgrG1-3 that are capped by proteins containing repeating proline-alanine-alanine-arginine motifs (PAAR). The inner tube of the tail complex is formed by the haemolysin-coregulated protein (Hcp) that is surrounded by the VipA/VipB outer tube. After the secretion process, ClpV ATPase disassembles and recycles the system (Joshi *et al.*, 2017). In *V. anguillarum* the T6SS provides the bacteria an ecological advantage. Under environmental conditions that mimic the fluctuations of the marine environment, the expression and secretion of Hcp was detected in non-O1 serotype strains (Tang *et al.*, 2016). Furthermore, the T6SS is involved in signal sensing mechanisms as it activates the expression of stress response regulators (Weber *et al.*, 2009).

2.3.5. Iron uptake mechanisms

Iron is an essential element for many metabolic functions in microorganisms. Its abundance in most environments does not correlate directly with its bioavailability. In natural conditions it is present in two redox states, as Fe^{2+} and Fe^{3+} , and these forms and their solubility are strongly influenced by pH and the presence of anions with which it can form complexes. In the presence of oxygen at neutral or slightly higher pH, iron is present as ferric hydroxides, and the alkaline seawater pH (pH 7.5 to 8.4) leads to a concentration in the nanomolar range of dissolved iron (Price and Morel, 1998). This concentration is far less than that needed by pathogens to survive, making iron a limiting factor for bacterial growth (Wandersman and Delepelaire, 2004). Iron is essential for the synthesis of enzymes that are vital for cellular processes, from cytochromes involved in cell respiration to the synthesis of nucleic acids and TCA enzymes (Andrews *et al.*, 2003; Crosa *et al.*, 2004). When available, iron is also presented as a challenge, since it can react with oxygen generating reactive oxygen species highly harmful for the cell (Cornelis *et al.*, 2011). Therefore, the acquisition of iron as well as its homeostasis are strictly regulated.

When facing an environment of iron limitation, most bacteria have developed specific mechanisms to scavenge it from environmental sources or from the host (Miethke, 2013). These systems include the direct contact with host iron-containing molecules such as transferrin or haem proteins or the synthesis and secretion of siderophores, secondary metabolites with high affinity for Fe^{3+} .

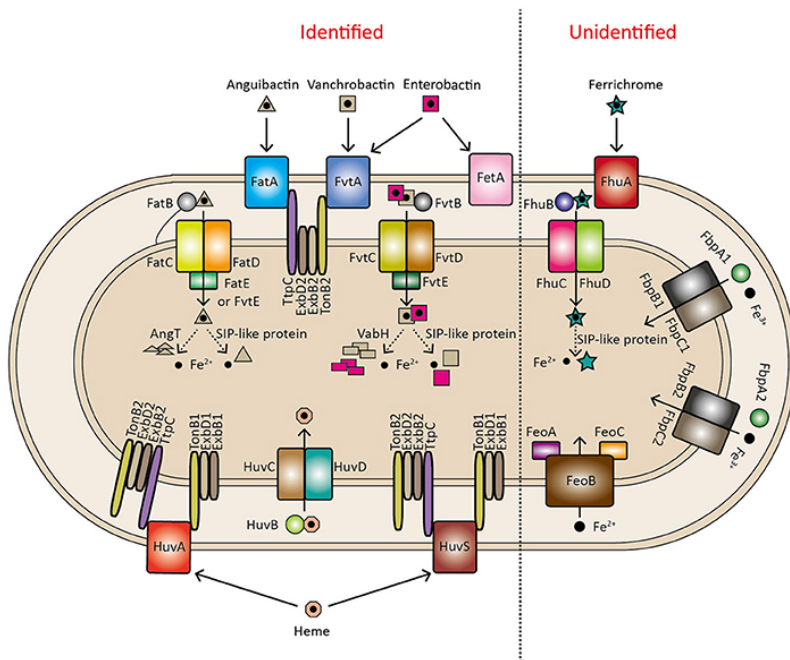


Figure I.5. Iron transport systems identified in *V. anguillarum*. Iron acquisition mediated by the siderophores anguibactin, vanchrobactin and xenosiderophores (enterobactin) are displayed. Other iron transport systems like haem uptake, use of ferrichrome, and utilization of ferrous and ferric iron are also represented. From Li and Ma, *Front. Cell. Infect. Microbiol.*, 2017. Authorization to reproduce in appendix 2.

In *V. anguillarum* different mechanisms of iron acquisition have been described (Li and Ma, 2017) (Figure I.5):

- Production of the siderophores anguibactin and vanchrobactin. Production and utilization of siderophores is one of the most important virulence factors. Biosynthesis, transport, and regulatory mechanisms have been characterized for both siderophore systems, anguibactin and vanchrobactin. However, only anguibactin role in virulence has been demonstrated. Anguibactin and vanchrobactin systems will be described below.
- Utilization of haem and haem-containing proteins. Haem transporters are widespread in pathogenic *Vibrios* (Kustusch *et al.*, 2011). Haem is found abundantly in fish tissues and potentially it is

a source of iron for the pathogen. However, free haem is not available as it is mostly present in haemoglobin or haemopexin and haptoglobin. Therefore, the utilization of haem as an iron source is facilitated by the activity of haemolysins that lyse host cells and consequently release the intracellular haem to the extracellular environment (Lemos and Balado, 2020). After its release, haem is captured by the outer membrane transporter HuvA. HuvA is essential for haem uptake as the deletion of this transporter disables the ability to grow with haem as the sole iron source, nonetheless it does not abolish haem-binding activity which suggest the presence of additional proteins with this function but not able to transport haem (Mazoy *et al.*, 2003). Haem uptake is an energy-dependent process, energized by TonB systems. Two TonB systems, TonB1 and TonB2 are involved in haem uptake, and the deletion of these systems leads to a defect in haem uptake and a decrease in virulence (Stork *et al.*, 2004). Some *V. anguillarum* strains that lack HuvA, have an additional gene, HuvS that assumes the same function (Mouriño *et al.*, 2004). The haem utilization gene cluster is composed of nine genes that encode proteins involved in haem uptake and utilization, HuvA, HuvZ, HuvX, TonB1, ExbB1, ExbD1, HuvB, HuvC and HuvD (Figure I.5). Single gene deletions demonstrated that *huvAZBCD* genes are essential for haem utilization as iron source (Mouriño *et al.*, 2004). After internalization via HuvA, the periplasmic protein HuvB delivers haem to the inner membrane complex HuvCD that transports it to the cytoplasm (Mouriño *et al.*, 2004). HuvZ is a putative haem storage protein (Wyckoff *et al.*, 2004) and HuvX would be an intracellular haem delivery protein (Sekine *et al.*, 2016) (Figure I.5). Nevertheless, the contribution of haem uptake systems to the virulence of *V. anguillarum* remains unclear.

- c) Moreover, additional iron transport systems are present in *V. anguillarum* genome, although their involvement in virulence is unclear. Four operons encode probable transport systems for unchelated ferrous (*feoABC*), ferric iron (*fbpABC1* and *fbpABC2*) and ferrichrome (*fhuABCD*) (Li and Ma, 2017):

- FeoABC system is likely the most ancient iron transport mechanism described to date due to its wide distribution among bacteria (Lau *et al.*, 2016). Despite the scarce characterization of the system, it is thought that FeoB forms the ferrous iron channel through the cytoplasmic membrane and FeoA and FeoC complement the functioning of the system (Payne *et al.*, 2016; Lau *et al.*, 2016). Nonetheless, remains unclear how ferrous iron access the periplasm through the outer membrane.
- Ferric iron transport has also been described in *Vibrios*. This transport is mediated by the ABC transporter FbpABC located in the cytoplasmic membrane. It has been proposed that ferric iron binds FbpA in the periplasm, then it is delivered to FbpBC in the cytoplasmic membrane and the hydrolysis of ATP favours the transport of iron to the cytoplasm (Payne *et al.*, 2016).
- Ferrichrome utilization has been reported in *V. anguillarum*, however the proteins involved in this process have not been characterized (Li and Ma, 2017).

3. IRON UPTAKE MEDIATED BY SIDEROPHORES IN *V. ANGUILLARUM*

Siderophores are small molecules with high affinity for Fe^{3+} that can scavenge iron from different sources like fish tissues or the environment. Structurally, siderophores are a diverse group of compounds and they are categorized based on the functional group – carboxylate, catecholate and hydroxamate – which confer different iron binding affinities (Hilder and Kong, 2010). There are also siderophores that contain more than one functional group as it is the case of yersiniabactin (Drechsel *et al.*, 1995). Harbouring different siderophore systems gives fitness advantages to bacteria, allowing them to survive in a wide range of environments (Bachman *et al.*, 2012; Holden and Bachman, 2015).

In *V. anguillarum* two iron uptake systems mediated by siderophores have been described to date: anguibactin and

vanchrobactin (Lemos *et al.*, 1988; Stork *et al.*, 2002; Balado *et al.*, 2006) (Figure I.6). While vanchrobactin is widespread in pathogenic and environmental *V. anguillarum* strains of serotypes O1 to O10, anguibactin is a plasmid-encoded system associated to highly virulent O1 strains (Actis *et al.*, 1986). The biosynthetic pathway of anguibactin and vanchrobactin has been deeply described and is accomplished by a series of non-ribosomal peptide synthases (NRPS) (Stork *et al.*, 2002; Crosa and Walsh, 2002; Balado *et al.*, 2006). Both siderophores share a common biosynthesis step which leads to the synthesis of the DHBA moiety (Lemos *et al.*, 2010). The genes involved in 2,3-dihydroxybenzoic acid (DHBA) synthesis were firstly identified in the chromosome of pJM1 harbouring isolates, but functional homologues are also present in the plasmid. Nonetheless, anguibactin and DHBA synthesis requires AngA whose only functional copy is located in the chromosome (Alice *et al.*, 2005).

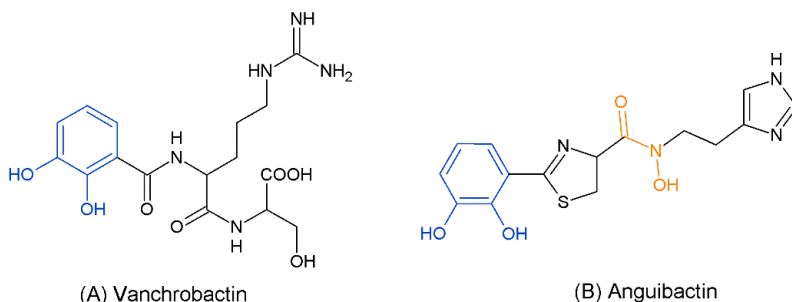


Figure I.6. Structure of the siderophores vanchrobactin (A) and anguibactin (B). Catecholate functional group is highlighted in blue and hydroxamate is highlighted in orange.

Most *V. anguillarum* highly pathogenic strains that belong to serotype O1 harbour a 65 kb plasmid. This plasmid, pJM1, confers the recipient bacteria the ability to synthesize and use the siderophore anguibactin (Figure I.7). A correlation can be established between the serotype and the presence of the pJM1 plasmid as it has been reported that the O1 side chain is essential for the stability of ferri-anguibactin outer membrane receptor FatA (Welch and Crosa, 2005). Structurally, anguibactin is a mixed siderophore as it contains catecholate and hydroxamate functional groups (Figure I.6.B) and most of the genes

that encode biosynthesis and transport functions are located in pJM1 plasmid (Stork *et al.*, 2002; Di Lorenzo *et al.*, 2003) (Figure I.7). The ferri-anguibactin complex is transported by the pJM1-harboured *fatABCD* operon (Di Lorenzo *et al.*, 2004; Stork *et al.*, 2004; Stork *et al.*, 2007). The ferri-anguibactin complex is recognized by the 86 kDa outer membrane transporter FatA, which facilitates its translocation through the outer membrane (Figure I.10) (López and Crosa, 2007; López *et al.*, 2007).

3.1. The vanchrobactin siderophore system

Virulent strains that lack the pJM1 plasmid synthesize a siderophore named vanchrobactin (Figure I.6 and I.7) (Lemos *et al.*, 1988; Balado *et al.*, 2006; Soengas *et al.*, 2006). The genes involved in vanchrobactin synthesis (*vabABCE*), and transport (*fvfA*) are widespread among environmental and pathogenic strains of all serotypes (Balado *et al.*, 2009). Notably, serotype O1 strains carrying pJM1-like plasmids do not produce vanchrobactin since its synthesis is disabled by the insertion of a plasmid-encoded insertion sequence (*IS1*) in *vabF*, the NRPS required for vanchrobactin synthesis (Figure I.7) (Naka *et al.*, 2008; Lemos *et al.*, 2010).

The presence of genes that encode the vanchrobactin siderophore system in the chromosome of pathogenic and environmental isolates, indicates that this may be the ancestral siderophore (Balado *et al.*, 2009). The anguibactin system could have been acquired through horizontal gene transfer and the higher affinity of anguibactin for iron might have led to the inactivation of the *vab* genes in favour of a more efficient system (Naka *et al.*, 2008).

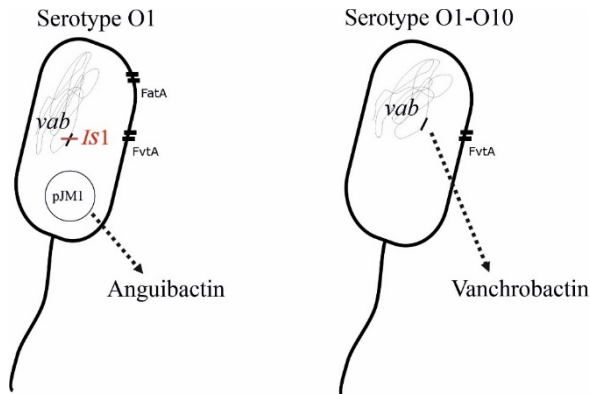


Figure I.7. Representation of the distribution of the vanchrobactin and anguibactin encoding genes. The *vab* genes are widespread among *V. anguillarum* serotypes O1-O10. In serotype O1 isolates that carry the plasmid pJM1, an insertion sequence inactivates the *vab* genes.

Vanchrobactin synthesis and transport functions are encoded by 13 genes that are clustered in a 26 kb chromosomal region (Figure I.8). The main biosynthetic functions are encoded by *vabABCE* which are involved in DHBA synthesis and activation (Figure I.11). *vabF* is the main biosynthetic gene, which encodes a NRPS responsible for the siderophore assembly (Balado *et al.*, 2006).

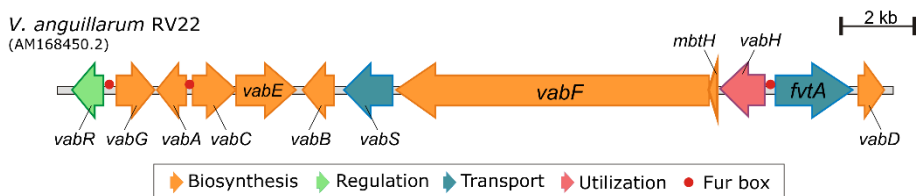


Figure I.8. Schematic representation of vanchrobactin gene cluster. Genes with related functions are represented with the same colour.

Upon synthesis, siderophores must be exported to complete its function as chelating agents, however the mechanisms behind this secretion process remain poorly studied. Two siderophore export systems have been described: an ATP-dependent efflux pump and a major facilitator superfamily protein (MFS) efflux pump (Li and Ma, 2017). Based on enterobactin export in *E. coli*, an export pathway has

been proposed for *V. anguillarum*. *vabS* would encode an MFS required for vanchrombactin export to the periplasm (Balado *et al.*, 2006) (Figure I.10).

After export to the extracellular environment, the ferri-siderophore complex must be internalized via specific outer membrane transporters by means of active transport. This process requires the TonB system (TonB dependent transporters, TBDT) (Nonaj *et al.*, 2010). Structurally, TBDTs are formed by a 22-stranded transmembrane β -barrel protein, which encloses a plug domain (Figure I.9). The plug domain is involved in ligand binding and acts as barrier to limit the access to the periplasm. At the N-terminus of this domain, the transporter contains the TonB box. When the ferri-siderophore complex binds to its cognate TBDT, a transduced signal is sent across the outer membrane and the TonB box suffers a rearrangement or unfolding which might lead to conformational changes in the extracellular loops, sequestering the ligand and allowing the interaction with the energy transducing system. The transduction system is composed by the periplasmic protein TonB and the inner membrane proteins ExbB and ExbD that acquire the energy from the proton motive force. The interaction between the periplasmic C-terminal domain of TonB and the TonB box in the TBDT induces conformational changes that allows the passage of the ferri-siderophore complex to the periplasmic space (Noinaj *et al.*, 2010).

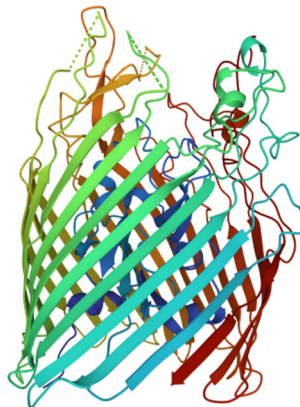


Figure I.9. Three-dimensional structure of the ferri-enterobactin receptor FepA from *Escherichia coli* (PDB ID: 1FEP).

Two TonB systems have been characterized in *V. anguillarum*, TonB1 and TonB2, however only TonB2 is essential for virulence (Stork *et al.*, 2004). The TonB2 complex is located at the inner membrane and is composed by TonB2, ExbB2, ExbD2 and TtpC (associated protein C). The TonB2 system plays a crucial role in ferri-vanchrobactin and xenosiderophores uptake (siderophores synthesized by other organisms). Ferri-vanchrobactin uptake is mediated by the outer membrane transporter FvtA, whose expression is dependent on the presence of the siderophore itself (Balado *et al.*, 2008; Balado *et al.*, 2009). In *V. anguillarum* RV22, the deletion of *fvtA* gene, encoding the outer membrane transporter, impairs the internalization of the ferri-siderophore complex and leads to a decrease in growth ability under iron-limiting conditions (Balado *et al.*, 2009). Besides FvtA, the uptake of xenosiderophores in *V. anguillarum* is accomplished through the transporter FetA (Figure I.10) (Naka and Crosa, 2012).

When in the periplasmic space, the ferri-vanchrobactin complex is anchored to the periplasmic protein FvtB and the complex is delivered to the cytoplasm through the ABC transporter, FvtCDE. This transporter is essential for ferri-vanchrobactin and ferri-xenosiderophores import (Figure I.10). (Naka *et al.*, 2013).

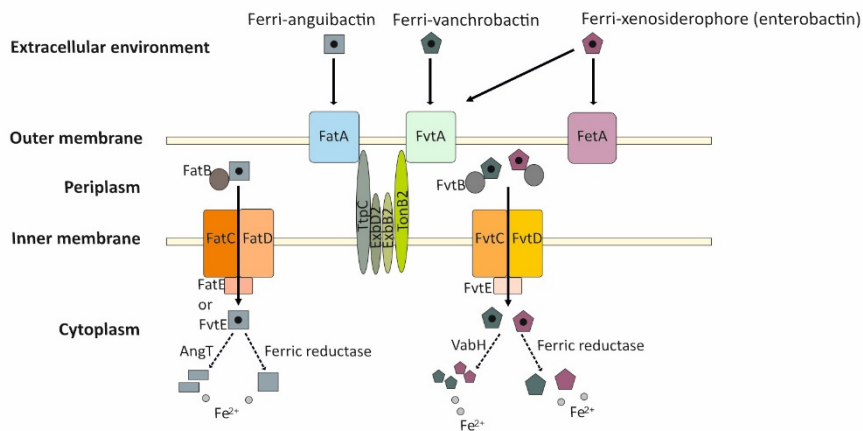


Figure I.10. Schematic representation of anguibactin and vanchrobactin siderophore systems.

Once in the cytoplasm, Fe^{3+} must be released from the ferri-siderophore complex to be used by the cell. Different strategies have

been reported for iron release: reduction of ferric iron and/or degradation/modification of siderophores (Figure I.10). Homology studies revealed that *vabH* encodes a probable cytoplasmic esterase, a Fes (ferric-enterobactin esterase) orthologue that is involved in enterobactin hydrolyzation during iron release (Brickman and McIntosh, 1992). *vabH* deletion impairs the growth of *V. anguillarum* under iron deficient conditions, although the production of the siderophore is not affected (Balado *et al.*, 2006). Additionally, a ferric reductase has been identified in *V. anguillarum* strains. This reductase is NADPH-dependent and shows high homology to *E. coli* siderophore-interacting protein (SIP) (Miethke *et al.*, 2011; Li *et al.*, 2015).

To date, the role of vanchrobactin in virulence of *V. anguillarum* RV22 has not been assayed in experimental challenges.

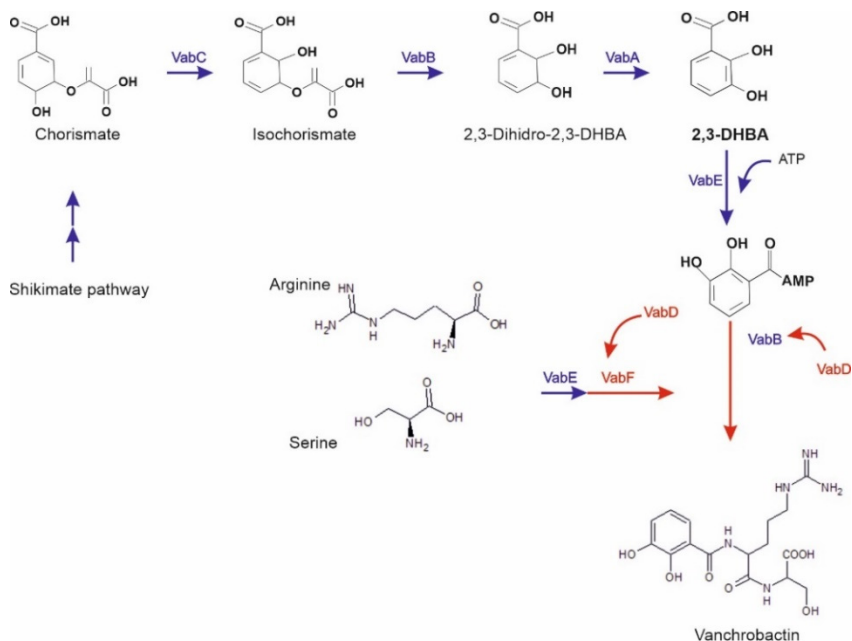


Figure I.11. Schematic representation of vanchrobactin biosynthetic pathway.

3.2. Evidence for a third siderophore in *V. anguillarum*

The genes involved in vanchrobactin synthesis and transport were characterized in the highly virulent strain *V. anguillarum* RV22 (Balado

et al., 2006). *V. anguillarum* RV22 is a serotype O2a strain that was isolated during a vibriosis outbreak affecting turbot in the Atlantic coast of northwest Spain (Toranzo *et al.*, 1987). After the vanchrobactin system inactivation, the resultant mutant strains showed an inability to grow in iron deficient conditions since apparently, they were impaired for siderophore synthesis (Balado *et al.*, 2006). However, the *V. anguillarum* RV22 $\Delta vabF$ mutant showed an intriguing phenotype. While siderophore production seemed disabled when *V. anguillarum* was cultivated at 25 °C, a residual siderophore production was still detected in CAS plates after growing the cells for longer periods at 15 °C (Figure I.12). *V. anguillarum* RV22 $\Delta vabF$ mutant does not produce vanchrobactin since it lacks the NRPS essential to assemble the siderophore from its constituents: 2,3-dihydroxybenzoic acid (DHBA), serine and arginine (Figure I.11). However, the synthesis of the catechol iron-chelating group (DHBA) was still accomplished and, thus, the observed phenotype in CAS plates was associated to the accumulation of this metabolite, since DHBA can retain a weak siderophore activity (Balado *et al.*, 2008).

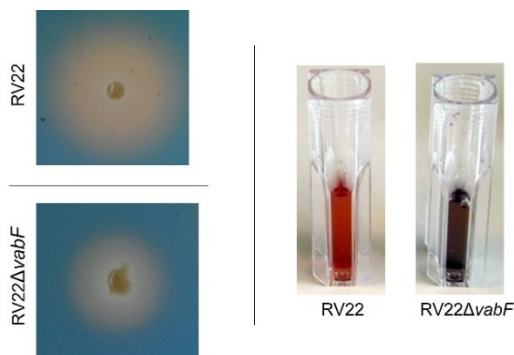


Figure I.12. Siderophore production in CAS Agar and CAS liquid assays of *V. anguillarum* RV22 wild-type and *vabF* mutant impaired for the synthesis of vanchrobactin.

Naka and colleagues sequenced the genome of *V. anguillarum* RV22 strain (Naka *et al.*, 2011) and the *in silico* analysis revealed the presence of a gene cluster that showed high homology to the piscibactin siderophore system. Piscibactin was firstly identified in *P. damselae*

subsp. *piscicida* (Souto *et al.*, 2012) and it is considered one of the most relevant virulence factors of this fish pathogen (Osorio *et al.*, 2015). In *P. damsela* subsp. *piscicida*, the functions related to synthesis and transport of piscibactin are encoded in a pathogenicity island located in a 69 kb conjugative plasmid, named pPHDP70 (Osorio *et al.*, 2015). This pathogenicity island resembles the HPI of *Yersinia* spp. and *E. coli* pathogenic strains encoding the siderophore yersiniabactin (Pelludat *et al.*, 1998; Osorio *et al.*, 2006; Souto *et al.*, 2012). The conjugative plasmid pPHDP70 was transmissible from *P. damsela* subsp. *piscicida* DI21 to *E. coli*, *Aeromonas salmonicida*, *V. anguillarum* and *V. alginolyticus*. When transferred to a *V. alginolyticus* strain impaired for vibrioferrin synthesis, it conferred this bacterium the ability to synthesize and use piscibactin as iron source (Osorio *et al.*, 2015).

The pathogenicity island encoding the piscibactin system shows a high homology to the high pathogenicity island present in *Yersinia* spp. that encodes the siderophore yersiniabactin (Dreschel *et al.*, 1995). *In silico* analysis of the protein sequence suggested that piscibactin is synthesized by a hybrid NRPS/PKS mechanism like the one described for yersiniabactin. However, the distinct domain organization indicates that piscibactin presents a different structure (Miller and Walsh, 2001; Miller *et al.*, 2002). Therefore, a biosynthetic pathway was proposed for piscibactin based on genetic data and on the pathway previously described for yersiniabactin (Souto *et al.*, 2012). Interestingly, the structure detected at the end of the purification process did not correspond to the terminal piscibactin molecule predicted based on the NRPS domain organization. In fact, the metabolite identified, is the result of the early release of the siderophore at module 5 (Souto *et al.*, 2012). Nonetheless, most detailed aspects of piscibactin synthesis and transport remain unknown since the construction of defective mutants in *P. damsela* subsp. *piscicida* is very difficult to accomplish due to the refractory nature of this bacterium to genetic manipulation. The presence of *irp* genes and the phenotype of the *vabF* mutant greatly suggest that *V. anguillarum* RV22, besides producing vanchrobactin, might synthesize, under specific growth conditions, piscibactin or a piscibactin-like siderophore. Thus, the identification of piscibactin as a

siderophore produced by *V. anguillarum* will be the main goal of this thesis.

4. KEY SIGNALS IN VIRULENCE FACTORS REGULATION

As an inhabitant of the marine and estuarine ecosystem, *V. anguillarum* must be able to adapt its physiology to the constantly changing aquatic environment. Fluctuations in salinity, nutrients availability and temperature are a constant trait of marine bacteria. Iron is essential for the bacterial metabolism, however when in excess it can be lethal. When intracellularly, iron that is free can be a catalyst for Haber-Weiss reactions and participate in Fenton reactions, generating toxic hydroxyl radicals (Kehrer, 2000; Touati, 2000). These hydroxyl radicals can then damage DNA, unsaturated lipids, and proteins (Imlay and Linn, 1988) thus when in excess, bacteria repress the iron uptake systems. A tight coordination and regulation must be achieved for the iron concentration to meet but not exceed the requirement for the metabolism. In *V. anguillarum* several regulation mechanisms have been described to date, however the master regulator of iron related genes is the negative regulator Fur.

Fur (Ferric uptake regulator) is the major regulator of iron metabolism and transport, and most virulence-related genes (Ratledge and Dover, 2000). It was firstly identified in *E. coli* as a sensor of intracellular iron concentration and it functions as an iron-binding transcriptional regulator (Litwin and Calderwood, 1994). In the presence of free/excess Fe^{2+} , Fur binds it, forming an iron-Fur complex that attaches to specific sites in the promoter region of iron regulated genes. These sites are termed Fur-boxes and a 21bp palindromic sequence has been identified (Balado *et al.*, 2008; Davies *et al.*, 2011). Although the Fur boxes are usually located in the -10 and -35 regions of promoters (Payne *et al.*, 2016), the location of the Fur box with respect to the transcription initiation site has been found to be variable (Davies *et al.*, 2011). When the Fe^{2+} -Fur complexes bind to these sites, the transcription is blocked leading to the down-regulation of those promoters containing Fur box motifs (Troxell and Hassan, 2013). Under iron limiting environments, Fur detaches from Fe^{2+} , being unable to bind to the Fur boxes, allowing the expression of genes for iron uptake.

In *V. anguillarum*, Fur regulates the expression of both siderophore systems, being involved in the blockage or derepression of genes encoding anguibactin and vanchrobactin synthesis and transport (Tolmasky *et al.*, 1994; Chen and Crosa, 1996; Chai *et al.*, 1998; Balado *et al.*, 2008).

Regarding the iron uptake system mediated by the siderophore vanchrobactin, a LysR-type transcriptional regulator (VabR) has been identified. Analysis of VabR revealed that its N-terminal domain bears a helix-turn-helix DNA binding motif. *vabR* encodes a regulatory factor that induces the expression of *vabG*, a biosynthetic gene involved in DHBA synthesis (Balado *et al.*, 2008). Vanchrobactin also plays an inducing role, when added exogenously it induces the expression of the biosynthetic genes. This effect is concentration dependent as increasing amounts of vanchrobactin lead to a linear increase in transcriptional activity of *fvfA* promoter (Balado *et al.*, 2008).

In addition to iron availability, other factors including quorum sensing, carbon sources, availability of oxygen, pH and temperature have been identified as signals that can modulate the expression of virulent factors including iron uptake systems (Carpenter and Payne, 2014; Payne *et al.*, 2016). The effect of temperature changes has been extensively studied in pathogens that infect mammals. The transcription of virulence factors is induced upon contact with the host which leads to a temperature shift from the environmental temperature to a higher temperature, 37 °C (Guijarro *et al.*, 2015). Usually, the host temperature is the optimal temperature for pathogens growth. Most of the mechanisms involved in temperature shift sensing are related to conformational changes in DNA, RNA, or in proteins (Konkel and Tilly, 2000). H-NS is a conserved repressor of virulence related genes with DNA and RNA binding activity (Stoebel *et al.*, 2008). At temperatures below 37 °C, H-NS binds to AT-rich DNA regions forming DNA-protein-DNA bridges blocking the movement of the RNA polymerase. When entering the host, the temperature rises to 37 °C which is the cue for the derepression. H-NS is released from the DNA, allowing the activation by transcriptional regulators and consequent expression of virulence genes (Guijarro *et al.*, 2015). The gene silence effect of H-NS is of particular importance in

Enterobacteriaceae as it regulates the expression of *virF* in *Shigella flexneri* (Falconi *et al.*, 1998) or *ssrB* in *Samonella enterica* (Fass and Groisman, 2009). Notably, H-NS and ToxR share part of their regulatory network in *V. cholerae* and ToxR antagonizes H-NS binding at shared promoter sites (Kazi *et al.*, 2016). ToxR is a global regulator of genome encoded genes as well as horizontal acquired DNA. It is the initiator of a regulatory cascade involved in the expression of major virulence factors, the cholerae toxin and the coregulated pili (Childers and Klose, 2007; Kazi *et al.*, 2016). For its optimal transcriptional activation, ToxR interacts with the transmembrane protein ToxS, which stabilizes its structure for correct functioning (DiRita and Mekalanos, 1991; Pfau and Taylor, 1998). ToxR expression is modulated by environmental cues such as pH, oxygen, temperature, and presence of concrete metabolites (Kazi *et al.*, 2016). It can directly induce the expression of virulence related genes or mediate their control through the AraC-like transcriptional regulator, ToxT (Higgins and DiRita, 1994).

Fish diseases outbreaks usually occur at a temperature below that of the optimal (TBO) growth of the pathogen. The regulation of virulence factors at TBO is different from those pathogens of warm-blood animals (Guijarro *et al.*, 2015). Several virulence genes have been identified as being induced at TBO, but the regulatory mechanisms are uncharacterized. In *Yersinia ruckeri*, the etiological agent of the enteric red mouth disease, several virulence factors are preferentially expressed at 18 °C than at the optimal bacterial growth temperature of 28 °C. In this pathogen, the operon that encodes the type IV secretion system, the haemolysin YhlA, the protease Yrp1 and the siderophore ruckerbactin have higher expression levels at 18 °C. *Vibrio salmonicida* causes disease in a temperature range of 10-20 °C and virulence factors such as biofilm formation or siderophore production are favoured at low temperatures (Guijarro *et al.*, 2015).

As an eurythermal bacterium, *V. anguillarum* can grow in a wide range of temperatures, from 10 to 42 °C being 25 °C considered its optimal growth temperature (Guérrin-Faubleé *et al.*, 1995). The water temperature is a factor that can directly enhance the occurrence of vibriosis (Le Roux *et al.*, 2015). Moreover, *V. anguillarum* is able to

produce disease outbreaks in a wide temperature range since it can infect cold- and warm-water farmed fish (Bellos *et al.*, 2015; Toranzo *et al.*, 2017; Ma *et al.*, 2017). Notably, the vibriosis outbreaks caused by *V. anguillarum* can occur at temperatures as low as 5 °C, being 15 °C the optimal temperature to cause vibriosis (Olafsen *et al.*, 1981; Austin and Austin, 2007; Bellos *et al.*, 2015). More recently, Lone Gram group showed that some *V. anguillarum* strains can produce 100% mortalities in infection challenges in cod (*Gadus morhua*), halibut (*Hippoglossus hippoglossus*) and turbot (*Scophthalmus maximus*) (Rønneseth *et al.*, 2017). Since these challenges were performed at 7, 9 and 16 °C respectively, the results suggest that some highly virulent *V. anguillarum* strains can cause high mortality ratios at temperatures that are below the optimal growth temperature and, thus, the adaptation to low temperatures should be considered in the regulation of virulence-related genes. These adaptations and the effect of temperature on expression of genes involved in siderophore synthesis and transport will be also studied in this thesis.

II. OBJECTIVES

II. OBJECTIVES

Two siderophore systems have been characterized in *V. anguillarum*: anguibactin, encoded by the pJM1 plasmid, and vanchrobactin, encoded by chromosomal genes. However, the presence in certain strains of *V. anguillarum* of genes with homology to *irp* genes encoding the siderophore piscibactin, as well as previous phenotypic evidence, suggest that piscibactin could be also produced by *V. anguillarum*. In addition, since *V. anguillarum* can infect diverse fish species living at very different temperatures, we hypothesized that a temperature-dependent regulation of virulence factors could play a relevant role in *V. anguillarum* versatility to cause disease.

Therefore, the main goals of the present thesis are:

1. Analyse the adaptations of *V. anguillarum* to low-iron availability and temperature changes that enable it to cause vibriosis in a wide diversity of fish species.
2. Characterize the genetic structure and regulation of the High-Pathogenicity Island encoding the siderophore piscibactin in *V. anguillarum*.
3. Determine the role of piscibactin in *V. anguillarum* virulence for fish.
4. Evaluate the use of FrpA and FvtA, the piscibactin and vanchrobactin outer membrane transporters, respectively, to design new strategies to prevent and control vibriosis in fish.

III. MATERIAL AND METHODS

III. MATERIAL AND METHODS

1. BACTERIAL STRAINS, PLASMIDS AND GROWTH CONDITIONS

The bacterial strains and plasmids used in this work are listed in Table III.1. *V. anguillarum* strains were grown routinely in Tryptic Soy Agar or broth supplemented until 1% of NaCl (TSA-1 or TSB-1) (Condalab). *Escherichia coli* strains were grown in Luria Bertani (LB) (Condalab). When required the media was supplemented with antibiotics at the following final concentrations: Ampicillin (Amp) 100 µg/mL or 60 µg/mL (stock solution in water at 100 mg/mL) (Fisher BioReagents), Kanamycin (Kan) at 50 µg/mL (stock solution in water at 50 mg/mL) (Sigma-Aldrich), Gentamycin (Gm) at 12 µg/mL (stock solution in water at 12 mg/mL) (NZYTech) and Rifampicin (Rif) at 50 µg/mL (stock solution in DMSO at 25 mg/mL) (Sigma-Aldrich). Bacterial strains stocks were stored at -80 °C in LB or TSB-1 with 32% (v/v) glycerol.

Growth assays under different iron availabilities were performed in CM9 minimal medium. CM9 contains: 6 g/L Na₂HPO₄, 3 g/L KH₂PO₄, 5 g/L NaCl, 1 g/L NH₄Cl, 1,47 mg/L CaCl₂, 12,04 mg/L MgSO₄, 0,5% glucose and 0,2% casamino acids pH 7.2 (Lemos *et al.*, 1988). To achieve iron limitation the chelating agents 2,2'-dipyridyl (TCI) or etilendiamine-di(*o*-hidroxifenil-acetic) acid (EDDHA) (Sigma-Aldrich) were added at the suitable concentrations.

Table III.1. Strains and plasmids used in this work (Kan^r, kanamycin resistance, Gm^r, gentamycin resistance, Amp^r, ampicillin resistance, Rif^r, rifampicin resistance).

Strain	Relevant characteristics	Source
<i>V. anguillarum</i>		
RV22	Wild-type serotype O2 strain isolated from diseased turbot (Spain), vanchrobactin and piscibactin producer, Amp ^r	Toranzo <i>et al.</i> , 1987
MB14	RV22 with in-frame deletion of <i>vabF</i> gene, piscibactin producer, Amp ^r	Balado <i>et al.</i> , 2006
MB67	RV22 with in-frame deletion of <i>vabD</i> gene, non-siderophore producer, Amp ^r	Balado <i>et al.</i> , 2008
MB280	RV22 with in-frame deletion of <i>irp1</i> gene, Amp ^r	This study
MB203	RV22 with in-frame deletion of <i>vabF</i> and <i>irp1</i> genes, Amp ^r	This study
MB299	MB203 carrying pPHDP70::Kan, Amp ^r Kan ^r	This study
ML208	RV22 with in-frame deletion of <i>vabF</i> and <i>frpA</i> genes, Amp ^r	This study
ML210	RV22 with in-frame deletion of <i>vabD</i> and <i>frpA</i> genes, Amp ^r	This study
ML168	RV22 with in-frame deletion of <i>vabF</i> and <i>araC1</i> genes, Amp ^r	This study
ML136	RV22 with in-frame deletion of <i>vabF</i> and <i>araC2</i> genes, Amp ^r	This study
ML293	RV22 with in-frame deletion of <i>vabF</i> and <i>h-ns</i> genes, Amp ^r	This study
ML270	RV22 with in-frame deletion of <i>vabF</i> and <i>toxR-5</i> genes, Amp ^r	This study
ML178	RV22 with in-frame deletion of <i>vabF</i> and <i>irp4</i> genes, Amp ^r	This study
ML772	RV22 with in-frame deletion of <i>vabF</i> and <i>irp8</i> genes, Amp ^r	This study
ML886	RV22 with in-frame deletion of <i>vabF</i> and <i>frpBC</i> genes, Amp ^r	This study
<i>Photobacterium damsela</i> subsp. <i>piscicida</i>		
DI21	Piscibactin producer strain (<i>irp</i> ⁺), Rif ^r	Toranzo <i>et al.</i> , 1991
AR84	DI21 cured of plasmid pPHDP70 (<i>irp</i> ⁻), non-piscibactin producer	Osorio <i>et al.</i> , 2015
<i>Escherichia coli</i>		
DH5α	Cloning strain	Laboratory strain
S17-1- λpir	RP4 (Kan::Tn7, Tc::Mu-1) <i>pro-82 λpir recA1 end A1 thiE1 hsdR17 creC510</i>	Herrero <i>et al.</i> , 1990
Plasmids		
pWKS30	Low-copy cloning vector, Amp ^r	Wang and Kushner, 1991
pNidKan	Suicide vector derived from pCVD442, Kan ^r	Mouriño <i>et al.</i> , 2004

pHRP309	Low-copy <i>lacZ</i> reporter plasmid, <i>mob</i> Gm ^r	Parales and Harwood, 1993
pSEVA651	Low-copy plasmid, <i>mob</i> Gm ^r	Martinez-Garcia, 2020
pPHDP70:: Kan	pPHDP70 with Kan ^r gene inserted, contains all necessary genes for piscibactin synthesis	Osorio <i>et al.</i> , 2015
pML119	pNidKan harbouring the construction for <i>araC2</i> deletion, Kan ^r	This study
pML141	pNidKan harbouring the construction for <i>araC1</i> deletion, Kan ^r	This study
pML144	pNidKan harbouring the construction for <i>irp4</i> deletion, Kan ^r	This study
pML187	pNidKan harbouring the construction for <i>frpA</i> deletion, Kan ^r	This study
pML254	pNidKan harbouring the construction for <i>toxR-S</i> deletion, Kan ^r	This study
pML282	pNidKan harbouring the construction for <i>h-ns</i> deletion, Kan ^r	This study
pML736	pNidKan harbouring the construction for <i>irp8</i> deletion, Kan ^r	This study
pML882	pNidKan harbouring the construction for <i>frpBC</i> deletion, Kan ^r	This study
pML519	pNidKan harbouring a functional version of <i>irp4</i> , Kan ^r	This study
pML777	pNidKan harbouring a functional version of <i>toxR-S</i> , Kan ^r	This study
pML796	pNidKan harbouring a functional version of <i>h-ns</i> , Kan ^r	This study
pML247	pSEVA651 harbouring a functional version of <i>araC1</i> , Gm ^r	This study
pML257	pSEVA651 harbouring a functional version of <i>frpA</i> , Gm ^r	This study
pMB12	<i>vabH</i> promoter fused to promoterless <i>lacZ</i> gene in pHRP309, Gm ^r	Balado <i>et al.</i> , 2008
pMB276	<i>frpA</i> promoter (<i>PfrpA</i>) fused to promoterless <i>lacZ</i> gene in pHRP309, Gm ^r	This study
pMB277	<i>araC1</i> promoter (<i>ParaC1</i>) fused to promoterless <i>lacZ</i> gene in pHRP309, Gm ^r	This study
pML212	<i>frpBC</i> promoter (<i>PfrpBC</i>) fused to promoterless <i>lacZ</i> gene in pHRP309, Gm ^r	This study
pML214	<i>araC2</i> promoter (<i>ParaC2</i>) fused to promoterless <i>lacZ</i> gene in pHRP309, Gm ^r	This study
pML258	<i>proC</i> promoter (<i>PproC</i>) fused to promoterless <i>lacZ</i> gene in pHRP309, Gm ^r	This study
pLP9	<i>frpA</i> promoter (<i>PfrpA_{pdp}</i>) fused to a promoterless <i>lacZ</i> gene in pHRP309, Gm ^r	This study
pLP28	<i>araC1</i> promoter (<i>ParaC1_{pdp}</i>) fused to a promoterless <i>lacZ</i> gene in pHRP309, Gm ^r	This study

2. DNA MANIPULATION AND CLONING

2.1. Genomic and plasmidic DNA extraction

Genomic DNA extraction was performed using the *Easy-DNA* Kit (Invitrogen). Plasmid DNA was extracted using the *GeneJET Plasmid Miniprep Kit* (Thermo Fisher Scientific). The extractions were performed following the manufacturer's instructions.

2.2. Polymerase chain reactions (PCR)

PCR reactions were carried out using the *NZYTaq II 2× Green Master Mix* (NZYTech), in a T100TM Thermal Cycler (Bio-Rad) in final volumes of 25 or 50 μ L. The *NZYTaq II 2× Green Master Mix* includes all the components needed for a PCR except for the specific primers and the DNA, i.e., Taq DNA polymerase, dNTPs, and the buffer necessary for the reactions. Primers were used to the final concentration of 0.1 μ M, elongation of the DNA chain was established as 1 min/kb and annealing temperatures were optimized for each primer set (from 52 °C to 58 °C) (Table III.2). PCR products were subjected to electrophoresis in an agarose gel (ranging from 1 to 2% depending on the size of the target fragment) in 1X TAE (40 mM Tris, 1 mM EDTA pH 8). RedsafeTM Nucleic Acid Staining Solution (iNtRON Biotechnology) was added to the solution for DNA detection. After running the gel, it was visualized in a transilluminator (Gelprinter Plus).

Table III.2. General parameters for PCR using the *NZYTaq II 2× Green Master Mix*.

PCR Parameters			
Cycle step	Temperature	Time	Number of cycles
Initial denaturation	95 °C	3 min	1
Denaturation	95 °C	30 s	30-35
Annealing	52-58 °C	30 s	
Extension	72 °C	1 min/kb	
Final Extension	72 °C	5 min	1

2.3. Cloning of DNA fragments

The desired fragment or insert was amplified by PCR and the plasmid vector was obtained through Miniprep. PCR products were loaded into a 1% agarose gel and the band obtained was cut and purified

using the *NucleoSpin Gel and PCR Clean-up Kit* (Macherey-Nagel). Both, purified PCR product (fragment) and plasmid DNA were digested with the same restriction enzymes (*FastDigest* from Thermo Scientific) to generate compatible ends. Additionally, the plasmid was dephosphorylated using *FastAP*TM Thermosensitive Alkaline Phosphatase (Thermo Fisher Scientific). The phosphatase eliminates phosphate groups at the 5' end which avoids the recircularization of the plasmids. After digestion the insert was cleaned using the phenol:chloroform method (Sambrook and Russell, 2006) and the plasmid was loaded in a 1% agarose gel to confirm the correct digestion and then purified. Then, insert and plasmid were mixed in a molar relation 5:1 with 1 U of T4 DNA Ligase (Thermo Fisher Scientific) in a final volume of 20 μ L. Ligations were incubated for at least 1 h at room temperature or overnight at 15 °C. Ligations were dialysed through 0.025 μ m MCE membrane filters (Millipore). After approximately 20 min the dialysed ligation was mixed with competent cells. Competent cells were obtained by growing *E. coli* DH5 α or S17-1- λ pir strains to mid exponential phase and pelleted through centrifugation at 4 °C, for 10 min at 8,000 rpm. Electrocompetent cells were centrifuged and washed two times with cold water and the final pellet was resuspended in 100 μ L of ultrapure water. For transformation, the previous mix was transferred to a 0.2 cm electroporation cuvette (Bio-Rad) and electroporated in a Gene Pulser electroporator (Bio-Rad). Electroporation was carried out with the following settings: 2.5 kv, 200 Ω and 25 μ F. The transformation was recovered with 1 mL LB and the cells were incubated at 37 °C with shaking at 120 rpm. After 1 h the transformed cells were pelleted by centrifugation, resuspended in 100 μ L of LB and plated onto LB plates supplemented with the suitable antibiotic.

2.4. Construction of mutant strains by allelic exchange

All the defective mutants used in this study were obtained by allelic exchange (Figure III.1). This technique is based on the substitution of the wild-type gene by a non-functional version that contains a deletion in the central region of the gene. Regions upstream and downstream of the gene of interest (including ca. 20 amino acids of each extreme of

the gene) were amplified by PCR. Restriction sites were added to each primer used for amplification, named as 1, 2, 3 and 4 (Table III.3) so that the correct orientation of the fragments is obtained. Both fragments corresponding to the upstream and downstream region of the gene were cloned into the low-copy number plasmid pWKS30 (Figure III.3) (Wang and Kushner, 1991). Then the construction was liberated from this plasmid through digestion with the enzymes *NotI* and *ApaI* and ligated into the suicide vector pNidKan (confers kanamycin resistance), digested with the same enzymes, and transformed into *E. coli* S17-1- λ *pir* competent cells (Mouriño *et al.*, 2004). pNidKan contains the *pir* dependent origin of replication and the *sacB* gene that confers sucrose sensitivity (Figure III.3). The construction was then mobilized to *V. anguillarum* strains RV22, RV22 Δ *vabF* or RV22 Δ *vabD* through conjugation on TSA-1 for 48 h at 25 °C. A first event of recombination occurred, and the cells were plated in 10-fold serial dilutions on TSA-1 plates supplemented with kanamycin and ampicillin.

The plasmid pNidKan is unable to replicate naturally in *V. anguillarum* as this bacterium lacks the *pir* gene, so it will only be maintained if it is integrated into the chromosome by homologous recombination with the wild-type gene. The first recombinant colonies, resistant to kanamycin and ampicillin, were grown in TSB-1 without selective pressure and after 5-10 consecutive passages, serial dilutions were plated onto LB plates supplemented with 15% sucrose. The plasmid confers sucrose sensitivity therefore only the cells that lost the plasmid will grow. This second event of recombination will generate a 50% of bacterial cells that will remain with the wild-type gene and 50% that will have a deleted copy in the chromosome. The cells that grew in sucrose plates were subjected to PCR to evaluate if they contained the mutated version of the gene. Therefore, the primers 1 and 4 were used to amplify the desired region (Table III.3). A PCR product of approximately 2 kb is an indicative of the deleted site as the revertant bacteria will amplify a larger region correspondent to the wild-type gene. The region subjected to the deletion was Sanger sequenced using primers 1 and 4 to verify that deletions were nonpolar.

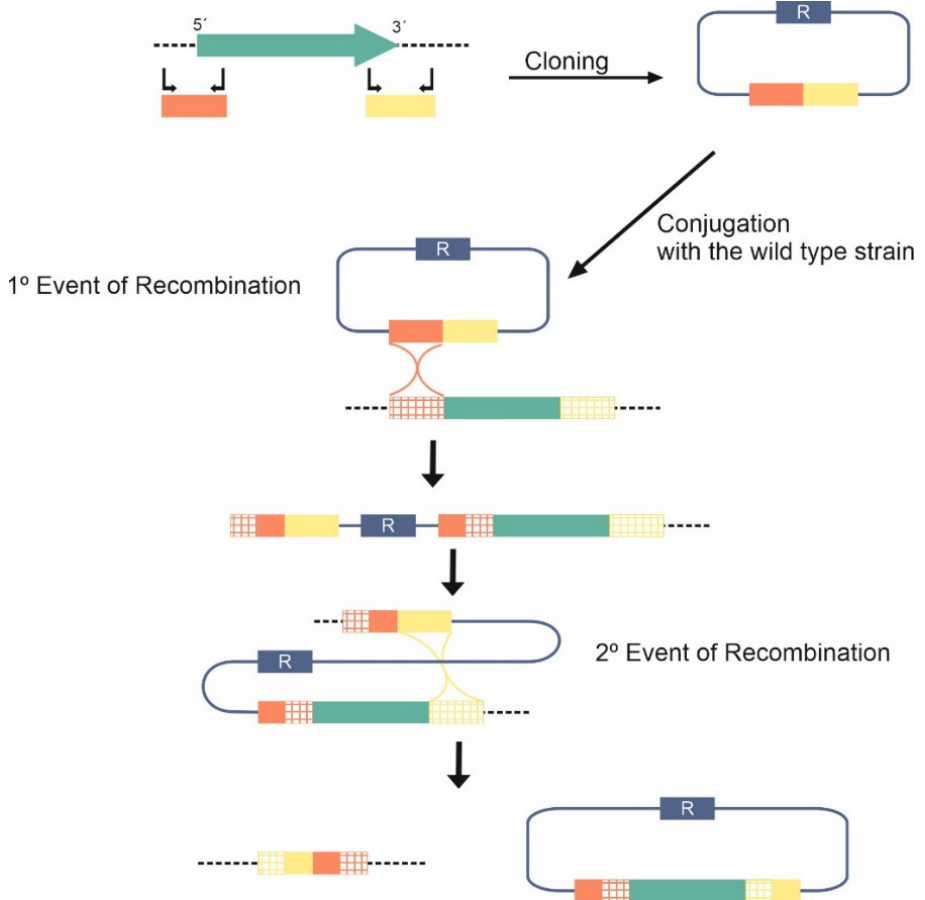


Figure III.1. Schematic representation of mutagenesis by allelic exchange. Upstream and downstream regions of the target gene were amplified by PCR and cloned into the suicide vector pNidKan. The resultant plasmid was introduced into *V. anguillarum* through conjugation and the transconjugants were selected based on the strain and plasmid resistance. The integration of the mutated version of the gene into the chromosome of *V. anguillarum* was accomplished through consecutive passages in non-selective media. This second event of recombination leads to the liberation of the wild-type gene in the plasmid and the generation of mutant strains.

Table III.3. Primers used for the construction of mutant strains by allelic exchange. Restriction sites are underlined in the primers sequence.

Oligonucleotide (5' -> 3')	Size (bp)
<i>irp1</i> mutant construction	
irp1_ang_1_XbaI*	1489
irp1_ang_2_BamHI	
irp1_ang_3_BamHI	1360
irp1_ang_4_EcoRI*	
<i>araC1</i> mutant construction	
AraC1_1_EcoRI*	927
AraC1_2_BamHI	
AraC1_3_BamHI	945
AraC1_4_XbaI*	
<i>araC2</i> mutant construction	
AraC2_1_EcoRI*	903
AraC2_2_BamHI	
AraC2_3_BamHI	954
AraC2_4_XbaI*	
<i>frpA</i> mutant construction	
1_FrpAang_XbaI*	750
2_FrpAang_BamHI	
3_FrpAang_BamHI	750
4_FrpAang_4_XhoI*	
<i>irp4</i> mutant construction	
1_Irp4ang_XbaI*	716
2_Irp4ang_PstI	
3_Irp4ang_PstI	861
4_Irp4ang_XhoI*	
<i>irp8</i> mutant construction	
1_Irp8_F_XbaI*	824
2_Irp8_R_BamHI	

3_Irp8_F_BamHI	CCGGGATCCCTGCTGACATTCTCCGTTAC	819
4_Irp8_R_XhoI*	GCCCTCGAGCATGGCTTGTTTCAGCGTCAT	
frpBC mutant construction		
1_FrpBC_R_NotI*	CCGGCGGCCGCTCTCAGCACGTGGAAAGCGA	1320
2_FrpBC_PstI_F	GGCCTGCAGGCTGCGCAGTTTATCCATTC	
3_FrpBC_PstI_R	CCGCTGCAGGCGCCTATCTTACTGCTTGA	995
4_FrpBC_KpnI_F*	GCCGGTACCGACCAATATCTCACCGTGAC	
h-ns mutant construction		
1_HNS_F_XbaI*	CGCTCTAGAGCGCCTAATACAATACCGA	888
2_HNS_R_BamHI	GCGGGATCCAGCGCTAGGCTACGAATAT	
3_HNS_F_BamHI	CCGGGATCCCAAGAGCAACTTGATGCAGG	800
4_HNS_R_XhoI*	GGCCTCGAGCCAATGCCAGAGGCAACAAT	
toxR-S mutant construction		
1_ToxR_F_XbaI*	CCGTCTAGAAGCGCGAGTTCCTTACAGTGA	746
2_ToxR_R_PstI	GCGCTGCAGCGTGAATCGGTAGCAAGGA	
3_ToxS_F_PstI	GGCCTGCAGGTCGACGTATTGATGTGCTC	626
4_ToxS_R_XhoI*	GCCCTCGAGGCGCAAGGTCAAGATGATGT	

* Primers used to verify the construction of mutants.

2.5. Complementation of mutant strains

The re-introduction of the wild-type gene would confirm that the phenotype of the mutant strains was the result of the deletion of a specific gene and not caused by mutations elsewhere in the bacterial genome as the mutant strains recover the parental phenotype. The plasmid pSEVA651 (Martínez-García *et al.*, 2020) was used to complement the allelic exchange mutants (Figure III.2). The entire gene and its promoter region were amplified by PCR and cloned into the vector. The amplification of the promoter region will ensure the expression of the gene as this plasmid does not bear a promoter. Restriction sites were added to the primers. Then, PCR product and plasmid were digested with the same enzymes to originate complementary ends (Table III.4). The plasmid and the gene to complement were transformed into *E. coli* S17-1- λ pir and plated onto LB plates supplemented with gentamycin. The colonies that carry the

plasmid with the gene to complement were mobilized by conjugation to the correspondent mutant strain. After 48 h at 25 °C the complemented cells were selected based on gentamycin and ampicillin resistance. The presence of the plasmid in *V. anguillarum* mutants was confirmed by PCR.

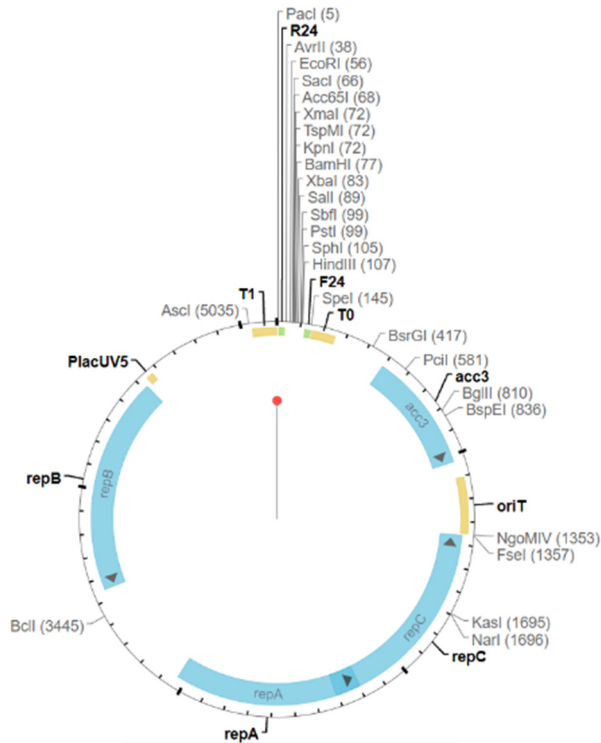


Figure III.2. pSEVA651 plasmid map. The plasmid harbours a resistant gene that allows the selection of strains that harbour the plasmid. This plasmid was used for the complementation of mutant strains.

Reversion to the wild type of *irp4*, *h-ns* and *toxR-S* mutants was accomplished by allelic exchange. To this purpose the complete wild type genes and flanking regions were PCR amplified using primers listed in Table III.4 and cloned in pCar109. Reintroduction of wild type genes and selection of the double recombination events was made as previously detailed (Figure III.1). After sucrose selection, bacteria were subjected to PCR with the same primer set to evaluate if they contained the wild-type or the mutated version of the gene. Therefore, the

complemented strains would bear a copy of the wild-type gene in the chromosome.

Table III.4. Primers used for the complementation of the mutant strains obtained through allelic exchange. Restriction sites are underlined in primers sequence.

Oligonucleotide (5' -> 3')	Size (bp)
<i>araC1</i>	
AraC1_comp_F_XbaI	1537
AraC1_comp_R_BamHI	
<i>frpA</i>	
1_FrpAang_comp_F_XbaI	2570
2_FrpAang_comp_R_BamHI	
<i>irp4</i>	
irp4_comp_F_NotI	2511
irp4_comp_R_ApaI	
<i>h-ns</i>	
HNS_comp_F_NotI	1329
HNS_comp_R_ApaI	
<i>toxR-S</i>	
ToxR-S_comp_F_NotI	2101
ToxR-S_comp_R_ApaI	

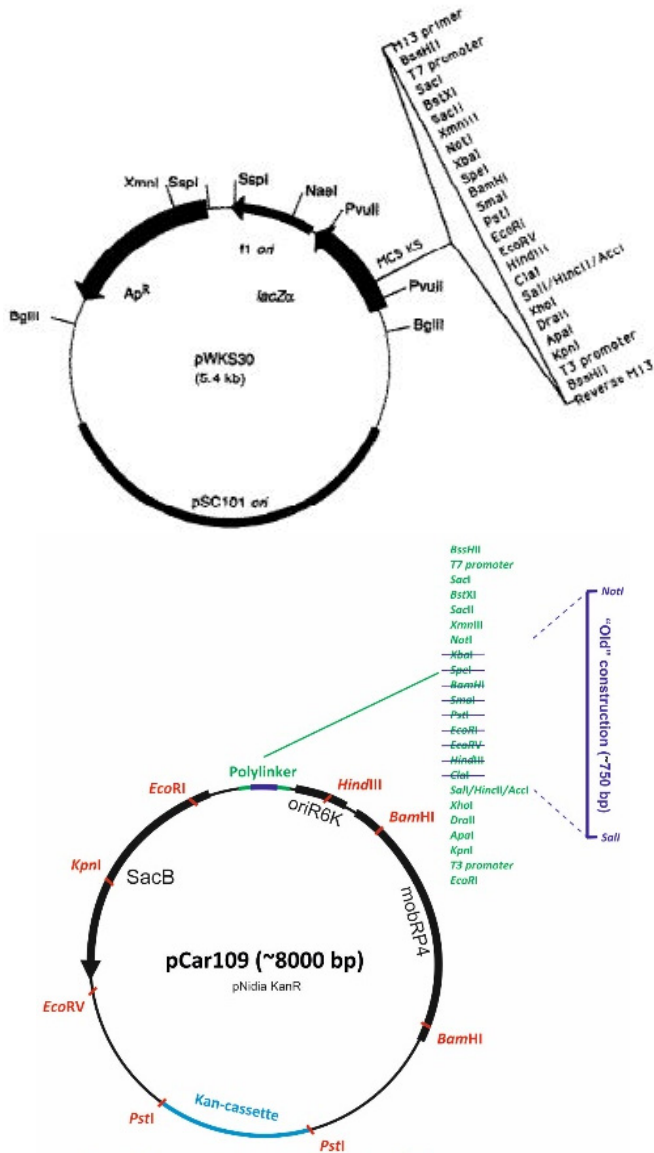


Figure III.3. pWKS30 and pCar109 (pNidKan) plasmids map. The low-copy plasmid pWKS30 harbours an ampicillin resistance gene. The pNidKan confers kanamycin resistance and the plasmid also harbours the sucrose sensitivity gene *sacB* and the *pir*-dependent origin of replication, *oriR6K*. Both plasmids were used for cloning. For the complementation of mutant strains, the wild-type gene was directly cloned into pNidKan.

3. RNA ANALYSIS

3.1. RNA purification and RT-PCR

The organization of *irp*-HPI was studied by reverse transcription PCR. *V. anguillarum* RV22 strain was grown in CM9 minimal medium supplemented with 5 μ M EDDHA or 10 μ M Fe₂(SO)₄ until OD₆₀₀ = 1.0. Cells were pelleted by centrifugation at 10,000 g for 10 min and total RNA was isolated with RNAwiz (Ambion) following the manufacturer's instructions. Reverse transcription reactions were performed with reverse transcriptase M-MLV RT (Invitrogen) using 1 μ g RNA pre-treated with RQ1 RNase-Free DNase (Promega). Primers used are listed in Table III.5. cDNA was obtained by amplification using a primer located at the 3'-end of *irp5* (Table III.5). This cDNA was then the template for a subsequent PCR reaction to ensure that the genes were co-transcribed using specific primers for *araC1* (PCR1). A negative control was performed using total RNA treated with DNase to confirm a possible contamination of the sample with genomic DNA. A PCR reaction using 100 ng of genomic DNA as template was used as a positive control.

Table III.5. Primers used to study the *irp*-HPI gene organization by RT-PCR.
RT-PCR experiments Size (bp)

RT	TTTGGAGATGAGTGCGACAC	
PCR1		
araC1_F	GATATGCGCTTTGACTGCCA	196
araC1_R	CTGTGAGACGGCATAACAAGC	

3.2. RNA sequencing

3.2.1. Growth conditions and total RNA extraction

V. anguillarum strain RV22 was grown in CM9 minimal medium (Lemos *et al.*, 1988) under different iron availabilities, iron limited conditions (50 μ M 2,2'-dipyridyl) and iron excess (10 μ M FeCl₃) at 25 °C or 15 °C. Bacterial cultures were grown until mid-exponential phase (OD₆₀₀ \approx 0.8) and the cells were harvested by centrifugation at 10,000 g for 10 min. Total RNA was isolated with RNAwiz (Ambion)

following the manufacturer's instructions. RNA was isolated from three independent experiments for each condition. RNA integrity was observed in a 1% agarose gel and the concentration was checked using the RNA 6000 Nano kit on the Bioanalyzer 2100 (Agilent Technologies, Palo Alto, CA). RNA was stored at -80 °C until further use.

3.2.2. cDNA library construction and sequencing

Construction of cDNA libraries and Illumina Sequencing was outsourced to FISABIO Sequencing and Bioinformatics Service (Valencia, Spain). Before the construction of independent cDNA libraries for whole-transcriptome sequencing, residual DNA and rRNA contamination was eliminated. An independent cDNA library represented each of the biological replicates and consisted of ca. of 20 M of 2 x 150 bp reads. Massive sequencing was performed in an Illumina Miseq using an NextSeq High Output 1 x 150 bp kit. RNAseq reads were deposited at NCBI Sequence Read Archive (accession number SRP213600).

3.2.3. Bioinformatic analysis and gene expression quantification

RNAseq data were analysed using the *Tuxedo* suite software programs (Ghosh and Chan, 2016). *Tophat* granted the alignment of the reads with *V. anguillarum* RV22 strain chromosome I and II (GenBank accession number GCA_000257185.1). Furthermore, *Cufflinks* assembled the mapped reads into possible transcripts to create a transcriptome assembly. Differentially expressed genes and transcripts were identified using *Cuffdiff*. The data obtained from *Cuffdiff* was analysed using the R package *CummeRbund* generating quality plots and figures. Finally, *Blast2GO* performed the functional annotation, enzyme code mapping and pathway analysis. Differentially expressed genes functional classification was obtained by COG database and KEGG and PSORTb v 3.0 was used for subcellular prediction (Yu *et al.*, 2010).

4. LACZ TRANSCRIPTIONAL FUSIONS AND β -GALACTOSIDASE ASSAYS

DNA fragments corresponding to the promoter regions of *V. anguillarum* RV22 strain *araC1* (renamed to *pbtA*), *araC2* (renamed to *pbtB*), *frpA*, *frpBC* and the house-keeping gene *proC* and *Photobacterium damsela* subsp. *piscicida* *araC1* and *frpA* were amplified by PCR (Table III.6). These fragments correspond to regions located upstream of the starting codon of each gene and the first nucleotides of the genes. These putative promoter regions were cloned upstream of the *lacZ* gene into the promoterless and low-copy number plasmid pHRP309 (Figure III.4).

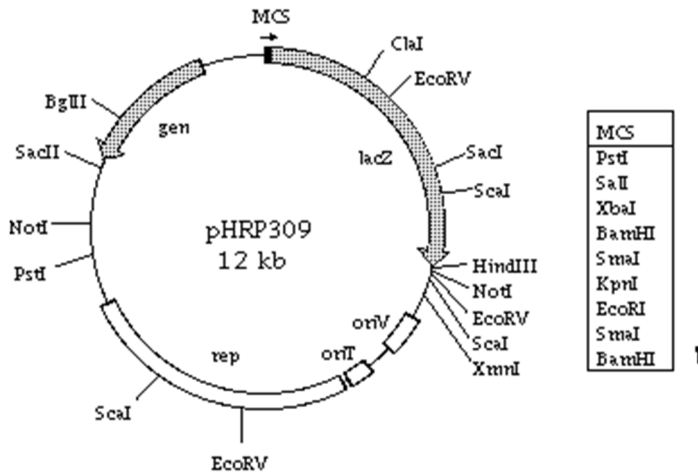


Figure III.4. pHRP309 plasmid map. Plasmid used for transcriptional fusions. The promoter region is cloned upstream of *lacZ*, the reporter gene.

This process led to the construction of the transcriptional fusions: *araC1*_{Vang}::*lacZ*, *araC2*_{Vang}::*lacZ*, *frpA*_{Vang}::*lacZ*, *frpBC*_{Vang}::*lacZ*, *proC*::*lacZ*, *araC1*_{Pdp}::*lacZ* and *frpA*_{Pdp}::*lacZ*. The constructs were then mobilized by conjugation from *E. coli* S17-1- λ *pir* to *V. anguillarum* RV22 and its derivative mutant strains or to *P. damsela* subsp. *piscicida*.

V. anguillarum and *P. damsela* subsp. *piscicida* strains carrying the promoter-*lacZ* fusions were grown in CM9 minimal medium under iron excess or under iron limited conditions (25 μ M 2,2'-dipyridyl) at

25 or 15 °C. When the cultures reached an OD₆₀₀ ca 0.3, the β -galactosidase activities were measured by the Method of Miller (Miller, 1992). The results shown are the mean of three independent experiments. Statistical significance was determined by student's *t*-test with a threshold *p* value <0.05 and *p*<0.001.

Table III.6. Primers used for amplification of the *irp*-HPI promoter regions in *V. anguillarum* and *P. damselae* subsp. *piscicida*.

Oligonucleotide (5' -> 3')	Size (bp)
<i>araC1</i>_{vang} promoter fusion construction	
irp_ang_pr2_F_BamHI	GCGGGATCCGCGATACACTCTTCGTAGTG
irp_ang_pr2_R_Xbal	GCGTCTAGAACGTTTCGGTAAGCGTATGG
	664
<i>araC2</i>_{vang} promoter fusion construction	
AraC1_F_P_Xbal	CCGTCTAGACTCGCGACTATTTACCAGCA
AraC2_R_P_BamHI	GGCGGATCCGATCACACAGCAACGTAACG
	656
<i>frpA</i>_{vang} promoter fusion construction	
irp_ang_pr1_F_BamHI	GCGGGATCCACTTTGCCACCCACCATTAC
irp_ang_pr1_R_Xbal	GCGTCTAGAAATCATGGCCACTTTCGAGTG
	695
<i>frpBC</i>_{vang} promoter fusion construction	
Transp_F_BamHI	CCGGGATCCGATAAGGTGACGCGATTTTC
Transp_R_Xbal	CGCTCTAGAAGCGGATGGTCAAGACTTTG
	746
<i>proC</i> promoter fusion construction	
1_proC_F_Xbal	GGCTCTAGATGTGCAAGAGGGCGCGTATA
2_proC_R_BamHI	CGCGGATCCGGCGACTAAGCCTGCAATAA
	498
<i>araC1</i>_{pdp} promoter fusion construction	
araC1_pF_Xbal	GGCTCTAGAACGTTAACTCGCCAAGTCT
araC1_pR_BamHI	CGCGGATCCCTGGTGTTGTTGCACCAGAGC
	1056
<i>frpA</i>_{pdp} promoter fusion construction	
frpA_pF_Xbal	CGCTCTAGACGATAGCTTAGCGACATCTC
frpA_pRI_BamHI	GGCGGATCCAGGGCTCAAGGTTGCAGCTA
	958

5. PHENOTYPIC CHARACTERIZATION

5.1. Growth promotion assays and siderophore production

V. anguillarum strains were grown in CM9 medium under different iron availabilities. Iron restrictive conditions were achieved by the addition of the iron chelator EDDHA at 5 μM or 2,2'-dipyridyl at 25, 50, 75 or 100 μM . Iron excess was obtained by the addition of 10 μM FeCl_3 or FeSO_4 . An overnight culture in TSB-1 of each strain was adjusted to an $\text{OD}_{600} = 0.5$, and a 1:50 dilution was inoculated in CM9 with the correspondent iron availability condition. The cultures were incubated for 48 h at 15 or 25 $^\circ\text{C}$ with shaking at 120 rpm. Growth (OD_{600}) was measured in a spectrophotometer (Hitachi U-2000).

Bacterial cultures grown in CM9 with 25 or 50 μM 2,2'-dipyridyl (condition that does not limit growth but is sufficient to induce siderophore production) were assayed for siderophore production with the Chrome Azurol-S (CAS) liquid assay (Schwyn and Neilands, 1987). This technique allows the detection of compounds that chelate iron. As the siderophores usually have a higher ability to chelate iron, they scavenge the iron from the Fe^{3+} -CAS complex releasing the CAS dye which results in a colour change from blue to red/orange. When the cultures reached an $\text{OD}_{600} = 0.8$, the cells were pelleted by centrifugation and cell-free supernatants and CAS reagent were mixed 1:1 and incubated at room temperature for 15 min. Quantification was performed by measuring A_{630} in a spectrophotometer (Hitachi U-2000). The results shown are the mean of three independent assays. Statistical significance was determined by student's *t*-test with a threshold *p* value <0.05 , <0.01 , <0.001 .

5.2. Cross-feeding assays

Cross-feeding assays were performed to evaluate if *V. anguillarum* mutant strains were able to synthesize, export or internalize siderophores. The indicators strains were challenged to use the siderophore produced by the tested strain. Indicator strains were grown in TSB-1 until $\text{OD}_{600} \approx 0.8$ and inoculated into 20 mL of CM9 minimal medium containing 0.8% agarose and supplemented with 90 or 120 μM 2,2'-dipyridyl and poured onto plates. Tested strains were grown in

TSA-1 plates supplemented with 50 μM 2,2'-dipyridyl to induce siderophore production. Then, a loopful of biomass was carefully placed onto the surface of the plates previously inoculated with the indicator strain and incubated 48 h at 25 °C. A growth halo of the indicator strain around the tested strain indicates that the indicator strain can use the siderophore produced by the tested strain.

5.3. Motility

Motility was assayed using the soft agar method. *V. anguillarum* RV22 was grown in CM9 until mid-exponential phase ($\text{OD}_{600} \approx 0.8$) and stabbed into CM9 containing 0.4% agar (soft agar) and supplemented with 10 μM FeCl_3 or 50 μM 2,2'-dipyridyl. After incubation at 15 or 25 °C for 48 h, the appearance of cloudiness around a central growth stripe was indicative of motility. *P. damselae* subsp. *piscicida* DI21 strain was used as a non-motile control. The experiment was performed three times.

5.4. Biofilm formation

The crystal violet assay was performed to evaluate biofilm formation. *V. anguillarum* RV22 was grown in glass tubes containing CM9 supplemented with 10 μM FeCl_3 or 50 μM 2,2'-dipyridyl and incubated at 15 or 25 °C until reaching an $\text{OD}_{600} \approx 0.8$. The bacterial cultures were gently discarded, and 10 mL of methanol 99% (Panreac) was added to each glass tube to fix the remaining attached bacteria. Methanol was discarded and 2 mL of crystal violet 2% (Biomérieux) was added to each tube. After 5 min, the excess of dye was rinsed off with tap water. The attached bacteria were then washed with PBS and let to air dry. The dye bound to the biofilm was solubilized with 10 mL glacial acetic acid 33% (v/v) (Panreac) and quantified by measuring the A_{570} in a spectrophotometer (Hitachi U-2000). The assay was performed three times. Statistical significance was determined by student's *t*-test with a threshold *p* value <0.05 .

5.5. Haemolytic activity

Haemolytic activity was evaluated using Columbia Blood Agar plates (Oxoid). *V. anguillarum* RV22 was grown in CM9 plates

supplemented with 2,2'-dipyridyl at 50 μ M and incubated at 15 or 25 $^{\circ}$ C for 48 and 24 h, respectively. A loopful of biomass was placed onto the surface of Columbia agar plates and haemolytic activity was observed after incubation at 15 or 25 $^{\circ}$ C for 48 h.

6. WESTERN BLOT ANALYSIS

V. anguillarum RV22 Δ vabF and RV22 Δ vabF Δ araC1 were grown overnight in TSB-1. The OD₆₀₀ was adjusted to 0.5 and a 1:50 dilution was inoculated in 10 mL CM9 medium supplemented with 2,2'-dipyridyl at 25 μ M. The cultures were incubated at 15 $^{\circ}$ C with shaking at 120 rpm and when reached an OD₆₀₀ = 0.8, the cells were pelleted by centrifugation at 4,000 rpm, for 30 min at 4 $^{\circ}$ C (Eppendorf Centrifuge 5810 R). The supernatant was discarded, and the pellet was resuspended in 5 mL of 10 mM Tris-HCl, NaCl 0,3%, pH 8.0. Cellular disruption was accomplished by sonication on ice (5 cycles of 30 sec). Then, to eliminate the cellular debris, the samples were centrifuged at 4,000 rpm for 30 min at 4 $^{\circ}$ C. For the isolation of membrane proteins, 1% sarkosyl was added and the samples were incubated at room temperature for 30 min. The samples were centrifuged at 40,000 rpm for 30 min at 4 $^{\circ}$ C (Beckman Coulter, Optima™ L-90K Ultracentrifuge) and the pellet was resuspended in 20 μ L of water, mixed 1:1 with SDS-PAGE loading buffer and loaded into a 12% polyacrylamide gel.

After the separation by SDS-PAGE, the transfer sandwich was prepared following the sequential order from anode to cathode: sponge, filter paper, gel, membrane, filter paper, sponge. The PVDF membrane was activated for 1 min in methanol. The transfer was done in a wet system using the transfer buffer 25 mM Tris, 190 mM glycine, 20% methanol, pH 8.3. The transfer was running at 100 V for 1 h at 4 $^{\circ}$ C. After the transfer, the PVDF membrane was blocked in blocking buffer (5% skim milk in TBST, Tris-buffered Saline with Tween 20, 20 mM Tris, 150 mM NaCl, 0.1% Tween 20, pH 7.5) for 1 h at room temperature with gentle shaking. The membrane was incubated overnight with a solution of primary antibody against the target protein (1:10,000 dilution of the anti-FrpA antibody in 3% blocking buffer). The blot was rinsed 5 times for 5 min in TBST and incubated with the secondary antibody (1:10,000 anti-rabbit IgG HRP conjugate antibody

in 3% blocking buffer) for 1 h at room temperature with gentle shaking. The signal was revealed using the Clarity™ Western ECL substrate (Bio-Rad). The blot was visualized in a Fujifilm LAS-3000.

6.1. Antibody anti-FrpA design

FrpA structure was modeled using SWISS-MODEL (Biasini *et al.*, 2014) (Figure III.5). FrpA loop 6 was selected because it is conserved between different protein versions and due to its external localization. Thus, the sequence of the short peptide PGGFSPAPRSSGDKNKYSP was used as antigen to get polyclonal anti-FrpA antibodies in rabbits. Rabbits immunization and purification of antibodies were ordered from GenScript.

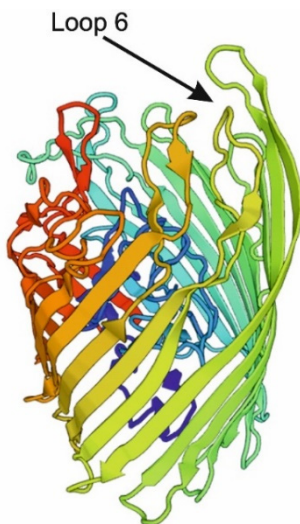


Figure III.5. Model of FrpA tertiary structure using SWISS-MODEL. Identification of loop 6.

7. BIOLOGICAL ACTIVITY OF PISCIBACTIN ANALOGUES

Some piscibactin analogues were synthesized by the Organic Chemistry Research Group of Prof. Carlos Jiménez at the University of A Coruña. The biological activity (capability to induce bacterial growth) of these compounds was analysed in 96-well microtiter plates with 200 μ L as final volume. Piscibactin and the analogues stock solution was prepared with methanol:milliQ water (1:1) and they were

used in the experiment at the final concentration of 20, 10, 2 and 0.2 μM .

V. anguillarum RV22 $\Delta vabD$, RV22 $\Delta vabD\Delta frpA$ and *P. damsela* subsp. *piscicida* DI21 were grown overnight in TSB-1. The OD₆₀₀ of each bacterial culture was adjusted to 0.5 and a final dilution of 1:20 (*V. anguillarum* strains) and 1:40 (DI21) were inoculated in CM9 media containing 75 μM 2,2'-dipyridyl (concentration that inhibits growth). Subsequently, piscibactin and its analogues were added at the suitable concentration. CM9 medium supplemented with 10 μM FeCl₃, or with 75 μM 2,2'-dipyridyl and non-inoculated medium were used as controls. The plate was incubated briefly at 25 °C with shaking at 120 rpm and then transferred to the iMarK Microplate reader (Bio-Rad) to record growth (OD₆₀₀) for 18 h. Each condition was done in duplicate in each plate and three independent experiments were performed. The results shown are the mean of the values obtained. Statistical significance was determined by student's *t*-test with a threshold *p* value <0.05.

8. ELECTROPHORETIC MOBILITY SHIFT ASSAY

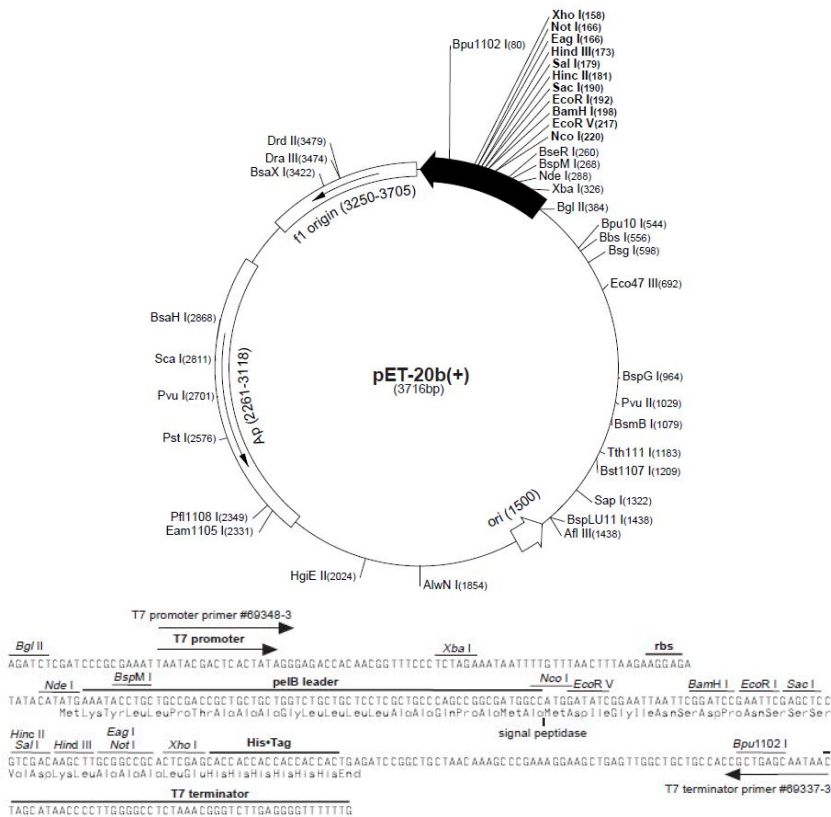
8.1. Cloning

V. anguillarum RV22 *pbtA* (*araC1*) and its N-terminal and C-terminal were cloned into the expression vector pET20b(+) (Figure III.6). Primers were designed to obtain each of the proteins with a His-tag at the C- or N-terminal. Primers used are listed in Table III.7.

Table III.7. Primers used to clone *pbtA* (*araC1*) and its N- and C-terminal domain into the expression vector pET20b(+). Restriction sites are underlined.

Oligonucleotide (5' -> 3')	Size (bp)
AraC1 with C-terminal His-tag	
AraC1_NdeI_F	<u>GCCATATGGTATCTAAAATGAATCG</u>
AraC1_XhoI_R	<u>CCGCTCGAGGGGACGTTGACGATGTTTCC</u>
AraC1 with N-terminal His-tag	
AraC1_F_NdeI_	<u>CGCCATATGCACCACCACCACCACCACAAT</u>
His-tagNTD	<u>CGTGTGATTTAAACC</u>
AraC1_XhoI_R_stop	<u>CCGCTCGAGTTAGGGACGTTGACGATGTTTCC</u>
AraC1 C-terminal with His-tag at the C-terminal	

CTD_F_NdeI	<u>CGCCATATG</u> T <u>CATCCCTTTCCAGTCG</u> AA <u>C</u>	342
AraC1_XhoI_R	CCGCTCGAGGGGACGTTGACGATGTTTC	
AraC1 C-terminal with His-tag at the N-terminal		
CTD_F_NdeI_	<u>CGCCATATG</u> CACCACCACCACCAC <u>CT</u> CATCC	
His-tag_NTD	CTTCCAGTCGAA <u>C</u>	342
AraC1_XhoI_R_stop	CCGCTCGAGTTAGGGACGTTGACGATGTTTC	
AraC1 N-terminal with His-tag at the C-terminal		
AraC1_NdeI_F	GCCATATGGTATCTAAAATGAATCG	645
NTD_R_XhoI	GCGCTCGAGCTCACTGTCTTTTTGTTGC	



pET-20b(+) cloning/expression region

Figure III.6. pET20b(+) plasmid map and sequence. The target genes were cloned using *NdeI* and *XhoI* restriction enzymes to liberate the *peIB* leader and clone the genes with a C-terminal His-tag. To obtain the His-tag at the N-terminal, primers were designed with a 6xHis-tag sequence in the forward primer.



8.2. Expression tests

Expression tests were performed to evaluate the conditions and the strains that express the proteins in higher concentrations. The vector carrying each construction to be tested was transformed into a set of seven chemocompetent *E. coli* strains. Chemocompetent cells were obtained by allowing the cells to grow until an OD₆₀₀ of 0.4-0.6. The culture was cooled down on ice for 15-20 min and then subjected to two centrifugations at 4,000 rpm at 4 °C for 10 min with incubations on ice in between. The pellet was gently resuspended with cold 50 mM CaCl₂. Transformation was carried out performing a thermic shock at 42 °C for 45 s. The recombinant bacteria were grown overnight at 37 °C in 10 mL LB supplemented with the correspondent antibiotic. From the overnight cultures, new cultures were obtained by adding inoculum to achieve a starting OD₆₀₀ = 0.07 in 45 mL of LB. The cultures were incubated at 37 °C, shaking at 200 rpm until achieving an OD₆₀₀ = 0.5. The culture was then subdivided into three cultures of 15 mL each. In one of the cultures the expression of the protein was immediately induced adding 0.5 μM IPTG and incubated for 4 h at 37 °C with shaking at 200 rpm. The remaining two cultures were acclimated at 17 °C and 25 °C for 20 min. Then the expression of the protein was induced by adding 0.5 μM IPTG and incubated overnight at 17 °C and 25 °C. The cultures were centrifuged at 4000 rpm for 10 min at 4 °C. The cells were resuspended in 1.7 mL of resuspension buffer (50 mM Tris, 500 mM NaCl, pH 8.0) and stored at -20 °C for at least 24 h. Bacteria were then lysed by sonication and samples corresponding to the total fraction and soluble fraction (obtained after centrifugation at 11,000 g for 20 min at 4°C) were collected. The samples were loaded in a 14% polyacrylamide gel and ran at 200 V in a Bio-Rad PowerPac Basic. The gel was stained with Coomassie Blue (g/L, 40% methanol, 10% acetic acid), destained in a solution of 40% methanol 10% acetic acid and visualized using Fujifilm LAS-3000.

8.3. Protein purification

Based on the expression tests, an *E. coli* strain and a temperature were selected to achieve the maximum protein yield. The same protocol

described for the expression tests was followed but with larger culture volumes (see Table III.8).

Table III.8. Strain, temperature, and culture volume used for protein purification.

Protein	Purification conditions		
	<i>E. coli</i> strain	Temperature	Volume
N-terminal Domain	BL21	17 °C	1 L
C-terminal Domain	BL21 plyS	37 °C	1 L
PbtA (AraC1)	Codon +	37 °C	2 L
	BL21	17 °C	2 L
	BL21	17 °C	6 L
	Solu	17 °C	6 L

After induction, the culture was incubated at the selected temperature (Table III.8). The cells were pelleted by centrifugation at 4,000 rpm for 30 min at 4 °C in a Beckman Avanti J-26 XP using the rotor JLA-8.1000. The supernatant was discarded, and the pellet resuspended in 40 mL of resuspension buffer (50 mM Tris, 500 mM NaCl, pH 8.0) and stored at -20 °C. The cells were lysed with a sonicator and then centrifuged at 17,000 rpm for 30 min at 4 °C in a Beckman Avanti J-26 XP using the rotor JA-25.50. Then a purification column C-50 (ABT) was prepared. Five mL of the high-density nickel resin (ABT) was added to the column, and it was subsequently washed with distilled water and resuspension buffer. Afterwards, the supernatant was added to the column and the flow through was collected. The column was washed and elutions with increasing imidazole concentration were sequentially added and collected (Table III.9).

Table III.9. List of buffers used for the purification process.

Buffer	Composition		
Resuspension buffer	50 mM Tris pH 8	500 mM NaCl	
Wash buffer	50 mM Tris pH 8	500 mM NaCl	20 mM Imidazole
Elution 100	50 mM Tris pH 8	500 mM NaCl	100 mM Imidazole
Elution 200	50 mM Tris pH 8	500 mM NaCl	200 mM Imidazole
Elution 400	50 mM Tris pH 8	500 mM NaCl	400 mM Imidazole

Samples corresponding to the total fraction (samples after sonication), soluble fraction (sonicated sample after centrifugation), flow through, elution 100, 200, 400 and resin were loaded in a 14% polyacrylamide gel. The elution that presented the highest amount of protein (larger band) was further concentrated. Concentration was performed by centrifugation at 4,000 rpm for 10 min at 4 °C using Vivaspin® centrifugal concentrators with a membrane cut-off lower than the protein of interested molecular weight. After concentration to a volume of approximately 1-3 mL the protein was transferred to a dialysis membrane (Spectra/Por® Dialysis Membrane, Spectrumlabs) previously washed with distilled water and resuspension buffer. The protein was incubated at 4 °C overnight in the dialysis membrane, floating in the resuspension buffer. Then the protein was centrifuged at 8,000 g for 15 min at 4 °C to eliminate any precipitation and its concentration was determined in a NanoDrop ND-1000 Spectrophotometer. The protein was kept at -80 °C until further use.

8.4. Electrophoretic Mobility Shift Assay (EMSA)

Electrophoretic mobility shift assay allows the study of DNA-protein interactions. The DNA of interest was amplified by PCR (Table III.10) and end-labelled with biotin using the Biotin 3' End DNA labelling Kit (Thermo Scientific™) following the manufacturer's recommendations.

Table III.10. Primers used to amplify *ParaC1*, *PfrpA* and *PfrpBC*.

Oligonucleotide (5'→3')	Size (bp)
<i>PpbtA (ParaC1)</i>	
AraC1_EMSA_F	TTCTTCCCCTAAAAAATGAC
AraC1_EMSA_R	TTTAGATACCATTCAAAAAT
<i>PfrpA</i>	
FrpA_1_EMSA_F	CAGGGTGCTCTCACGCCCTAA
FrpA_EMSA_R	CGAATCTGTTTTCTGTGGT
<i>PfrpA</i>	
FrpA_4_EMSA_F	AAAAATAGACGACCCGATCT
FrpA_5_EMSA_R	CTGTGGTATCCATATTGAAC
<i>PfrpBC</i>	
FrpBC_EMSA_F	AATAAAGCTCCATAAATGGA

FrpBC_1_EMSA_R	ATACATCTTCGTAGACAGGG	
PfrpBC		
FrpBC_EMSA_F	AATAAAGCTCCATAAATGGA	
FrpBC_12_EMSA_R	GGTGGGCTAGTTACGACTAA	100

The EMSA was performed using the LightShift® Chemiluminescent EMSA Kit (Thermo Scientific™). Binding reactions were performed as in Table III.11. Binding reactions were incubated for 30 min at 21 °C and loaded in a 5% 0.5x TBE gel. The gel was running at 100V for 1 h at 4 °C. The proteins were then transferred to a positively charged nylon membrane in a wet system (0.5x TBE) at 380 mA for 30 min at 4 °C. The resultant membrane was immediately UV-crosslinked and further treated following the manufacturer's instructions.

Table III.11. Components of the binding reactions. Each reaction contained the 3' end biotin labelled DNA and 0.2 or 1 pmol of the protein. To R3 was added an excess of specific unlabelled DNA.

Binding Reactions						
Component	Final amount	R1	R2(0.2)	R2(1)	R3(0.2)	R3(1)
Ultrapure water		8 µL	6.96 µL	5.4 µL	---	---
10x binding buffer (10 mM Tris, 50 mM KCl, 1 mM DTT, pH 7.5)	1x	2 µL				
50% glycerol	5%	2 µL				
1 M KCl	150 mM	3 µL				
100 mM MgCl ₂	5 mM	1 µL				
20 mM EDTA	1 mM	1 µL				
BSA	0.3 mg/mL	2 µL				
Unlabelled DNA	2.5 pmol	-	-	-	---	---
Protein CTD/NTD	0.2 pmol	-	1.04/ 1.42 µL	-	1.04/ 1.42 µL	-
Protein CTD/NTD	1 pmol	-	-	2.6/ 1.42 µL	-	2.6/ 1.42 µL
Biotin labeled DNA	25 fmol	1 µL				
Total volume		20 µL				

9. EXPERIMENTAL INFECTIONS

Fish virulence assays were performed using sole fingerlings (*Solea senegalensis*) of 10-15 g that are naturally infected with *V. anguillarum*. Fish were divided in groups of 30 individuals and acclimated at the temperature tested and maintained in 50 L seawater tanks with aeration. Fish were inoculated intraperitoneally with 0.1 mL of a bacterial suspension obtained by resuspending in saline solution (0.85% NaCl) several colonies from a fresh TSA-1 culture. The suspension was adjusted to an $OD_{600} = 0.5$ and the inoculum used was a 10-fold serial dilution of this suspension. The precise number of injected bacterial cells was determined by colony plate counting in TSA-1. Control groups were inoculated with 0.1 mL of saline solution and maintained at the correspondent temperature during the time frame of the experiment (7-12 days). Mortalities were recorded daily and statistically significant differences in percentage of survival were determined using the Kaplan-Meier method with Mantel-Cox log-rank test using SPSS (version 20; IBM SPSS Inc., Chicago, IL). *P*-values were considered significant when $p < 0.05$; < 0.01 and 0.001 . The Relative Percentage of Survival was determined following: $RPS = [1 - (\% \text{ mortality of the vaccinated groups} / \% \text{ mortality in the control group})] \times 100$.

The assay was executed at the Experimental Aquarium of the University of Santiago de Compostela. The protocols for animal experimentation used followed the current Spanish and European legislation and have been approved by the Bioethics Committee of the University of Santiago de Compostela (Procedure Code 15004/14/003).

10. VACCINATION ASSAYS

10.1. Immunization

Vaccination assays were performed to evaluate the protection generated by classical bacterins and the recombinant proteins rFrpA and rFvtA against *V. anguillarum* infection occurred at 18 and 24 °C. The cross-protection of FrpA_{Vang} against a *P. damsela* subsp. *piscicida* infection was also evaluated (Table III.12).

The assay was performed using Senegalese sole (*Solea senegalensis*) fish fingerlings of approximately 10 g. The assay was executed at the Experimental Aquarium of the University of Santiago de Compostela. The fish were acclimated for seven days in 100 L tanks of seawater, with recirculation and continuous aeration at 18 °C. After acclimation, fish were separated in 6 groups that were subjected to the following treatments: rFrpA or rFvtA subunit vaccine; *V. anguillarum* RV22 or *P. damselae* subsp. *piscicida* DI21 bacterins; Freund's adjuvant control; and PBS (non-immunized control).

Table III.12. Representation of the treatments, number of fish and temperature of the experimental challenge.

Immunization		
Treatment	Number of fish	Temperature of experimental infection (°C)
Bacterin RV22	100	18
		22
Bacterin DI21	50	22
rFrpA	100	18
		22
rFvtA	100	18
		24
Freund's Adjuvant	100	18
		22
		24
PBS	100	18
		22
		24

The recombinant proteins rFrpA and rFvtA were diluted in PBS leading to a final concentration of 0.6 mg/mL and fish belonging to those groups injected intraperitoneally with 100 µL of an emulsion of recombinant protein and Freund's adjuvant (Sigma-Aldrich) in a 1:1 proportion (complete Freund's adjuvant was used for the first immunization and the incomplete one in the second immunization). Each fish was immunized with 30 µg of protein. Both recombinant proteins were purified from *E. coli* cultures expressing the proteins from the corresponding genes cloned in plasmid pET20b(+). They were elaborated by Prof. Carlos Jiménez group of Organic Chemistry of the University of A Coruña.

The bacterins were obtained by growing aerobically *V. anguillarum* RV22 and *P. damselae* subsp. *piscicida* DI21, in TSB-1 at 25 °C with shaking. When the cultures reached an OD₆₀₀ ca. 0.9, the cells were inactivated by the addition of 37% formaldehyde (PanReac) at 10 mL/L of culture. The suspension was incubated for 4 h with shaking (120 rpm) at 25 °C. To assure the inactivation of the cells, 100 µL of the suspension was plated in duplicate in TSA-1 and incubated at 25 °C and 37 °C. The bacterins were stored at 4 °C until the immunization. Fish were injected intraperitoneally with 100 µL of the correspondent bacterin.

Two control groups were established, PBS and Freund's adjuvant. Fish belonging to the PBS control group were injected intraperitoneally with 100 µL of sterile PBS. Fish belonging to the Freund's adjuvant group were also injected intraperitoneally with an emulsified solution of adjuvant in PBS (1:1).

Two immunizations were performed. The first one at day 0 and a second immunization or a booster vaccination at day 30. Complete Freund's adjuvant was used in the first immunization and incomplete Freund's adjuvant in the booster dose. Sixty days after the first immunization, experimental infection challenges with *V. anguillarum* or *P. damselae* subsp. *piscicida* were performed at 18, 22 or 24 °C (see Table III.12). Fish were injected intraperitoneally with 100 µL of a suspension of *V. anguillarum* RV22 or *P. damselae* subsp. *piscicida* DI21 with ca 5x10⁵ CFU/mL. Mortality was followed daily.

10.2. Determination of antibody levels by ELISA

The levels of antibodies were determined at three time points, before the first immunization (day 0), before the second immunization (day 30) and before the experimental infection (day 60). Blood was extracted from 5 fish of each group by puncturing the caudal vein. Blood was incubated at 4 °C to coagulate and after approximately two hours, the serum was collected and mixed with glycerol 1:1 (v/v) to freeze it at -20 °C until use.

The level of antibodies generated by the administration of each treatment described above was evaluated by an indirect ELISA immunoassay (*Enzyme-Linked ImmunoSorbent Assay*) (Figure III.7).

The monoclonal IgM anti-Gourami antibody (*Osphronemus goramy*) (AQUATIC Diagnostics Ltd) was used to detect the level of IgG in fish serum. The anti-IgG Gourami antibodies have demonstrated to be effective in the determination of antibodies levels produced in sole fish (Valderrama *et al.*, 2019). ELISA was performed following the manufacturer's recommendations (AQUATIC Diagnostics Ltd). As primary antigen, that immobilized in the wells of the ELISA plate, was used the purified protein, rFrpA or rFvtA (10 ng in each well) or the bacterins (100 μL /well). Consequently, the fish antibodies able to recognize rFrpA, rFvtA and whole cells were immobilized in the well. The primary antigens were incubated overnight at 4 °C and then the wells were washed with TTBS (0.5% Tween 20, Tris 50 mM, NaCl 0.15 M, pH 7.5). The antigens were blocked with 5% skim milk in TBS (Tris 50 mM, NaCl 0.15 M, pH 7.5) and incubated for 1 hat 25 °C. After washing with TTBS, 50 μL of each serum (from a 1:100 dilution) were added to each well and the plate was incubated for 30 min at 25 °C. After another wash, 50 μL /well of a 1:1000 dilution of the monoclonal IgG mouse anti-Gourami IgM antibody (AQUATIC Diagnostics Ltd) was added. Subsequently, 50 μL /well of a 1:1000 dilution of the anti-mouse IgG (Bio-Rad) was used to detection. This IgG produced in goat is conjugated to the enzyme peroxidase that allows the quantification through a colorimetric reaction using the Kit TMB-peroxidase (Bio-Rad). After the incubation with the substrate for 30 min at 25 °C in the dark, the reaction was blocked with 1 N H_2SO_4 . The appearance of a yellow colour is indicative of the presence of antibodies and its intensity is directly dependent on the level of antibodies present. The resultant antibody level was quantified by measuring the A_{450} in an iMarK Microplate Reader (Bio-Rad). Antibody levels were determined in triplicate and the results shown are the average of the levels detected.

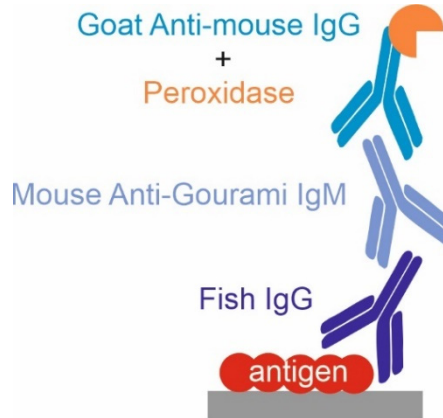


Figure III.7. Schematic representation of the indirect ELISA assay used to determine the level of antibodies IgG in fish serum.

11. BIOINFORMATIC ANALYSIS

11.1. *irp*-HPI structure and distribution

The presence of the *irp*-HPI genomic island was screened in 43 *V. anguillarum* strains whose genome is deposited in GenBank. The whole nucleotide sequence of *V. anguillarum* RV22 *irp*-HPI and the regions immediately upstream and downstream were used as a query in a BlastN search. Those nucleotide sequences that resulted in a significant alignment were downloaded and a multiple alignment of the conserved regions was obtained using MAUVE (Darling *et al.*, 2010). This alignment allowed the analysis of the genomic island structure and the identification of its insertion point. Furthermore, putative Fur-boxes were identified using the database PRODORIC Release 8.9, *Virtual Footprint Promoter Matches* (<http://www.prodoric.de>). The BlastP algorithm was used to analyse the homology of each protein from *V. anguillarum* and *P. damselae* subsp. *piscicida*.

11.2. Promoter sequence analysis and phylogenetic reconstitution

BlastN searches (nr/nt) and whole-genome shotgun (wgs) NCBI databases were performed using as a query the nucleotide sequence of *V. anguillarum* RV22 *irp*-HPI, 250 bp upstream of *pbtA* to *frpA* stop codon (sequence ID. AEZB01000030, 30437-35095). Homologous

sequences were clustered in promoter types by similarity, thus each type included sequences sharing 100% of coverage and $\geq 99.5\%$ of nucleotide identity. Representative sequences of each type were downloaded from NCBI and aligned using MUSCLE (MEGA X suite). Phylogenetic tree was inferred using p-distances (Transitions + Transversions) and Neighbour-Joining method. All ambiguous positions were removed for each sequence pair (pairwise deletion option). There was a total of 3,377 positions in the final dataset. Sequence alignments, nucleotide pairwise p-distances and evolutionary analyses were conducted in MEGA X (Kumar *et al.*, 2018).

11.3. FrpA phylogenetic analysis

The phylogenetic analysis of the piscibactin outer membrane transporter FrpA was performed using MEGA6 (Tamura *et al.*, 2013). Firstly, BlastN searches in the nucleotide collection (nr/nt) and whole-genome shotgun (wgs) from NCBI databases were performed, using *frpA* nucleotide sequence of *V. anguillarum* RV22 as a query. *frpA* homologs were downloaded from NCBI and aligned using MUSCLE (MEGA 6 suite). The phylogenetic tree was constructed by the neighbour-joining method with a bootstrap method of 1000 replicates using MEGA 6 software.

IV. RESULTS AND DISCUSSION

IV. RESULTS AND DISCUSSION

1. ADAPTATIONS OF *V. ANGUILLARUM* THAT ENABLE IT TO CAUSE VIBRIOSIS IN WARM-AND COLD-WATER FISH SPECIES

1.1. EFFECT OF TEMPERATURE IN THE GROWTH KINETICS AND VIRULENCE OF *V. ANGUILLARUM*

To analyse the virulence properties of *V. anguillarum*, an experimental infection at cold (15 °C) and warm (25 °C) water temperatures was performed. *Solea senegalensis* was chosen as the fish model organism because it is naturally exposed to temperature shifts from 12 to 26 °C (Arjona *et al.*, 2010). Thereby, the temperatures used in this experiment were in its thermal limit which would not impact the immune response (Fletcher and Secombes, 2015). Groups of 30 fish were acclimated at the correspondent water temperature of 15 °C or 25 °C. The control groups, one per each temperature, were inoculated intraperitoneally with 0.1 mL of saline solution (0.85% NaCl). No mortality was observed during the experiment time frame in the control groups. Fish were inoculated intraperitoneally with the same dose of *V. anguillarum* RV22 strain ($2-5 \times 10^5$ CFU per fish) and mortalities were accounted for 10 days (Figure IV.1.B). Interestingly, the mortality observed was significantly higher at cold (15 °C) than at warm (25 °C) water temperature. Seven days post infection, a mortality of 95% was observed at 15 °C, and no more deaths were registered until the end of the experiment. At 25 °C, the mortality rate was considerably lower, reaching 63%, 9 days post infection (Figure IV.1.B).

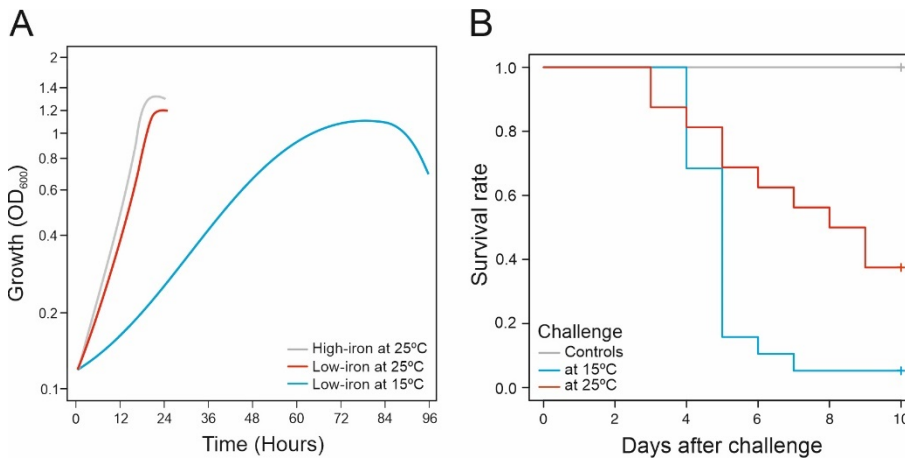


Figure IV.1. Influence of temperature in growth and virulence of *V. anguillarum*. (A) *V. anguillarum* was grown in iron deficiency at 15 and 25 °C and in iron excess at 25 °C. Growth was monitored for 24 h (25 °C) or 96 h (15 °C). (B) Senegalese sole fingerlings were experimentally infected with *V. anguillarum* RV22 and kept at 15 or 25 °C. Mortality was recorded for 10 days.

These results clearly contrast with the rapid growth phenotype presented by *V. anguillarum* RV22 strain at 25 °C. When grown at 15 °C, RV22 never reached the maximal OD₆₀₀ observed at 25 °C (OD₆₀₀ ca 1.35). There were not differences in the growth curve at 25 °C with high iron availability or with low iron availability. Nonetheless, under low iron conditions, RV22 did not achieve the maximal OD₆₀₀ of 1.35. At 15 °C, RV22 displayed a slow growth rate and a long log phase, which lasted almost 60 hours, reaching its maximum OD₆₀₀ ca. 1.1 after 84 hours. After this, a rapid decay in the OD₆₀₀ was observed (Figure IV.1.A).

The growth capacity shown by RV22 at 25 °C contrasts with the considerably higher virulence demonstrated at 15 °C. We hypothesize that this observation may be the result of an up-regulation of virulence factors at cold-water temperature. The temperature-dependent regulation of virulence factors is a characteristic of pathogenic bacteria that infect ectothermic hosts such as fish, where the infection process generally occurs at temperatures below that of the optimal growth

(TBO) (Guijarro *et al.*, 2015). However, these regulatory mechanisms are yet poorly characterized.

1.2. TRANSCRIPTOMIC ADAPTATIONS OF *V. ANGUILLARUM* TO GROWTH UNDER LOW IRON AVAILABILITY AT COLD OR WARM TEMPERATURE

An RNAseq experiment was conducted to analyse the expression pattern of *V. anguillarum* RV22 during growth at low- and high-water temperature. The expression level of each gene was analysed in conditions that would mimic the environment faced by the pathogen when infecting cold- (15 °C) or warm- (25 °C) water adapted fish species. To this purpose, *V. anguillarum* RV22 was grown in CM9 minimal medium supplemented with 50 µM 2,2'-dipyridyl reducing iron availability, a condition that mimics the main signal that bacteria find during host colonization (Skaar, 2010). In addition, the expression pattern when *V. anguillarum* was grown in iron availability (10 µM FeCl₃) was used as control to define the genes that are regulated by iron limitation (Figure IV.2).

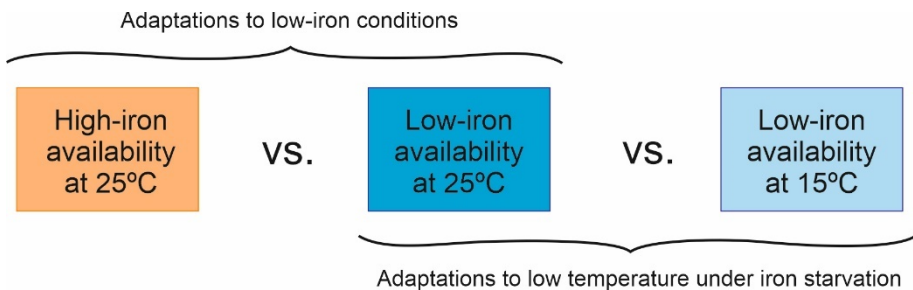


Figure IV.2. Experimental design to evaluate the transcriptomic changes of *V. anguillarum* RV22 strain to iron availability and temperature shift.

The comparative transcriptome analysis under low-iron and high-iron availability at 25 °C revealed 948 differentially expressed genes (DEGs) (Figure IV.3). 511 genes were down-regulated and 437 were up-regulated under low iron availability. For a better interpretation of the results, the differentially expressed genes were grouped into 19 functional KEGG categories (Figure IV.4).

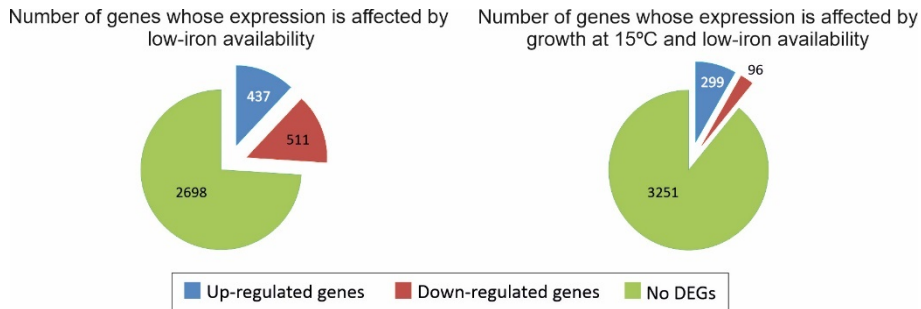


Figure IV.3. Differentially expressed genes (DEGs) identified under iron deficiency and low temperature (15 °C).

The results showed profound changes in global cellular metabolism adaptations and, most notably, the induction of virulence-related genes. Most of the down-regulated DEGs encode functions related to signal transduction (T), energy metabolism (C), cell motility (N) and translation and ribosome structure (J). By contrast, functions related to replication, recombination, and repair (L), cell wall/membrane biogenesis (M), and inorganic ion transport (P) are induced under low iron. In addition, the number of DEGs down- and up-regulated related to amino acids (E) and carbohydrate metabolism (G) functions, as well as some transcriptional factors (K), were equilibrated, which would suggest that the adaptation to grow under iron deprivation implies changes in amino acid and carbohydrate requirements.

Most DEGs identified at low-temperature (15 °C) under low iron availability were up-regulated (299 DEGs) (Figure IV.3). The most represented functional groups were related to amino acids metabolism and transport (E), DNA replication, recombination, and repair (L), cell wall/membrane (M), and inorganic ion transport (P) (Figure IV.4). Interestingly, the slow growth rate observed at 15 °C did not correlate to a drastic change in the expression pattern of genes related to the energetic metabolism, as it was similar at 25 °C and 15 °C (Figure IV.4). In fast growing cells there is a direct correlation between the growth rate and ribosome content, as the machinery responsible for protein synthesis such as ribosomes, tRNA and translation factors have a determinant role in maintaining exponential growth (Bremer and Dennis, 2008). When temperature drops to 15 °C, there was a significant

down-regulation of genes related to synthesis of large and small subunits of ribosomes and tRNA biogenesis (J). Growth under iron starvation at 15 °C is a limiting condition that requires low levels of ribosomal proteins and polypeptide synthesis for bacterial growth (Bremer and Dennis, 2008). Additionally, components of amino acids and carbohydrates transport systems (ABC transporters and phosphotransferase systems) were also down-regulated. The slower growth phenotype of RV22 at 15 °C might be the result of a decrease in nutrient import.

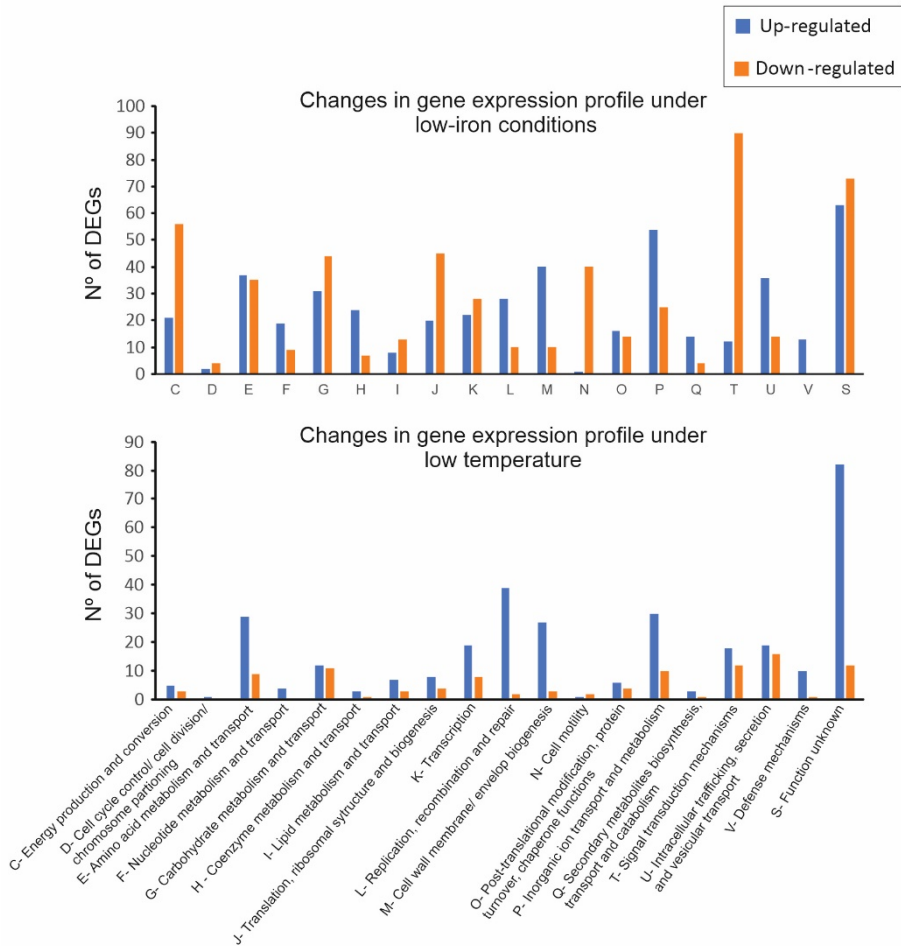


Figure IV.4. DEGs classified under KEGG categories. Number of DEGs up- and down-regulated under iron limitation at 25 °C and at 15 °C.

1.3. METABOLIC ADAPTATIONS TO GROWTH UNDER IRON STARVATION

The reduction of iron levels within the host environment constitutes a defence mechanism against bacterial pathogens. These conditions are a signal that a pathogen detects when it initiates the host colonization, consequently bacterial cells adapt their metabolism to iron starvation conditions (Skaar, 2010). According to our results, *V. anguillarum* responds to iron starvation redirecting the central metabolism to increase iron availability. The bacterium down-regulates genes encoding enzymes that participate in pathways with high-iron requirement like TCA cycle, in which some Fe-S containing enzymes participate, favouring glycolysis and pentose phosphate pathway as energy and metabolite sources (Table IV.1). Seven DEGs encoding enzymes of the glycolytic pathway were up-regulated. Conversely, the expression of genes encoding TCA cycle functions decreased (Table IV.1). These observations suggest a systemic up-regulation of glycolysis and a down-regulation of TCA cycle upon iron starvation, which would lead to a comparable increase in pyruvate for subsequent use in fermentative pathways as opposed to the TCA cycle. Even though the inhibition of TCA cycle makes the metabolism less energetically effective, glycolysis generates pyruvate, nicotinamide adenine dinucleotide (NADH), and other metabolic intermediates used by major biosynthetic pathways (Carlos *et al.*, 2018). Besides, the pentose phosphate pathway can also generate NADPH, ribose 5-phosphate and erythrose 4-phosphate that can be used in other biosynthetic pathways such as fatty acid biosynthesis, nucleotide and nucleic acid biosynthesis and aromatic amino acids biosynthesis (Carlos *et al.*, 2018). Notably, HexR a regulator that represses the activity of the central carbon metabolism (Leyn *et al.*, 2011) was down-regulated (Table IV.1).

Table IV.1. Relevant differentially expressed genes related to metabolism. Darker colour denotes higher expression. Fold change values with $p < 0.05$ are shown. ns, no significant differences.

Gene	Description	Expression level (FPKM)			Fold change	
		Fe(+) 25°C	Fe(-) 25°C	Fe(-) 15°C	Fe(+) 25°C vs Fe(-) 25°C	Fe(-) 25°C vs Fe(-) 15°C
Central metabolic regulator						
<i>iscR</i> (WP_026027698.1)	DNA-binding transcription factor	394.841	1701.96	1981.35	4.3	ns
<i>erpA</i> (WP_026027518.1)	Iron-sulfur cluster insertion protein	84.1258	198.739	342.876	2.4	ns
<i>hexR</i> (WP_019281735.1)	Repressor of central carbon metabolism	9.79078	10.442	40.3567	-	3.9
Glycolysis						
<i>pgm</i> (WP_019281944.1)	Phosphoglucomutase	43.9	189.5	222.3	4.3	ns
<i>pfkA</i> (WP_029388378.1)	6-phosphofructokinase	380.9	1341.1	1335.1	3.5	ns
<i>fbaA</i> (WP_013857804.1)	Fructose-bisphosphate aldolase	355.5	744.4	621.4	2.1	ns
<i>gapdH</i> (WP_010317219.1)	Glyceraldehyde-3-phosphate dehydrogenase	682.7	1716.5	1942.2	2.5	ns
<i>pgk</i> (WP_026027969.1)	Phosphoglycerate kinase	336.5	1068.9	1006.5	3.2	ns
<i>gpmI</i> (WP_019282807.1)	2,3-biphosphoglycerate-independent phosphoglyceromutase	215.7	1124.0	811.6	5.2	ns
<i>pykF</i> (WP_029388154.1)	Pyruvate kinase	202.5	448.2	338.2	2.2	ns
TCA cycle						
<i>glTA</i> (WP_019281581.1)	Citrate (S)-synthase	161.6	51.5	125.0	-3.1	2.4
<i>mdh</i> (WP_017043806.1)	Malate dehydrogenase	1498.4	631.1	803.8	-2.4	ns
<i>fumA</i> (WP_029388383.1)	Fumarate hydratase	565.0	211.3	249.5	-2.7	ns
<i>sdhA</i> (WP_013856347.1)	Succinate dehydrogenase flavoprotein subunit	2750.5	616.5	505.4	-4.5	ns
<i>sdhB</i> (WP_013856348.1)	Succinate dehydrogenase iron-sulfur subunit	729.2	139.4	121.2	-5.2	ns
<i>sdhC</i> (WP_019281580.1)	Succinate dehydrogenase cytochrome b556	831.0	87.9	50.4	-9.5	ns
<i>sdhD</i> (WP_010318675.1)	Succinate dehydrogenase, anchor protein	2088.6	241.8	151.6	-8.6	ns
<i>frdABCD</i>	Fumarate reductase	531.0	58.5	50.0	-8.3	ns
<i>frdA</i> (WP_013855868.1)	Fumarate reductase flavoprotein subunit	712.5	90.2	104.1	-7.9	ns
<i>frdB</i> (WP_017046770.1)	Fumarate reductase iron-sulfur subunit	453.2	86.6	51.5	-5.2	ns
<i>frdC</i> (WP_017043204.1)	Fumarate reductase subunit C	360.2	44.1	34.4	-8.2	ns
<i>frdD</i> (WP_010317640.1)	Fumarate reductase subunit D	156.0	13.2	10.0	-11.8	ns
<i>sucB</i> (WP_019281578.1)	Dihydropyrimidine succinyltransferase	973.3	392.7	283.3	-2.5	ns
Pentose phosphate pathway						
<i>zwf</i> (WP_029388423.1)	Glucose-6-phosphate dehydrogenase	30.9	175.2	282.4	5.7	ns
<i>gnd</i> (WP_019283138.1)	6-phosphogluconate dehydrogenase	33.3	303.8	468.3	9.1	ns
<i>fbaA</i> (WP_013857804.1)	Fructose-bisphosphate aldolase	355.5	744.4	621.4	2.1	ns
<i>glpX</i> (WP_019282901.1)	Fructose 1,6-bisphosphatase	69.8	153.3	125.9	2.2	ns
<i>pfkA</i> (WP_029388378.1)	6-phosphofructokinase	380.9	1341.1	1335.1	3.5	ns
Respiratory chain						
WP_019281580.1	Cytochrome b556	831.0	87.9	50.4	-9.5	ns
WP_019281630.1	Cytochrome C	426.2	15.7	17.5	-27.2	ns
WP_013855655.1	Cytochrome C	143.6	67.7	79.4	-2.1	ns
WP_019282134.1	Cytochrome C	1575.6	117.0	89.4	-13.5	ns
WP_026028567.1	Cytochrome C nitrate reductase	60.4	11.1	5.3	-5.4	ns
WP_026027333.1	Cytochrome C oxidase, cbb3-type, subunit I, II and III	3461.0	194.6	174.0	-5.7	ns
WP_013856895.1	Cytochrome C oxidase, cbb3-type, subunit I	194.7	34.3	42.0	-5.7	ns
WP_010320252.1	Cytochrome C oxidase, cbb3-type, subunit II	1490.3	269.5	238.8	-5.5	ns
WP_013856895.1	Cytochrome C oxidase, cbb3-type, subunit III	1776.0	280.1	241.2	-6.3	ns
WP_026027913.1	Cytochrome C biogenesis protein CcsB	292.3	73.9	143.9	-4.0	ns
WP_017046505.1	Cytochrome B	2181.5	363.3	272.1	-6.0	ns
WP_002540812.1	ATP synthase FO, C subunit	589.7	216.3	293.3	-2.7	ns
WP_013855589.1	ATP synthase FO, A subunit	451.7	138.1	198.0	-3.3	ns
WP_013855588.1	FOF1 ATP synthase subunit I	1275.7	532.1	711.7	-2.4	ns
WP_013856176.1	NADH-quinone reductase, F subunit	1261.3	418.3	340.7	-3.0	ns
WP_013856175.1	Ubiquinone oxidoreductase, E subunit	332.8	131.5	100.3	-2.5	ns
WP_005457265.1	Cytochrome BD oxidase subunit I	294.3	600.5	373.1	2.0	ns
<i>rsxB</i> (WP_013857280.1)	Electron transport complex protein RnfB	6.9	27.2	19.5	3.9	ns
<i>rsxE</i> (WP_029388436.1)	Electron transporter RsxE	83.7	201.6	149.3	2.4	ns
<i>rsxC</i> (WP_000949708.1)	Electron transporter RnfC	12.0	48.5	36.3	4.0	ns
<i>rsxD</i> (WP_006963070.1)	Electron transporter RnfG	6.3	21.9	11.1	3.5	ns

Many genes related to respiratory chain like cytochromes were down-regulated at low iron availability. Iron-sulfur (Fe-S) containing proteins were extensively down-regulated at low iron availability. Fe-S proteins are crucial for cell metabolism since they are involved in numerous biological processes, ranging from energy metabolism, e.g., TCA cycle and respiratory chain, to DNA repair. Interestingly, among low-iron induced DEGs (a 4.3-fold increase) was *iscR*, which encodes a transcriptional regulator that senses the cellular Fe-S status and adjust transcription of genes encoding several Fe-S assembly factors, Fe-S enzymes, Mn²⁺-containing enzymes like superoxide dismutase and ribonucleotide reductase, and additional genes with functions, such as biofilm formation, colicin K synthesis, and RNA metabolism (Lim and Choi, 2014; Santos *et al.*, 2015). Furthermore, IscR homologs play a role in virulence (Mettert and Kiley, 2015). Notably, the essential respiratory protein A, *erpA*, a Fe-S biogenesis-related gene essential for respiratory metabolism was 2.4-fold induced (Loiseau *et al.*, 2007). In addition, energy production through respiratory chain should be balanced, thus alternative members of the respiratory chain were up-regulated at low iron availability: the Rbf complex, the YdjA-like NAD(P)H nitroreductase, the electron transporter RxE, and oxidoreductase (Table IV.1).

Bacteria also adjust the amino acid metabolism to the environmental requirements (Table IV.2). Under iron starvation, valine, leucine and isoleucine degradation routes were down-regulated as the expression of five DEGs encoding enzymes for these functions diminished. Conversely, arginine, phenylalanine, tyrosine and tryptophan biosynthesis, as well as cysteine, methionine, glycine, serine and threonine metabolism were up-regulated.

Table IV.2. Relevant amino acids metabolism, synthesis and degradation related genes differentially expressed. Darker colour denotes higher expression. Fold change values with $p < 0.05$ are shown. ns, no significant differences.

Gene	Description	Expression level (FPKM)			Fold change	
		Fe(+) 25°C	Fe(-) 25°C	Fe(-) 15°C	Fe(+) 25°C vs Fe(-) 25°C	Fe(-) 25°C vs Fe(-) 15°C
Histidine metabolism						
<i>hutH</i> (WP_017048047.1)	Histidine ammonia-lyase	65.4	8.8	11.4	-7.4	ns
<i>hutU</i> (WP_019283311.1)	Urocanate hydratase	50.4	6.5	15.7	-7.8	2.4
<i>hutI</i> (WP_029388451.1)	Imidazolonepropionase	19.1	1.8	6.1	-10.5	ns
<i>hutG</i> (WP_029388450.1)	Formimidoylglutamase	24.0	1.6	3.4	-14.6	ns
Valine, leucine and isoleucine degradation						
<i>lpd</i> (WP_026027892.1)	Dihydrolipoamide dehydrogenase	4.0	0.9	1.8	-4.4	ns
<i>fadI</i> (WP_019283104.1)	3-ketoacyl-CoA thiolase	275.1	62.5	83.3	-4.4	ns
<i>ascA</i> (WP_010319642.1)	Acetoacetyl-CoA synthetase	86.3	28.1	28.6	-3.1	ns
Arginine biosynthesis						
<i>aspC</i> (WP_019282378.1)	Aspartate aminotransferase	360.1	685.7	879.7	1.9	ns
<i>argA</i> (WP_026027647.1)	Amino-acid N-acetyltransferase	122.5	281.2	448.0	2.3	ns
<i>argB</i> (WP_010317663.1)	Acetylglutamate kinase	626.9	1206.1	2213.7	1.9	ns
<i>argC</i> (WP_019282443.1)	N-acetyl-gamma-glutamyl-phosphate reductase	420.3	1096.0	1610.6	2.6	ns
<i>argG</i> (WP_017043213.1)	Argininosuccinate synthase	1719.3	4046.0	5666.2	2.4	ns
Phenylalanine, tyrosine and tryptophan biosynthesis						
<i>trpE</i> (WP_019281982.1)	Anthranilate synthase subunit I	77.6	380.6	149.7	4.9	-2.5
<i>trpG</i> (WP_019281983.1)	Amidotransferase of anthranilate synthase	136.8	908.7	174.4	6.6	-5.2
<i>trpC</i> (WP_019281984.1)	Phosphoribosylanthranilate isomerase	62.4	365.5	213.5	5.9	ns
<i>trpB</i> (WP_013857145.1)	Tryptophan synthase, beta subunit	683.4	4147.6	1021.0	6.1	-4.1
<i>trpR</i> (WP_013857539.1)	<i>trp</i> operon repressor	230.221	450.574	435.671	2.0	ns
<i>phhA</i> (WP_019282676.1)	Phenylalanine 4-monooxygenase	80.3	39.0	29.5	-2.1	ns
<i>tyrA</i> (WP_017043283.1)	Chorismate mutase	272.8	561.8	322.7	2.1	ns
<i>nadB</i> (WP_017046483.1)	L-aspartate oxidase	84.3	283.9	314.6	3.4	ns

Arginine is an amino acid required to synthesize the siderophore vanchrobactin (Soengas *et al.*, 2006). The biosynthesis of the aromatic amino acids phenylalanine, tyrosine and tryptophan was 4- to 6-fold up-regulated. Regarding the synthesis of phenylalanine and tyrosine from chorismate, three enzymes intervene in the process. The conversion of tyrosine to the immediate precursor, 4-hydroxyphenylpyruvate and the conversion of phenylalanine to the precursor phenylpyruvate is also up-regulated. Moreover, the conversion of phenylalanine to tyrosine was repressed, as the activity of the enzyme phenylalanine-4-hydroxylase PhhA, was down-regulated. Five DEGs encoding enzymes involved in the synthesis of tryptophan were up-regulated. Notably there was an up-regulation of the tryptophan transcriptional repressor that regulates the expression of the *trp* operon in response to its intracellular levels. The biosynthetic process that leads to the synthesis of these aromatic amino acids generates an intermediate, chorismate, essential for the synthesis of siderophores (Balado *et al.*, 2008). The genes *hutGHIU* involved in histidine metabolism were also down-regulated. Four DEGs encoding enzymes that are involved in the degradation of L-histidine to L-glutamate were down-regulated. This reaction results in L-glutamate

that can be involved in a fermentation process leading to the formation of acetate, pyruvate and ammonia or histidine that can also be converted in TCA cycle intermediates (Kastenmuller *et al.*, 2009). Interestingly, there was an up-regulation of a gene encoding a histidine decarboxylase, involved in the decarboxylation of histidine to form histamine. Histamine has been reported as a metabolite that can induce immune responses, specifically it is associated with HFP- histamine fish poisoning and consequently can act as a virulence factor (Barancin *et al.*, 1998; Barcik *et al.*, 2017).

Table IV.3. Relevant fatty acid metabolism related genes differentially expressed. Darker colour denotes higher expression. Fold change values with $p < 0.05$ are shown. ns, no significant differences.

Gene	Description	Expression level (FPKM)			Fold change	
		Fe(+) 25°C	Fe(-) 25°C	Fe(-) 15°C	Fe(+) 25°C vs Fe(-) 25°C	Fe(-) 25°C vs Fe(-) 15°C
Fatty acid metabolism						
<i>fadA</i> (WP_019281690.1)	Protoporphyrinogen oxidase	102.334	16.7644	22.7837	-6.1	ns
<i>fadB</i> (WP_019281689.1)	Fatty acid oxidation complex subunit alpha	247.2	33.3	38.3	-7.4	ns
<i>fadE</i> (WP_019282302.1)	Acyl-CoA dehydrogenase	448.51	42.9246	40.7234	-10.4	ns
<i>fadJ</i> (WP_019283103.1)	Fatty acid oxidation protein subunit alpha	318.8	62.4	93.3	-5.1	ns
<i>fadI</i> (WP_019283104.1)	3-ketoacyl-CoA thiolase	275.1	62.5	83.3	-4.4	ns

Fatty acids represent not only a carbon source for the energetic metabolism but also a source for bacterial membrane remodeling. The membrane phospholipid content affects its permeability and consequently bacterial survival in changing environments and persistence within the host. Beyond the alteration of membrane homeostasis, fatty acids may change *Vibrio* species virulence phenotype. It has been reported that in *V. cholerae* the incorporation of specific fatty acids enhance motility, biofilm formation, cholera toxin secretion and antibiotic resistance (Chatterjee *et al.*, 2007; Moravec *et al.*, 2017). Under iron starvation, there is a down-regulation of 5 DEGs related to fatty acid metabolism (Table IV.3).

1.4. EXPRESSION OF VIRULENCE FACTORS AT WARM- AND COLD-WATER TEMPERATURE UNDER IRON STARVATION

Bacterial pathogens must express virulence factors that enable them to colonise and grow within the host. Bacteria face a drastic shift in iron availability upon host encounter (Skaar, 2010). Low-iron adaptations were described in most bacterial pathogens including *E.*

coli, *V. cholerae* and *Staphylococcus aureus* (Andrews *et al.*, 2003; Mey *et al.*, 2005; Friedman *et al.*, 2006) and it is well established that low-iron up-regulates the expression of most virulence factors. To date several virulence factors have been described in *V. anguillarum*. They include LPS, motility and chemotaxis, iron uptake mechanisms and extracellular products with haemolytic and proteolytic activity (Li and Ma, 2017; Toranzo *et al.*, 2017).

The adaptation to iron starvation produced the up-regulation of genes related to LPS, different systems for iron acquisition, the haemolysins RTX, Vah1 and Vah3, outer membrane proteins associated with the efflux of metabolites (OmpA, OmpC and OmpV), and Type VI Secretion Systems. The temperature-dependent expression of virulence factors is detailed below.

1.4.1. Lipopolysaccharide and exopolysaccharide related genes

V. anguillarum lipopolysaccharide has endotoxic activity and allows the pathogen to adhere and persist within the host by evading the immune system (Boesen *et al.*, 1999). It is constituted by three regions, lipid-A, core polysaccharide, and the O-antigen that confers the endotoxic activity, antigenic properties and induce immunological responses (Boesen *et al.*, 1999; Lindell *et al.*, 2012). Interestingly, LPS composition, specifically the O-antigen polysaccharide side chains, influences the bactericidal effect of the complement system (Boesen *et al.*, 1999). It has been reported that *V. anguillarum* isolates resistant to serum were pathogenic for Atlantic salmon (Austin *et al.*, 1995). This indicates a direct correlation between serum resistance and survival of *V. anguillarum* in the fish host (Boesen *et al.*, 1999).

The genes involved in capsular polysaccharide production are encoded by a biosynthesis operon (VAR_RS0112290-VAR_RS0112465) and by the transport and assemble genes *wza-wzc* (*wziab*, VAR_RS0107285-VAR_RS0107295) and *wbfB-wbfD* (VAR_RS0107305-VAR_RS0107315) (Croxatto *et al.*, 2007; Naka *et al.*, 2011). *V. anguillarum* EPS is essential for the attachment of the pathogen to the host skin, preventing its removal by natural sloughing of fish mucus (Croxatto *et al.*, 2007). Moreover, the attachment to fish skin by formation of a biofilm would boost the colonization and

proliferation of *V. anguillarum* (Weber *et al.*, 2010). In *E. coli*, *wza* gene encodes an outer membrane lipoprotein that forms a channel essential for the export of polysaccharides (Drummel-Smith and Whitfield, 2000). The other genes in this operon, *wzb* and *wzc* catalyse the polymerization of the exported polysaccharides (Drummel-Smith and Whitfield, 1999; Wugeditsch *et al.*, 2001). EPS provides an environment full of nutrients and exoenzymes and promotes the cooperation between cells, forming biofilms (Croxatto *et al.*, 2007).

RNAseq results showed that there was an up-regulation (2.6-fold increase) of genes related to LPS/EPS biosynthesis, assemble and export under iron starvation (Table IV.4). This result suggests that the expression of LPS and EPS related genes increase under iron starvation, allowing the bacteria to evade host's defences and survive within the host. In addition, genes encoding functions related to exopolysaccharide transport and assemble showed maximal expression (a 2.7-fold increase) at low temperature (Table IV.4) but statistically significant differences were not found.

Table IV.4. Expression level and fold change of LPS and EPS related genes. Darker colour denotes higher expression. Fold change values with $p < 0.05$ are shown. ns, no significant differences.

Gene	Expression level (FPKM)			Fold change	
	Fe(+) 25°C	Fe(-) 25°C	Fe(-) 15°C	Fe(+) 25°C vs Fe(-) 25°C	Fe(-) 25°C vs Fe(-) 15°C
LPS biosynthesis					
WP_019282749.1	10.3232	23.2583	67.0299	2.3	2.9
WP_019282750.1	28.6925	64.1388	104.614	2.2	ns
WP_019282751.1	23.5349	38.716	61.25	ns	ns
WP_019282752.1	67.7342	119.016	139.861	ns	ns
WP_010317081.1	8.25886	16.686	38.0145	ns	ns
WP_019282753.1	36.9733	86.5046	175.719	2,3	ns
WP_019282754.1	40.5841	100.161	162.17	ns	ns
WP_010317086.1	33.0327	72.7726	126.36	ns	ns
WP_019282755.1	43.3658	173.618	264.417	4.0	ns
WP_019282756.1	44.0879	91.7012	176.738	ns	ns
WP_019282757.1	25.7907	90.9073	128.23	ns	ns
WP_019282758.1	11.7846	32.6429	49.7433	ns	ns
WP_019282759.1	7.76503	10.8502	14.1291	ns	ns
WP_019282760.1	2.45572	8.98473	13.8316	ns	ns
WP_019282761.1	8.89288	30.298	51.1257	3.4	ns
WP_019282762.1	21.6241	65.5437	95.3489	3.0	ns

WP_019282763.1	11.351	41.3446	72.5237	3.6	ns
WP_010317120.1	13.5146	29.2668	55.3569	ns	ns
WP_019282765.1	34.0807	71.2537	141.751	ns	ns
WP_019282766.1	117.277	194.436	290.968	ns	ns
WP_019282767.1	83.7276	166.189	262.383	ns	ns
WP_043004658.1	97.1849	214.714	398.852	2.2	ns
WP_019282768.1	31.22	64.9891	103.531	2.1	ns
WP_029388338.1	9.62516	21.9041	25.758	2.3	ns
WP_019282770.1	0.296127	3.66849	16.2737	ns	4.4
WP_019282771.1	0.767859	1.29479	6.03082	ns	4.7
WP_029388340.1	5.49534	22.6863	55.7805	4.1	2.5
WP_019282773.1	17.7071	36.6227	59.9883	ns	ns
WP_019282774.1	32.6509	73.2255	51.5516	2.2	ns
LPS transport and assemble					
wzb (WP_029388235.1)	11.6347	28.21	54.8375	2.4	ns
wza (WP_019282252.1)	8.47715	23.5381	81.5519	2.8	3.5
wzi (WP_019282253.1)	22.2108	68.5437	192.299	3.1	2.8
wbfB (WP_019282254.1)	1.00805	2.61944	10.0848	ns	3.8
wbfC (WP_019282255.1)	0.379411	1.37967	5.07576	ns	ns
wbfD (WP_019282256.1)	5.20315	9.65681	21.6635	ns	2.2
Exopolysaccharide					
Biosynthesis	24.2	63.4	106.3	2.6	ns
Transport and assemble	9.7	26.5	72.1	2.6	2.7

To corroborate the RNAseq results, the biofilm formation was tested *in vitro* under the same conditions used for RNAseq. *V. anguillarum* RV22 was grown at 25 °C under iron excess and iron restriction and at 15 °C under iron deficiency. After achieving the exponential phase, the cells in solution were discarded and those attached to the tube were stained with crystal violet. The quantification showed that there were no significant differences in biofilm formation of cells grown under iron excess or under iron starvation at 25 °C (Figure IV.5). However, a significant increase in biofilm formation was observed when the cells were grown under iron deficit at 15 °C (Figure IV.5).

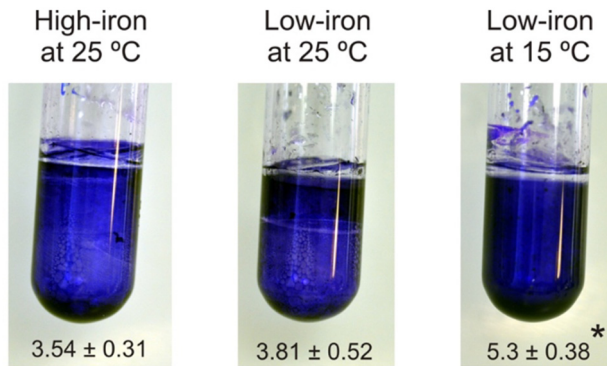


Figure IV.5. Biofilm formation under iron excess at 25 °C and iron deficit at 25 and 15 °C. The cells attached to the tube were used to quantify the biofilm formation by adding crystal violet.

1.4.2. Type VI Secretion System and outer membrane proteins

V. anguillarum genome harbours two T6SS, the T6SS1 is encoded in chromosome II and T6SS2 is encoded in chromosome I. The T6SS was firstly described in *V. cholerae* (Pukatzki *et al.*, 2006) and is involved in a variety of functions, from pathogenesis to biofilm formation and stress sensing (Bingle *et al.*, 2008; Bernard *et al.*, 2010). Interestingly, T6SS1 was ca. 10-fold more expressed under iron excess than T6SS2, which was almost silenced under this condition. Both T6SS1 and T6SS2 were 3.5-fold and 10.2-fold, respectively, up-regulated under iron starvation (Table IV.5). However, at 25 °C under iron deficit the T6SS1 shows a higher expression pattern than T6SS2 (FRPKM of 548 for the T6SS1 and 173 for the T6SS2). Interestingly, each system responds distinctively to temperature. While the T6SS1 is preferentially expressed at warm-temperature showing a down-regulation of gene expression at 15 °C (3.5-fold decrease), the T6SS2 requires cold-temperature to be significantly expressed. These temperature drop resulted in a global 2.6-fold change increase in T6SS2 expression while T6SS1 maintained a basal expression level under all tested conditions. These results suggest that T6SS2 needs a conjugation of environmental signals to be expressed. Though, T6SS1 may have an unspecific environmental role in *V. anguillarum* impacting its environmental fitness at both cold- and warm-water temperature,

T6SS2 role must be more niche specific. In addition, as both systems respond to low iron availability by increasing their expression, Fur must directly repress these genes (Chakraborty *et al.*, 2011; Brunet *et al.*, 2011).

The presence of more than one T6SS gene cluster in a bacterial genome has been previously reported (Bingle *et al.*, 2008), suggesting the presence of different functions and diverse regulatory mechanisms (Cascales, 2008; Bernard *et al.*, 2010; Schwarz *et al.*, 2010). In *V. anguillarum* the inactivation of T6SS2 did not result in a significant loss of virulence (Weber *et al.*, 2009; Tang *et al.*, 2016) however the inactivation of the T6SS1 or T6SS2 did impact the fitness *in vivo* (Guanhua *et al.*, 2018). T6SS2 has also been reported to be involved in the regulation of extracellular proteases expression via the stress-response regulator RpoS and the quorum-sensing regulator VanT (Weber *et al.*, 2009). Notably, the expression pattern of the T6SS2 shows high discrepancies between *V. anguillarum* serotypes. Its expression varies from undetectable levels to high levels of expression under warm marine like conditions (Tang *et al.*, 2016). This suggests that unidentified elements encoded outside the T6SS2 gene cluster might modulate its expression (Tang *et al.*, 2016). The present work results show that *V. anguillarum* serotype O2 strain RV22 expresses the T6SS2 when grown under iron deficit at low temperatures, reinforcing the notion that there is a high heterogenicity among *V. anguillarum* strains.

Table IV.5. Expression level and fold change of T6SS related genes. Darker colour denotes higher expression. Fold change values with $p < 0.05$ were shown. ns, no significant differences.

Gene	Expression level (FPKM)			Fold change	
	Fe(+) 25°C	Fe(-) 25°C	Fe(-) 15°C	Fe(+) 25°C vs Fe(-) 25°C	Fe(-) 25°C vs Fe(-) 15°C
T6SS1					
<i>vipA</i> (WP_050934223.1)	814.443	2542.05	843.377	3.1	-3.0
<i>vipB</i> (WP_026027753.1)	549.576	1947.43	562.651	3.5	-3.5
lysozyme (WP_013868295.1)	175.989	951.569	255.543	5.4	-3.7
<i>vasA</i> (WP_019282041.1)	27.2836	87.4775	33.3469	3.2	-2.6
<i>vasB</i> (WP_019282042.1)	53.479	169.466	42.6442	3.2	-4.0
<i>fha</i> (WP_019282043.1)	76.1711	360.377	77.2212	4.7	-4.7
<i>vasL</i> (WP_019281677.1)	27.7933	73.3933	21.8023	2.6	-3.4
<i>vasK</i> (WP_017045001.1)	40.6847	124.476	23.7704	3.1	-5.2
<i>vasJ</i> (WP_019281678.1)	98.3314	347.132	53.0565	3.5	-6.5
<i>vasI</i> (WP_019281679.1)	13.6323	34.1923	7.73133	ns	ns
<i>vasH</i> (WP_029388109.1)	67.254	188.39	35.6307	2.8	-5.3
<i>clpB</i> (WP_029388110.1)	48.4923	222.433	51.9803	4.6	-4.3
<i>vasF</i> (WP_050928076.1)	55.282	262.42	43.7926	4.7	-6.0
<i>vasE</i> (WP_017044997.1)	17.8958	77.1511	21.8753	4.3	-3.5
<i>vasD</i> (WP_019281682.1)	152.144	551.612	121.142	3.6	-4.6
T6SS2					
WP_013856698.1	3.12719	54.2805	45.8229	17.4	ns
<i>vtsl</i> (WP_019282546.1)	1.34988	13.0757	27.973	9.7	2.1
<i>vtsh</i> (WP_013856696.1)	2.857	39.8497	85.4617	13.9	2.1
<i>vtsg</i> (WP_019282547.1)	3.47447	51.6916	114.048	14.9	ns
<i>vtst</i> (WP_019282548.1)	5.25545	86.7504	104.071	16.5	ns
<i>vtse</i> (WP_029189804.1)	0.988325	26.5766	73.3223	ns	ns
<i>vtstD</i> (WP_019282549.1)	0.766437	28.3116	79.6949	36.9	2.8
<i>vtsc</i> (WP_013856691.1)	1.21379	14.9605	55.5803	ns	ns
<i>vtstB</i> (WP_019282550.1)	2.02319	38.3401	60.443	19.0	ns
<i>vtstA</i> (WP_013856689.1)	1.75907	49.4278	124.767	28.1	2.5
<i>clpV</i> (WP_019282551.1)	2.44775	33.3544	106.206	13.6	3.2
<i>vasB</i> (WP_019282552.1)	1.83427	33.0786	74.851	ns	ns
<i>vasA</i> (WP_017082793.1)	3.71716	23.035	88.1314	6.2	3.8
lysozyme (WP_010446924.1)	11.8391	90.4735	289.851	7.6	ns
<i>vipB</i> (WP_013856684.1)	6.51395	34.8136	106.012	5.3	ns
<i>vipB</i> (WP_004731267.1)	54.793	559.506	2403.55	10.2	4.3
<i>vipA</i> (WP_013856682.1)	84.2777	1021.22	3450.89	12.1	ns
<i>hcp</i> (WP_013856681.1)	57.3981	283.076	800.058	4.9	2.8
<i>vasL</i> (WP_029189803.1)	101.404	1040.56	2192.04	10.3	ns
<i>vgrG</i> (WP_029388295.1)	18.0072	230.97	557.787	12.8	2.4
WP_029189801.1	7.43758	66.973	137.501	ns	ns
PARR domain (WP_013856676.1)	3.92307	18.1195	52.0806	4.6	2.9
T6SS1	154.5	548.3	156.4	3.5	-3.5
T6SS2	16.9	173.1	451.3	10,2	2.6

The outer membrane of Gram-negative bacteria functions as a barrier that blocks the free entrance/secretion of compounds. One of the components present in high number are non-specific outer membrane proteins (OMP). These pore-forming proteins allow the passive transport of molecules such as nutrients and hydrophilic compounds, are involved in antibiotic resistance and allow the adaptative response of the cell to environmental changes such as temperature, pH and osmolarity (Delcour, 2009; Kao *et al.*, 2009; Choi and Lee 2019).

In the present study three differentially expressed genes encoding OMP proteins were identified (Table IV.6). While *ompA* and *ompV* were induced under low iron at 25 °C (3.5 and 6.4-fold increase, respectively), *ompC* was preferentially expressed at 15 °C, resulting in a 11.5-fold increase. OmpA plays a crucial role in the attachment to host cells during the invasion process and is also involved in the evasion of host defence mechanisms (Confer and Ayalew, 2013). OmpV is one of the major outer membrane proteins in *V. cholerae* and it is highly immunogenic (Stevenson *et al.*, 1985). OmpC is involved in membrane integrity maintenance and resistance to antibiotics (Choi and Lee., 2019). In addition, OmpC synthesis is favoured by high osmolarity and warm temperatures (Davey *et al.*, 1998).

Table IV.6. Expression level and fold change of outer membrane proteins related genes. Darker colour denotes higher expression. Fold change values with $p < 0.05$ were shown. ns, no significant differences.

Gene	Expression level (FPKM)			Fold change	
	Fe(+) 25°C	Fe(-) 25°C	Fe(-) 15°C	Fe(+) 25°C vs Fe(-) 25°C	Fe(-) 25°C vs Fe(-) 15°C
Outer membrane permeases					
<i>ompA</i> (WP_017045950.1)	236.738	829.038	439.803	3.5	ns
<i>ompC</i> (WP_019282894.1)	8.07736	8.92047	102.636	ns	11.5
<i>ompV</i> (WP_019282463.1)	35.3357	224.713	305.061	6.4	ns

1.4.3. Haemolysins

The haemolytic and cytotoxic activities of *V. anguillarum* are important virulence factors for fish. Some cytotoxic proteins have been characterized to date including *empA*, *vah1* cluster (*vah1* and *plp* genes), *vah2-5* haemolysins and the multifunctional autoprocessing Rtx toxin (MARTX, *rtxACHBDE*) (Li *et al.*, 2008). These haemolysins are

the ones responsible for the characteristic haemorrhagic septicaemia of vibriosis (Hirono *et al.*, 1996; Li *et al.*, 2008). The genome of *V. anguillarum* RV22 encodes the Vah1-3 and MARTX toxins (does not contain *empa*, *vah4* nor *vah5*). Interestingly, while *vah2* was almost constitutively expressed in all assayed conditions (statistically significant differences were not observed), *vah1*, *vah3* and MARTX were significantly induced when *V. anguillarum* was grown under low iron. *vah1* and *vah2* showed high expression levels under iron excess conditions (FRKM of 1439 and 1194, respectively). These findings contrast with the low expression levels of MARTX and *vah3* (FRPKM of 60.4 and 105, respectively). MARTX is expressed only when the bacterium senses low iron availability, increasing 10.6-fold the operon transcription (Table IV.7).

Notably, while *vah1* maximal expression was observed under low-iron at 25 °C (FPKM of 4190), MARTX is highly expressed at 15 °C (*rtxA* FPKM of 415 at 25 °C and 1399 at 15 °C), showing a general 2.4-fold increase. Thus, each haemolysin is preferentially expressed at a different temperature.

Table IV.7. Expression levels and fold change of haemolysin-encoding genes. Darker colour denotes higher expression. Fold change values with $p < 0.05$ are shown. ns, no significant differences.

Gene	Expression level (FPKM)			Fold change	
	Fe(+) 25°C	Fe(-) 25°C	Fe(-) 15°C	Fe(+) 25°C vs Fe(-) 25°C	Fe(-) 25°C vs Fe(-) 15°C
Haemolysins					
<i>vah2</i> (WP_010317353.1)	1194.68	936.151	665.078	ns	ns
<i>vah1</i> (WP_019282664.1)	1439.24	4190.97	2080.54	2.9	ns
<i>vah3</i> (WP_019282064.1)	105.953	224.066	269.647	2.1	ns
MARTX					
<i>rtxA</i> (WP_019282576.1)	35.3543	415.329	1399.13	11.7	3.4
<i>rtxC</i> (WP_010848330.1)	33.3572	418.414	983.098	12.5	2.3
<i>rtxH</i> (WP_013856638.1)	280.614	2960.8	6558.39	10.6	2.2
<i>rtxB</i> (WP_019282577.1)	4.45415	44.0058	180.25	9.9	4.1
<i>rtxC</i> (WP_010319619.1)	5.10154	56.6148	276.16	11.1	4.9
<i>rtxD</i> (WP_017047016.1)	3.2314	24.6371	95.0801	7.6	3.9
<i>rtxA</i> CHBDE	60.4	653.3	1582.0	10.6	2.4

MARTX and Vah1 are the main responsible for the haemolytic and cytotoxic activities of *V. anguillarum* in fish (Hirono *et al.*, 1996; Li *et al.*, 2008). MARTX depends on the expression of six genes (*rtxABCHBDE*), which encode a potent toxin RtxA, a toxin activator RtxC, and the specialized TISS RtxDBE, responsible for RtxA secretion (Li *et al.*, 2008). Both haemolysins have a cytotoxic effect on Atlantic salmon kidney cells and only a *vah1 rtxA* double mutant was no longer cytotoxic. Though, when the implication of MARTX and Vah1 in virulence was studied using Atlantic salmon as fish model, only strains containing a *rtxA* deletion had reduced virulence. Consequently, it was proposed as a major virulence factor for *V. anguillarum* (Li *et al.*, 2008). Remarkably, the water temperature used in the experimental infection was not mentioned (Li *et al.*, 2008), however, salmon infections should occur at a low temperature of ca 15 °C, the temperature that favours MARTX maximal expression. Therefore, the implication of MARTX in virulence in the reported works could be overestimated as both haemolysins expression is temperature dependent.

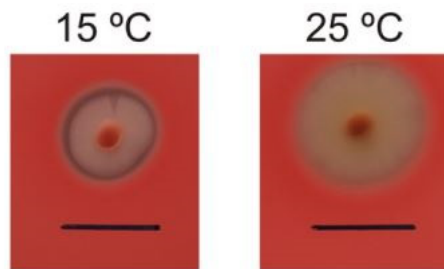


Figure IV.6. Haemolytic activity of *V. anguillarum* at 15 and 25 °C. A loopful of cells grown in iron deficiency was placed onto sheep blood agar plates and the haemolytic activity was observed by the appearance of a translucent halo.

To evaluate the effect of temperature in *V. anguillarum* haemolytic activity, a loopful of biomass of RV22 strain, cultured in CM9 plates supplemented with 50 μM of the chelating agent 2,2'-dipyridyl, was placed onto sheep blood agar plates (Figure IV.6) After incubation at 25 or 15 °C, the appearance of a translucent halo around the biomass is indicative of haemolytic activity. A higher translucency of the haemolytic halo was detected when cells were grown at 15 °C, but a

larger halo was observed at 25 °C. These results indicate that different haemolysins are produced at 15 and 25 °C. (Figure IV.6).

1.4.4. Chemotaxis and Motility

Chemotaxis and motility have been recognized as virulence related factors (Larsen *et al.*, 2004; Guanhuo *et al.*, 2018). Conversely to what was observed for other virulence factors, genes related to chemotaxis and flagellum synthesis were significantly down-regulated, between 3.6- and 2.1-fold, when *V. anguillarum* was grown under low iron availability. In addition, a significant down-regulation of these genes was observed when the temperature was dropped to 15 °C. Although genes encoding structural components of the flagellar system were down-regulated, they exhibited a high basal expression and some proteins of the flagellar motor were even induced, however, no statistically significant differences were observed (Table IV.8).

V. anguillarum exhibits rapid motility by means of a polar flagellum and the chemotactic motility is essential for virulence when the host encounters the pathogen in the aqueous environment (O'Toole *et al.*, 1999). Interestingly *V. anguillarum* responds chemotactically to a wide range of chemoattractants allowing the infection of different fish epithelia (O'Toole *et al.*, 1999). *V. anguillarum* is chemotactic in a wide temperature range nonetheless the optimal temperature for chemotaxis is 25 °C congruent with its optimal growth temperature (Larsen *et al.*, 2004). In fact, *V. anguillarum* responds chemotactically to fish skin and intestinal mucus, however the flagellum is only essential for the initial steps of infection. The flagellum may act as a motility organelle or has an adhesin for binding mucosal tissue and *V. anguillarum* swimming speed is also temperature dependent as it is reduced at low temperatures (Ormonde *et al.*, 2000; Larsen *et al.*, 2004). Once the pathogen has invaded the host, the flagellum is not needed for the progression of vibriosis (Milton *et al.*, 1996; O'Toole *et al.*, 1996).

Table IV.8. Expression levels and fold change of chemotaxis and motility related genes. Darker colour denotes higher expression. Fold change values with $p < 0.05$ were shown. ns, no significant differences.

Gene	Expression level (FPKM)			Fold change	
	Fe(+) 25°C	Fe(-) 25°C	Fe(-) 15°C	Fe(+) 25°C vs Fe(-) 25°C	Fe(-) 25°C vs Fe(-) 15°C
Chemotaxis and Motility					
<i>cheW</i> (WP_038170663.1)	2033.18	713.796	466.965	-2.8	ns
WP_026027244.1	256.73	108.131	78.4109	ns	ns
<i>cheY</i> (WP_017045237.1)	701.776	308.252	282.219	-2.3	ns
<i>cheA</i> (WP_019281574.1)	1079.22	388.021	409.818	-2.8	ns
<i>cheZ</i> (WP_017045236.1)	6726.19	2224.29	2189.51	-3.0	ns
<i>cheY</i> (WP_033197405.1)	3960.36	682.6	626.479	-5.8	ns
<i>fliA</i> (WP_010318887.1)	2318.56	493.279	352.914	-4.7	ns
<i>flhG</i> (WP_010318888.1)	1594.56	398.287	333.352	-4.0	ns
<i>flhF</i> (WP_019281575.1)	1204.46	260.841	208.399	-4.6	ns
<i>flhA</i> (WP_013856364.1)	80.239	45.1634	36.9497	ns	ns
<i>sixA</i> (WP_017042529.1)	3480.22	960.556	378.878	-3.6	-2.5
<i>fliE</i> (WP_026028064.1)	1104.24	440.209	339.411	-2.5	ns
WP_026028065.1	82.0278	72.2388	94.2691	ns	ns
WP_013856306.1	74.9664	38.7162	34.272	ns	ns
WP_017045739.1	98.6652	55.1108	44.2178	ns	ns
<i>fliS</i> (WP_010318718.1)	9202.2	1267.04	1278.27	-7.3	ns
<i>fliD</i> (WP_019281598.1)	542.424	202.725	180.483	-2.7	ns
<i>flaG</i> (WP_013856302.1)	41456.6	15525.9	8205.19	-2.7	ns
<i>flaB</i> (WP_026028066.1)	10285.3	3051.42	2738.72	-3.4	ns
<i>flaB</i> (WP_019281599.1)	4917.86	790.794	899.291	-6.2	ns
<i>flaB</i> (WP_019281600.1)	697.139	104.123	157.355	-6.7	ns
<i>fliN</i> (WP_010318705.1)	197.341	104.657	90.697	ns	ns
<i>fliM</i> (WP_013856317.1)	173.746	71.1982	81.0141	-2.4	ns
<i>fliL</i> (WP_000796796.1)	725.779	238.571	164.089	-3.0	ns
WP_017048845.1	1261.68	243.46	305.046	-5.2	ns
<i>flgF</i> (WP_006881570.1)	236.927	82.0141	54.171	-2.9	ns
<i>flgE</i> (WP_026027395.1)	619.483	338.421	385.431	ns	ns
<i>flgD</i> (WP_013856252.1)	992.065	333.312	220.056	-3.0	ns
<i>flgC</i> (WP_010319383.1)	5470.65	1634.97	992.253	-3.3	ns
<i>flgB</i> (WP_013856251.1)	4452.93	1073.12	771.889	-4.1	ns
<i>cheR</i> (WP_013856250.1)	2118.36	310.161	347.366	-6.8	ns

(cont.)					
<i>chew</i> (WP_013856249.1)	2889.64	683.392	557.727	-4.2	ns
<i>flgA</i> (WP_043004140.1)	112.189	189.412	240.587	ns	ns
<i>flgM</i> (WP_013856247.1)	1657.65	279.441	266.407	-5.9	ns
<i>flgN</i> (WP_013856246.1)	849.376	226.752	245.953	-3.7	ns
<i>flgP</i> (WP_017043110.1)	2526.36	595.867	355.34	-4.2	ns
WP_013856244.1	401.789	80.6444	86.1174	-5.0	ns
<i>flgT</i> (WP_019281754.1)	339.406	148.865	107.485	-2.3	ns
VAR_RS0102305	21834.7	33357.1	22907.7	ns	ns
WP_026027396.1	1396.51	880.517	498.776	ns	ns
<i>flaA</i> (WP_017045944.1)	7543.89	2803.26	1071.3	-2.7	-2.6
<i>flgL</i> (WP_019281751.1)	356.513	192.279	107.453	ns	ns
<i>flgK</i> (WP_019281752.1)	182.764	87.2139	40.9505	-2.1	-2.1
<i>flaC</i> (WP_026029038.1)	22960.9	1829.66	1880.75	-12.5	ns
<i>flgJ</i> (WP_013856257.1)	63.5011	50.5542	43.3766	ns	ns
<i>flgI</i> (WP_019281753.1)	110.014	73.702	60.0677	ns	ns
<i>flgH</i> (WP_017045947.1)	95.3077	61.1727	34.6172	ns	ns
<i>flgG</i> (WP_010319379.1)	154.99	75.1964	53.9199	-2.1	ns
VAR_RS0102350	206.088	75.1498	50.6109	-2.7	ns
WP_019281759.1	28.3258	34.4234	44.4516	ns	ns
WP_019281760.1	13.2131	15.6022	25.9253	ns	ns
WP_019281761.1	14.7701	10.0167	9.17567	ns	ns
WP_019281762.1	173.367	51.4949	43.6861	-3.4	ns
WP_019281763.1	658.807	228.179	237.553	-2.9	ns
WP_043004148.1	284.354	126.086	114.275	-2.3	ns
WP_019281765.1	1131.32	173.517	112.271	-6.5	ns
<i>fliL</i> (WP_013855488.1)	473.644	129.04	99.0488	-3.7	ns
<i>motB</i> (WP_017044193.1)	1016.9	357.034	341.787	-2.8	ns
<i>pomA</i> (WP_013857399.1)	2871.64	828.47	582.023	-3.5	ns
<i>motX</i> (WP_013855917.1)	1576.73	596.259	907.818	-2.6	ns
<i>motY</i> (WP_010318471.1)	84.8421	28.7748	22.8028	-2.9	ns
<i>cheWYAZ</i>	2130.5	598.5	487.6	-3.6	ns
Flagella operon	3134.4	1404.9	970.7	-2.1	ns

An *in vitro* experiment was performed to confirm the motility of *V. anguillarum* under iron availability and iron limitation. *V. anguillarum* colonies were stabbed in the centre of a tube containing soft agar supplemented with iron or the iron chelator 2,2'-dipyridyl. The tubes were incubated at 25 or 15 °C.

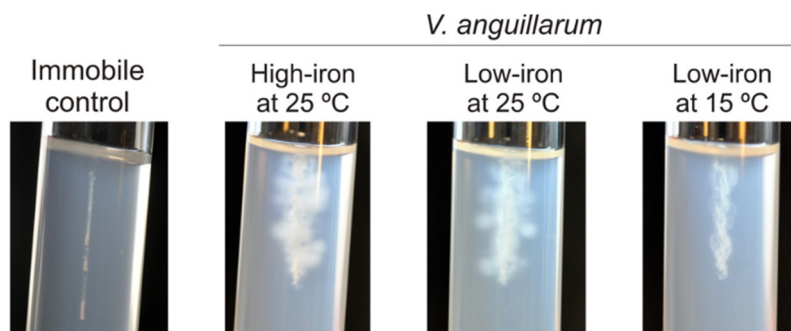


Figure IV.7. *V. anguillarum* motility observed under iron excess at 25 °C and iron restriction at 25 and 15 °C. *V. anguillarum* colonies were stabbed into soft agar and the appearance of cloudiness indicated motility.

The appearance of cloudiness around the central puncture indicates motility. When compared to a non-motile bacterium, *V. anguillarum* motility was higher under iron availability. Under iron starvation and when the temperature dropped to 15 °C, the flagellar motility tended to decrease (Figure IV.7).

1.4.5. Iron uptake systems

Bacteria can acquire iron, an element essential for metabolic pathways and intracellular survival, by synthesizing specialized systems. Iron can be obtained directly from the host haem group or haem containing proteins or by the production of high-affinity extracellular ferric-chelators, siderophores (Wandersman and Delepelaire, 2004).

V. anguillarum genome harbours genes that encode functions related to the acquisition and utilization of the haem group (*huvABCDZX*) (Mouriño *et al.*, 2004), the acquisition of ferrous iron (*feoABC*) (Lemos and Osorio, 2010) and two siderophore systems, the

chromosomally encoded vanchrobactin (*vabABCDEFGHRSR mbtH*) and piscibactin (*araCIC2* and *irp*).

Iron acquisition systems are strongly up-regulated under iron starvation (Table IV.9). *feoB*, that mediates ferrous iron acquisition (Lemos and Osorio, 2010), was 5.9-fold induced. *huvBCDZX* genes encoding haem uptake and utilization system (Mouriño *et al.*, 2004) showed a 26.4-fold increase in their transcription level. Notably, both siderophore systems presented an up-regulation. Vanchrobactin *vabABCDEFGHRSR mbtH* genes showed a global 60-fold change increase, while piscibactin *araCIC2* and *irp* genes showed an 8.2-fold increase. At 25 °C the vanchrobactin siderophore system is strikingly more expressed than piscibactin showing more than a 20-fold change difference in expression (FRPKM of 917.3 for vanchrobactin and 41.9 for piscibactin). Ferri-siderophores and the haem group are internalized through specific outer membrane transporters. This process is mediated by the inner membrane potential achieved through the energy transducing TonB-ExbB-ExbD system (TonB1 and TonB2 systems) whose expression increased upon iron starvation, 45.4- and 17.4-fold increase (Table IV.9). The vanchrobactin outer membrane receptor gene *fvfA* was preferentially expressed at 25 °C, showing a 173.7-fold change increased expression.

Notably, piscibactin biosynthetic and uptake genes were greatly up-regulated at low temperature. At 15 °C under iron deprived conditions, *araCIC2* and *irp* genes achieved the maximal FRPKM of 219.6. Under this condition, the genes *araCI*, encoding the putative AraC-like transcriptional regulator, and *frpA*, the gene encoding the putative outer membrane transporter for the ferri-piscibactin complex, are among the most up-regulated genes as their transcription showed a 6.8- and 3.9-fold increase. Interestingly, at 15 °C, *huvA*, the haem group outer membrane receptor gene, showed its maximal expression level, FRPKM 1287.1. Genes *frpB* and *frpC* encode the putative inner membrane ABC transporters and their expression level increased at 15 °C, showing a 3.7- and 4.6-fold increase. When in the cytosol, the ferri-siderophores complexes are dissociated for further use. This function might be accomplished by reductases and interestingly the locus WP_017045538.1 was induced under iron restriction (18.1-fold

change), and it would encode an uncharacterized putative ferric-siderophore utilization protein. All results put together greatly suggest that the genes that encode piscibactin are among the most induced genes at cold-temperatures. The work carried out to characterize the mechanisms involved in the temperature-dependent regulation of *irp*-HPI genomic element, which encodes the piscibactin siderophore system, are detailed below in Chapter IV.3.

Table IV.9. Expression level and fold change of iron uptake systems related genes. Darker colour denotes higher expression. Fold change values with $p < 0.05$ were shown. ns, no significant differences.

Gene	Expression level (FPKM)			Fold change	
	Fe(+) 25°C	Fe(-) 25°C	Fe(-) 15°C	Fe(+) 25°C vs Fe(-) 25°C	Fe(-) 25°C vs Fe(-) 15°C
<i>feoB</i> (WP_017045230.1)	213.2	1255.9	589.1	5.9	-2.1
Heme uptake system					
<i>huvA</i> (WP_029388256.1)	6.3	212.3	1287.1	33.9	6.1
<i>huvZ</i> (WP_017044790.1)	5.1	143.0	186.3	27.8	ns
<i>huvX</i> (WP_026027544.1)	144.4	3558.2	1592.7	24.6	-2.2
<i>huvB</i> (WP_019282390.1)	8.0	383.0	268.0	47.6	ns
<i>huvC</i> (WP_010319753.1)	24.5	145.2	85.9	5.9	ns
<i>huvD</i> (WP_043004479.1)	3.4	284.5	65.4	84.0	-4.4
<i>huvBCDXZ</i>	23.2	611.3	490.4	26.4	ns
<i>tonBexbBD</i>	5.7	258.5	309.3	45.4	ns
<i>tonB2exbB2D2ttpC</i>	33.0	573.5	394.0	17.4	ns
Vancomycin system					
<i>vabB</i> (WP_019281789.1)	51.1	6875.3	4367.6	134.6	ns
<i>vabS</i> (WP_019281790.1)	7.0	139.8	112.7	20.0	ns
<i>vabF</i> (WP_019281791.1)	14.5	758.5	601.6	52.2	ns
<i>mbtH</i> (WP_019281792.1)	1.3	367.0	225.6	ns	ns
<i>vabH</i> (WP_019281793.1)	3.1	383.9	492.7	125.1	ns
<i>fvtA</i> (WP_019281795.1)	20.2	3511.5	1767.0	173.7	ns
<i>vabD</i> (WP_017045634.1)	3.8	244.3	125.9	64.8	-1.9
<i>tonB</i> (WP_050934211.1)	12.8	47.6	124.4	3.7	2.6
<i>vabR</i> (WP_029388129.1)	1.8	28.2	30.8	15.4	ns
<i>vabG</i> (WP_019281786.1)	11.2	1037.3	927.6	92.7	ns
<i>vabA</i> (WP_013857267.1)	92.7	717.7	691.5	7.7	ns
<i>vabC</i> (WP_043004165.1)	10.9	1940.7	2476.8	177.6	ns
<i>vabE</i> (WP_019281788.1)	6.4	334.7	523.4	52.4	ns
<i>vabABCDEFGHSR mbtH</i>	15.3	917.3	700.7	60.0	ns

Piscibactin system					
<i>araC1</i> (WP_019281874.1)	0.7	120.9	825.5	172.9	6.8
<i>araC2</i> (WP_019281875.1)	0.7	12.2	47.4	16.7	3.9
<i>frpA</i> (WP_019281876.1)	0.9	123.2	479.0	135.1	3.9
<i>irp8</i> (WP_019281877.1)	0.4	19.6	69.5	45.4	3.5
<i>irp2</i> (WP_019281878.1)	0.2	25.5	110.9	125.0	4.3
<i>irp5</i> (WP_019281883.1)	0.4	50.9	307.8	ns	ns
<i>irp9</i> (WP_019281882.1)	0.8	84.2	529.3	99.8	ns
<i>irp4</i> (WP_019281881.1)	0.8	54.0	157.0	ns	ns
<i>irp3</i> (WP_019281880.1)	0.4	25.9	87.6	ns	ns
<i>irp1</i> (WP_019281879.1)	0.4	42.4	187.7	97.4	4.4
<i>frpB</i> (WP_017046020.1)	1.5	32.1	119.9	21.6	3.7
<i>frpC</i> (WP_019281884.1)	1.1	15.0	69.5	13.8	4.6
<i>araC1C2</i> and <i>irp</i> genes	5.1	41.9	219.6	8.2	5.2
Ferri-siderophore reductase					
WP_017045538.1	100.998	1828.74	1981.8	18.1	ns

1.5. SUMMARY OF CHAPTER 1

Transcriptomic data gives a new insight into the physiological adaptations of *V. anguillarum* that enable this bacterium to infect fish that live at different temperatures. The results revealed a deep adaptation of *V. anguillarum* to grow under iron restrictive conditions. Genes related to the energetic metabolism were down-regulated whereas virulence related genes were induced under this condition. Chemotaxis, motility and T6SS1 are preferentially expressed at 25 °C. Conversely, the haemolysin RTX, T6SS2 and genes related to exopolysaccharide assembly and transport were induced by a temperature shift to 15 °C. Concretely, iron limitation induced the expression of siderophores however their relevance varies with temperature. The piscibactin siderophore system is one of the most up-regulated virulence factor at 15 °C, while vanchrobactin, seems to be the preferential system to supply iron at 25 °C. Notably, in *V. anguillarum* temperature and iron availability are key signals for the expression of virulence factors. Their expression varies between temperatures, which indicates a different relevance for the infection of cold- and warm-water adapted fish species.

2. CHARACTERIZATION OF THE PISCIBACTIN GENOMIC ISLAND (*irp*-HPI) AND IDENTIFICATION OF ELEMENTS REQUIRED FOR PISCIBACTIN PRODUCTION AND UTILIZATION

2.1. *V. ANGUILLARUM irp*-HPI GENOMIC ISLAND (*irp*-HPI_{VANG})

V. anguillarum RV22 genome harbours an *irp* gene cluster, with a size of about 40 kb, located in chromosome II between locus AEH34691 and AEH34692. This cluster shows a similar gene structure and a homology at the amino acid level between 52 and 66% when compared to its ortholog counterpart located in the plasmid pPHDP70 of *P. damselae* subsp. *piscicida*. As reported for pPHDP70, RV22 *irp* gene cluster contains all the genes necessary for piscibactin synthesis and utilization, however an *entD* homolog is absent (Figure IV.8). *entD* encodes a 4'-phosphopantetheinyl transferase required to activate the peptide synthesis domains of NRPS. Although an *entD* is not present in the piscibactin gene cluster, the vanchrobactin gene cluster in strain RV22 harbours a gene encoding the same function, *vabD* that could complement in *trans* the other siderophore system (Figure I.8).

The *irp* gene cluster shows some of the marked characteristics of genomic islands acquired via horizontal gene transfer. Apart from its A+T high content (G+C content of ca. 46.7%), adjacent to the *irp* gene cluster there are three *orfs* that encode a putative transposon belonging to the Tn7 superfamily (Figure IV.8). These transposons are associated with the insertion of horizontally acquired genes that are not inserted near tRNAs. The nucleotide sequence of these *orfs* show an 86% identity to *V. parahaemolyticus* pathogenicity island (Vp-PAI), suggesting that *irp* genes are part of a genomic island, which was named as *irp*-HPI_{Vang}.

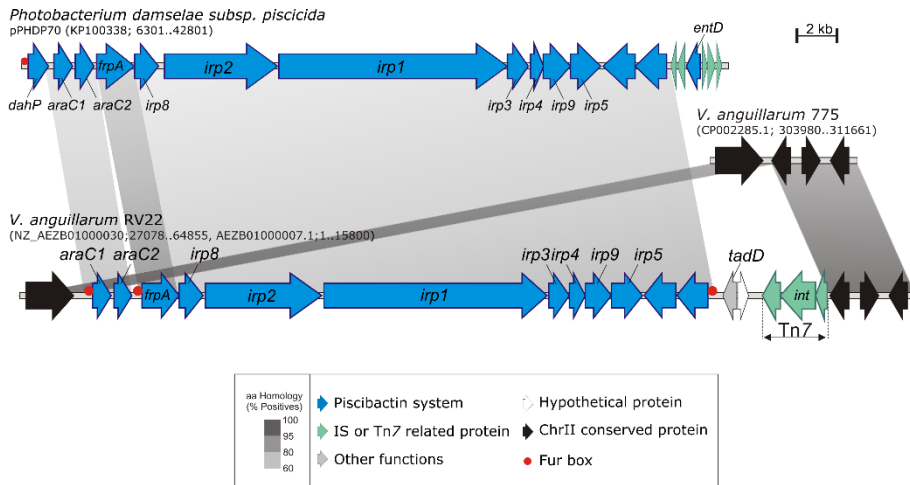


Figure IV.8. Comparison between the piscibactin gene cluster of *V. anguillarum* RV22 strain and *P. damsela subsp. piscicida*.

To evaluate the distribution of the *irp* genomic island among different *V. anguillarum* strains, an *in silico* search using 43 genomes available in GenBank was performed (Table IV.10). Results showed that the *irp* gene cluster is present in several strains including some highly pathogenic isolates harbouring an active vanchrobactin siderophore system (Table IV.10). The prevalence of the *irp* gene cluster in highly virulent strains suggests a relevant role in virulence. Interestingly, some of these pathogenic strains (H1610, 90-11-286, 178/90, DSM 21597 and 91-7-154), have been associated with high virulence for larvae of cod, turbot, and halibut in experimental infections where the animals were maintained at 7 °C, 9 °C and 16 °C respectively (Rønneseth, *et al.*, 2017). These data suggest that piscibactin genes are widespread among different *V. anguillarum* strains that can infect cold- and warm-water adapted fish species. Remarkably, the presence of the piscibactin gene cluster appears to be incompatible with the presence of the anguibactin encoding plasmid pJM1, so none of the analysed strains showed the simultaneous presence of the piscibactin and anguibactin systems.

Table IV.10. Distribution of vanchrobactin, piscibactin and anguibactin gene clusters in several *V. anguillarum* strains whose genome is available in GenBank. Grey shadow indicates active systems in each genome.

Strain	Serotype	Vanchrobactin	Piscibactin	Anguibactin	Assembly
775	O1	(+)	-	+	GCA_000217675.1
M3	O1	(+)	-	+	GCA_000462975.1
N B10	O1	(+)	-	+	GCA_000786425.1
90 -11 -286	O1	+	+	-	GCA_001660505.1
MVAV6203	O1	(+)	-	+	GCA_002163795.1
87 -9 -116	O1	(+)	-	+	GCA_002211505.1
JLL237	O1	+	+	-	GCA_002211985.1
S3 4/9	O1	+	+	-	GCA_002212005.1
VIB43	O1	+	+	-	GCA_002287545.1
ATCC -68554	O1	(+)	-	+	GCA_002291265.1
MVM425	O1	(+)	-	+	GCA_003031205.1
96F	O1	+	-	-	GCA_000257165.1
A023	O1	+	-	-	GCA_001989675.1
87 -9 -117	O1	(+)	-	+	GCA_001989715.1
91 -8 -178	O1	(+)	-	+	GCA_001989735.1
178/90	O1	(+)	-	+	GCA_001989755.1
261/91	O1	(+)	-	+	GCA_001989775.1
Ba35	O1	(+)	-	+	GCA_001989795.1
T265	O1	(+)	-	+	GCA_001989815.1
51/82/2	O1	(+)	-	-	GCA_001989855.1
LMG12010	O1	(+)	-	+	GCA_001989875.1
S2 2/9	O1	+	+	-	GCA_001989895.1
9014/8	O1	(+)	-	+	GCA_001989915.1
87 -9 -116	O1	(+)	-	-	GCA_001989935.1
90 -11 -287	O1	(+)	-	+	GCA_001990025.1
91 -7154	O1	(+)	-	+	GCA_001990045.1
601/90	O1	(+)	-	+	GCA_001990065.1
6018/1	O1	(+)	-	+	GCA_001990085.1
VA1	O1	(+)	-	+	GCA_001990105.1
VIB 93	O1	(+)	-	+	GCA_001990125.1
VIB 18	O1	(+)	-	+	GCA_001998845.1
VIB12	O2	+	+	-	GCA_002310335.1
ATCC 14181	O2	+	-	-	GCA_001718015.1
DSM 21597	O2	+	+	-	GCA_001989995.1
M93	O2a	+	-	-	GCA_002901125.1
HI610	O2a	+	+	-	GCA_001989835.1
RV22	O2a	+	+	-	GCA_000257185.1
HI618	O2b	(+)	-	-	GCA_002078035.1
4299	O2b	+	-	-	GCA_001989655.1
CNEVA NB11008	O3	+	+	-	GCA_002212025.1
PF430 -3	O3	+	-	-	GCA_001989695.1
PF7	O3	+	-	-	GCA_001997225.1
PF4	O3	+	-	-	GCA_002813835.1

Thode and colleagues (2018) showed that while some siderophore systems are present only in a determined lineage of *Vibrionaceae*, others such as piscibactin have a wide distribution and are present in several phylogenetic lineages, which would be explained by the fact that it is encoded in a horizontally transferable element which would have contributed decisively to its dissemination among *Vibrionaceae* species.

2.2. PRODUCTION OF PISCIBACTIN BY *V. ANGUILLARUM* RV22

To ascertain the production and utilization of piscibactin by *V. anguillarum* RV22, cross-feeding assays were initially performed (Figure IV.9). As indicator strains in these assays, we used *V. anguillarum* RV22 and a derivative mutant defective in *vabD* gene. This mutant, previously obtained (Balado *et al.*, 2008), is unable to produce any siderophore. The utilization of the siderophore produced by the tested strains, results in the appearance of a growth halo around the biomass of the tested strain.

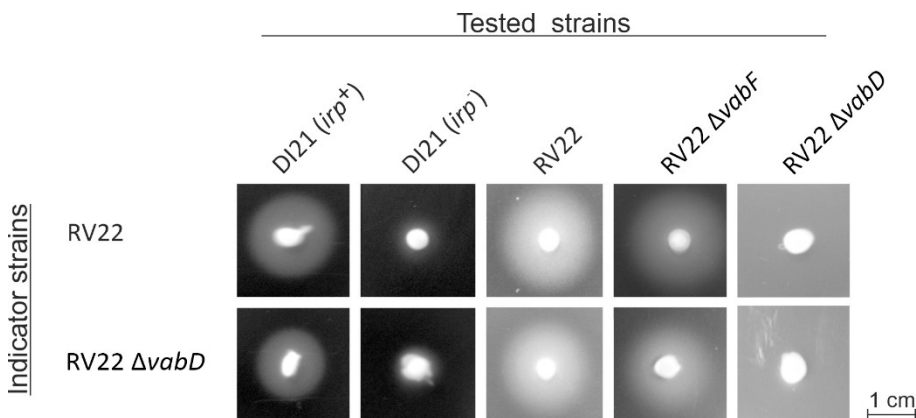


Figure IV.9 Cross-feeding assay to determine the production and utilization of piscibactin as iron source. The growth halo around the biomass of the tested strains (DI21 *irp*⁺, DI21 *irp*⁻, RV22, RV22 Δ *vabF* and RV22 Δ *vabD*) indicates that the indicator strain (RV22 and RV22 Δ *vabD*) can use the siderophore produced by the tested strain to overcome iron limitation.

Both indicator strains, RV22 and RV22 Δ *vabD*, could be cross fed by a piscibactin producing strain, *P. damsela* subsp. *piscicida* DI21 *irp*⁺. The *P. damsela* subsp. *piscicida* DI21 mutant strain impaired for

the synthesis of piscibactin, DI21 *irp*⁻, did not promote the growth of any of the indicator strains. RV22 $\Delta vabF$ (unable to produce vanchrobactin) could cross-feed both indicator strains indicating that a second siderophore, must be synthesized. Growth halos were not observed in any of the indicators when RV22 $\Delta vabD$ was used as tested strain. This result confirms that *vabD* is essential for the synthesis of vanchrobactin and piscibactin and that RV22 $\Delta vabD$ does not produce any siderophore.

The cross-feeding assays indicate that *V. anguillarum* produces piscibactin or a piscibactin-like siderophore. In a previous work, a method was developed for the isolation of piscibactin from cell-free supernatants of *P. damselae* subsp. *piscicida* (Souto *et al.*, 2012), therefore the same methodology was applied to ascertain whether *V. anguillarum* RV22 synthesizes piscibactin in addition to vanchrobactin. The chemical work was performed in collaboration with the group of Dr. Carlos Jiménez, an Organic Chemistry research group at the University of A Coruña.

V. anguillarum RV22 was grown under iron limited conditions and GaBr₃ was added to stabilize the siderophore. Liquid chromatography-mass spectrometry (LC-MS) was applied and the first siderophore to be detected was vanchrobactin with a retention time of 2.74 min. The complex siderophore-Ga(III) was detected with the same retention time as the one for *P. damselae* subsp. *piscicida* (*t_R* 9.56 min) (Figure IV.10).

Additionally, the same methodology was applied for the detection of siderophores in the mutant strains RV22 $\Delta vabF$ (impaired to synthesize vanchrobactin) and RV22 $\Delta vabD$ (mutant for the 4'-phosphopantetheinyl transferase). In the RV22 $\Delta vabF$ mutant only the complex piscibactin-Ga(III) was detected, showing a retention time of 9.71 min. In RV22 $\Delta vabD$ mutant, neither siderophore was detected, confirming that *vabD* is essential for the synthesis of both siderophores, vanchrobactin and piscibactin.

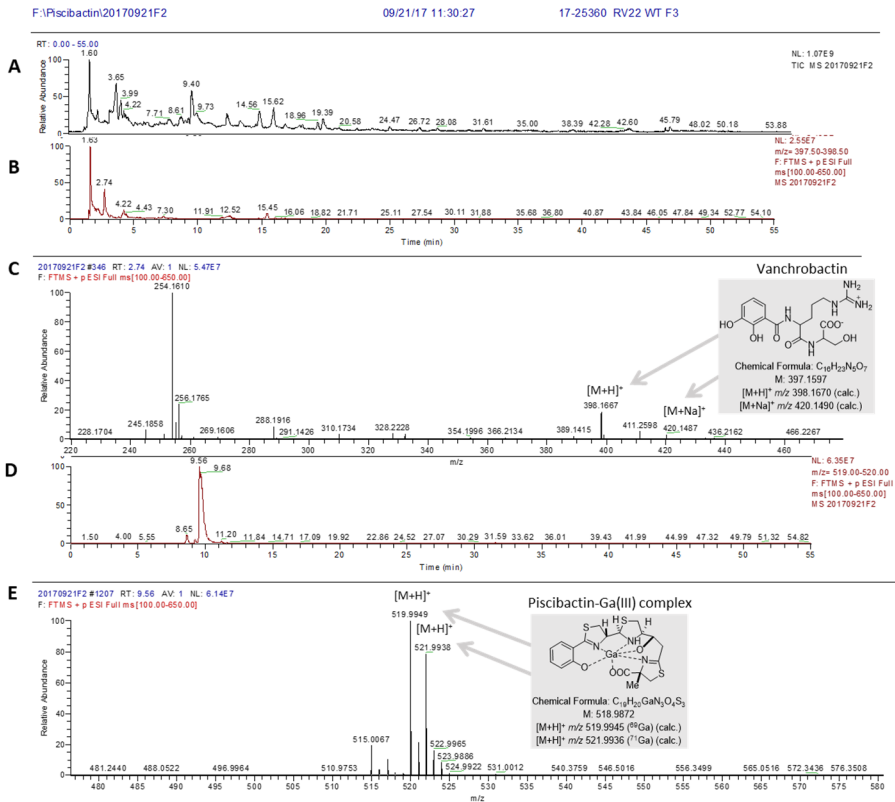


Figure IV.10. LC-MS chromatograms for the detection of vanchrobactin and piscibactin-Ga(III) complex in *V. anguillarum* RV22. (A) Total ion chromatogram (B) Extracted mass chromatogram showing the peak with the retention time of 2.74 min. (C) Peak with the retention time 2.74 min identified as vanchrobactin. (D) Extracted mass chromatogram showing the peak with the retention time of 9.56 min. (E) Peak with the retention time 9.56 min identified as piscibactin-Ga(III) complex.

The synthesis of more than one siderophore can enhance cell fitness and consequently niche flexibility and pathogenesis (Garcia *et al.*, 2011; Cordero *et al.*, 2012; Dumas *et al.*, 2013). The synthesis of multiple siderophores has been reported in the fish pathogen *Aeromonas salmonicida* that synthesizes acinetobactin and amonabactin (Balado *et al.*, 2015).

The use of siderophores synthesized by other organisms the so-called siderophore piracy, is well documented. The acquisition of

xenosiderophores has been reported in *Pseudomonas fluorescens*, that down-regulates genes involved in pyoverdine and enantiopyochelin synthesis and up-regulates the expression of the outer membrane transporter *foxA* when in the presence of *Streptomyces ambofaciens*. Though, the synthesis of more than one siderophore increases the possibility of one of the siderophores not been available for the competitors (McRose *et al.*, 2018). Furthermore, synthesis of multiple siderophores can also be a strategy to limit iron availability in the environment and restrict it to competitors. Additionally, siderophores can also act as metallophors and uptake other metals besides iron, allowing the bacteria survival in other environments. For instance, yersiniabactin is involved in zinc acquisition and protects the cell against copper toxicity during infection (Chaturvedi *et al.*, 2012; Bobrov *et al.*, 2014; Koh and Henderson, 2015; Holden *et al.*, 2016).

Multiple siderophores can also work synergistically in the acquisition of iron. Siderophores with different iron affinities can be synthesized under diverse iron availabilities. In *Azotobacter vinelandii*, azotobactin is only synthesized under strong iron limitation (McRose *et al.*, 2018). Piscibactin, yersiniabactin and pyochelin share some structural characteristics and it has been reported that the co-expression of yersiniabactin with other catecholate siderophores improves the virulence of uropathogenic *E. coli* (Crosa and Walsh, 2002; Garcia *et al.*, 2011; Souto *et al.*, 2012).

2.3. CHARACTERIZATION OF FUNCTIONS REQUIRED FOR PISCIBACTIN PRODUCTION

The high pathogenicity island *irp*-HPI includes genes that putatively encode functions related to the synthesis (*irp1-5* and *irp9*), transport (*frpABC* and *irp8*), and regulation (*araC1* and *araC2*) of the piscibactin siderophore system. Nonetheless, many aspects about piscibactin synthesis and transport remain unknown. The genes *irp1* and *irp2* showed an amino acid similarity of 52% and 57%, respectively, with its ortholog counterpart from *P. damsela* subsp. *piscicida*. In this bacterium, Irp1 showed the functional structure of a NRPS/PKS with a similarity of 62% to *Y enterocolitica* HMWP1 (Osorio *et al.*, 2006). The insertional inactivation of *irp1* in *P. damsela*

subsp. *piscicida*, impaired the bacterium to produce siderophores and to grow under iron deficient conditions (Osorio *et al.*, 2006). Therefore, *irp1* would encode a large NRPS/PKS involved in the synthesis of piscibactin (Osorio *et al.*, 2006; Souto *et al.*, 2012). Notably, the refractory nature of *P. damsela* subsp. *piscicida* to genetic manipulation, did not allow the construction of mutant strains using the allelic exchange strategy. Moreover, the role of the type II thioesterase Irp4 in the release of the nascent siderophore from the multienzymatic complex remains uncharacterized. The other aspects uncharacterized concern the route of export and internalization of the siderophore. *irp8* encodes a putative exporter that belongs to the major facilitator superfamily, *frpA* encodes a putative TonB-dependent outer membrane transporter and *frpB* and *frpC* putatively encode an ABC transporter but no experimental evidence has been conducted yet.

2.3.1. Deletion of *irp1* impairs piscibactin synthesis

To study the role of *irp1* in piscibactin synthesis and consequently evaluate the contribution of piscibactin to growth under iron deficiency, a deletion mutant of *irp1* was constructed in a RV22 wild-type and RV22 $\Delta vabF$ background. The growth ability of the resultant mutants, RV22 $\Delta irp1$ (impaired for the synthesis of piscibactin), RV22 $\Delta vabF\Delta irp1$ (impaired for the synthesis of vanchrobactin and piscibactin), as well as RV22 and RV22 $\Delta vabD$ was measured under iron limited conditions by supplementing the CM9 minimal medium with the chelating agent EDDA (strong chelating agent) or 2,2'-dipyridyl (weak chelating agent) (Figure IV.11).

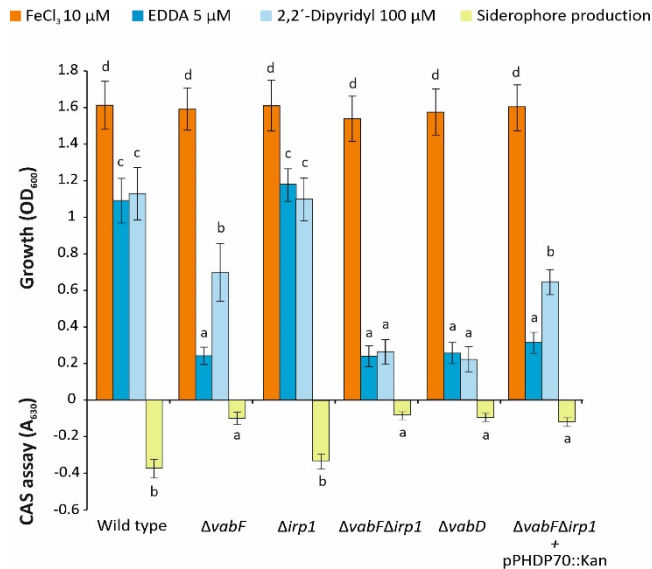


Figure IV.11. Growth ability of *V. anguillarum* RV22 and its derivative mutants. Growth was measured under iron excess (10 μM FeCl₃) or iron starvation by the addition of 5 μM EDDA or 100 μM 2,2'-dipyridyl. Siderophore production was determined using the CAS liquid assay. Bars labelled with the same letters (a, b, c, d) did not show statistically significant differences (student's *t*-test).

Under iron excess, no statistically significant differences were observed for the tested strains, as all of them reached an OD₆₀₀ ca. 1.6. However, under iron restrictive conditions different growth phenotypes emerged. When 5 μM of EDDA was added, the parental strain RV22 and the mutant RV22 Δ*irp1* (impaired for piscibactin synthesis) showed no significant differences in growth (OD₆₀₀ ca. 1.1). Regarding RV22 Δ*vabF*, that only produces piscibactin, there was a significant decrease in growth achieved, showing a phenotype like RV22 Δ*vabF*Δ*irp1* (OD₆₀₀ ca. 0.2). These results suggest that the inactivation of the vanchrobactin siderophore system strongly impacts the growth ability of *V. anguillarum* under strong iron deficiency (EDDA). Surprisingly, when 2,2'-dipyridyl was used as chelating agent, RV22 Δ*vabF* reached a growth close to 35% of the growth observed for the wild-type strain, OD₆₀₀ = 0.7. RV22 Δ*irp1* showed a growth capacity indistinguishable from that of RV22. RV22 Δ*vabF*Δ*irp1* and RV22 Δ*vabD* had a similar growth potential and it was identical for both chelating agents. To determine siderophore production, cell-free supernatants of cultures

grown with 50 μ M 2,2'-dipyridyl were evaluated for siderophore activity with the CAS liquid assay. RV22 and RV22 $\Delta irp1$ showed the highest siderophore production ca. -0.35. Although RV22 $\Delta vabF$ showed an intermediate growth, siderophore production was residual. Interestingly, siderophore production in RV22 $\Delta vabF$ was indistinguishable from that observed for RV22 $\Delta vabF\Delta irp1$ and RV22 $\Delta vabD$ (A₆₃₀ ca. -0.1). When RV22 $\Delta vabF\Delta irp1$ mutant was complemented with plasmid pPHDP70 from *P. damsela* subsp. *piscicida* that harbours the *irp* genes, the parental phenotype was restored (Figure IV.11).

Evaluation of siderophore production by the CAS assay revealed that the growth potential directly correlates to the synthesis of vanchrobactin as the mutant impaired for vanchrobactin synthesis (RV22 $\Delta vabF$) showed extremely low levels of siderophore production. In fact, the siderophore production phenotype of RV22 $\Delta vabF$ was similar to the mutants RV22 $\Delta vabD$ and RV22 $\Delta vabF\Delta irp1$, both impaired for the synthesis of vanchrobactin and piscibactin. These results suggest that *irp1* encodes biosynthetic functions as its deletion in a $\Delta vabF$ background impaired siderophore synthesis and the growth under iron limited conditions. Furthermore, vanchrobactin may be the primary siderophore of *V. anguillarum* and a more efficient source of iron since piscibactin efficiency as siderophore seems to be dependent on the iron source.

2.3.2. *Irp4* is required for piscibactin synthesis

Many natural products such as siderophores are produced by multimodular non-ribosomal peptide synthetases (NRPS) and polyketide synthases (PKS) from the assembling of different amino acids and polyketide moieties, respectively. Each module of a NRPS/PKS incorporates a single precursor into the nascent product that will remain covalently attached to the peptidyl carrier protein (PCP) domain (Schwarzer *et al.*, 2003). Thus, the final product must be released from the final PCP by a C-terminal type I thioesterase domain (TE I) present in the last NRPS/PKS of the route (Drake *et al.*, 2016).

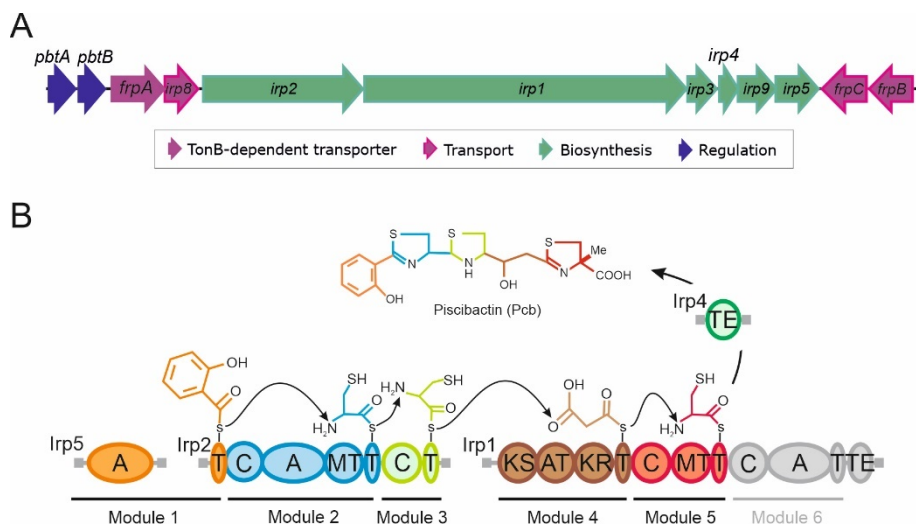


Figure IV.12. Genetic organization of piscibactin gene cluster in *V. anguillarum* (*araC1* and *araC2* were renamed to *pbtA* and *pbtB*, respectively) (A) and biosynthetic model for piscibactin assembly showing module organization and predicted substrate of Irp5, Irp2 and Irp1. Conserved domain annotation: A - adenylation, T - aryl or peptidyl carrier protein, C - condensation, MT - methyltransferase, KS - ketoacyl synthase, AT - acyltransferase, KR - ketoacyl reductase, TE - thioesterase.

The piscibactin system possesses a C-terminal TE domain as part of the NRPS/PKS enzyme Irp1 in addition to a separate gene (*irp4*) that encodes a putative external TE (Figure IV.12). *irp4* is located between the biosynthetic genes *irp3* and *irp9* (Figure IV.12.A) with which it is co-transcribed (see below). The translated product of *irp4* showed sequence similarity (42% of identity, 56% similarity) to type II thioesterases such as YbtT from NRPS/PKS biosynthetic pathway of yersiniabactin (Ohlemacher *et al.*, 2018). In addition, Irp4 contains the characteristic conserved thioesterase signature motif GHSMG from the amino acid position 99 to 103 (Geoffroy *et al.*, 2000). This finding suggests that *irp4* encodes a functional type II TE. To analyse the role of Irp4 in piscibactin production, a defective mutant for this gene was constructed in RV22 Δ *vabF* background where the production of vanchrobactin was abolished and so this mutant strain only synthesizes piscibactin. Then, the resultant RV22 Δ *vabF* Δ *irp4* mutant was challenged to grow and produce siderophores under different iron

availability conditions (Figure IV.13).

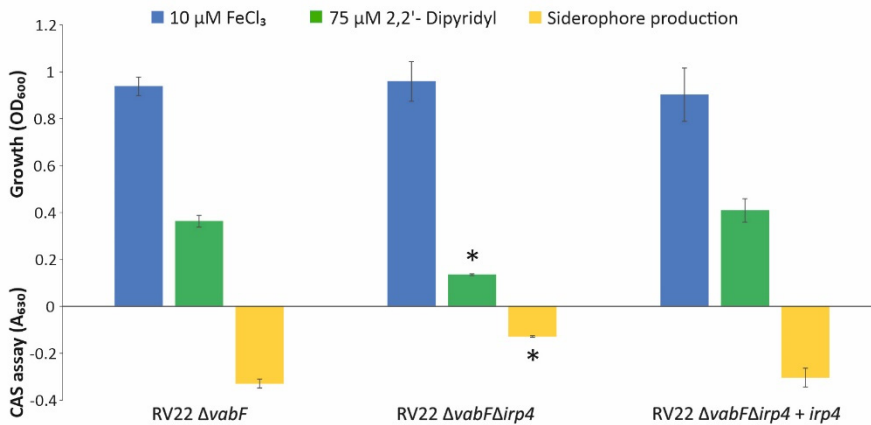


Figure IV.13. Growth ability of *V. anguillarum* RV22 strain, RV22 $\Delta vabF\Delta irp4$ and complemented strain. Parental and mutant strain were grown in CM9 medium under iron excess or iron deprived conditions. Cultures grown in CM9 supplemented with 25 μM 2,2'-dipyridyl were used to test siderophore production using the liquid CAS assay. Asterisk denotes statistically significant differences, * $p < 0.05$ (student's *t*-test).

As shown in Figure IV.13, parental strain RV22 $\Delta vabF$ and RV22 $\Delta vabF\Delta irp4$ mutant were able to grow under iron excess conditions, showing indistinguishable growth capacity. By contrast, RV22 $\Delta vabF\Delta irp4$ mutant was impaired to grow under iron-restricted conditions, achieved by the addition of 2,2'-dipyridyl at 75 μM to CM9 minimal medium. This mutant reached an OD_{600} ca. 0.15 when challenged to grow under stringent iron deprived conditions. Further evaluation of siderophore content in the culture supernatants of both strains showed that the deletion of *irp4* caused a strong decrease in siderophore production compared to the parental strain RV22 $\Delta vabF$ (Figure IV.13). The siderophore production measured using the liquid CAS assay revealed that the mutant strain achieved an A_{630} ca. -0.18. Moreover, piscibactin was not detected in the cell-free supernatants of RV22 $\Delta vabF\Delta irp4$ by LC-MS analysis. When this mutant $\Delta irp4$ was complemented with a functional version of the *irp4* gene, it recovered the parental phenotype both in terms of growth ability and siderophore production (Figure IV.13).

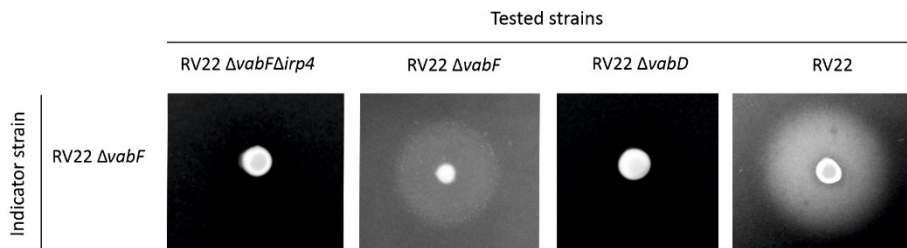


Figure IV.14. Cross-feeding assay to evaluate the production of piscibactin by the tested strains RV22 $\Delta vabF\Delta irp4$, RV22 $\Delta vabF$, RV22 $\Delta vabD$ and RV22. A growth halo around the biomass of the tested strains indicates the use of the siderophore by the indicator strain.

In addition, a cross-feeding assay was performed to analyse the synthesis of piscibactin by the mutant RV22 $\Delta vabF\Delta irp4$, using RV22 $\Delta vabF$ as indicator strain. A growth halo indicates the utilization of the piscibactin produced by the tested strain (Figure IV.14). The tested strains RV22 $\Delta vabF$, that produces piscibactin, and RV22, that produces both piscibactin and vanchrobactin, induced the growth of the indicator strain. Nonetheless, RV22 $\Delta vabF\Delta irp4$ and RV22 $\Delta vabD$ showed identical phenotypes and were not able to cross-feed the RV22 $\Delta vabF$ strain (Figure IV.14). These results provide further evidence that the thioesterase encoded by *irp4* is required for piscibactin synthesis.

Usually, external type II thioesterases (TE II) are related to editing functions as they can remove non-extendable structures to promote the continuous flow of several rounds of biosynthesis by liberating the CP domains of NRPS/PKS from precursors (Drake *et al.*, 2016). Piscibactin is a yersiniabactin-like siderophore and yersiniabactin system also possesses a C-terminal TE domain as part of the NRPS/PKS synthetase HMWP1 and an external TE named YbtT (Pelludat *et al.*, 1998). Both TE domains are functional and ensure appropriate levels of yersiniabactin production (Bobrov *et al.*, 2002). While the internal C-terminal TE releases the complete siderophore from the multienzymatic complex, YbtT avoids the formation of aberrant molecules that would block siderophore synthesis (Bobrov *et al.*, 2002). Thus, although YbtT is not required for bacterial growth, it is needed for yersiniabactin maximal production as it prevents the incorporation of erroneous

precursors that could inhibit the biosynthesis pathway (Ohlemacher *et al.*, 2018). Piscibactin biosynthetic pathway is constituted by the NRPS/PKSs Irp5, Irp2 and Irp1 which form a synthesis complex organized in 6 modules (Figure IV.12.B). Irp1 contains an internal C-terminal thioesterase domain that would release the complete siderophore at the final step of biosynthesis (Irp1 module 6). However, the predicted final product of the route was not detected neither in *P. damselae* subsp. *piscicida* (Souto *et al.*, 2012) nor in *V. anguillarum* supernatants (data not shown), and the piscibactin chemical structure is in accordance with the early release of the nascent siderophore at domain 5 (Figure IV.12.B). Since *irp4* defective mutant lacks siderophore production, the results greatly suggest that Irp4 is required for piscibactin production since it mediates the early liberation of the siderophore from Irp1.

Piscibactin is part of an intriguing and complex system as its labile and unstable nature once synthesized, leads to its rapid degradation to intermediate forms which greatly difficult its detection (Souto *et al.*, 2012). The inability to detect the predicted final siderophore structure questions the role of the C-terminal thioesterase. It cannot be ruled out that module 6 would be non-functional or that its product may be a cryptic metabolite that is synthesized only under specific conditions. Nonetheless, the loss of Irp4 activity abolishes siderophore production denoting a direct role of Irp4 in piscibactin synthesis and in its release from the NRPS/PKS multienzymatic system.

2.3.3. Irp8 is involved in piscibactin export

When bacteria sense a low iron environment, siderophore synthesis is induced. Upon synthesis, siderophores must be exported to the extracellular environment to scavenge iron to fulfil the cell requirements (Ratledge and Dover, 2000). The mechanisms behind the secretion of siderophores remain poorly characterized in most bacteria. Two major siderophore export systems have been described: ATP-dependent efflux pumps (Seeger and van Veen, 2009) and the major facilitator superfamily (MFS) (Fluman and Bibi, 2009). In the *irp*-HPI, *irp8* encodes a putative exporter MFS-like. Irp8 is a polytopic protein, spanning the membrane several times, with 12 domains that represent

transmembrane segments typically found in this type of efflux pumps (Furrer *et al.*, 2002). A three-dimensional structure model based in its closest homologue was constructed using SWISS-MODEL (Figure IV.15)

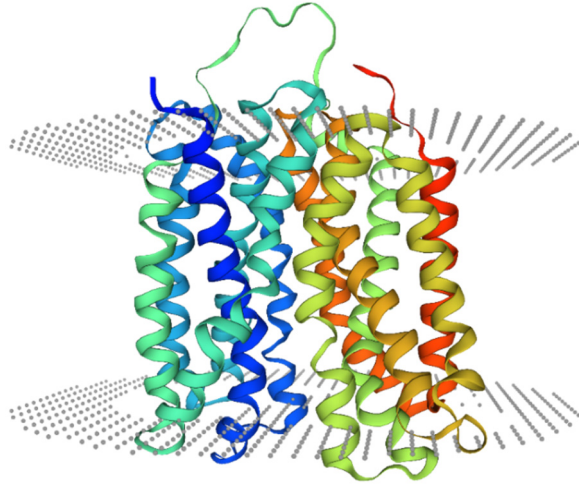


Figure IV.15. Three-dimensional structure of the exporter Irp8 created using SWISS-MODEL and based on the MFS closest homolog.

To analyse the role of Irp8 in piscibactin exporting route, an in-frame deletion mutant was constructed, and the resultant mutant was challenged to grow under different iron availability conditions: iron excess, CM9 minimal medium supplemented with 10 μM FeCl_3 and iron limited conditions, CM9 medium supplemented with 75 μM 2,2'-dipyridyl. Siderophore production in the parental strain and in its derivative Δirp8 mutant was evaluated in cell-free supernatants of cultures grown under weak iron deprived conditions (CM9 + 25 μM 2,2'-dipyridyl) (Figure IV.16). When grown in iron excess (addition of 10 μM FeCl_3), the mutant RV22 $\Delta\text{vabF}\Delta\text{irp8}$ showed a growth capacity indistinguishable from that of the parental strain RV22 ΔvabF . Both strains achieved an OD_{600} ca. 0.9. However, when challenged to grow under stringent iron limitation by the addition of 2,2'-dipyridyl at 75 μM , both strains showed opposite growth phenotypes. While the parental strain had a 55% decrease in its growth ability when compared to iron excess conditions (OD_{600} ca. 0.4), the Δirp8 mutant achieved

growth levels significantly lower (OD_{600} around 0.2) when grown under strong iron limited conditions (Figure IV.16). The decrease in growth of RV22 $\Delta vabF\Delta irp8$ also correlates with a lower siderophore production. Nonetheless, the deletion of the putative exporter *irp8* did not totally abolished siderophore production. The mutant strain achieved an A_{630} ca. -0.15. This siderophore production might indicate that residual amounts of piscibactin or intermediates that retain siderophore activity are still secreted to the extracellular medium which also correlates to the intermediate growth phenotype observed.

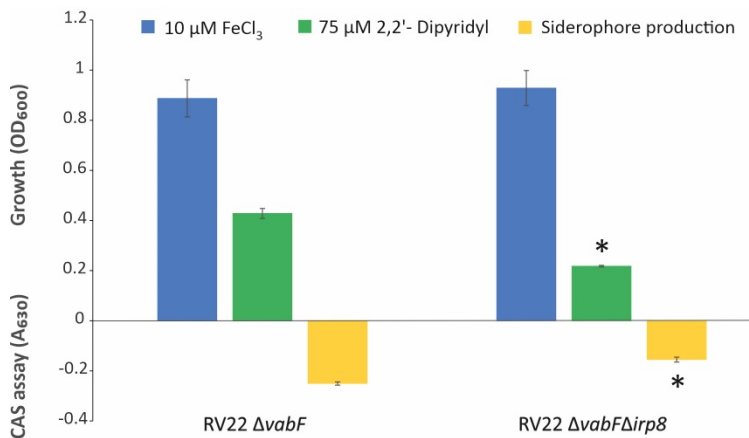


Figure IV.16. Growth ability of *V. anguillarum* RV22 $\Delta vabF$ and RV22 $\Delta vabF\Delta irp8$ in iron excess (10 μM $FeCl_3$) or iron deficiency (75 μM 2,2'-dipyridyl). Siderophore production was quantified in cell-free supernatants of cultures grown in CM9 supplemented with 25 μM 2,2'-dipyridyl. Asterisk denotes statistically significant differences, * $p < 0.05$ (student's *t*-test).

To evaluate the ability of the $\Delta irp8$ mutant strain to produce piscibactin, a cross-feeding assay was performed (Figure IV.17). The RV22 $\Delta vabD$ strain can grow under iron limited conditions using the siderophore produced by RV22 $\Delta vabF$ and RV22. However, the RV22 $\Delta vabF\Delta irp8$ mutant was unable to cross-feed RV22 $\Delta vabD$ strain. This result clearly suggests that RV22 $\Delta vabF\Delta irp8$ mutant is deficient in siderophore export and *Irp8* is involved in the secretion process of piscibactin.

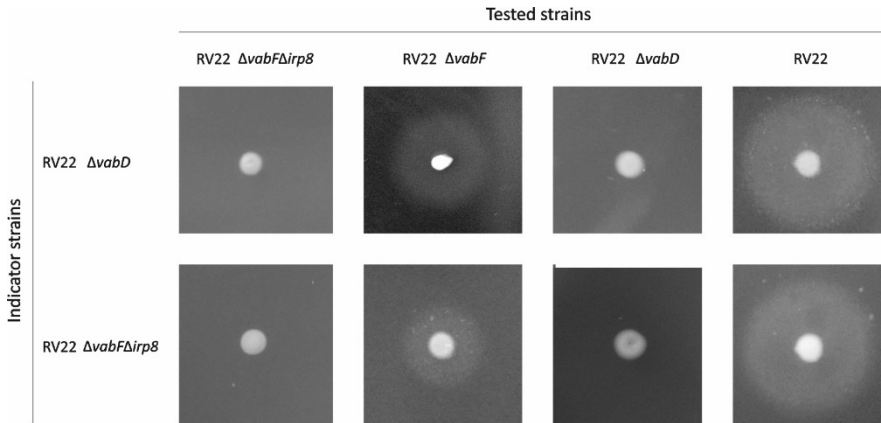


Figure IV.17. Cross-feeding assay to evaluate the ability of the tested strains (RV22 $\Delta vabF\Delta irp8$, RV22 $\Delta vabF$, RV22 $\Delta vabD$ and RV22) to produce siderophores that the indicator strain could use to grow under iron limited conditions.

Previous studies on siderophores export routes suggest that most exporter deletion mutants show intermediate siderophore production and growth phenotype when compared to the parental strain (Furrer *et al.*, 2002; Balado *et al.*, 2006). These phenotypes may be due to the presence of alternative secretion routes or the passive secretion of subproducts of siderophore synthesis that still show some activity when measured by the CAS assay (Furrer *et al.*, 2002; Balado *et al.*, 2006). The enterobactin siderophore export system in *E. coli* is one of the best characterized routes (Furrer *et al.*, 2002; Horiyama and Nishino, 2014). Enterobactin is exported to the periplasm through EntS, a major facilitator transporter (Furrer *et al.*, 2002). An EntS homolog, VabS, was also identified in *V. anguillarum*. VabS is involved in the secretion of the siderophore vanchrobactin (Balado *et al.*, 2006). Nonetheless, the secretion of secondary metabolites requires at least three components: an active efflux pump (eg. EntS, VabS and Irp8), a membrane fusion protein that connects the pump to the outer membrane, and a channel located at the outer membrane that allows the passage of the siderophore (Furrer *et al.*, 2002). Enterobactin is captured in the periplasm by the RND transporters AcrB, AcrD and MdtABC and then exported to the extracellular environment through the outer membrane

channel TolC (Bleuel *et al.*, 2005; Horiyama and Nishino, 2014). The involvement of a RND efflux system has been described for vibriobactin secretion in *V. cholerae* (Kunkle *et al.*, 2017). According to this, it can be hypothesized that the MFS mediated efflux pump Irp8 of *V. anguillarum* secretes piscibactin to the periplasm and yet undetermined components export the siderophore to the extracellular environment.

2.4. PISCIBACTIN CONTRIBUTES SIGNIFICANTLY TO *V. ANGUILLARUM* VIRULENCE

To study the contribution of piscibactin and vanchrobactin to *V. anguillarum* virulence, an experimental infection was performed using turbot fingerlings. The virulence assay was performed at 18-20 °C, temperature at which turbot are naturally maintained at fish farms. The fish were inoculated intraperitoneally with a dose of $2-4 \times 10^4$ CFU of the correspondent strain: RV22 wild-type strain or its derivative mutants (RV22 $\Delta vabF$, RV22 $\Delta irp1$, RV22 $\Delta vabF\Delta irp1$, RV22 $\Delta vabD$, and the complemented strain (RV22 $\Delta vabF\Delta irp1$ + pPHDP70). The fish were monitored for 7 days, and death events were daily registered (Figure IV.18). Five days post infection, the wild-type strain RV22 and the mutant impaired for vanchrobactin synthesis (RV22 $\Delta vabF$), produced mortalities in the same range, 80% and 88%, respectively. The fish challenged with the mutant that only synthesizes vanchrobactin, RV22 $\Delta irp1$, produced 56% mortality 6 days post infection. Conversely, the mutants unable to synthesize neither vanchrobactin nor piscibactin, RV22 $\Delta vabF\Delta irp1$ and RV22 $\Delta vabD$, reached a mortality of 12% and 8%, respectively, 7 days post infection. Notably, when piscibactin production was restored by gene complementation *in trans*, RV22 $\Delta vabF\Delta irp1$ + pPHDP70, the complemented strain reached 78% mortality, 6 days after infection (Figure IV.18). These results denote the strong effect of siderophores production, and in particular piscibactin production, in *V. anguillarum* virulence. At the tested conditions, when the fish were maintained at 18-20 °C during the experimental infection, piscibactin contributed more significantly than vanchrobactin to virulence.

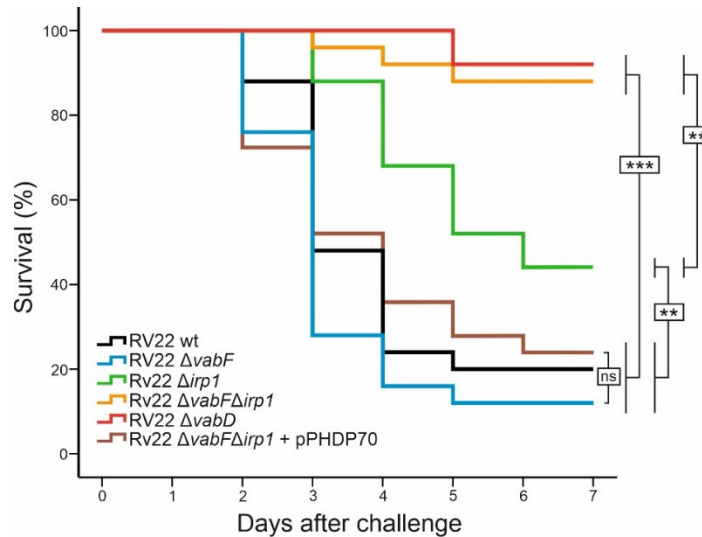


Figure IV.18. Percentage of survival, after 7 days, of fish challenged with RV22, RV22 $\Delta vabF$, RV22 $\Delta irp1$, RV22 $\Delta vabF\Delta irp1$, RV22 $\Delta vabD$ and RV22 $\Delta vabF\Delta irp1$ + pPHDP70. Statistically significant differences are marked with asterisks. * $p < 0.05$; ** $p < 0.01$; *** $p < 0.001$; ns, no statistically significant differences.

Remarkably, the inactivation of the piscibactin siderophore system did not impact greatly the ability of *V. anguillarum* to grow under iron restrictive conditions (Figure IV.11). In this case, vanchrobactin would be the siderophore that allows an efficient internalization of iron to the cell *in vitro*. Notably, piscibactin is only an efficient source of iron when the iron limitation is not stringent. However, these results clearly contrast with the virulence assay. The mutant strain that only synthesizes piscibactin achieved the maximal virulence and the inactivation of the piscibactin system resulted in a severe loss of virulence. In the infection challenge, the synthesis of piscibactin is sufficient to achieve a high virulence degree and, thus, vanchrobactin production could be more related to the survival in the environment.

2.5. CHARACTERIZATION OF FERRI-PISCIBACTIN UPTAKE

irp-HPI harbours genes that would encode the ferri-piscibactin uptake machinery (*frpABC*). Concretely, *frpA* would encode the putative outer membrane transporter for ferri-piscibactin acquisition

and *frpBC* the ABC transporter involved in ferri-piscibactin passage through the inner membrane.

2.5.1. FrpA and FrpBC are involved in ferri-piscibactin uptake

To analyse the role of FrpA and FrpBC in piscibactin uptake, an in-frame deletion mutant of each gene was constructed in a RV22 $\Delta vabF$ (impaired for vanchrobactin synthesis) background. Mutants and parental strains were grown in minimal medium under different iron availability conditions (Figure IV.19). When grown under iron excess, parental RV22 $\Delta vabF$ and mutant strains RV22 $\Delta vabF\Delta frpA$ and RV22 $\Delta vabF\Delta frpBC$ showed indistinguishable growth potentials. The RV22 $\Delta vabD$ mutant strain unable to synthesize both piscibactin and vanchrobactin also demonstrated the same growth ability, achieving an OD₆₀₀ ca. 1. However, when challenged to grow under strong iron deficit conditions by supplementing the CM9 minimal medium with 50 μM 2,2'-dipyridyl, the parental strain and its mutant derivatives showed different growth abilities. While the parental strain and RV22 $\Delta vabF\Delta frpA$ were able to grow under iron deficit, the $frpBC^-$ mutant showed a decrease in its growth potential. The parental strain achieved an OD₆₀₀ ca. 0.74 whereas the $frpBC^-$ mutant strain had a significant decrease in OD₆₀₀ to ca. 0.18. When the conditions passed to a more stringent iron restriction (75 μM 2,2'-dipyridyl), the growth phenotype of the mutant strains showed a marked decrease. Both mutant strains $frpA^-$ and $frpBC^-$ achieved an OD₆₀₀ ca. 0.18 and 0.1, respectively. Interestingly, the growth ability of RV22 $\Delta vabF\Delta frpBC$ was similar to that of the mutant strain impaired for siderophore synthesis. Remarkably, iron deficit impacts in a greater extent the growth of $frpBC^-$. This reduced growth ability contrasts with the siderophore production. The RV22 $\Delta vabF\Delta frpA$ and RV22 $\Delta vabF\Delta frpBC$ mutant strains showed an A₆₃₀ with similar levels as the parental strain, ca. -0.25 (Figure IV.19). Complementation of the RV22 $\Delta vabF\Delta frpA$ mutant strain with *frpA* wild-type gene, restored the parental phenotype. These results suggest that piscibactin is present in the extracellular environment, but it is not being internalized which impaired RV22 $\Delta vabF\Delta frpA$ growth under iron restriction. In addition,

FrpBC has an active role in the ability of RV22 $\Delta vabF$ to grow under iron deficit.

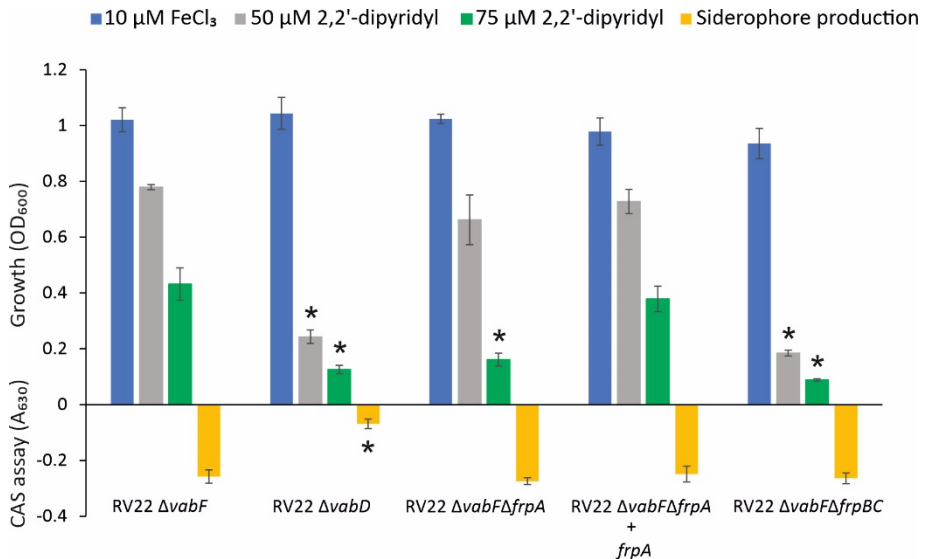


Figure IV.19. Growth ability of *V. anguillarum* RV22 $\Delta vabF$ and its derivative mutant strains RV22 $\Delta vabF\Delta frpA$ and RV22 $\Delta vabF\Delta frpBC$. Parental and mutant strains were challenged to grow under iron excess and iron restrictive conditions. Siderophore production was evaluated using the liquid CAS assay. Asterisks denote statistically significant differences, * $p < 0.05$ (student's *t*-test).

Furthermore, a cross-feeding assay showed that RV22 $\Delta vabF\Delta frpA$ can cross-feed its parental strain to use the siderophore produced by the tested strains. Thus, piscibactin secreted by RV22 $\Delta vabF\Delta frpA$ supports the growth of RV22 $\Delta vabF$ under iron deficit. However, RV22 $\Delta vabF\Delta frpA$ was unable to use the siderophore piscibactin produced by both RV22 $\Delta vabF$ and RV22 $\Delta vabF\Delta frpA$. These results suggest that FrpA must act as the outer membrane transporter for the ferri-piscibactin complex (Figure IV.20). Notably, RV22 $\Delta vabF\Delta frpBC$ can cross-feed its parental strain RV22 $\Delta vabF$. Conversely, RV22 $\Delta vabF\Delta frpBC$ cannot grow when cross-fed by piscibactin producing strains (RV22 $\Delta vabF\Delta frpBC$ and RV22 $\Delta vabF$). These results suggest that while the piscibactin export is accomplished, ferri-piscibactin internalization route was abolished at a concrete step.

Thus, FrpBC is required for the internalization of the ferri-piscibactin complex.

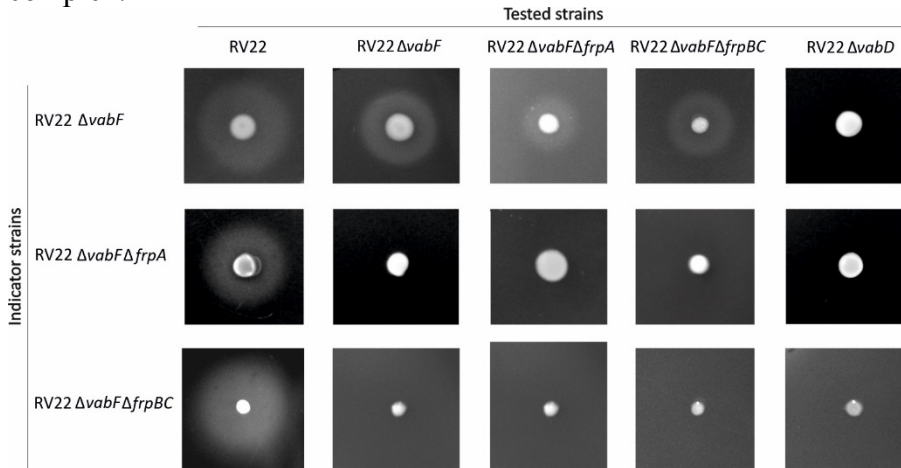


Figure IV.20. Cross-feeding assay to evaluate the production of siderophore by the tested strains (RV22, RV22 $\Delta vabF$, RV22 $\Delta vabF\Delta frpA$, RV22 $\Delta vabF\Delta frpBC$ and RV22 $\Delta vabD$) and its use by the indicator strains (RV22 $\Delta vabF$, RV22 $\Delta vabF\Delta frpA$ and RV22 $\Delta vabF\Delta frpBC$). A growth halo indicates the utilization of the siderophore by the indicator strain.

Interestingly, it has been reported that some ferri-siderophores complexes are dissociated in the periplasm and the reduced iron is internalized via the Feo system (Shin *et al.*, 2019). Nonetheless, the dramatic decrease in the ability to grow under weak iron restrictive conditions and the inability to be cross-fed by piscibactin producing strains indicates that FrpBC is required for the import of the ferri-piscibactin complex to the cytoplasm. Notably, ABC transporters have also been identified as the proteins that allow the internalization of ferri-anguibactin and ferri-vanchrobactin in *V. anguillarum* (Köster *et al.*, 1991; Naka *et al.*, 2013). The ferri-siderophore import occurs in a stepwise manner. Firstly, it must pass the outer membrane through a TonB-dependent transporter. Once the complex is at the periplasm it is combined with a periplasmic lipoprotein and then passes through the ABC transporter to be delivered at the cytoplasm (Li and Ma, 2017).

2.5.2. Distribution of *frpA* in different bacteria and phylogenetic analysis

The piscibactin siderophore system was firstly described in *P. damsela* subsp. *piscicida* (Osorio *et al.*, 2015). It was later reported that the *irp*-HPI genomic island is widespread among *Vibrionaceae*, specially in species grouped in the *Harveyi* and *Splendidus* clades (Thode *et al.*, 2018). Therefore, depending on the bacterial species there are some homologues of *frpA*, encoding different versions of the piscibactin transporter FrpA. To evaluate FrpA versions distribution, a BlastN search was performed using as a query *V. anguillarum frpA* sequence. Then, the sequences found were used to construct a phylogenetic tree (Figure IV.21).

The resultant phylogenetic tree showed that FrpA is widespread not only in *Vibrionaceae*, but it is also present in gamma-proteobacteria like *Shewanella*, *Marinomonas* and enterobacteria like *Xenorhabdus*, *Photorhabdus* and *Providencia*, displaying similarities higher than 62% (Figure IV.21). *V. anguillarum* is clustered in a clade with *V. ordalii* and *V. qinghaiensis*. In addition, these sequences are clustered with a bootstrap of 100 with several *V. cholerae frpA* sequences which reflect a close relationship between the *irp*-HPI elements present in the genome of these species. *P. damsela* subsp. *piscicida frpA* (*frpA_{Pdp}*) is clustered with *Vibrio* species generally related to bivalve molluscs infections such as *Vibrio ostreicida*, *Vibrio coralliilyticus* and *Vibrio neptunius* (Dubert *et al.*, 2017). The gene encoding the outer membrane receptor FrpA of *V. anguillarum* (*frpA_{Vang}*) shares a 66% homology identity and 81% similarity with the version of *frpA* present in the *P. damsela* subsp. *piscicida* genome (*frpA_{Pdp}*).

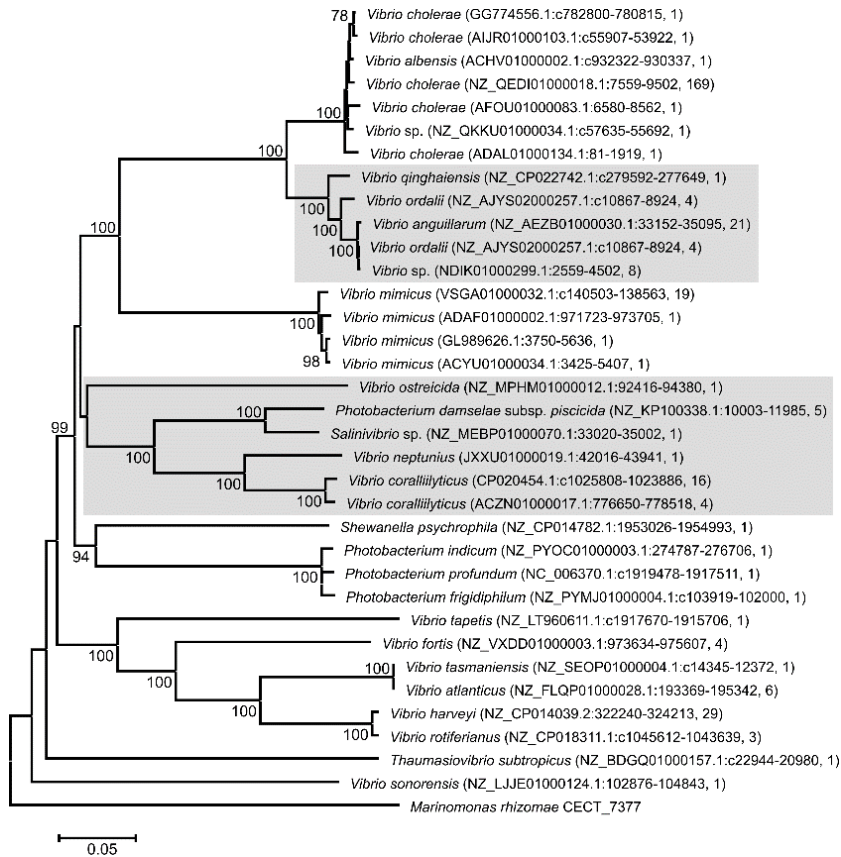


Figure IV.21. Phylogenetic tree of *frpA* homologues. Sequences are identified by species name, accession number and number of related genes deposited in GenBank. The tree was drawn to scale and branch length represents nucleotide p-distances. Bootstrap values higher than 70% are shown.

2.5.3. Structural requirements in piscibactin analogues to be transported through FrpA

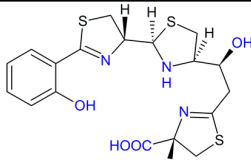
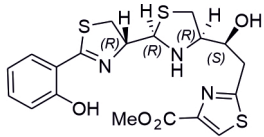
Outer membrane transporters are generally specific for its cognate ligand; however, some cases of ligand plasticity have been reported (Andrews *et al.*, 2003; Ghysels *et al.*, 2005; Naikare *et al.*, 2013; Wyckoff *et al.*, 2015; Rey-Varela *et al.*, 2019). As an example, the amonabactin outer membrane transporter FstC of the fish pathogen, *Aeromonas salmonicida* is one of the most versatile transporters, since

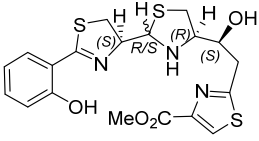
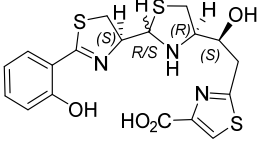
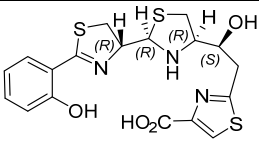
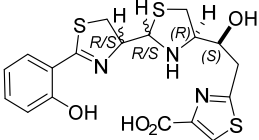
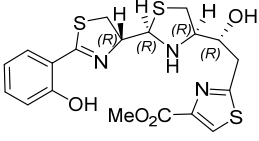
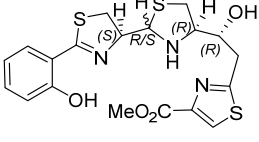
it can internalize the four natural amonabactin forms and some biscatecholate analogues (Rey-Varela *et al.*, 2019).

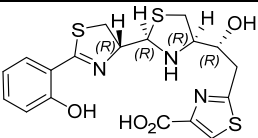
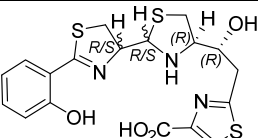
Once FrpA was identified as the outer membrane transporter for piscibactin (section above), some piscibactin analogues were designed and synthesized by the Organic Chemistry group (Prof. Carlos Jiménez) at the University of A Coruña, and their ability to be internalized via FrpA was evaluated. Thus, the structural requirements for piscibactin transport were studied.

The structures of the compounds tested are presented in Table IV.11. All piscibactin analogues tested have the substitution of the thiazoline group present in piscibactin for a thiazole ring. This modification would stabilize the compound. In addition, two sets bearing the thiazole ring were synthesized differentiating in the configuration of the hydroxyl group at C-13 position (13*S*, 13*R*) and have an altered configuration at C-9 and/or C-10. Moreover, the analogues bear a methyl ester or a carboxyl group. Evaluation of the biological activity of these compounds will allow the definition of the chemical groups involved in iron(III) chelation and/or the recognition by the piscibactin transporter FrpA.

Table IV.11. Structure of the natural piscibactin (1) and chemically synthesized analogues. The analogues have a thiazole ring among which two groups were designed that differ in the configuration at C-13 position. The analogues also have altered configuration at C-9 and/or C-10 and bear a methyl ester or a carboxyl group.

Piscibactin			1
13 <i>S</i> (natural configuration)	Methyl ester group	 Chemical Formula: C ₁₉ H ₂₁ N ₃ O ₄ S ₃ Exact Mass: 451,0694	6a

13S (natural configuration)	Methyl ester group	 <p>Chemical Formula: C₁₉H₂₁N₃O₄S₃ Exact Mass: 451,0694</p>	6b/c
	Carboxylic acid group	 <p>Chemical Formula: C₁₈H₁₉N₃O₄S₃ Exact Mass: 437,0538</p>	7b/c
		 <p>Chemical Formula: C₁₈H₁₉N₃O₄S₃ Exact Mass: 437,0538</p>	7a
		 <p>Chemical Formula: C₁₈H₁₉N₃O₄S₃ Exact Mass: 437,0538</p>	7a-d
13R (Non-natural configuration)	Methyl ester group	 <p>Chemical Formula: C₁₉H₂₁N₃O₄S₃ Exact Mass: 451,0694</p>	8a
		 <p>Chemical Formula: C₁₉H₂₁N₃O₄S₃ Exact Mass: 451,0694</p>	8b/c

¹³ R (Non-natural configuration)	Carboxylic acid group	 <p>Chemical Formula: C₁₈H₁₉N₃O₄S₃ Exact Mass: 437,0538</p>	9a
		 <p>Chemical Formula: C₁₈H₁₉N₃O₄S₃ Exact Mass: 437,0538</p>	9a-d

2.5.3.1. Piscibactin analogues activity in *V. anguillarum*

To analyse the ability of *V. anguillarum* to use the piscibactin analogues as iron source, an in-frame deletion mutant of *frpA* was constructed in a RV22 $\Delta vabD$ background, which is impaired for piscibactin and vanchrobactin synthesis. Thus, the growth achieved in growth promotion assays by the *frpA*(+) (RV22 $\Delta vabD$) and *frpA*(-) (RV22 $\Delta vabD\Delta frpA$) strains would be proportional to the biological activity of the analogues tested. The biological activity of the chemically synthesized analogues was compared to the natural piscibactin (Figure IV.22). Under strong iron deprived conditions, piscibactin efficiently promoted the growth of the *frpA*(+) strain. For each concentration tested, 20, 10, 2 and 0.2 μM , piscibactin showed the highest siderophore activity of all the compounds. Interestingly, the growth achieved by the *frpA*(+) strain only decreased when piscibactin was added at the lowest concentration of 0.2 μM . As expected, the addition of piscibactin at 10 μM did not promote the growth of the *frpA* deletion mutant, confirming that FrpA mediates the uptake of the ferri-piscibactin in *V. anguillarum*.

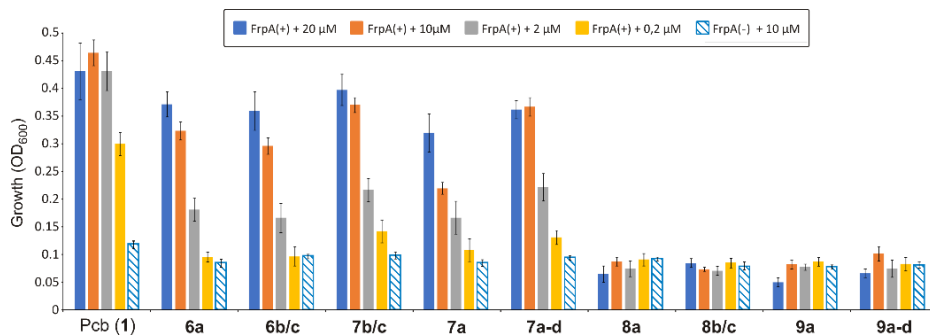


Figure IV.22. Growth promotion assay. RV22 $\Delta vabD$ (*frpA*(+)) and RV22 $\Delta vabD\Delta frpA$ (*frpA*(-)), were challenged to grow in minimal medium under iron limited conditions and use piscibactin or chemically synthesized analogues as iron source.

The assay revealed that despite being less effective in growth promotion than the natural piscibactin, all the 13*S*-thiazole piscibactin analogues (compounds 6a, 6b/c, 7b/c, 7a and 7a-d) promoted the growth of the *V. anguillarum frpA*(+) at all tested concentrations. Similarly, to piscibactin, none of the analogues promoted the growth of the *frpA*(-) strain. Conversely, the analogues 8a-c and 9/a-d bearing the configuration 13*R* at the C-13 position did not support the growth of neither *V. anguillarum frpA*(+) nor *frpA*(-) strains (Figure IV.22).

To assess the ability of each analogue to chelate iron, a CAS liquid assay was performed. Piscibactin and the 13*S* analogues 6 and 7 showed a positive CAS result indicating that they can chelate iron. By contrast, the analogues 8 and 9 bearing the 13*R* configuration, gave a negative CAS result, which explains their inability to promote *V. anguillarum* growth. Notably, although the analogue 7b/c exhibited a higher biological activity than its methyl ester 6b/c and thiazole 7a counterpart, the differences were not statistically significant. Globally, it can be observed that the 13*S* thiazole analogues 6 and 7 showed similar activities which suggests that the configuration at the position C-9 and C-10 had no major influence on the biological activity of these analogues. These results suggest that the configuration of the hydroxyl group at C-13 is essential for iron(III) chelation and consequently for the recognition by the outer membrane transporter FrpA. Remarkably, the activity shown by analogues 6 and 7 indicates that the substitution

of the thiazoline ring for a more stable thiazole ring and/or the presence of a methyl ester group instead of a carboxylic acid functionality did not affect the recognition of the analogues by FrpA. These groups would not constitute key structural elements of the siderophore and may not interact in a particular manner with the recognition domain of FrpA.

2.5.3.2. Piscibactin analogues activity in *P. damsela* subsp. *piscicida*

P. damsela subsp. *piscicida* DI21 strain was used to evaluate the ability of a piscibactin producing strain to use the piscibactin analogues tested as iron source. DI21 was assayed to grow under iron deficiency using the thiazole analogues 6a and 7a-d (Figure IV.23). The results showed that the 13S analogues were efficiently internalized by *P. damsela* subsp. *piscicida* via FrpA_{Pdp}. Notably, this transporter exhibited almost the same specificity for the chemically synthesized analogues and the natural piscibactin. At the tested concentrations, the growth achieved showed no significant differences regarding all the compounds tested (Figure IV.23).

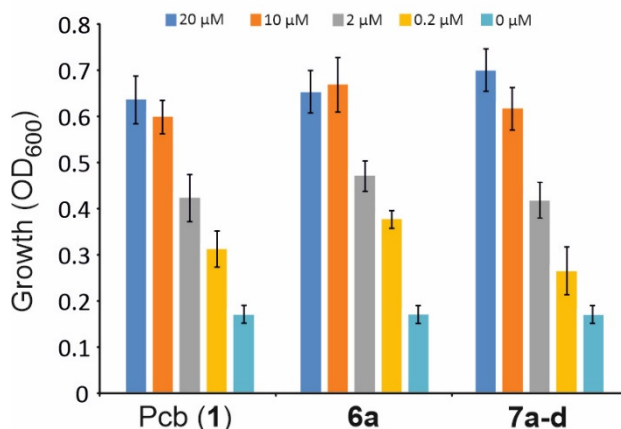


Figure IV.23. Growth promotion assay. *P. damsela* subsp. *piscicida* DI21 strain was challenged to grow in minimal medium under iron deficit conditions and use piscibactin or chemically synthesized analogues 6a and 7a-d as iron source.

2.6. SUMMARY OF CHAPTER 2

The characterization of the *irp*-HPI_{Vang} genomic island revealed the genetic organization of the gene cluster and the identification of piscibactin as a siderophore synthesized by *V. anguillarum* RV22. Additionally, this high pathogenicity island is present in the genome of non-harboring pJM1-like isolates, mainly belonging to serotype O1. An interplay between vanchrobactin and piscibactin siderophore systems has been described, as the synthesis of piscibactin is strictly dependent on the presence of *vabD*, encoding 4'-phosphopantetheinyl transferase functions, and located in the *vab* gene cluster.

irp-HPI_{Vang} encodes functions related to the synthesis, transport, and regulation of the piscibactin system. However, most aspects were never characterized. Here, the role of Irp1, Irp4, Irp8, FrpA and FrpBC in piscibactin synthesis and transport was elucidated. Irp1 is a NRPS/PKS essential for piscibactin synthesis. Piscibactin is consistent with the early release on the nascent molecule from NRPS enzymatic line. The results showed that the type II thioesterase Irp4 is involved in this process. In addition, the predicted final product of the piscibactin route was never detected and the inactivation of *irp4* abolished piscibactin production. Once synthesized, the siderophore must be exported to the extracellular environment presumably in a stepwise manner. The total components of this process were not characterized, nonetheless the MFS Irp8 is involved in piscibactin export in *V. anguillarum*. The ferri-piscibactin complex enters the cell through high affinity transporters in a TonB-dependent manner. FrpA was characterized as the specific transporter for the ferri-piscibactin complex as its deletion impaired growth under iron limiting conditions and the mutant strain could not be cross fed by piscibactin producing strains. Once in the periplasm, the ferri-piscibactin complex is internalized via the ABC transporter FrpBC.

The synthesis of piscibactin analogues allowed the definition of the configuration of C-13 as essential for the recognition by the outer membrane transporter FrpA. Notably, the piscibactin analogues were used as iron source since they could be efficiently internalized through the FrpA versions of both *V. anguillarum* and *P. damsela* subsp. *piscicida*. These results greatly suggest that piscibactin analogues could

be used as carriers of antimicrobial compounds to develop novel antimicrobials effective not only against *V. anguillarum* and *P. damsela* subsp. *piscicida*, but also against a large diversity of *irp*-HPI bearing bacteria, including the human pathogen *V. cholerae* or bivalve molluscs pathogens such as *V. ostreicida*, *V. neptunius* and *V. coralliilyticus*.

3. IDENTIFICATION OF REGULATORS INVOLVED IN *IRP-HPI* GENE EXPRESSION

3.1. *IRP-HPI* IS PREFERENTIALLY EXPRESSED AT COLD TEMPERATURES

The synthesis of siderophores as of any virulence factor is metabolically expensive for the cell. So, siderophore-related genes expression must be tightly regulated to be synthesized only when they are strictly necessary (Cornelis *et al.*, 2011).

To study the influence of iron availability and temperature in piscibactin gene expression modulation, we firstly defined the transcriptional organization of the gene cluster. Reverse-transcriptase PCR reactions were performed to ascertain whether the piscibactin genes are expressed as an operon.

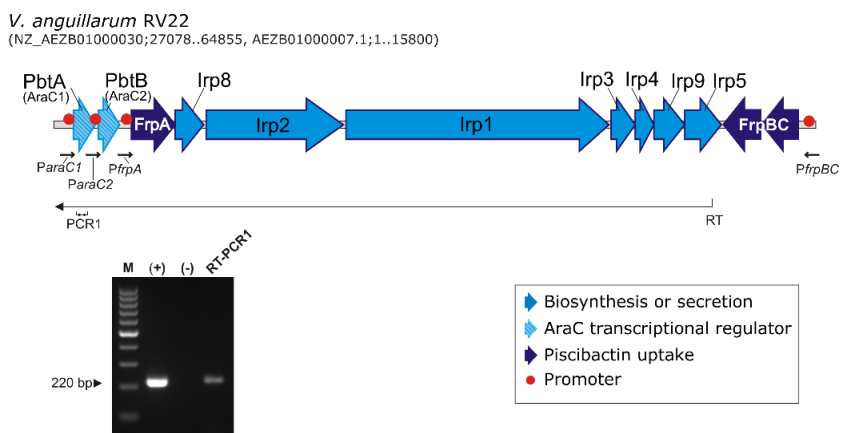


Figure IV.24. Genetic map of *irp*-HPI gene organization and result of the RT-PCR design to evaluate the transcription of the gene cluster.

Results showed that the gene cluster is transcribed in a polycistronic mRNA that includes *araC1*, *araC2*, *frpA*, *irp1-5*, *irp8* and

irp9 (Figure IV.24). Thus, the genes involved in piscibactin synthesis, transport and regulation are co-transcribed from the promoter region located upstream of *araC1*. Despite the co-transcription from *araC1* promoter region, the presence of additional promoter(s) cannot be excluded since putative Fur-box motifs are found in the intergenic region of *araC2-frpA*. Moreover, several regions have a large size compatible with the presence of a promoter. Therefore, the presumptive promoters of the *irp*-HPI genomic island located upstream of *araC1* (*ParaC1*), the intergenic region *araC1-araC2* (*ParaC2*) and *araC2-frpA* (*PfrpA*) and the region upstream of *frpBC* (*PfrpBC*) were cloned into the promoterless plasmid pHRP309 upstream of the *lacZ* gene (Figure IV.24). The plasmids were then mobilized into RV22 Δ *vabF* and the transcriptional levels measured by means of β -galactosidase activity under low- and high-iron availability and at 15 °C (temperature considered enough to cause vibriosis) and 25 °C. As constitutive control was used the house-keeping gene promoter *proC*, *PproC* (Savioz *et al.*, 1990) (Figure IV.25).

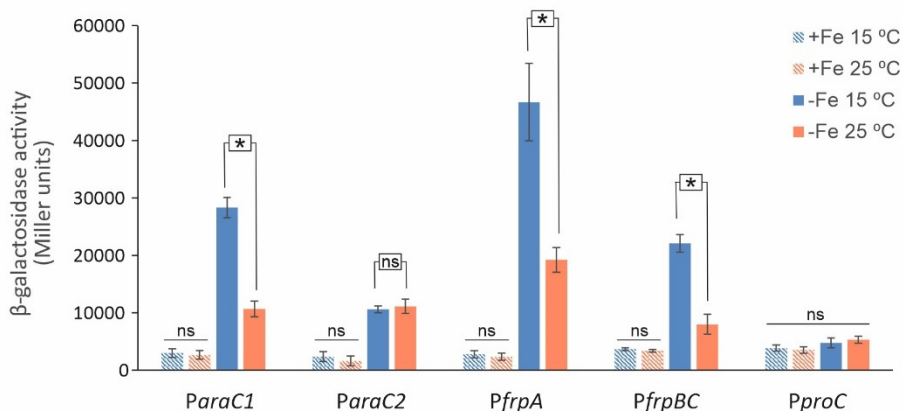


Figure IV.25. Transcriptional activity of *irp*-HPI_{vang} promoters. The promoters were cloned into pHRP309 and mobilized by conjugation to RV22 Δ *vabF*. The transcriptional levels were measured under iron excess and iron restriction at 15 and 25 °C. Asterisks denote statistical significance, * $p < 0.05$; ns, no statistically significant differences.

All the tested piscibactin promoters produced significant β -galactosidase activity indicating that these regions serve as transcription

starts. Interestingly, *PfrpA* showed the highest activity, which can imply that it is the main promoter of the gene cluster (Figure IV.25). Under iron availability, the promoters showed low levels of transcriptional activity. Fur (iron uptake regulator) is a well-known regulator of iron metabolism and of most virulence-related genes, repressing their expression when intracellular iron concentration increases (Ratledge and Dover, 2000). Most notably, there is a direct correlation between temperature and piscibactin system promoters activity. The activity of piscibactin promoters *ParaC1*, *PfrpA* and *PfrpBC* decreased significantly when the bacterium was grown at 25 °C (Figure IV.25). *ParaC1*, *PfrpA* and *PfrpBC* activity showed a 2.8, 2.4 and 2.4-fold decrease, respectively. By contrast, the activity of *ParaC2* remained constant at both temperatures. The constitutive promoter *PproC* was also tested under the same conditions of temperature and iron availability and no significant differences were found in its transcriptional levels. These findings suggest that the expression of piscibactin transporters, *frpA* and *frpBC*, and regulatory gene, *araC1*, is favoured at lower temperatures, corroborating the results of the transcriptomic analysis (see Chapter IV.1). Thus, the piscibactin operon would be silent at warm temperature and highly expressed at cold temperatures.

3.2. REGULATORS INVOLVED IN *IRP*-HPI GENE EXPRESSION MODULATION

To confer fitness advantages, horizontally transferred DNA is subjected to a precise regulatory control by the recipient's genome that allows genes to be expressed under the control of specific signals for the benefit of the microbe (Stoebel *et al.*, 2008). Bacteria possess tools to silence the expression of horizontally acquired genes such as H-NS. Conversely, horizontally acquired DNA usually encodes transcriptional regulators that promote their own expression (Stoebel *et al.*, 2008). The *irp*-HPI encodes two AraC-like transcriptional regulators. The AraC family of transcriptional regulators is extensively distributed in bacteria, and they are involved in a wide variety of cellular processes. Their function evolves around the regulation of carbon metabolism, stress response and virulence (Gallegos *et al.*, 1997). In *V. anguillarum*

RV22, the analysis of piscibactin genomic island reveals the presence of two putative AraC-like transcriptional regulators. Therefore, AraC1 and AraC2 might exert some influence in the expression of piscibactin uptake and biosynthetic genes.

3.2.1. *araC1* (*pbtA*) deletion impairs growth under iron limited conditions

Generally, the regulation of iron uptake systems is mediated by the negative transcriptional regulator Fur. Conversely, other transcriptional regulators have been identified as exerting a positive regulation in the expression of biosynthetic and transport genes. Regarding the regulation of piscibactin expression, two candidate genes are present in this cluster – *araC1* and *araC2*. These putative transcriptional regulators belong to the AraC family as they present the characteristic two-domain organization, a conserved C-terminal domain that is composed of a helix-turn-helix structure and a variable N-terminal domain (Gallegos *et al.*, 1997).

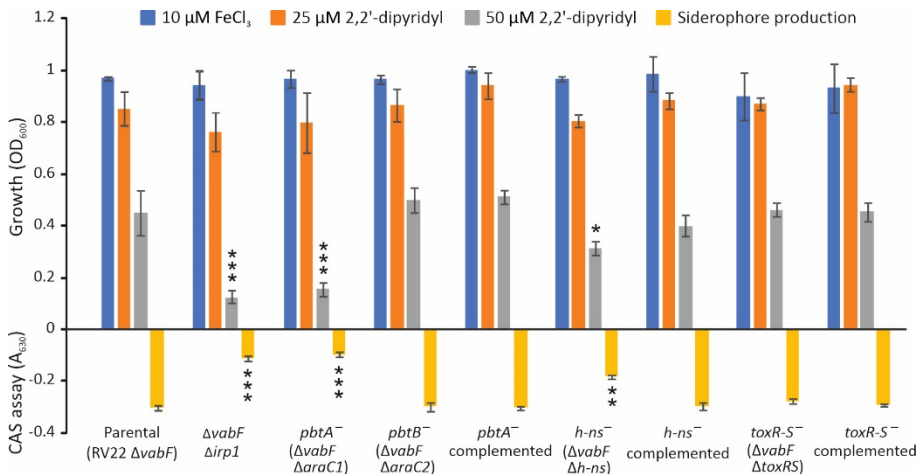


Figure IV.26. Growth ability of parental (RV22 Δ*vabF*) and derivative mutant strains (RV22 Δ*vabF*Δ*irp1*, RV22 Δ*vabF*Δ*pbtA*, RV22 Δ*vabF*Δ*pbtB*, RV22 Δ*vabF*Δ*h-ns* and RV22 Δ*vabF*Δ*toxR-S*) in iron excess and iron deficient conditions. Siderophore production was quantified using the liquid CAS assay. Asterisks denote statistically significant differences, * $p < 0.05$; ** $p < 0.01$; *** $p > 0.001$.

To evaluate the role of *araC1* and *araC2* in the regulation of piscibactin expression, in-frame deletion mutants for each gene were constructed in the piscibactin producer *V. anguillarum* $\Delta vabF$ strain and the resultant mutants were challenged to grow in different iron availability conditions. Iron deprived conditions were accomplished by adding the chelating agent 2,2'-dipyridyl to CM9 minimal medium, conversely FeCl_3 10 μM was added to achieve iron excess (Figure IV.26). When the mutants were grown under iron excess or weak iron deprived conditions (25 μM 2,2'-dipyridyl), no statistically significant differences were found when compared to the parental strain. The growth of the tested strains fluctuated around an OD_{600} ca. 1.0 under iron excess and ca. 0.8 under weak iron deprived conditions. However, when the iron availability changed to a more stringent condition (75 μM 2,2'-dipyridyl), different growth phenotypes appeared. While *araC2* deletion mutant showed a growth like that of the parental strain (OD_{600} ca. 0.5), the deletion of *araC1* dramatically reduced the ability to grow in strong iron deprived conditions as this mutant only achieved an OD_{600} of 0.15. Interestingly, an equivalent phenotype was found for the mutant impaired to synthesize the siderophores piscibactin and vanchrobactin (RV22 $\Delta vabF\Delta irp1$). When these mutants were assayed for siderophore production using the liquid CAS assay, the *araC2* mutant showed a siderophore production in the same range as the parental strain (A_{630} ca. -0.35) whereas the *araC1* mutant showed similar levels as the mutant impaired for siderophore synthesis (A_{630} ca. -0.1). When the *araC1* mutant was complemented *in trans* with a functional version of the gene, the original phenotype was restored (Figure IV.26).

These results suggest that *araC1* would encode a transcriptional regulator directly involved in piscibactin synthesis while *araC2* is apparently not essential. Due to its active role in piscibactin synthesis, *araC1* was renamed to *pbtA* (piscibactin regulator A) and *araC2* to *pbtB* (piscibactin regulator B).

3.2.2. The global regulators ToxR-S and H-NS play indirect roles in the regulation of the *irp*-HPI_{Vang} gene expression

The expression of virulence factors encoded in pathogenicity islands can be under the control of factors encoded in the island, such as the above identified piscibactin regulator PbtA, as well as factors located elsewhere in the recipient bacteria genome. Two of the most relevant conserved regulators characterized are H-NS, which is involved in HGT genes transcription blocking, and ToxR that mediates the regulation of virulence factors in a range of pathogenic *Vibrios* (Herrington *et al.*, 1988; Peterson and Mekalanos, 1988; Lee *et al.*, 2000; Whitaker *et al.*, 2012). Thus, the hypothetical role of the global regulators H-NS and ToxR-S in the expression of the piscibactin system was evaluated.

In-frame deletion mutants for *h-ns* and *toxR-S* were constructed and these mutants were challenged to grow under different iron availability conditions (Figure IV.26). Under iron excess (10 μ M FeCl₃) or weak iron deprived conditions (25 μ M 2,2'-dipyridyl), both mutant strains showed a growth phenotype like that of the parental. Though, the phenotype presented by these mutants when grown under iron deprived conditions is divergent. *h-ns* deletion resulted in a decrease in growth (maximum OD₆₀₀ ca. 0.30) under strong iron restriction. The diminished growth ability directly correlates with a decrease in siderophore production, showing an A₆₃₀ around -0.18. Surprisingly, the *toxR-S* mutant showed a growth and siderophore production phenotype indistinguishable from that of the parental strain. When both mutant strains were complemented with the wild-type version of the gene, the parental phenotype was fully restored. These results suggest that the global regulator H-NS is required to achieve the maximum production of piscibactin, whereas ToxR-S is not essential for piscibactin production.

3.2.3. PbtA and H-NS are needed for full virulence of *V. anguillarum*

Attending to the results described above, PbtA and H-NS are required to achieve maximum piscibactin production. To study the probable role of PbtA and H-NS in *V. anguillarum* virulence, infection

challenges were performed in sole fingerlings (Figure IV.27). ToxR-S was excluded from the virulence test since its role in *Vibrionaceae* virulence has been fully characterized (Childers and Klose, 2007; Zhang *et al.*, 2018).

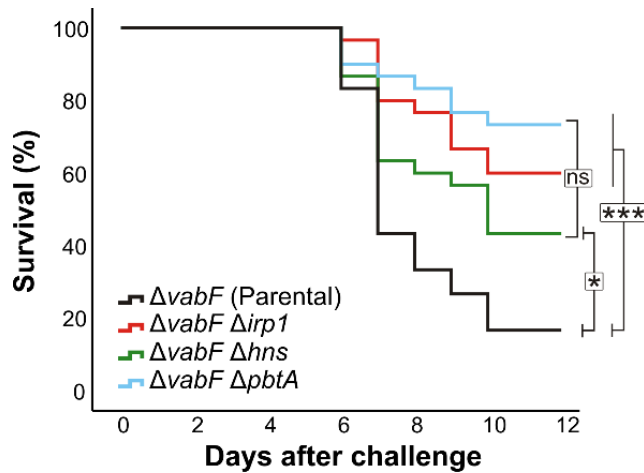


Figure IV.27. Survival rate of sole fingerlings infected with *V. anguillarum* RV22 $\Delta vabF$ and its derivative mutant strains $\Delta irp1$, Δhns and $\Delta pbtA$. Asterisks denote statistical significance, * $p < 0.05$; *** $p < 0.001$; ns, no statistically significant differences.

The virulence of *V. anguillarum* $\Delta pbtA$ and Δhns mutants was evaluated and compared to the parental strain RV22 $\Delta vabF$ and to RV22 $\Delta vabF \Delta irp1$, a mutant unable to produce any siderophore. Fish were inoculated with a dose of $2-3 \times 10^3$ CFU per fish while controls were injected with saline solution. The control group did not show any mortality in the time frame of the experiment. The survival curve of the fish group challenged with the parental strain RV22 $\Delta vabF$ showed 80% mortality, 10 days post infection, however $\Delta pbtA$ defective mutant showed a significant reduction in mortality (Figure IV.27). In the same time frame, $\Delta pbtA$ mutant produced a mortality of ca. 20% and its survival curve showed no statistically significant differences with the one obtained for the RV22 $\Delta vabF \Delta irp1$ mutant that is impaired to synthesize any siderophore. Moreover, hns deletion also led to a decrease in virulence for fish, as the mutant showed a reduction of

mortality when compared to the parental strain. Ten days after infection, the *h-ns* mutant achieved its maximal mortality of around 45%. Furthermore, the survival curve did not show statistically significant differences when compared to the one obtained for $\Delta pbtA$ and RV22 $\Delta vabF\Delta irp1$ (Figure IV.27).

In *V. anguillarum*, H-NS has been reported as a regulator of haemolytic activity and cytotoxicity. *h-ns* deletion resulted in an increase of haemolytic activity and an increased cytotoxicity against ASK cells, indicating that H-NS acts as a repressor of haemolysin gene expression (Mou *et al.*, 2013). It is interesting to note that PbtA and H-NS are required for *V. anguillarum* full virulence. In addition, as both regulators are necessary for the maximum production of piscibactin, the results strongly confirm the essential role of siderophores and specifically piscibactin for *V. anguillarum* virulence.

3.2.4. PbtA is the main expression modulator of genes encoding piscibactin synthesis and transport

As shown above, piscibactin gene cluster is co-transcribed in a polycistronic mRNA spanning from *pbtA* to *irp9*. We have shown above that *PpbtA* and *PfrpA* are the main promoters of the *irp*-HPI_{Vang} genomic island. Thus, to analyse the role of the putative transcriptional regulator PbtA in the expression of the piscibactin gene cluster and re-evaluate the role of PbtA, the activity of piscibactin promoters *PpbtA* and *PfrpA* was measured in a *pbtA*⁻ (RV22 $\Delta vabF\Delta pbtA$) and *pbtB*⁻ (RV22 $\Delta vabF\Delta pbtB$) background under cold (15 °C) and warm temperatures (25 °C) and compared to the parental strain RV22 $\Delta vabF$. The results are shown in Figure IV.28. The deletion of *pbtB* did not alter the transcriptional levels of *PpbtA* nor *PfrpA* since both promoters showed the same expression pattern as that observed for the parental strain at 15 and 25 °C and followed a temperature dependent expression pattern. This result agrees with the growth capacity and siderophore production of the *pbtB* mutant (see above). However, deletion of *pbtA* resulted in the complete loss of activity of *PfrpA*. Notably, the expression of *PpbtA* in the $\Delta pbtA$ mutant still followed a temperature dependent pattern, showing ca. of 20,000 and 9,000 units at 15 and 25 °C, respectively, transcriptional levels equivalent to those observed in

the parental strain (Figure IV.28). Thereby, *pbtA* deletion did not alter the expression of its own promoter. The evaluation of *PpbtA* and *PfrpA* activities in the complemented strain was not possible since plasmids pSEVA651 and pHRP309 have the same gentamycin resistance marker. However, and as it was shown above, the complementation of the *pbtA* mutant with the wild-type gene restored the original phenotype (Figure IV.26).

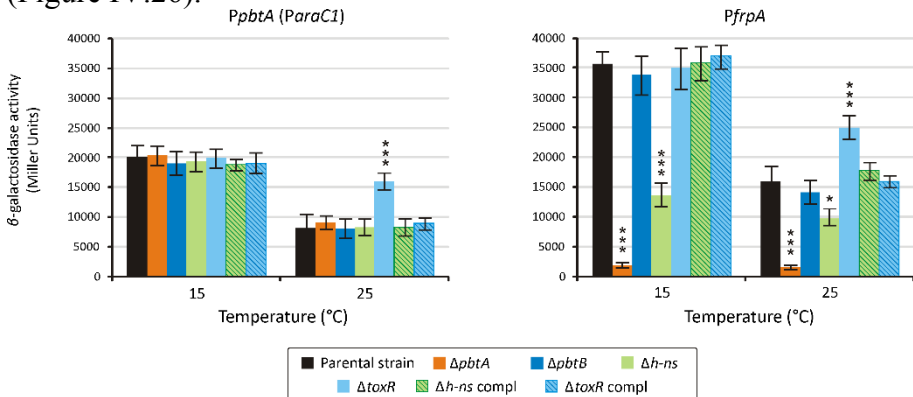


Figure IV.28. Transcriptional activity of *PpbtA* and *PfrpA* in $\Delta pbtA$, $\Delta pbtB$, $\Delta toxR$ -S and $\Delta h-ns$, measured in CM9 minimal medium supplemented with 25 μ M 2,2'-dipyridyl, at 15 °C and 25°C. Asterisks denote statistically significant differences, * p <0.05, *** p <0.001.

AraC-like transcriptional regulators have been described as exerting a positive regulatory function in different siderophore systems. These regulators are involved in the induction of both biosynthetic and transport gene expression. In *Bordetella pertussis*, AlcR up-regulates the expression of alcaligin siderophore biosynthesis and transport (Brickman *et al.*, 2001), in *Vibrio vulnificus* the regulator DesR induces the transport of ferrioxamine B (Tanabe *et al.*, 2005) and in *Pseudomonas aeruginosa* the regulator PchR is required for the maximal expression of pyochelin biosynthesis and transport genes (Michel *et al.*, 2005). The results obtained in this work suggest that the inactivation of *pbtA* disables piscibactin biosynthesis and transport, impairing *V. anguillarum* to grow under iron limited conditions (Figure IV.26). Conversely, *pbtB* inactivation did not result in any phenotypic nor gene expression change. Therefore, *pbtB* role remains unclear. In *Yersinia pestis*, the AraC-like regulator YbtA activates the expression

of specific promoters related to yersiniabactin synthesis and uptake (Anisimov *et al.*, 2005). In contrast to what was found for *V. anguillarum* PbtA, YbtA activates the expression of its own promoter (Fetherson *et al.*, 1996; Anisimov *et al.*, 2005). Additionally, although *ybtA* deletion blocks the synthesis of yersiniabactin, the virulence phenotype shown by the mutant is intermediate between the wild-type strain and the biosynthetic mutant (Smati *et al.*, 2017). In *V. anguillarum*, *pbtA* deletion resulted in a significant decrease in virulence for sole fingerlings, at the same level as the mutant unable to synthesize siderophores (Figure IV.27).

To confirm the silencing of gene *frpA* in the absence of PbtA, *V. anguillarum* RV22 $\Delta vabF\Delta pbtA$ and its parental strain RV22 $\Delta vabF$, were grown under iron deficiency and their outer membrane protein fractions were obtained. The presence of the outer membrane transport protein FrpA was evaluated by SDS-PAGE separation and detection by western blot using a specific anti-FrpA antibody (Figure IV.29). The detection of a unique band of ca 70 kDa, congruent with the molecular weight of FrpA (68 kDa), in the sample corresponding to the parental strain (Figure IV.29.B) corroborates the specificity of this antibody. In the outer membrane fraction of the *pbtA* defective mutant only residual amounts of FrpA were detected (Figure IV.29.A). This result corroborates that the inactivation of the transcriptional regulator PbtA blocks the expression of the piscibactin gene operon, avoiding an efficient synthesis of the proteins required for piscibactin synthesis and uptake.

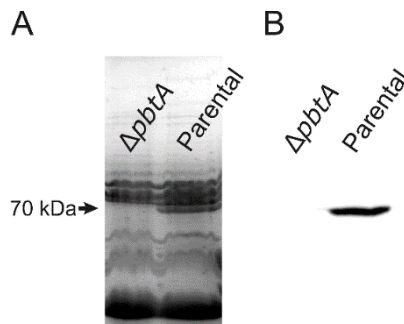


Figure IV.29. Protein pattern of the outer membrane components of *V. anguillarum* separated by SDS-PAGE (A) and detection of the outer membrane transporter FrpA by western blot (B), in the mutant RV22 $\Delta vabF\Delta pbtA$ and in the parental RV22 $\Delta vabF$ strain.

In addition, the transcriptional activity of *PpbtA* and *PfrpA* was also evaluated in an *h-ns*⁻ and *toxR-S*⁻ background (Figure IV.28). Remarkably, while the activity of the *PpbtA* in the *h-ns* mutant was indistinguishable from that of the parental strain at both temperatures (ca. 20,000 units at 15 °C and 9,000 units at 25 °C), *PfrpA* activity showed a reduction of ca. 60% at 15 °C and ca. 20% at 25 °C (Figure IV.28). Conversely, in a *toxR-S*⁻ background, *PpbtA* activity increased 2-fold and *PfrpA* activity increased 30% at 25 °C. Interestingly, no significant changes in the transcriptional levels of both promoters were observed at 15 °C. The complemented strains showed expression levels indistinguishable from those of the parental strain.

Regarding ToxR regulatory role in piscibactin siderophore expression, the results shown in this work suggest an intricate activity. The deletion of the global regulator ToxR-S did not cause appreciable changes in the ability of *V. anguillarum* to grow under iron restrictive conditions nor caused differences in the ability to produce siderophore at low temperatures (Figure IV.26). Though, when evaluating the transcriptional levels at 25 °C, an increase in *PpbtA* and *PfrpA* activities was noted. Although piscibactin is preferentially expressed at lower temperatures, the deletion of *toxR-S* appears to unblock the piscibactin synthesis at 25 °C. This finding suggests that *irp-HPI*_{*Vang*} might be in some way part of the ToxR regulon (Figure IV.30).

AraC-like regulators can be part of a larger regulon that can act in a cascade manner as a response to environmental signals. ToxR is a regulatory protein that is essential for virulence in a range of different pathogenic Vibrios (Herrington *et al.*, 1988; Peterson and Mekalanos, 1988; Lee *et al.*, 2000; Whitaker *et al.*, 2012). ToxR mediates the control of several virulence factors through the activation of the AraC-like transcriptional regulator ToxT. ToxT directly responds to environmental cues and activates the transcription of virulence related promoters (Higgins and DiRitta, 1994; Skorupski and Taylor, 1997; Childers and Klose, 2007). In the human pathogen *V. cholerae*, ToxR regulates the expression of the main virulence factors including cholera toxin and the toxin-coregulated pili (Herrington *et al.*, 1988; Peterson and Mekalanos, 1988). In *V. anguillarum*, ToxR is not a major regulator

of virulence factors since its inactivation shows a slight decrease in virulence (Okuda *et al.*, 2001; Wang *et al.*, 2002).

Gram-negative bacteria possess tools to silence the expression of horizontally acquire genes. H-NS is a global repressor implicated in the process of xenogenetic silencing (Stoebel *et al.*, 2008; Prajapat and Saini, 2012). H-NS function is based on binding to DNA motifs creating DNA-protein-DNA bridges that block the movement of the RNA polymerase, the so-called transcription silencing (Stoebel *et al.*, 2008). H-NS has been characterized as a repressor of virulence genes expression specially in pathogens that infect mammals, where the infection occurs at a temperature higher than the optimal growth temperature of the pathogen (Guijarro *et al.*, 2015). In these cases, temperature acts as an environmental cue to release the repressor activity allowing the induction of promoters by transcriptional activators (Guijarro *et al.*, 2015).

In this study, the *h-ns* mutant showed a decrease in growth capacity and siderophore production under iron restrictive conditions. Interestingly, a lower transcriptional activity of the *PfripA* was noted at both warm and cold temperatures. Thus, this suggests that H-NS must exert an indirect effect on the expression of piscibactin biosynthesis and transport genes (Figure IV.30). Notably, *PpbtA*, whose product is required for the transcriptional activity of *PfripA*, was not affected by *h-ns* deletion as it did not affect the transcriptional activity of *PpbtA*. Therefore H-NS would not have any regulatory effect on the expression of the transcriptional activator PbtA.

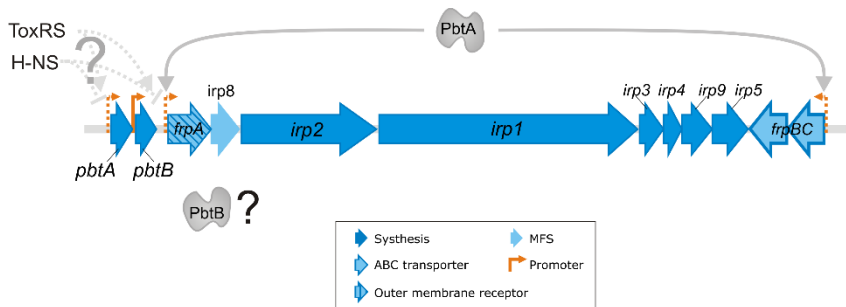


Figure IV.30. Schematic representation of the regulatory mechanisms behind *irp*-HPI gene expression.

3.2.5. Purification of PbtA and its N- and C-terminal domains

The inactivation of *pbtA* disables piscibactin synthesis and transport, which results in a dramatic decrease in the degree of virulence. In addition, PbtA was confirmed as the transcriptional activator directly required for the expression of the piscibactin siderophore system. PbtA is a member of the AraC/XylS family of transcriptional regulators and includes the well characterized and conserved C-terminal domain, comprised by ca. 100 amino acids, and containing the characteristic two helix-turn-helix motifs (Gallegos *et al.*, 1997). The N-terminal domain, comprised by the first 200 amino acids, is the variable region that would be involved in dimerization and/or binding of small effector proteins (Childers *et al.*, 2011). Both domains are usually joined by a flexible linker region (Gallegos *et al.*, 1997).

To evaluate the interaction of PbtA with the target DNA, the total protein (PbtA) and its domains (N- and C-terminal) were cloned into the pET20b(+) expression vector. The resulting protein would be expressed with 6x His-tag at the N- or C-terminal.

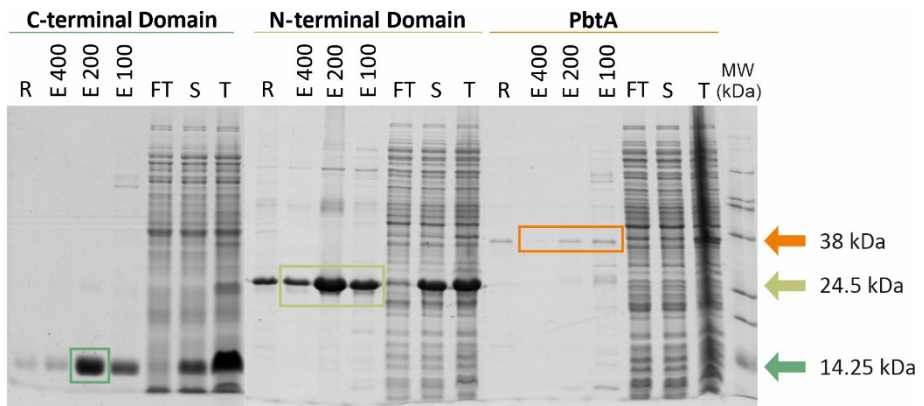


Figure IV.31. Protein pattern of the total fraction (T), soluble fraction (S), flow through (FT), elution 100 mM imidazole (E100), elution 200 mM imidazole (E200), elution 400 mM imidazole (E400) and resin (R) of PbtA, N and C-terminal domains obtained during the purification process.

Several attempts were done to purify PbtA in the soluble fraction. Different *E. coli* expression strains and growth conditions were used;

however, the protein was present in vestigial amounts and contaminated with other protein products (Figure IV.31). The N- and the C-terminal domains were satisfactorily produced. Large amounts were detected in the elutions (Figure IV.31). Unfortunately, the total PbtA protein was poorly soluble and could not be purified. Moreover, during concentration the protein was degraded, and contaminants and products of PbtA degradation were being concentrated (PbtA in Figure IV.32). Finally, PbtA was discarded from further use.

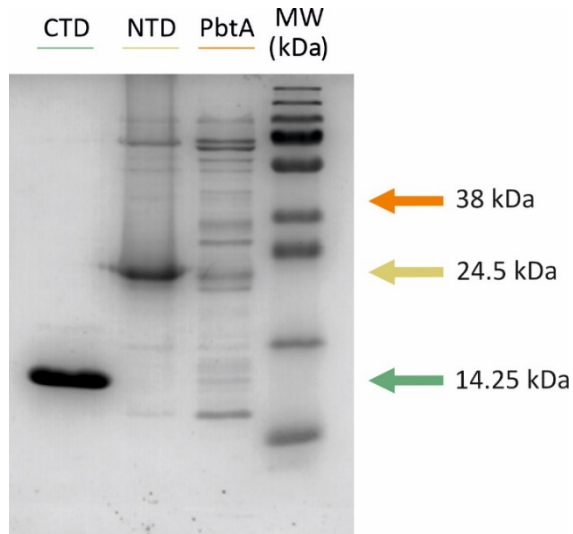


Figure IV.32. Protein patterns of the purified proteins. CTD (C-terminal domain) was free of contaminants while NTD (N-terminal domain) had contaminants with higher and lower molecular weights. PbtA was present in low amount, and it was severely contaminated.

Regarding the N-terminal domain, the three elutions with increasing imidazole concentrations (E100, E200 and E400) were used for protein concentration, whereas for the C-terminal domain only the Elution 200 was used. Attending to Figure IV.31, Elution 200 had large amounts of C-terminal protein, so only this fraction was used for protein concentration to avoid a possible protein precipitation. After purification, concentration, and dialysis, 5 μg of each protein were loaded in a 14 % polyacrylamide gel and visualized for the presence of contaminants. The C-terminal domain (CTD in Figure IV.32) was

present in the form of a consistent band with the expected molecular weight (14.25 kDa). Remarkably, no contaminants were detected in the sample corresponding to this domain. Regarding the N-terminal domain (NTD in Figure IV.32), the protein was purified in significant amounts although it was not completely depleted of contaminants. Several bands with molecular weights higher and lower than the N-terminal domain (24.5 kDa) were present in the final protein. Nonetheless, the ratio of N-terminal domain:contaminants is favourable for the target protein thus it could be used in further experiments.

3.2.6. PbtA interacts directly with the piscibactin promoters *PfrpA* and *PfrpBC*

As shown above (section 3.1) expression of both *PfrpA* and *PfrpBC* promoters is regulated by environmental signals such as iron levels and temperature assuring that both transporters are expressed only when they are needed. To test whether PbtA binds directly the piscibactin promoters and to define the DNA interaction motif, the sequence upstream of *pbtA* ATG start codon (*PpbtA*), the intergenic region of *pbtB-frpA* (*PfrpA*) and the region upstream of *frpBC* ATG star codon (*PfrpBC*) were subjected to DNA-protein interaction analysis by Electrophoretic Mobility Shift Assay (EMSA). The binding reactions were performed as in Table III.11 (Material and Methods).

Results showed that the C-terminal domain of PbtA did not bind the *pbtA* promoter (Figure IV.33, lanes 2 and 3). This result is congruent with that previously described, since PbtA does not regulate its own expression. Notably, PbtA C-terminal domain effectively binds *frpA* and *frpBC* promoters (Figure IV.33, lanes 7-8 and 12-13), the N-terminal domain of PbtA did not cause a mobility shift of any promoter (neither *frpA*, *frpBC* nor *pbtA* promoters) (Figure IV.33, lanes 17 and 18). The specificity of the interaction was confirmed by the addition of cold unlabelled specific DNA which prevented the shift (Figure IV.33, lanes 9-10 and 14-15). These results showed that the C-terminal domain of PbtA has a DNA-binding activity.

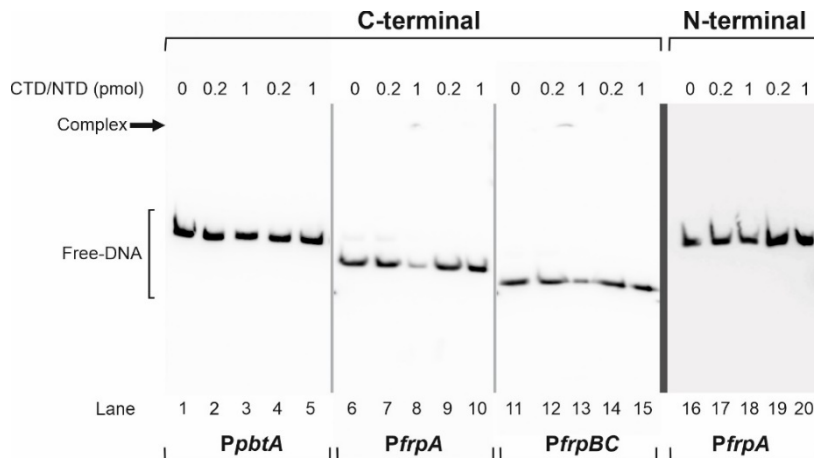


Figure IV.33. PbtA binding to PpbtA, PfrpA and PfrpBC was analysed by EMSA. Lanes 1, 6, 11 and 16 corresponds to the free probe. Lanes 2, 3, 7, 8, 12, 13, 17 and 18 corresponds to DNA with 0.2 or 1 pmol of CTD/NTD. Lanes 4, 5, 9, 10, 14, 15, 19 and 20 corresponds to the reaction containing DNA, CTD/NTD and an excess of unlabelled specific DNA.

Mobility in a native gel depends on the protein's charge. Surprisingly, CTD of PbtA has a $pI = 10.43$, which is higher than the pH of buffer and gel (8.3) used for electrophoresis. When the pH is lower than the pI , the proteins are positively charged, which prevents their migration in the gel. The protein-DNA complexes were identified by the decrease in free DNA band intensity (when compared to the reaction that only contains DNA, Figure IV.33, lanes 6 and 11) and the appearance of a band at the top of the gel, indicative of the difficulty of the complex to enter the gel.

Several internal sequences of PfrpA and PfrpBC were also subjected to EMSA. Finally, the 136 bp and 100 bp sequence regions immediately upstream of *frpA* and *frpBC* ATG start codon were characterized as the minimal regions involved in the interaction with PbtA C-terminal domain (Figure IV.34). Both regions include -35 and -10 putative motif regions, where the RNA polymerase specifically binds. Interactions between AraC transcriptional activators and RNA polymerase have been described (Hulbert and Taylor, 2002). Many AraC family members have binding sites that are in proximity or overlap the -35 region (Class II promoters) or have binding sites located

upstream of the – 35 positions (Class I promoters). From the EMSA data nor *PfrpA* neither *PfrpBC* can be classified as class I or II promoters because the minimal region that induced the shift harbours the -35 region and is extended beyond this sequence.

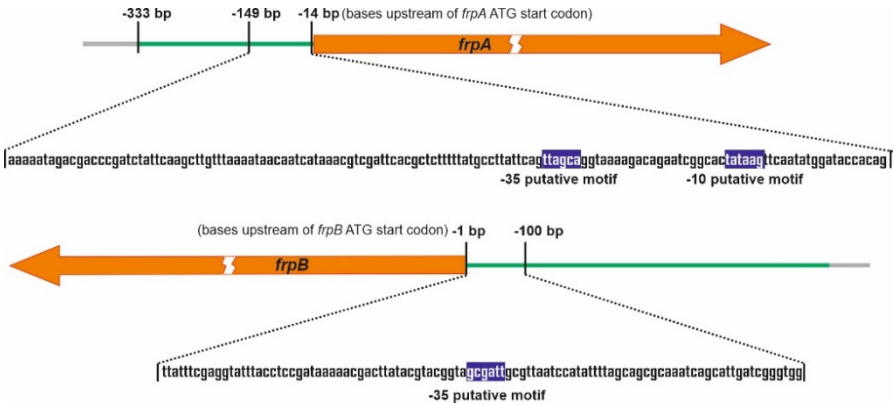


Figure IV.34. Identification of *PfrpA* and *PfrpBC* minimal regions experimentally proved to bind PbtA C-terminal domain. Both regions harbour -10 and -35 putative motif regions.

AraC family members tend to recognize asymmetric binding sites and A-rich DNA sequences. ExsA from *Pseudomonas aeruginosa*, binds to a consensus sequence, TNAAAANA, located near the -50 position from the transcriptional start site (Hovey and Frank, 1995) and tox-boxes are characterized by a conserved 5' poly (T) and a variable 3' end rich in AT nucleotides varying their position in relation to the transcriptional start site (Dittmer and Withey, 2012). *frpA* and *frpBC* promoter regions identified by the EMSA assay, both lay in an AT-rich region and a consensus sequence could not be determined which prevents the prediction of PbtA binding site.

ToxT is the closest homolog of PbtA, however, their ability to bind to promoters seem to be different. Our results greatly suggest that PbtA C-terminal domain binds piscibactin promoters *PfrpA* and *PfrpBC* as a monomer. Interestingly, the C-terminal domain of ToxT is unable to cause a mobility shift when in a monomer (Prouty *et al.*, 2005). In addition, the interaction between N-terminal domains is essential for the transcriptional activation thus, ToxT binds adjacent tox-boxes,

dimerizes leading to promoter activation (Prouty *et al.*, 2005). The impossibility to use the native total protein PbtA in the EMSA assay, did not allow to analyse the N-terminal domain function. From these results, the N-terminal domain would not be involved in DNA binding. However, further works must be performed to elucidate the role of PbtA as an environmental sensor.

3.2.7. *irp*-HPI is widespread in *Vibrionaceae* and contains several versions of *frpA* and *pbtA* promoters

The spread of selectively favoured virulence factors by horizontal gene transfer facilitates the emergence of novel diseases (Bruto *et al.*, 2017; Le Roux and Blokesch, 2018). Horizontally transferred genes not always are expressed in the recipient genome, because of possible incompatibilities in promoter sequences, different codon usage and/or excessive energy cost (Ochman *et al.*, 2000; Park and Zhang, 2012). A precise regulatory control by the recipient's genome must allow the expression of these genes under specific environmental signals (Stoebel *et al.*, 2008). The piscibactin siderophore system is widespread among *Vibrionaceae* including *V. cholerae*, *V. ordalii*, *V. neptunius* *P. damsela* subsp. *piscicida* or *P. profundum* (Thode *et al.*, 2018) and several versions of the *irp*-HPI genomic island exist.

The alignment of *irp*-HPI genomic islands from different species from the human pathogen *V. cholerae* to the psychrophilic marine bacterium *Shewanella psychrophila*, showed that the sequences immediately upstream of *pbtA* ATG start codon (*pbtA* promoter region) (Figure IV.36) and the *pbtB-frpA* intergenic region (*frpA* promoter region) (Figure IV.37) present major differences between the analysed species. Attending to their similarity, different types of piscibactin promoters *PpbtA* and *PfrpA* could be defined. Remarkably, the distribution of each promoter type (*PpbtA* and *PfrpA* sequences) did not match with the *irp*-HPI phylogenetic lineages (Figure IV.35). Thus, several *irp*-HPI lineages exist, and extensive differences are present specifically in intergenic regions where *PpbtA* and *PfrpA* are located.

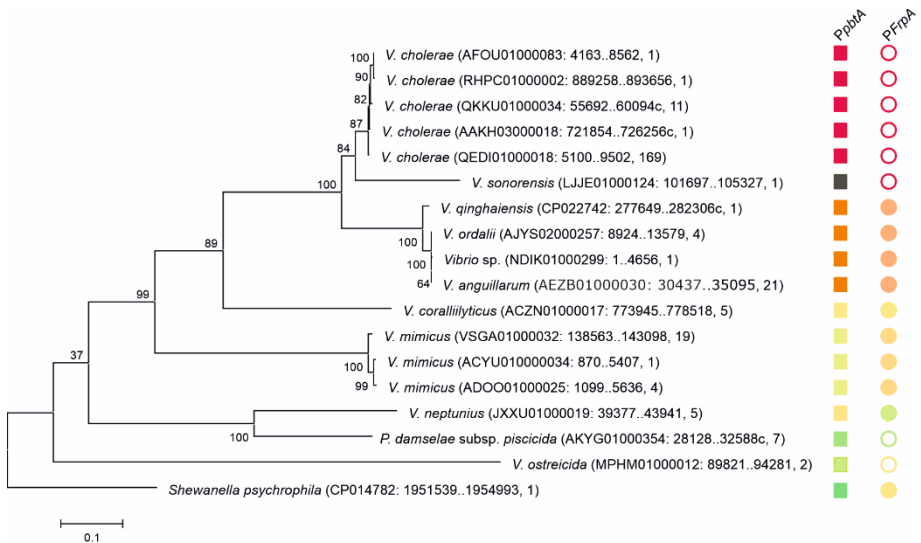


Figure IV.35. Phylogenetic tree of *pbtA-frpA* region (sequence between 250 bp upstream of *pbtA* and *frpA* stop codon) and distribution of *PpbtA* and *PfrpA* promoter versions. Sequences are identified by species name, sequence ID, region and number of related sequences deposited in GenBank. The tree was drawn to scale and the branch length represents the evolutionary distance. Different versions of *PpbtA* (squares) and *PfrpA* (circles) are represented and filled circles correspond to *frpA* long version while empty circles represent the short version. Closely related promoter sequences are represented with the same colour.

The sequences that showed the highest level of variability are found in *pbtB-frpA* intergenic region. Nonetheless, a conserved region located ca. 100 bp immediately upstream of *frpA* start codon is present in all *pbtB-frpA* sequences (Figure IV.37). The region located downstream of *pbtB* stop codon showed higher differences possibly indicating that deletions and/or insertions events might have occurred. From this analysis, different types of promoters have been recognized based on the length of the sequence (Figure IV.35). The *irp*-HPI genomic island of *V. anguillarum*, *V. ordalii* and *V. qinghaiensis* contains a long *pbtB-frpA* intergenic region with a size of ca. 360 bp. Conversely, *P. damsela* subsp. *piscicida*, *V. ostreicida*, *V. sonorensis* and *V. cholerae*, that are grouped apart in the phylogenetic tree (Figure IV.35), harbour a shorter intergenic region sequence whose nucleotide length is between 100 and 140 bp. This shorter version lacks the

segment immediately downstream of *pbtB* stop codon (Figure IV.37). Additionally, an intermediate promoter version could also be identified, and it was present in *V. mimicus* and *V. neptunius* (Figure IV.37). The high variability presented by both promoter regions, located upstream of *pbtA* (*PpbtA*) and *pbtB-fipA* intergenic region (*PfrpA*) could imply the existence of different expression patterns among strains that harbour the *irp*-HPI genomic island.

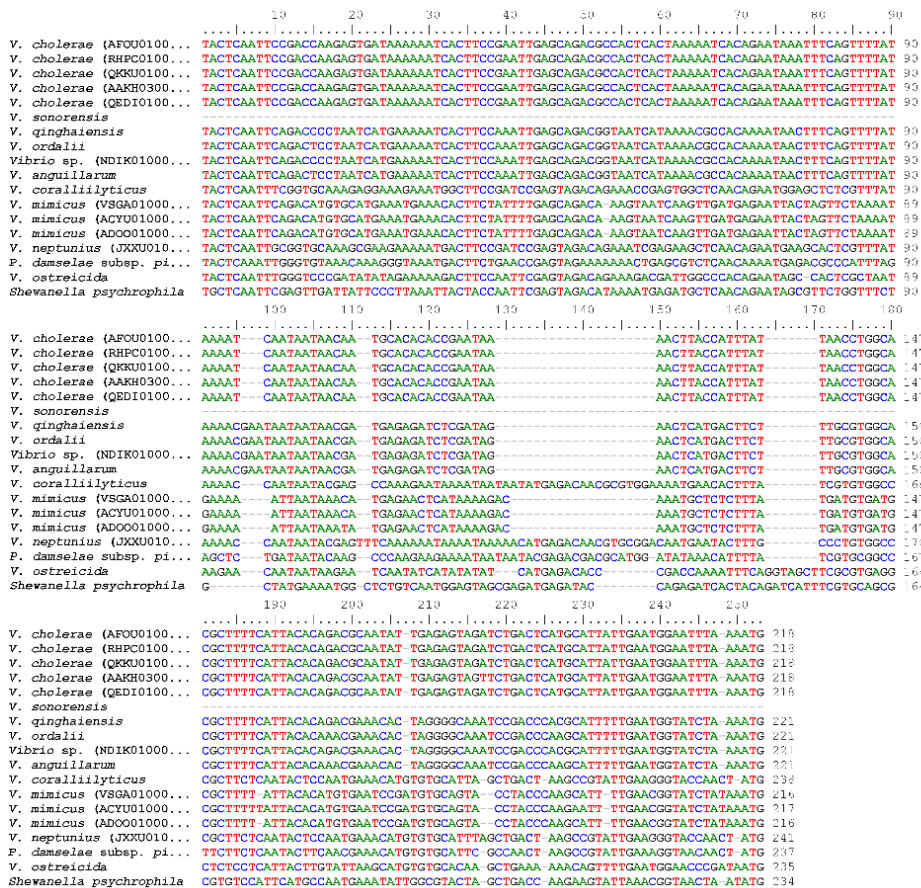


Figure IV.36. Alignment of representative versions of *PpbtA* (250 bp upstream of *pbtA* ATG start codon)

IV. Results and Discussion

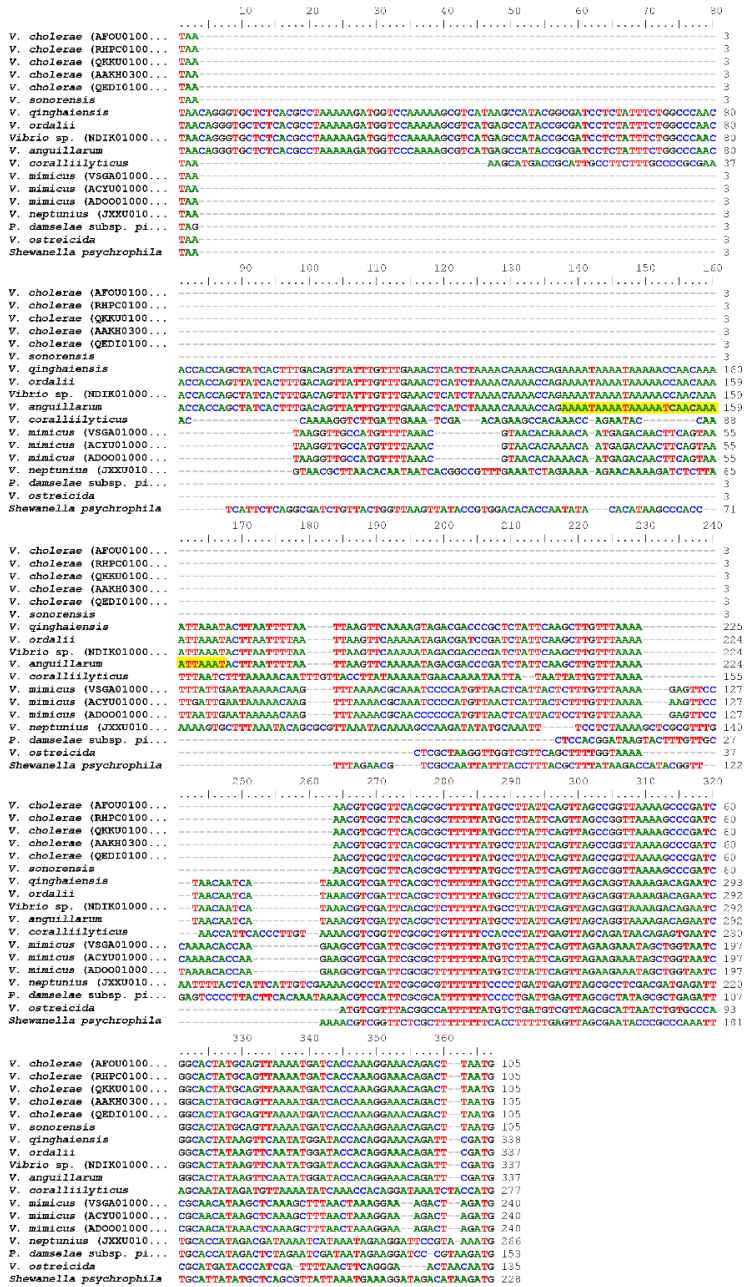


Figure IV.37. Alignment of representative versions of *PfrpA* (*pbtB-frpA* intergenic region between *pbtB* stop codon and *frpA* ATG start codon).

3.2.8. *irp*-HPI expression pattern results from the interaction of the type of promoter and other elements in the genome

The piscibactin siderophore system was firstly identified in the marine pathogen *P. damsela* subsp. *piscicida* and it is a key virulence factor in this relevant fish pathogen (Osorio *et al.*, 2015). Notably, the expression pattern of *irp*-HPI described for *V. anguillarum* is incompatible with the ecology of *P. damsela* subsp. *piscicida*, as this pathogen causes disease outbreaks when the water temperature is above 20 °C (Romalde, 2002; Toranzo *et al.*, 2005; Bellos *et al.*, 2015).

To study the expression of *P. damsela* subsp. *piscicida* *irp*-HPI genomic island (*irp*-HPI_{*Pdp*}) and compare it to the expression of *V. anguillarum* *irp*-HPI (*irp*-HPI_{*Vang*}), *lacZ* fusions of *irp*-HPI_{*Pdp*} promoters were obtained and evaluated. Thus, the sequences immediately upstream of *pbtA* and *frpA* from *P. damsela* subsp. *piscicida* (*PpbtA_{Pdp}* and *PfrpA_{Pdp}*) were cloned into the promoterless plasmid pHRP309 upstream of the *lacZ*, and the transcriptional levels were assayed at 15 °C and 25 °C under low iron availability (Figure IV.38.A).

Native evaluation of the expression pattern of each piscibactin promoter of *P. damsela* subsp. *piscicida* showed that they differ considerably from that observed in *V. anguillarum* (Figure IV.38.A and C). The expression pattern of *PpbtA_{Pdp}* in *P. damsela* subsp. *piscicida* showed almost the same transcriptional activity at 15 °C and at 25 °C (Figure IV.38.A), which suggests that piscibactin genes do not follow a temperature-dependent expression pattern in this bacterium contrarily to what was describe in *V. anguillarum* (see above). In addition, *PpbtA_{Pdp}* showed a 3-fold lower activity in *P. damsela* subsp. *piscicida* (Figure IV.38.A) than its counterpart *PpbtA_{Vang}* in *V. anguillarum* (Figure IV.38.C). Unexpectedly, while *PfrpA_{Vang}* in *V. anguillarum* achieved ca. 50,000 β-galactosidase units at 15 °C, the activity of *PfrpA_{Pdp}* was almost undetectable (<750 U) suggesting that the shorter *pbtB*-*frpA* intergenic region found in the *irp*-HPI_{*Pdp*} does not constitute a transcriptional promoter (Figure IV.38.A and C). As this bacterium lacks a *PfrpA*, all piscibactin genes should be expressed from *PpbtA*. A large operon that includes regulator, biosynthesis and transporter functions would be co-transcribed. Interestingly, *PpbtA_{Pdp}* did not

follow a temperature-dependent expression pattern in *P. damselae* subsp. *piscicida* and the transcriptional activity of the operon is significantly lower than that observed in *V. anguillarum*.

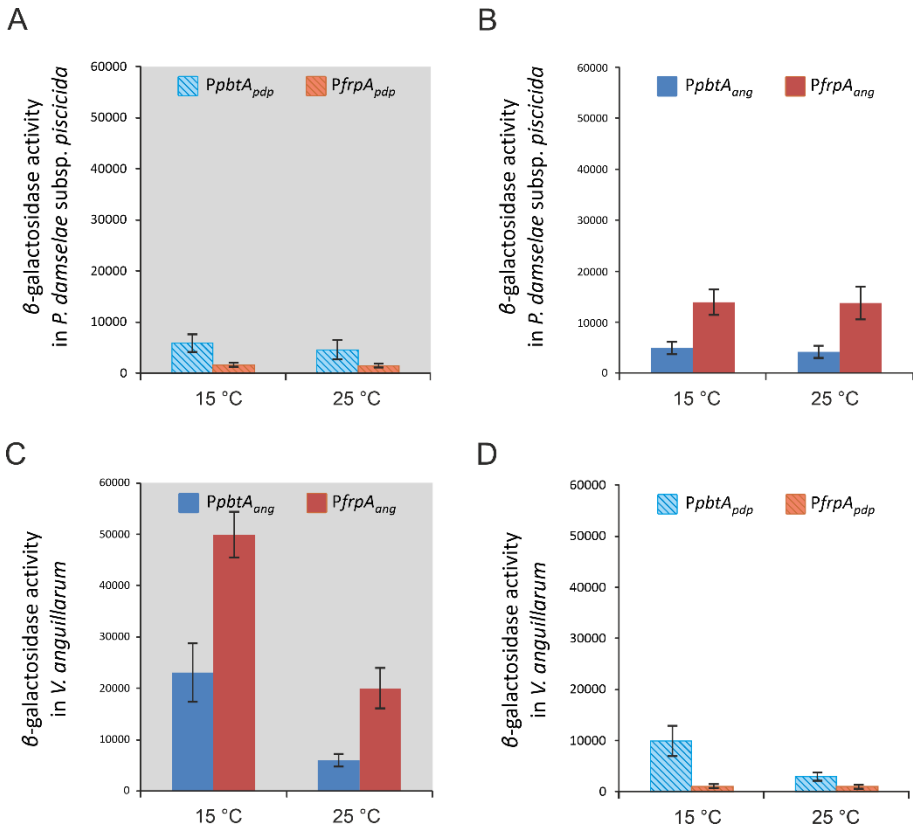


Figure IV.38. Transcriptional activity of *PfrpA* and *PpbtA* from *P. damselae* subsp. *piscicida* and *V. anguillarum* (the grey background corresponds to native transcriptional activity) (A and C) and correspondent heterologous transcriptional activity (B and D) assayed under iron limitation at 15 and 25°C.

This evaluation did not completely clarify if the different expression patterns are due to differences in promoter versions or are due to factors encoded in the respective recipient bacterial genome. To ascertain this aspect, heterologous evaluation of each promoter LacZ fusion was performed under the same conditions. Results in Figure

IV.38 showed that both versions of the *irp* promoters, either *PpbtA_{Pdp}* and *PfrpA_{Pdp}* or *PpbtA_{Vang}* and *PfrpA_{Vang}*, had ca. 3-fold less transcriptional activity in *P. damselae* subsp. *piscicida* (Figure IV.38.A and B) than *PpbtA_{Vang}* and *PfrpA_{Vang}* in *V. anguillarum* (Figure IV.38.C). The expression level achieved by *PpbtA_{Vang}* in *P. damselae* subsp. *piscicida* was like that shown by the native evaluation of *PpbtA_{Pdp}* in *P. damselae* subsp. *piscicida*. Notably, while the transcriptional activity of *PpbtA_{Vang}* and *PfrpA_{Vang}* in *P. damselae* subsp. *piscicida* did not show differences between temperatures (Figure IV.38.B), the promoter *PpbtA_{Pdp}* showed a 3-fold higher transcriptional activity at 15 °C than at 25 °C when assayed in *V. anguillarum* (Figure IV.38.D). In contrast, *PfrpA_{Pdp}* did not show transcriptional activity when measured in *V. anguillarum*, confirming that the short *pbtB-frpA* intergenic sequence does not serve as transcriptional initiator (Figure IV.38.D). Notably, when inserted in *V. anguillarum*, *irp*-HPI_{Pdp} was activated at low temperature but the opposite did not occur. When *PpbtA_{Vang}* and *PfrpA_{Vang}* were inserted in *P. damselae* subsp. *piscicida*, the transcriptional activity of both promoters did not respond to the environmental temperature. These results greatly suggest that *irp*-HPI temperature-dependent expression pattern would be a property more related to the presence of an activator in the recipient bacteria genome that enhances the transcription of *PpbtA* when temperature decreases than an inherent property of the *irp*-HPI genomic island. Thus, *irp*-HPI expression pattern would result from long-range interaction of *irp*-HPI type with the recipient genome regulatory factors.

3.3. SUMMARY OF CHAPTER 3

Piscibactin production would be preferentially expressed at cold temperature. The transcriptional levels of the *PpbtA*, *PfrpA* and *PfrpBC* significantly increased upon temperature shift to 15 °C. Inactivation of *pbtA* disables piscibactin biosynthesis and transport, impairing *V. anguillarum* to grow under iron limited conditions. Therefore, PbtA was characterized as the most prominent modulator of piscibactin *irp* genes expression in *V. anguillarum*. PbtA deletion abolished the expression of the piscibactin outer membrane receptor and biosynthetic functions. PbtA C-terminal domain interacts directly with ca. 100 bp

region located upstream of *PfrpA* and *PfrpBC* start codon. The impossibility to purify PbtA total protein did not allow to determine the N-terminal domain function and if PbtA acts as an environmental sensor. Moreover, elements encoded elsewhere in the genome, *h-ns* and *toxR-S* are indirectly involved in the expression of the system. The deletion of *h-ns* resulted in a decrease in the transcriptional levels of *PfrpA* at 15 °C and 25 °C indicating that H-NS is required for the maximum expression of piscibactin siderophore system. The deletion of both *pbtA* and *h-ns* caused a significant decrease in virulence for fish, confirming the relevance of piscibactin in the pathogenesis of *V. anguillarum*. Interestingly, the deletion of the conserved regulator *toxR-S* showed a different effect. It resulted in an increased expression of *PfrpA* and *PpbtA* at 25 °C. The increased transcriptional levels suggest that ToxR-S may be involved in the modulation of piscibactin *irp* genes at 25 °C, acting as a repressor of transcription at warm temperature. Notably, the widespread distribution and the existence of different versions of the *irp*-HPI suggests a long-term evolution of this pathogenicity island in *Vibrionaceae*. The temperature-dependent expression of *irp*-HPI is the result of the interaction between piscibactin activator PbtA and regulator(s) harboured in *V. anguillarum* genome. The results greatly suggest that piscibactin production enables *V. anguillarum* to infect cold adapted fish species.

4. UTILITY OF THE SIDEROPHORES OUTER MEMBRANE TRANSPORTERS TO DEVELOP NEW VACCINES AGAINST VIBRIOSIS

The components of the iron acquisition systems could be used to generate novel methods of prevention and control of infectious diseases in aquaculture. In this chapter the use of the outer membrane transporters FrpA and FvtA will be explored to use in the elaboration of subunit vaccines against vibriosis in fish.

4.1. USE OF SIDEROPHORE TRANSPORTERS FVTA AND FRPA TO DEVELOP VACCINES AGAINST VIBRIOSIS

The development of subunits vaccines requires the identification of the pathogen proteins with immunogenic properties that can generate protection. Furthermore, the selected protein must be expressed during the infection process and must be located at the surface of the pathogen to be available to the host immune system. Iron acquisition systems mediated by siderophores are recognized as relevant virulence factors and are essential for the survival of the pathogen within the host (Ballouche *et al.*, 2009). These characteristics make them excellent candidates for the development of new antibacterial therapies. The *irp*-HPI that encodes the piscibactin siderophore system is widespread among diverse marine bacterial pathogens and thus it could be used as a target to prevent disease outbreaks from a diverse number of pathogens. In *P. damsela* subsp. *piscicida*, the piscibactin outer membrane transporter FrpA_{Pdp} has been shown to be an immunogenic protein and an excellent candidate to formulate vaccines for fish (Valderrama *et al.*, 2019).

4.1.1. Fish immunization assay

Experimental immunizations and subsequent infection challenges were performed to study whether vanchrobactin (FvtA) and piscibactin

(FrpA) outer membrane transporters could be used for the development of vaccines against *V. anguillarum* infections. Recombinant proteins of FrpA (rFrpA) and FvtA (rFvtA) were obtained by cloning each gene in the plasmid pET20b(+), expressed in *E. coli* and the native proteins were purified from the outer membrane fractions. These procedures were made by the group of Prof. Carlos Jiménez (University of A Coruña) as part of a coordinated research project.

Table IV.12. Treatment employed to each fish group.

Group	Treatment
Non-vaccinated	PBS
Freund's control	Freund's Adjuvant:PBS
<i>V. anguillarum</i> bacterin control	RV22 inactivated cells
<i>P. damselae</i> subsp. <i>piscicida</i> (<i>Pdp</i>) bacterin control	DI21 inactivated cells
rFrpA	30 µg rFrpA
rFvtA	30 µg rFvtA

To test FvtA and FrpA immunogenicity and further protection, 6 groups of sole fish (*Solea senegalensis*) fingerlings were inoculated intraperitoneally with the correspondent treatment (Table IV.12). Two control groups were established: non-vaccinated control and Freund's adjuvant. Freund's adjuvant was selected since it is commonly used in the study of subunits vaccines as it stimulates the immune response (Dadar *et al.*, 2017). The fish of either rFrpA or rFvtA groups were inoculated with an emulsion containing the recombinant protein diluted in PBS and Freund's adjuvant. The bacterin control groups were treated with a classical bacterin after growing *V. anguillarum* RV22 strain (Bacterin *V. anguillarum*) or *P. damselae* subsp. *piscicida* DI21 strain (Bacterin *Pdp*) in TSB-1 at 25 °C.

Two immunizations were performed (Figure IV.39). The first one at day 0 and a second immunization or a booster vaccination at day 30. In addition, before each immunization, on day 0 and 30, and 30 days after the booster immunization, on day 60, a blood sample was extracted from 5 fish from each group to evaluate the level of antibodies generated against the recombinant proteins and bacterins used in the immunizations (Figure IV.39). Sixty days after the first immunization, experimental infection challenges were performed to evaluate the degree of protection conferred by the treatments.

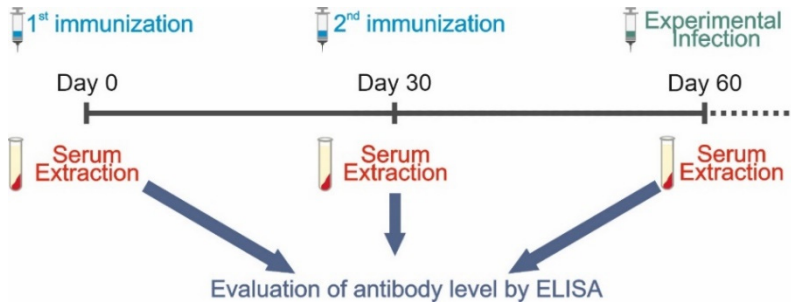


Figure IV.39. Schematic representation of the experimental design. Two immunizations were performed 30 days apart. After 60 days, an experimental infection was performed to evaluate the protection conferred by the treatments. Serum was extracted before each immunization and experimental infection to evaluate the antibody levels.

4.1.2. FrpA and FvtA are immunogenic proteins

Immunogenicity is the ability of an antigen to activate the immune system and generate an immune response. The level of antibodies generated after each immunization was evaluated by ELISA. This assay allowed the quantification of the antibodies generated against the recombinant proteins rFrpA and rFvtA and against the whole cells (bacterins) of either *V. anguillarum* (anti-RV22) or *Pdp* (anti-*Pdp*).

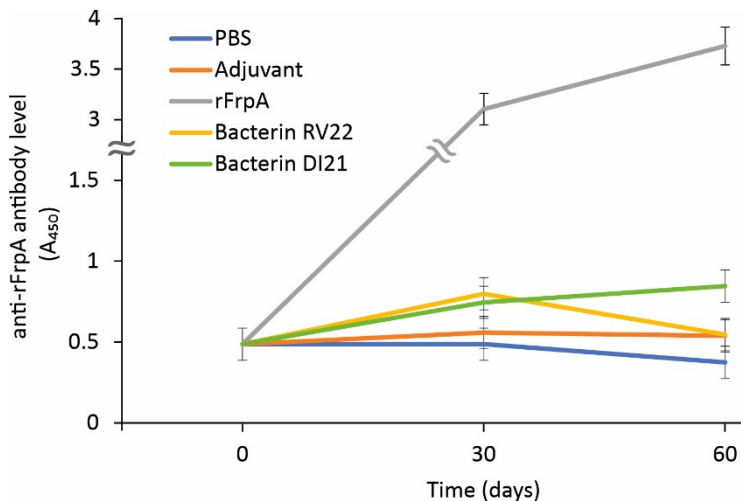


Figure IV.40. Anti-rFrpA antibody levels detected by ELISA in the serum of fish immunized with PBS, Freund's adjuvant, rFrpA, bacterin RV22 and bacterin DI21.

First, an ELISA assay was performed to evaluate the level of antibodies generated against rFrpA (anti-rFrpA antibodies) (Figure IV.40). Fish treated with the recombinant protein rFrpA showed high antibody levels, measured at A_{450} of 3.1 at day 30, and increased to 3.7 at day 60, after the second immunization (Figure IV.40). This antibody levels were significantly higher than that observed for the groups treated with bacterins. Fish treated with the RV22 bacterin revealed a fluctuation in the antibody levels. At the time of the second immunization this group of fish showed an $A_{450} = 0.8$ and it slightly decreased to 0.55 at day 60. Regarding the fish group treated with the DI21 bacterin, the antibody levels increased over time. After the second immunization, the A_{450} increased from 0.75 to 0.85. The control group treated with PBS showed a basal antibody level of ca. 0.4. Moreover, the control group treated with Freund's adjuvant showed an antibody level after the second immunization at the same level as that observed for the RV22 bacterin (Figure IV.40). These results suggest that rFrpA is highly immunogenic. Thus, the low levels of antibodies anti-rFrpA found in the fish immunized with bacterin, either RV22 or DI21, must be due to low FrpA content in the cells that form the bacterin.

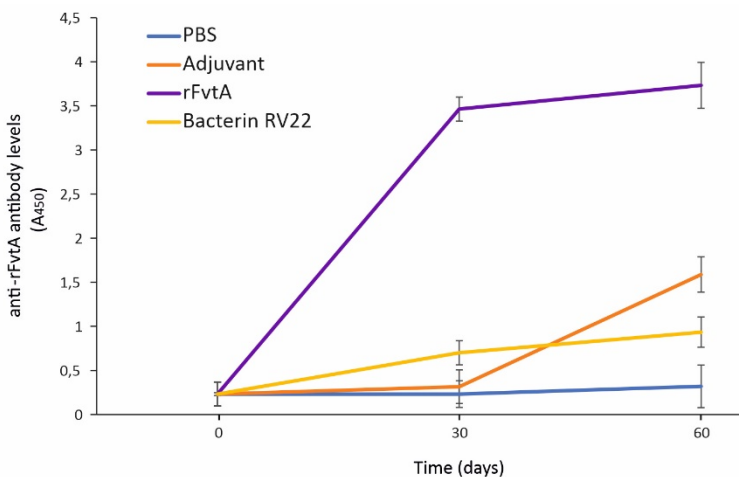


Figure IV.41. Anti-rFvtA antibody levels detected by ELISA in the serum of fish immunized with PBS, Freund's adjuvant, rFvtA and bacterin RV22.

When the antibody levels against rFvtA (anti-rFvtA antibodies) were measured (Figure IV.41) in serum from fish immunized with the recombinant protein rFvtA. The values obtained were high, achieving the maximum after the second immunization (A_{450} ca. 3.7). Remarkably, the anti-rFvtA antibody levels at day 60 of the control group immunized with Freund's adjuvant were higher than those obtained for the fish group immunized with the RV22 bacterin. After the second immunization, the antibody titer of the fish group immunized with the adjuvant increased, reaching an A_{450} ca. 1.5, whereas the bacterin immunized fish showed an A_{450} ca. 0.8. The fish control group immunized with PBS showed a residual level of anti-rFvtA antibodies. These results suggest that rFvtA is also a highly immunogenic protein. Though, the low levels of antibodies anti-rFvtA found in the fish immunized with RV22 inactivated whole cells, indicates a scarce presence of FvtA in the cells that form the bacterin.

Fish immunized with any bacterin, either RV22 or DI21 bacterins, showed the maximum level of antibodies among all the treatments against their respective bacterial whole cells (Figure IV.42 and IV.43). Fish groups immunized with one of the recombinant proteins, rFrpA or rFvtA, have low anti-RV22 or anti-*Pdp* antibody levels compared to the bacterins (Figure IV.42 and IV.43). The most plausible explanation is that the content of FrpA in the outer membrane of the cells might be low. The classical vaccines, bacterins, are obtained by allowing the cells to grow in a rich medium, which does not correspond to the conditions faced by the pathogen when within the host. In *V. anguillarum* the most relevant virulence factors are expressed under iron deficiency, therefore using these stringent conditions would improve the level of antigens (van Oirschot, 1997). Nonetheless, the use of these conditions could also lead to the accumulation of factors with toxic effects (Ebanks *et al.*, 2004).

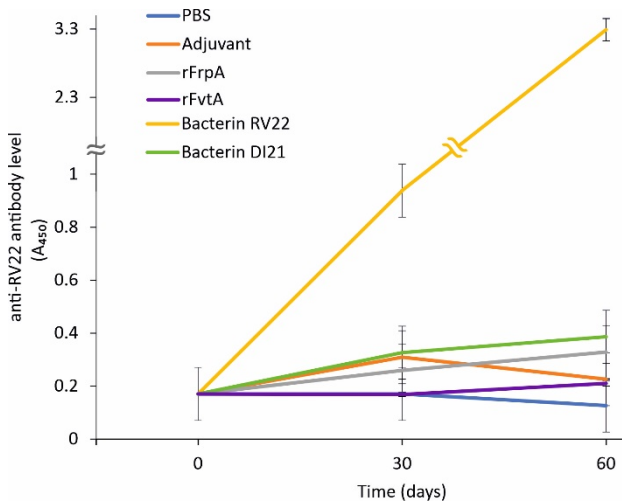


Figure IV.42. Anti-RV22 antibody levels detected by ELISA in the serum of fish immunized with PBS, Freund’s adjuvant, rFrpA, rFvtA, bacterin RV22 and bacterin DI21.

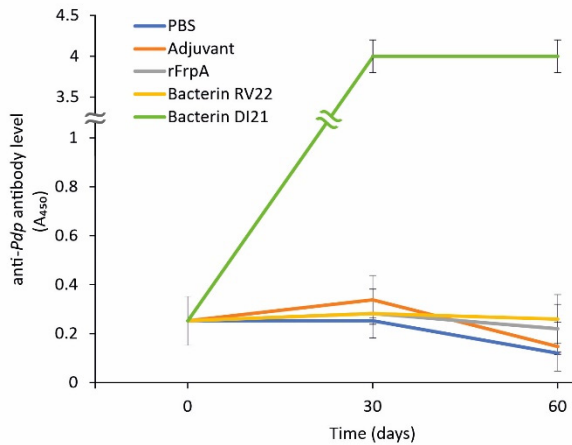


Figure IV.43. Anti-Pdp antibody levels detected by ELISA in the serum of fish immunized with PBS, Freund’s adjuvant, rFrpA, bacterin RV22 and bacterin DI21.

The results of immunogenicity assays suggest that FrpA and FvtA are immunogenic proteins, and both induce an intense immune response since the first dose, which suggests that both proteins could be used as antigens in vaccine formulations. The generation of antibodies anti-

rFrpA showed a similar pattern as the generation of antibodies anti-RV22 and anti-rFvtA, where a second immunization promotes the maximal production of antibodies. One of the advantages of using subunits vaccines is that a booster immunization stimulates the immune system to generate a longer protection (Esmailkhani *et al.*, 2016). Interestingly, when *Pdp* bacterin was used as antigen, the generation of antibodies achieved the maximal level upon the first immunization. The booster dose did not significantly increase the antibody level.

The results suggest that both recombinant proteins, either rFrpA and rFvtA, are immunogenic and, therefore, the correlation between immunogenic response generated and protection conferred against pathogens infection must be evaluated.

4.1.3. Evaluation of protection in experimental infections

Considering the subunits vaccines, the immunization with proteins in their native conformation would generate a higher level of protection (Valderrama *et al.*, 2019) as it also assures that the epitopes present in the outer membrane are the same as in the vaccine. Nonetheless, the level of antibodies generated after the immunization with an antigen does not always correlate with protection against the pathogen as not all the antigens induce an adaptative immune response and memory (Ellis, 1999). Since expression of FvtA and FrpA in *V. anguillarum* is favoured at warm- and cold-temperatures, respectively, the infection challenges with *V. anguillarum* were made at warm-water temperature (24 °C), to evaluate protection conferred by FvtA, and at colder water temperature (18 °C) to evaluate FrpA. Both challenges were done in sole (*Solea senegalensis*) fingerlings. The possible cross protection of rFrpA from *V. anguillarum* against *P. damselae* subsp. *piscicida* was tested at 22 °C, temperature at which *Pdp* natural outbreaks occur.

a) Protection conferred by rFvtA against *V. anguillarum* at warm-water temperature

To evaluate the use of rFvtA in subunit vaccines against *V. anguillarum*, fish immunized with the treatments described above were maintained at a water temperature of 24 °C and were injected intraperitoneally with 100 µL of a *V. anguillarum* suspension with

ca. 5×10^5 CFU/mL (Figure IV.44). At this temperature, the vancomycin siderophore system is significantly expressed and, thus, FvtA could be a good antigen candidate to develop new vaccines. The fish group immunized with PBS began to die one day post infection and on day 5 a 100% of mortality was observed. The fish group immunized with Freund's adjuvant showed a similar survival curve and only 10% of fish survived. Interestingly, the fish group immunized with rFvtA showed a survival rate of 25%, 8 days post infection. Notably, the fish group immunized with RV22 bacterin showed a remarkable survival rate of 98%. These results indicate that fish immunized with a classical RV22 bacterin, composed of inactivated whole cells grown in iron excess at 25 °C significantly protects against a *V. anguillarum* infection at temperatures above 24 °C. Although it is expressed at this temperature, FvtA does not generate high levels of protection. The antigen content of the bacterin clearly surpasses the infectiveness of *V. anguillarum* when the infection occurs at 24 °C.

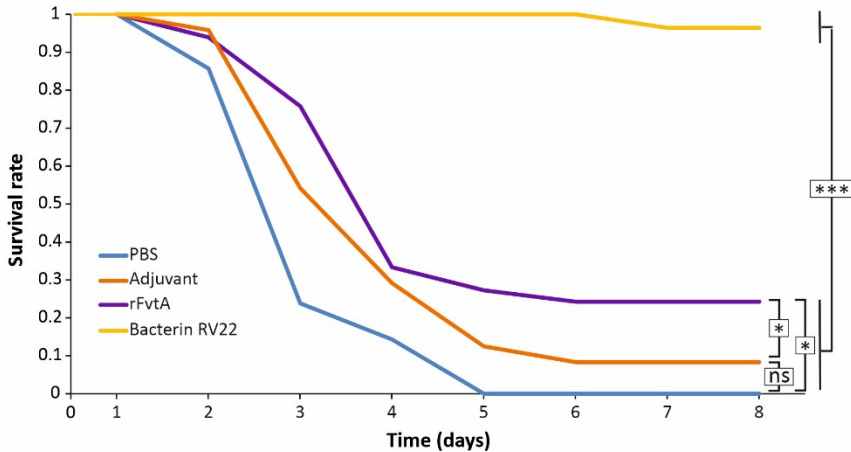


Figure IV.44. Survival rate of fish maintained at 24 °C and experimentally challenged with 5×10^5 CFU/mL of a *V. anguillarum* suspension. Mortality was followed daily. Asterisks denote statistical significance, * $p < 0.05$, *** $p < 0.001$, ns, no statistically significant differences.

b) Protection conferred by rFrpA against *V. anguillarum* at cold-water temperature

Fish treated with rFrpA exhibited high levels of IgG in their serum. Therefore, to evaluate the protection conferred by this vaccine against *V. anguillarum* and *Pdp*, a series of experimental infection challenges were performed. To this purpose, each immunized fish group (Table IV.12) was divided into two groups and the experimental infections were performed at 18 °C to evaluate protection against *V. anguillarum* and at 22 °C for *P. damsela* subsp. *piscicida* to mimic the natural infection conditions. In addition, the protection conferred by FvtA at cold water temperature was also evaluated.

Fish maintained at a water temperature of 18 °C were injected intraperitoneally with 100 µL of a *V. anguillarum* suspension with ca. 5×10^5 CFU/mL. The mortality events were followed and registered daily, and the relative survival rate was defined for each of the treatments (Figure IV. 45).

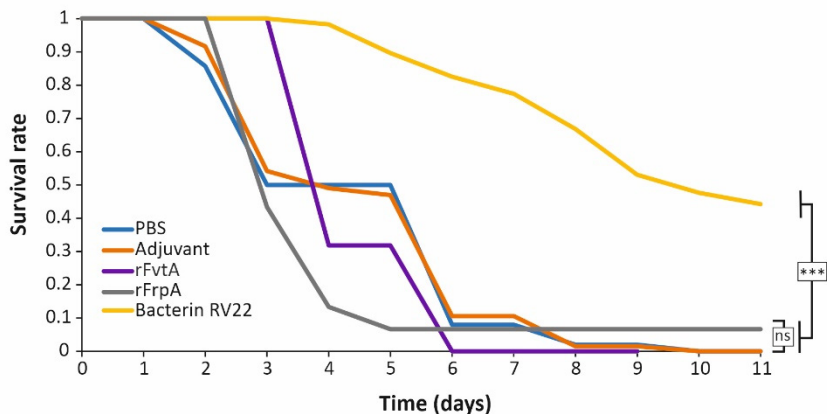


Figure IV.45. Survival rate of fish maintained at 18 °C and experimentally challenged with 5×10^5 CFU/mL of a *V. anguillarum* suspension. Mortality was followed daily. Asterisks denote statistical significance, *** $p < 0.001$, ns, no statistically significant differences.

Mortality events started 3 days post infection in fish challenged with *V. anguillarum* (Figure IV.45). As expected, fish of the

control group immunized with PBS began to die 2 days post infection. This group achieved a mortality rate of 100% on day 8 after infection. Similarly, the fish immunized with Freund's adjuvant showed a mortality curve as that observed for the PBS control group. Five days post infection, the fish immunized with rFrpA showed a survival rate of ca. 10%. This survival curve remained stable until the end of the experiment. Fish immunized with rFvtA showed a drastic decrease in the survival rate 4 days post infection and a mortality rate of 100% was achieved 6 days post infection. Remarkably, the survival curve of fish immunized with the RV22 bacterin was significantly different. Mortality started on day 4 post infection and a constant decrease in the survival curve was observed. At the end of the experiment, this fish group showed a survival rate of 46%. Notably, the RV22 bacterin generated an intermediate protection against a *V. anguillarum* infection at 18 °C. These results suggest that rFrpA and rFvtA did not generate a significant level of protection when compared to the RV22 bacterin against a *V. anguillarum* infection at 18 °C. As described above, the bacterin was obtained by growing the cells in a rich medium at 25 °C. Under these conditions most virulence factors and particularly iron uptake system are silenced. Although FrpA and FvtA are immunogenic proteins they did not generate a high level of protection against *V. anguillarum* infection at 18 °C.

c) Protection conferred by rFrpA against *P. damsela* subsp. *piscicida* (*Pdp*)

Since *irp*-HPI is widespread in *Vibrionaceae*, the cross protection conferred by FrpA of *V. anguillarum* against other fish bacterial pathogens such as *Pdp* was evaluated.

Fish maintained at 22 °C were injected intraperitoneally with 100 µL of a *Pdp* suspension with ca. 5×10^5 CFU/mL. Mortality was followed daily, and the survival curve was obtained for each treatment (Figure IV. 46). The survival curves obtained after the experimental infection with *P. damsela* subsp. *piscicida* at 22 °C, revealed a different outcome (Figure IV.46). 4 days post infection the PBS control group, achieved a mortality of 100%. The fish

immunized with Freund's adjuvant showed an intermediate survival, as 7 days post infection it achieved a survival rate of 46%. Fish immunized with DI21 bacterin showed a remarkable survival rate, since 7 days post infection this group had a survival rate of around 80%. Surprisingly, the group treated with rFrpA generated a 63% survival rate. This means that FrpA from *V. anguillarum* can generate protection against *P. damsela* subsp. *piscicida* infection at 22 °C at notable levels, compared with the DI21 bacterin. These results confirm previous work that showed FrpA as a good candidate to elaborate subunit vaccines against *Pdp* (Valderrama *et al.*, 2019). As *P. damsela* subsp. *piscicida* infection occurs at a temperature closer to the one used for bacterin elaboration, the antigens present in this bacterin resemble those encountered during the infection process which increased the protection against *P. damsela* subsp. *piscicida*.

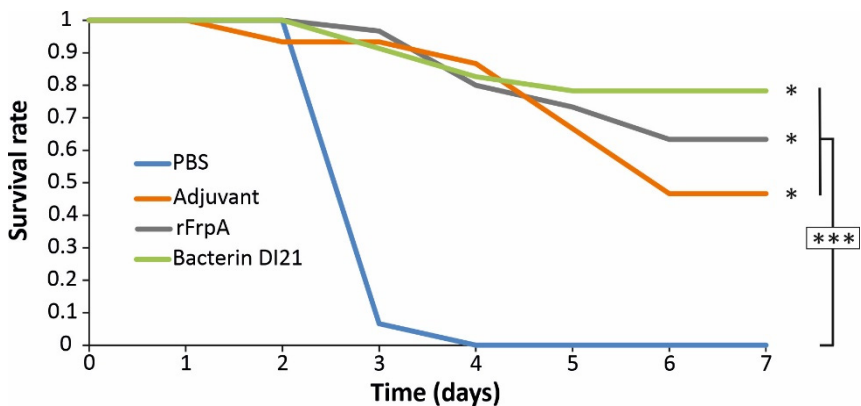


Figure IV.46. Survival rate of fish maintained at 22 °C and experimentally challenged with 5×10^5 CFU/mL of a *P. damsela* subsp. *piscicida* suspension. Mortality was followed daily. Asterisks denote statistical significance, * $p < 0.05$, *** $p < 0.001$.

The subunit vaccines are based on antigenic components of a specific pathogen therefore, the immune response is focused against it (Hansson *et al.*, 2000). The outer membrane proteins are natural candidates for this vaccine formulation due to its external localization and immunogenicity. Nonetheless, the feasibility of this method is

strictly dependent on the *in vitro* production of significant amounts of the protein, the manipulation of the vector and the expression of the protein in its native conformation. The utilization of siderophore transporters in subunit vaccines is a promising strategy. The previous results of our group using FrpA from *Pdp* to protect sole against photobacteriosis (Valderrama *et al.*, 2019) is a good demonstration. The immunization with FuyA, the yersiniabactin transporter, or the siderophore transporters Hma, IutA or IreA showed protection against uropathogens (Brumbaugh *et al.*, 2013). Likewise, immunization with Iron, the enterobactin receptor in *E. coli* has shown also promising results (Russo *et al.*, 2003). The main advantage of using the siderophores transport systems is that they are essential virulence factors that are significantly expressed during the infection process (Ebanks *et al.*, 2004).

Our results, although rather preliminary, suggest that the efficacy of the *V. anguillarum* RV22 bacterin decreases when the infection challenge is performed at lower temperatures. Several vaccine formulations are commercially available against vibriosis (Frans *et al.*, 2011). All of them consist in the inactivation of bacteria (serotype O1 and O2) by formalin or heat. However, vibriosis outbreaks still occur, mainly caused by serotype O2 in cold-adapted fish species such as cod (Mikkelsen *et al.*, 2007). To improve protection, these vaccine formulations can be enriched with extracellular products, outer membrane proteins or lipopolysaccharides (Frans *et al.*, 2011). The outer membrane receptors for the ferri-siderophore complex are antigenic proteins and good candidates for vaccine enrichment (Valderrama *et al.*, 2019). In this concern, DNA vaccines based on the major outer membrane protein OmpU and the metalloprotease EmpA have shown promising results (Kumar *et al.*, 2007; Yang *et al.*, 2009). It is tempting to speculate that a bacterin made of inactivated whole cells grown at 18 °C or lower temperatures could improve protection of those fish species farmed at cold-water temperature. Moreover, it is remarkable how FrpA from *V. anguillarum* could generate a significant cross protection against an *irp*-HPI harbouring pathogen such as *P. damsela* subsp. *piscicida*.

The demonstration that FrpA from *V. anguillarum* generated protection against an *irp*-HPI harbouring pathogen like *Pdp*, suggests that FrpA could be a good candidate to develop subunit vaccines against diverse pathogens, mainly of the genus *Vibrio* and *Photobacterium*.

4.2. SUMMARY OF CHAPTER 4

Siderophore outer membrane transporters are good candidates for vaccine development as they are expressed during the infection process. Although the results demonstrated that both FrpA and FvtA are immunogenic proteins, the fish immunization assays revealed that the recombinant proteins did not confer a significant protection against *V. anguillarum* infection. These findings showed that protection against a pathogen does not directly correlate with antibody levels as other factors must be considered in subunit vaccines formulation, such as antigen concentration or adjuvants. Interestingly, *V. anguillarum* version of FrpA (rFrpA_{Vang}) conferred cross protection against the infection of the *irp*-HPI harbouring pathogen *P. damsela* subsp. *piscicida*. These results suggest that the widespread distribution of *frpA* among *Vibrionaceae*, could be used to formulate multivalent vaccines against a diversity of pathogens.

V. CONCLUSIONS

V. CONCLUSIONS

1. *V. anguillarum* modulates the expression of virulence factors in response to iron levels and, most notably, in response to temperature. Genes related to chemotaxis, motility, the T6SS1 and the siderophore vanchrobactin are preferentially expressed at the optimal growth temperature (25 °C). Conversely, genes related to exopolysaccharide assembly and transport, the haemolysin RTX, T6SS2, and the siderophore piscibactin, achieve their maximal expression below the optimal growth temperature (at 15 °C).
2. The production of a concrete array of virulence factors in response to temperature implies that each virulence factor might have different relevance for virulence in cold- and warm-water cultivated fish species. Thus, disease caused by *V. anguillarum* is multifactorial and context dependent.
3. Highly virulent *V. anguillarum* strains lacking the anguibactin siderophore system harbour the High-Pathogenicity Island *irp*-HPI and produce two siderophores, vanchrobactin and piscibactin. Piscibactin is essential for *V. anguillarum* virulence whereas the role of vanchrobactin would be more related to environmental survival. The piscibactin system is one of the most up-regulated virulence factors at 15 °C. The acquisition of *irp*-HPI by horizontal gene transfer enhances niche flexibility enabling the recipient bacteria to infect cold- and warm-water adapted fish species.
4. The High-Pathogenicity Island *irp*-HPI encodes the functions required for the synthesis, transport, and regulation of the piscibactin system. The unique exception is the 4'-phosphopantetheinyl transferase activity, whose function is complemented by the vanchrobactin operon. Inactivation of either *irp1* or *irp4* abolished piscibactin production. Thus, while Irp1 is a large

NRPS/PKS essential for piscibactin synthesis, the type II thioesterase Irp4 is involved in the release of the nascent siderophore from the biosynthetic enzymatic line. The MFS Irp8 mediates piscibactin export.

5. The ferri-piscibactin complex enters the cell through the TonB-dependent outer membrane transporter FrpA and the inner membrane ABC transporter FrpBC. The configuration of C-13 is essential for piscibactin iron chelation and its further recognition by the outer membrane transporter FrpA.
6. Synthetic piscibactin analogues are internalized through different FrpA homologues present in pathogenic bacteria such as *V. anguillarum* and *P. damselae* subsp. *piscicida*. Thus, piscibactin analogues could be used to vectorize antimicrobial compounds against a wide range of pathogens employing the Trojan Horse strategy.
7. The temperature-dependent expression of *irp*-HPI is the result of the interaction between piscibactin activator PbtA and regulator(s) harboured in *V. anguillarum* genome. PbtA is the main modulator of *irp* genes expression and directly interacts with the piscibactin promoters *PfrpA* and *PfrpBC*. The widespread distribution of *irp*-HPI homologues and the existence of different expression patterns between bacterial species suggests a long-term evolution of this pathogenicity island in *Vibrionaceae*.
8. The outer membrane siderophore transporters FrpA and FvtA are immunogenic proteins, but they did not confer a significant protection against *V. anguillarum* infection. However, cross protection conferred by the *V. anguillarum* FrpA against *irp*-HPI harbouring pathogen such as *P. damselae* subsp. *piscicida* and its widespread distribution among *Vibrionaceae*, makes it an excellent target to improve multivalent vaccines to prevent outbreaks caused by pathogenic *Vibrio*-like bacteria.

VI. REFERENCES

VI. REFERENCES

- Actis, L. A., Fish, W., Crosa, J. H., Kellerman, K., Ellenberger, S.R., Hauser, F. M. and Sanders-Loehr, J. (1986) Characterization of anguibactin, a novel siderophore from *Vibrio anguillarum* 775 (pJM1). *J. Bacteriol.* 167(19): 57-65. doi: 10.1128/jb.167.1.57-65.1986.
- Adams, A. (2019) Progress, challenges and opportunities in fish vaccine development. *Fish Shellfish Immunol.* 90: 210-214. doi: 10.1016/j.fsi.2019.04.066.
- Alice, A. F., López, C. S. and Crosa, J. H. (2005) Plasmid- and chromosome-encoded redundant and specific functions are involved in biosynthesis of the siderophore anguibactin in *Vibrio anguillarum* 775: a case of chance and necessity? *J. Bacteriol.* 187(6): 2209-2214. doi: 10.1128/JB.187.6.22.09-2214.2005.
- Andrews, S. C., Robinson, A. K., and Rodriguez-Quinones, F. (2003) Bacterial iron homeostasis. *FEMS Microbiol. Rev.* 27 (2-3): 215-237. doi: 10.1111/j.1365-2109.2004.01165.x.
- Anisimov, R., Brem, D., Heesemann, J., and Rakin, A. (2005). Transcriptional regulation of high pathogenicity island iron uptake genes by YbtA. *Int. J. Med. Microbiol.* 295(1): 19-28. doi: 10.1016/j.ijmm.2004.11.007.
- APROMAR. (2020). Aquaculture in Spain. Report prepared by the Spanish Aquaculture Business Association (APROMAR): www.apromar.es.
- Arjona, F. J., Ruiz-Jarabo, I., Vargas-Chacoff, L., Martín Del Río, M. P., Flik, G., Mancera, J. M., *et al.* (2010). Acclimation of *Solea senegalensis* to different ambient temperatures: implications for thyroidal status and osmoregulation. *Mar. Biol.* 157(6): 1325-1335. doi: 10.1007/s00227-010-1412-x.
- Austin, B., Alsina, M., Austin, D. A., Blanch, A. R., Grimont, F., Grimont, P. A. D., Jofre, J., Koblavi, S., Larsen, J. L., Pedersen, K., Tiainen, T., Verdonck, L. and Swings, J. (1995). Identification and typing of *Vibrio anguillarum*: a comparison of different methods. *System. Appl. Microbiol.* 18: 285-302. doi: 10.1016/S0723-2020(11)80400-5.

- Austin, B., and Austin, D. A. (2007). *Epizootiology: gram-negative bacteria, in Bacterial fish Pathogens*. Springer Praxis Books, (Dordrecht: Springer). doi: 10.1007/978-1-4020-6069-4_8.
- Austin, B. (2010) Vibrios as casual agents of zoonoses. *Vet. Microbiol.* 140 (3-4): 310-317. doi: 10.1016/j.vetmic.2009.03.015.
- Bachman, M. A., Lenio, S., Schmidt, L., Oyler, J. E. and Weiser, J. N. (2012) Interaction of lipocalin 2, transferrin, and siderophores determines the replicative niche of *Klebsiella pneumoniae* during pneumonia. *mBio*.3(6): e00224-11. doi: 10.1128/mBio.00224-11.
- Balado, M., Osorio, C.R., and Lemos, M.L. (2006) A gene cluster involved in the biosynthesis of vanchrobactin, a chromosome-encoded siderophore produced by *Vibrio anguillarum*. *Microbiology* 152(12): 3517–3528. doi: 10.1099/mic.0.29298-0.
- Balado, M., Osorio, C. R., and Lemos, M. L. (2008) Biosynthetic and regulatory elements involved in the production of the siderophore vanchrobactin in *Vibrio anguillarum*. *Microbiology* 154(5): 1400–1413. doi: 10.1099/mic.0.2008/016618-0.
- Balado, M., Osorio, C. R. and Lemos, M. L. (2009) FvtA is the receptor for the siderophore vanchrobactin in *Vibrio anguillarum*: utility as a route of entry for vanchrobactin analogues. *Appl. Environ. Microbiol.* 75(9): 2775–2783. doi: 10.1128/AEM.02897-08.
- Balado, M., Souto, A., Vences, A., Careaga, V., Valderrama, K., Segade, Y., Rodríguez, J., Osorio, C. R., Jiménez, C. and Lemos, M. L. (2015) Two catechol siderophores, acinetobactin and amonabactin, are simultaneously produced by *Aeromonas salmonicida* subsp. *salmonicida* sharing part of the biosynthetic pathway. *ACS Chem. Biol.* 10(12): 2850–2860. doi: 10.1021/acscchembio.5b00624.
- Ballouche, M., Cornelis, P. and Baysse, C. (2009) Iron metabolism: a promising target for antibacterial strategies. *Recent Pat. Antiinfect. Drug Discov.* 4(3): 190-205. doi: 10.2174/157489109789318514.
- Barancin, C. E., Smoot, J. C., Findlay, R. H. and Actis, L. A. (1998) Plasmid-mediated histamine biosynthesis in the bacterial fish pathogen *Vibrio anguillarum*. *Plasmid*. 39(3): 235-244. doi: 10.1006/plas.1998.1345.
- Barcik, W., Wawrzyniak, M., Akdis, C. A. and O'Mahony, L. (2017) Immune regulation by histamine and histamine-secreting bacteria. *Curr. Opin. Immunol.* 48: 108-113. doi: 10.1016/j.coi.2017.08.011.

- Bellos, G., Angelidis, P., and Miliou, H. (2015) Effect of temperature and seasonality principal epizootiological risk factor on vibriosis and photobacteriosis outbreaks for European sea bass in Greece (1998-2013). *J. Aquac. Res. Dev.* 6(5): 338. doi: 10.4172/2155-9546.1000338.
- Ben-Haim, Y., Thompson, F. L., Thompson, C. C., Cnockaert, M. C., Hoste, B., Swings, J. and Rosenberg, E. (2003) *Vibrio coralliilyticus* sp. nov., a temperature-dependent pathogen of the coral *Pocillopora damicornis*. *Int. J. Syst. Evol. Microbiol.* 53(1): 309–315. doi: 10.1099/ij.s.0.02402-0.
- Bernard, C. S., Brunet, Y. R., Gueguen, E., and Cascales, E. (2010). Nooks and crannies in type VI secretion regulation. *J. Bacteriol.* 192(15): 3850–3860. doi: 10.1128/JB.00370-310.
- Biasini, M., Bienert, S., Waterhouse, A., Arnold, K., Studer, G., Schmidt, T., Kiefer, F., Cassarino, T. G., Bertoni, M., Bordoli, L. and Schwede, T. (2014) SWISS-MODEL: modelling protein tertiary and quaternary structure using evolutionary information. *Nucleic Acids Res.* 42: W252-258. doi: 10.1093/nar/gku340.
- Bingle, L. E., Bailey, C. M. and Pallen, M. J. (2008) Type VI secretion: a beginner's guide. *Curr. Opin. Microbiol.* 11(1): 3-8. doi: 10.1016/j.mib.2008.01.006.
- Bleuel, C., Grosse, C., Taudte, N., Scherer, J., Wesenberg, D., Krauss, G. J., Nies, D. H. and Grass, G. (2005) TolC is involved in enterobactin efflux across the outer membrane of *Escherichia coli*. *J. Bacteriol.* 187(19): 6701-6707. doi: 10.1128/JB.187.19.6701-6707.2005.
- Bobrov, A. G., Geoffroy, V. A. and Perry, R. D. (2002) Yersiniabactin production requires the thioesterase domain of HMWP2 and YbtD, a putative phosphopantetheinylate transferase. *Infect. Immun.* 70(8): 4204-4214. doi: 10.1128/IAI.70.8.4204-4214.2002.
- Bobrov, A. G., Kirillina, O., Fetherston, J. D., Miller, M. C., Burlison, J. A., and Perry, R. D. (2014). The *Yersinia pestis* siderophore, yersiniabactin, and the ZnuABC system both contribute to zinc acquisition and the development of lethal septicaemic plague in mice. *Mol. Microbiol.* 93(4): 759–775. doi: 10.1111/mmi.12693.
- Boesen, H. T., Pedersen, K., Larsen, J. L., Koch, C. and Ellis, A. E. (1999) *Vibrio anguillarum* resistance to rainbow trout (*Oncorhynchus mykiss*) serum: role of O-antigen structure of lipopolysaccharide. *Infect. Immunol.* 67(1): 294-301. doi: 10.1128/IAI.67.1.294-301.1999.

- Bremer, H. and Dennis, P. P. (2008) Modulation of chemical composition and other parameters of the cell at different exponential growth rates. *EcoSal. Plus.* 3(1): 1-49. doi: 10.1128/ecosal.5.2.3.
- Brickman, T. J. and McIntosh, M. A. (1992) Overexpression and purification of ferric enterobactin esterase from *Escherichia coli*. Demonstration of enzymatic hydrolysis of enterobactin and its iron complex. *J. Biol. Chem.* 267(17): 12350-12355.
- Brickman, T. J., Kang, H. Y., and Armstrong, S. K. (2001) Transcriptional activation of *Bordetella* alcaligin siderophore genes requires the AlcR regulator with alcaligin as inducer. *J. Bacteriol.* 183(2): 483-489. doi: 10.1128/JB.183.2.483-489.2001.
- Brudeseth, B. E., Wiulsrød, R., Frediksen, B. N., Lindmo, K., Løkling, K.-E., Bordevik, M., Steine, N., Klevan, A. and Gravningen, K. (2013) Status and future perspectives of vaccines for industrialised fin-fish farming. *Fish and Shellfish Immunol.* 35(6): 1759-1768. doi: 10.1016/j.fsi.2013.05.029.
- Brumbaugh, A. R., Smith, S. N. and Mobley, H. L. T. (2013) Immunization with the yersiniabactin receptor, FyuA, protects against pyelonephritis in a murine model of urinary tract infection. *Infect. Immun.* 81(9): 3309-3316. doi: 10.1128/IAI.00470-13.
- Brunet, Y. R., Bernard, C. S., Gavioli, M., Llobès, R. and Cascales, E. (2011) An epigenetic switch involving overlapping Fur and DNA methylation optimizes expression of a Type VI secretion gene cluster. *Plos Genet.* 7(7): e1002205. doi: 10.1371/journal.pgen.1002205.
- Bruto, M., James, A., Petton, B., Labreuche, Y., Chenivesse, S., Alunno-Bruscia, M., Polz, M. F. and Le Roux, F. (2017) *Vibrio crassostreae*, a benign oyster colonizer turned into a pathogen after plasmid acquisition. *ISME J.* 11: 1043-1052. doi: 10.1038/ismej. 2016.162.
- Buller, N. B. (2004) *Bacteria from Fish and other Aquatic Animals: A Practical Identification Manual*. CABI Publishing, Wallingford, UK.
- Busschaert, P., Frans, I., Crauwels, S., Zhu, B., Willems, K., Bossier, P., Michiels, C., Verstrepen, K., Lievens, B. and Rediers, H. (2015) Comparative genome sequencing to assess the genetic diversity and virulence attributes of 15 *Vibrio anguillarum* isolates. *J. Fish Dis.* 38(9): 795-807. doi: 10.1111/jfd.12290.
- Canestri, G. (1893) La mallattia dominante delle anguille. *Atti Instituto Veneto*

- Sci. Lett. Ed. Arti.* 7: 809-814.
- Carlos, A. R., Weis, S. and Soares, M. P. (2018) Cross-Talk between iron and glucose metabolism in the establishment of disease tolerance. *Front. Immunol.* 9: 2498. doi: 10.3389/fimmu.2018.02498.
- Carpenter, C. and Payne, S. M. (2014) Regulation of iron transport systems in *Enterobacteriaceae* in response to oxygen and iron availability. *J. Inorg. Biochem.* 133: 110-117. doi: 10.1016/j.jinorgbio.2014.01.007.
- Cascales, E. (2008) The type VI secretion toolkit. *EMBO Rep.* 9(8): 735-741. doi:10.1038/embor.2008.131.
- Chai, S., Welch, T.J. and Crosa, J. H. (1998) Characterization of the interaction between Fur and the iron transport promoter of the virulence plasmid in *Vibrio anguillarum*. *J. Biol. Chem.* 273(50): 33841-33847. doi: 10.1074/jbc.273.50.33841.
- Chakraborty, S., Sivaraman, J., Leung, K. Y. and Mok, Y.-K. (2011) Two-component PhoB-PhoR regulatory system and ferric uptake regulator sense phosphate and iron to control virulence genes in type III and VI secretion systems of *Edwardsiella tarda*. *J. Biol. Chem.* 286(45): 39417-39430. doi: 10.1074/jbc.M111.295188.
- Chatterjee, A., Dutta, P. K. and Chowdhury, R. (2007) Effect of fatty acids and cholesterol present in bile on expression of virulence factors and motility of *Vibrio cholerae*. *Infect. Immun.* 75(4): 1946-1953. doi: 10.1128/IAI.01435-06.
- Chatuverdi, K. S., Hung, C. S., Crowley, J. R., Stapleton, A. E. and Henderson, J. P. (2012) The siderophore yersiniabactin binds copper to protect pathogens during infection. *Nat. Chem. Biol.* 8(8): 731-736. doi: 10.1038/nchembio.1020.
- Chen, Q. and Crosa, J. H. (1996) Antisense RNA, Fur, iron, and the regulation of iron transport genes in *Vibrio anguillarum*. *J. Biol. Chem.* 271(31): 18885-18891. doi: 10.1074/jbc.271.31.18885.
- Childers, B. M., and Klose, K. E. (2007). Regulation of virulence in *Vibrio cholerae*: the ToxR regulon. *Future Microbiol.* 2(3): 335-344. doi: 10.2217/17460913.2.3.335.
- Childers, B. M., Cao, X., Weber, G. G., Demeler, B., Hart, P. J. and Klose, K. E. (2011) N-terminal residues of the *Vibrio cholerae* virulence regulatory protein ToxT involved in dimerization and modulation by fatty acids. *J.*

Biol. Chem. 286(32): 28644-28655. doi: 10.1074/jbc.M111.258780.

- Choi, U. and Lee, C.-R. (2019) Distinct roles of outer membrane porins in antibiotic resistance and membrane integrity in *Escherichia coli*. *Front. Microbiol.* 10: 953. doi:10.3389/fmicb.2019.00953.
- Confer, A. W. and Ayalew, S. (2013) The OmpA family of proteins: roles in bacterial pathogenesis and immunity. *Vet. Microbiol.* 163(3-4): 207-222. doi: 10.1016/j.vetmic.2012.08.019.
- Cordero, O. X., Ventouras, L.-A., DeLong, E. F. and Polz M. F. (2012) Public good dynamics drive evolution of iron acquisition strategies in natural bacterioplankton populations. *Proc. Natl. Acad. Sci. USA.* 109(49): 20059–20064. doi: 10.1073/pnas.1213344109.
- Cornelis, P., Wei, Q., Andrews, S. C., and Vinckx, T. (2011). Iron homeostasis and management of oxidative stress response in bacteria. *Metallomics.* 3(6): 540–549. doi: 10.1039/c1mt00022e.
- Crosa, J. H. and Walsh, C. T. (2002) Genetics and assembly line enzymology of siderophore biosynthesis in bacteria. *Microbiol. Mol. Biol. Rev.* 66(2): 223–249. doi: 10.1128/MMBR.66.2.223-249.2002.
- Crosa, J. H., Payne, S. M., and Mey, A. R. (2004). *Iron Transport in Bacteria*. Washington, DC: ASM Press.
- Croxatto, A., Lauritz, J., Chen, C., and Milton, D. L. (2007). *Vibrio anguillarum* colonization of rainbow trout integument requires a DNA locus involved in exopolysaccharide transport and biosynthesis. *Environ. Microbiol.* 9(2): 370–382. doi: 10.1111/j.1462-2920.2006.01147.x.
- Dadar, M., Dhama, K., Vakharia, V. N., Hoseinifar, S. H., Karthik, K., Tiwari, R., Khandia, R., Munjal, A., Salgado-Miranda, C. and Joshi, S. K. (2017) Advances in aquaculture vaccines against fish pathogens: global status and current trends. *Rev. Fisheries Sci. and Aquac.* 25(3): 184-217. doi: 10.1080/23308249.2016.1261277.
- Darling, A. E., Mau, B. and Perna, N. T. (2010) progressiveMauve: multiple genome alignment with gene gain, loss and rearrangement. *PLoS One.* 5(6): e11147. doi: 10.1371/journal.pone.0011147.
- Davey, M. L., Hancock, R. E. and Mutharia, L. M. (1998) Influence of culture conditions on expression of the 40-kilodalton porin protein of *Vibrio anguillarum* serotype O2. *Appl. Environ. Microbiol.* 64(1): 138-146. doi: 10.1128/AEM.64.1.138-146.1998.

- Davies, B. W., Bogard, R. W. and Mekalanos, J. J. (2011) Mapping the regulon of *Vibrio cholerae* ferric uptake regulator expands its known network of gene regulation. *Proc. Natl. Acad. Sci. USA*. 108(30): 12467-12472. doi: 10.1073/pnas.1107894108.
- Delcour, A. H. (2009) Outer membrane permeability and antibiotic resistance. *Biochem. Biophys. Acta*. 1794(5): 808-816. doi: 10.1016/j.bbapap.2008.11.005.
- Denkin, S. M., and Nelson, D. R. (1999). Induction of protease activity in *Vibrio anguillarum* by gastrointestinal mucus. *Appl. Environ. Microbiol.* 65(8): 3555– 3560. doi: 10.1128/AEM.65.8.3555-3560.1999.
- Denkin, S. M. and Nelson, D. R. (2004) Regulation of *Vibrio anguillarum* *empA* metalloprotease expression and its role in virulence. *Appl. Environ. Microbiol.* 70(7): 4193-4204. doi: 10.1128/AEM.70.7.4193-4204.2004.
- Di Lorenzo, M., Stork, M., Tomalsky, M. E., Actis, L. A., Farrell, D., Welch, T. J., Crosa, L. M., Wertheimer, A. M., Chen, Q., Salinas, P., Waldbeser, L. and Crosa, J. H. (2003) Complete sequence of virulence plasmid pJM1 from the marine fish pathogen *Vibrio anguillarum* strain 775. *J. Bacteriol.* 185 (19): 5822-5830. doi: 10.1128/JB.185.19.5822-5830.2003.
- Di Lorenzo, M., Stork, M. Alice, A. F., López, C. S. and Crosa, J. H. (2004) *Vibrio – Iron transport in bacteria*. Crosa, J. H., Mey, A. R. and Payne, S. M. (eds). Washington, DC, USA: ASM Press, 16: 241-255. doi: 10.1128/9781555816544.ch16.
- DiRita, V. J. and Mekalanos, J. J. (1991) Periplasmic interaction between two membrane regulatory proteins, ToxR and ToxS, results in signal transduction and transcriptional activation. *Cell*. 64(1): 29-37. doi: 10.1016/0092-8674(91)90206-e.
- Dittmer, J. B. and Withey, J. H. (2012) Identification and characterization of the functional toxboxes in the *Vibrio cholerae* cholera toxin promoter. *J. Bacteriol.* 194(19): 5255-5263. doi: 10.1128/JB.00952-12.
- Drake, S. L., DePaola, A. And Jaykus, L. A. (2007) An overview of *Vibrio vulnificus* and *Vibrio parahaemolyticus*. *Comp. Rev. Food Sci. Food Safe.* 6(4): 120-144. doi: 10.1111/j.1541-4337.2007.00022.x.
- Drake, E. J., Miller, B. R., Shi, C., Tarrasch, J. T., Sundlov, J. A., Allen, C. L., Skiniotis, G., Aldrich, C. C. and Gulick, A. M. (2016) Structures of two distinct conformations of holo-non ribosomal peptide synthases.

Nature. 529: 235-238. doi: 10.1038/nature16163.

- Drechsel, H., Stephan, H., Lotz, R., Haag, H., Zähler, H., Hantke, K. and Jung, G. (1995) Structure elucidation of yersiniabactin, a siderophore from highly virulent *Yersinia* strains. *Liebigs Ann. Chem.* 1995(10): 1727-1733. doi: 10.1002/jlac.1995199510243.
- Drummelsmith, J. and Whitfield, C. (1999) Gene products required for surface expression of the capsular form of the group 1 K antigen in *Escherichia coli* (O9a:K30). *Mol. Microbiol.* 31(5): 1321-1332. doi: 10.1046/j.1365-2958.1999.01277.x.
- Drummelsmith, J. and Whitfield, C. (2000) Translocation of group 1 capsular polysaccharide to the surface of *Escherichia coli* requires a multimeric complex in the outer membrane. *EMBO J.* 19(1): 57-66, doi: 10.1093/emboj/19.1.57.
- Dubert, J., Barja, J. L. and Romalde, J. L. (2017) New insights into pathogenic vibrios affecting bivalves in hatcheries: present and future prospects. *Front. Microbiol.* 8: 762. doi: 10.3389/fmicb.2017.00762.
- Dumas, Z., Ross-Gillespie, A. and Kümmerli, R. (2013) Switching between apparently redundant iron-uptake mechanisms benefits bacteria in changeable environments. *Proc. Biol. Sci.* 280(1764): 20131055. doi: 10.1098/rspb.2013.1055.
- Ebanks, R. O., Dacanay, A., Goguen, M., Pinto, D. M. and Ross, N. W. (2004) Differential proteomic analysis of *Aeromonas salmonicida* outer membrane proteins in response to low iron and *in vivo* growth conditions. *Proteomics* 4(4): 1074–1085. doi: 10.1002/pmic.200300664.
- Ellis, A. E. (1999) Immunity to bacteria in fish. *Fish Shellfish Immunol.* 9(4): 291–308. doi: 10.1006/fsim.1998.0192.
- Ellis, A. E. (2001) Innate host defense mechanisms of fish against viruses and bacteria. *Dev. Comp. Immunol.* 25 (8–9): 827–39. doi: 10.1016/s0145-305x(01)00038-6.
- Esmailkhani, H., Rasooli, I., Nazarian, S. and Sefid, F. (2016) *In vivo* validation of the immunogenicity of recombinant *Baumannii* acinetobactin utilization A protein (RBauA). *Microb. Pathog.* 98: 77–81. doi: 10.1016/j.micpath.2016.06.032.
- Falconi, M., Colonna, B., Prosseda, G., Micheli, G. and Gualerzi, C. O. (1998) Thermoregulation of *Shigella* and *Escherichia coli* EIEC pathogenicity.

- A temperature-dependent structural transition of DNA modulates accessibility of *virF* promoter to transcriptional repressor H-NS. *EMBO J.* 17(23): 7033-7043. doi: 10.1093/emboj/17.23.7033.
- FAO. 2020. The State of World Fisheries and Aquaculture 2020. Sustainability in action. Rome. <https://doi.org/10.4060/ca9229en>.
- Fass, E. and Groisman, E. A. (2009) Control of *Salmonella* pathogenicity island-2 gene expression. *Curr. Opin. Microbiol.* 12(2): 199-204. doi: 10.1016/j.mib.2009.01.004.
- Fetherston, J. D., Bearden, S. W., and Perry, R. D. (1996). YbtA, an AraC-type regulator of the *Yersinia pestis* pesticin/yersiniabactin receptor. *Mol. Microbiol.* 22(2): 315–325. doi: 10.1046/j.1365-2958.1996.00118.x.
- Fletcher, T. C., and Secombes, C. J. (2015) *Immunology of Fish*. Chichester: John Wiley & Sons Ltd.
- Fluman, N. and Bibi, E. (2009) Bacterial multidrug transport through the lens of the major facilitator superfamily. *Biochim. Biophys. Acta.* 1794(5): 738-747. doi: 10.1016/j.bbapap.2008.11.020.
- Frans, I., Michiels, C. W., Bossier, P., Willems, K. A., Lievens, B. and Rediers, H. (2011) *Vibrio anguillarum* as a fish pathogen: virulence factors, diagnosis and prevention. *J. Fish Dis.* 34(9): 643-661. doi: 10.1111/j.1365-2761.2011.01279.x.
- Friedman, D. B., Stauff, D. L., Pishchany, G., Whitwell, C. W., Torres, V. J. and Skaar, E. P. (2006) *Staphylococcus aureus* redirects central metabolism to increase iron availability. *PLoS Pathog.* 2(8): e87. doi: 10.1371/journal.ppat.0020087.
- Furrer, J. L., Sanders, D. N., Hook-Barnard, I. G. and McIntosh, M. A. (2002) Export of the siderophore enterobactin in *Escherichia coli*: involvement of a 43 kDa membrane exporter. *Mol. Microbiol.* 44(5): 1225–1234. doi: 10.1046/j.1365-2958.2002.02885.x.
- Gallegos, M. T., Schleif, R., Bairoch, A., Hofmann, K., and Ramos, J. L. (1997). AraC/XylS family of transcriptional regulators. *Microbiol. Mol. Biol. Rev.* 61(4): 393–410. doi: 10.1128/mmbr.61.4.393-410.1997.
- Garcia, E. C., Brumbaugh, A. R. and Mobley, H. L. T. (2011) Redundancy and specificity of *Escherichia coli* iron acquisition systems during urinary tract infection. *Infect. Immun.* 79(3): 1225–1235. doi: 10.1128/IAI.01222-10.

- Geoffroy, V. A., Fetherston, J. D. and Perry, R. D. (2000) *Yersinia pestis* YbtU and YbtT are involved in synthesis of the siderophore yersiniabactin but have different effects on regulation. *Infect. Immun.* 68(8): 4452-4461. doi: 10.1128/IAI.68.8.4452-4461.2000.
- Ghysels, B., Ochsner, U., Möllman, U., Heinisch, L., Vasil, M., Cornelis, P. and Matthijs, S. (2005) The *Pseudomonas aeruginosa* *pirA* gene encodes a second receptor for ferrienterobactin and synthetic catecholate analogues. *FEMS Microbiol. Lett.* 246(2): 167–174. doi: 10.1016/j.femsle.2005.04.010.
- Ghosh, S. and Chan, C.-K. K. (2016) Analysis of RNA-Seq data using TopHat and Cufflinks. *Methods Mol. Biol.* 1374: 339-3361. doi: 10.1007/978-1-4939-3167-5_18.
- Grisez, L., Chair, M., Sorgeloos, P. and Ollevier, F. (1996) Mode of infection and spread of *Vibrio anguillarum* in turbot *Scophthalmus maximus* larvae after oral challenge through live feed. *Dis. Aquat. Org.* 26: 181-187. doi: 10.3354/dao026181.
- Guanhua, Y., Wang, C., Wang, X., Ma, R., Zheng, H., Liu, Q., Zhang, Y., Ma, Y. and Wang, Q. (2018) Complete genome sequence of the marine fish pathogen *Vibrio anguillarum* and genome-wide transposon mutagenesis analysis of genes essential for *in vivo* infection. *Microbiol. Res.* 216: 97-107. doi: 10.1016/j.micres.2018.08.011.
- Guérin-Faubleé, V., Rosso, L., Vigneulle, M. and Flandrois, J. P. (1995) The effect of incubation temperature and sodium chloride concentration on the growth kinetics of *Vibrio anguillarum* and *Vibrio anguillarum*-related organisms. *J. Appl. Bacteriol.* 78(6): 621-629. doi: 10.1111/j.1365-2672.1995.tb03108.x.
- Guijarro, J. A., Cascales, D., García-Torrico, A. I., García-Domínguez, M. and Méndez, J. (2015) Temperature-dependent expression of virulence genes in fish-pathogenic bacteria. *Front. Microbiol.* 6: 700. doi: 10.3389/fmicb.2015.00700.
- Hansen, M. J., Kudirkiene, E. and Dalsgaard, I. (2020) Analysis of 44 *Vibrio anguillarum* genomes reveals high genetic diversity. *PeerJ.* 8: e10451. doi: 107717/peerj.10451.
- Hansson, M., Nygren, P. A. and Ståhl, S. (2000) Design and production of recombinant subunit vaccines. *Biotechnol. Appl. Biochem.* 32(2): 95-107. doi: 10.1042/ba20000034.

- Henderson, J. C., Zimmerman, S. M., Crofts, A. A., Boll, J. M., Kuhns, L. G., Herrera, C. M. and Trent, M. S. (2016) The power of asymmetry: architecture and assembly of the Gram-negative outer membrane lipid bilayer. *Annu. Rev. Microbiol.* 70: 255-278. doi: 10.1146/annurev-micro-102215-095308.
- Herrero, M., de Lorenzo, V. and Timmis, K. N. (1990) Transposon vectors containing non-antibiotic resistance selection markers for cloning and stable chromosomal insertion of foreign genes in Gram-negative bacteria. *J. Bacteriol.* 172(11): 6557-6567. doi: 10.1128/jb.172.11.6557-6567.1990.
- Herrington, D. A., Hall, R. H., Losonsky, G., Mekalanos, J. J., Taylor, R. K. and Levine, M. M. (1988) Toxin, toxin-coregulated pili, and the *toxR* regulon are essential for *Vibrio cholerae* pathogenesis in humans. *J. Exp. Med.* 168(4): 1487-1492. doi: 10.1084/jem.168.4.1487.
- Hider, R. C., and Kong, X. (2010) Chemistry and biology of siderophores. *Nat. Prod. Rep.* 27(5): 637–657. doi: 10.1039/b906679a.
- Higgins, D. E. and DiRita, V. J. (1994) Transcriptional control of ToxT, a regulatory gene in the ToxR regulon of *Vibrio cholerae*. *Mol. Microbiol.* 14(1): 17-29. doi: 10.1111/j.1365-2958.1994.tb01263.x.
- Hirono, I., Masuda, T. and Aoki, T. (1996) Cloning and detection of the hemolysin gene of *Vibrio anguillarum*. *Microb. Pathog.* 21(3): 173-182. doi: 10.1006/mpat.1996.0052.
- Holden, V. I., and Bachman, M. A. (2015) Diverging roles of bacterial siderophores during infection. *Metallomics.* 7(6): 986–995. doi: 10.1039/c4mt00333k.
- Holden, V. I., Breen, P., Houle, S., Dozois, C. M. and Bachman, M. A. (2016) *Klebsiella pneumoniae* siderophores induce inflammation, bacterial dissemination, and HIF-1 α stabilization during pneumonia. *mBio.* 7(5): e01397-16. doi: 10.1128/mBio.01397-16.
- Holland, M. C. H. and Lambris, J. D. (2002) The complement system in teleosts. *Fish Shellfish Immunol.* 12(5): 399-420. doi: 10.1006/fsim.2001.0408).
- Holt, J. G., Krieg, N. R., Sneath, P. H. A., Staley, J. T. and Williams, S. T. (1994) *Group 5. Facultative anaerobic Gram-negative rods. Genus Vibrio.* Ed. William R. Hensyl. *Bergey's Manual of Determinative Bacteriology.* 9th ed. 192, 260-261. Williams & Wilkins.

- Horiyama, T. and Nishino, K. (2014) AcrB, AcrD, and MdtABC multidrug efflux systems are involved in enterobactin export in *Escherichia coli*. *PLoS One*. 9(9): e108642. doi: 10.1371/journal.pone.0108642.
- Hovey, A. K. and Frank, D. W. (1995) Analyses of the DNA-binding and transcriptional activation properties of ExsA, the transcriptional activator of the *Pseudomonas aeruginosa* exoenzyme S regulon. *J. Bacteriol.* 177(15): 4427-4436. doi: 10.1128/jb.177.15.4427-4436.1995.
- Hulbert, R. R. and Taylor, R. K. (2002) Mechanism of ToxT-dependent transcriptional activation at the *Vibrio cholerae* *tcpA* promoter. *J. Bacteriol.* 184(20): 5533-5544. doi: 10.1128/JB.184.20.5533-5544.2002.
- Imlay, J. A. and Linn, S. (1988) DNA damage and oxygen radical toxicity. *Science*. 240(4857): 1302-1309. doi: 10.1126/science.3287616.
- Joshi, A., Kostiuk, B., Rogers, A., Teschler, J., Pukatzki, S. and Yildiz, F. H. (2017) Rules of engagement: The Type VI Secretion System in *Vibrio cholerae*. *Trends Microbiol.* 25(4): 267-279. doi: 10.1016/j.tim.2016.12.003.
- Kao, D.-Y., Cheng, Y.-C., Kuo, T.-Y., Lin, S.-B., Lin, C. C., Chow, I.-P. and Chen, W.-J. (2009) Salt-responsive outer membrane proteins of *Vibrio anguillarum* serotype O1 as revealed by comparative proteome analysis. *J. Appl. Microbiol.* 106(6): 2079-2085. doi: 10.1111/j.1365-2672.2009.04178.x.
- Kastenmüller, G., Schenk, M. E., Gasteiger, J. and Mewes, H.-W. (2009) Uncovering metabolic pathways relevant to phenotypic traits of microbial genomes. *Genome Biology*. 10: R28. doi: 10.1186/gb-2009-10-3-r28.
- Kazi, M. I., Conrado, A. R., Mey, A. R., Payne, S. M. and Davies, B. W. (2016) ToxR antagonizes H-NS regulation of horizontally acquired genes to drive host colonization. *PLoS Pathog.* 12(4): e1005570. doi: 10.1371/journal.ppat.1005570.
- Kehrer, J. P. (2000) The Haber-Weiss reaction and the mechanisms of toxicity. *Toxicology*. 149(1): 43-50. doi: 10.1016/s0300-483x(00)00231-6.
- Koh, E., and Henderson, J. P. (2015) Microbial copper-binding siderophores at the host-pathogen interface. *J. Biol. Chem.* 290(31): 18967–18974. doi: 10.1074/jbc.R115.644328.

- Konkel, M. E. and Tilly, K. (200) Temperature-regulated expression of bacterial virulence genes. *Microbes Infect.* 2(2): 157-166. doi: 10.1016/s1286-4579(00)00272-0.
- Köster, W. L., Actis, L. A., Waldbeser, L.S., Tolmasky, M. E. and Crosa, J. H. (1991) Molecular characterization of the iron transport system mediated by the pJM1 plasmid in *Vibrio anguillarum* 775. *J. Biol. Chem.* 266(35): 23829-23833. doi: 10.1016/S0021-9258(18)54358-1.
- Kumar, S. R., Parameswaran, V., Ahmed, V. P. I., Musthaq, S. S. and Hameed, A. S. S. (2007) Protective efficiency of DNA vaccination in Asian seabass (*Lates calcarifer*) against *Vibrio anguillarum*. *Fish Shellfish Immunol.* 23(2): 316-326. doi: 10.1016/j.fsi.2006.11.005.
- Kumar, S., Stecher, G., Li, M., Knyaz, C. and Tamura, K. (2018) MEGA X: molecular evolutionary genetics analysis across computing platforms. *Mol. Biol. Evol.* 35(6): 1547-1549. doi: 10.1093/molbev/msy096.
- Kunkle, D. E., Bina, X. R. and Bina, J. E. (2017) The *Vibrio cholerae* VexGH RND efflux system maintains cellular homeostasis by effluxing vibriobactin. *mBio.* 8(3): e00126-17. doi: 10.1128/mBio.00126-17.
- Kustusch, R. J., Kuehl, C. J. and Crosa, J. H. (2011) Power plays: iron transport and energy transduction in pathogenic vibrios. *Biometals.* 24(3): 559-566. doi: 10.1007/s10534-011-9437-2.
- Larsen, M. H., Blackburn, N., Larsen, J. L. and Olsen, J. E. (2004) Influences of temperature, salinity, and starvation on the motility and chemotactic response of *Vibrio anguillarum*. *Microbiology* 150(5): 1283-1290. doi: 10.1099/mic.0.26379-0.
- Lau, C. K. Y., Kreuwulak, K. D. and Vogel, H. J. (2016) Bacterial ferrous iron transport: The Feo system. *FEMS Microbiol. Rev.* 40(2): 273-298. doi: 10.1093/femsre/fuv049.
- Le Morvan, C., Troutaud, D. and Deschaux, P. (1998) Differential effects of temperature on specific and nonspecific immune defences in fish. *J. Exp. Biol.* 201(2): 165-168.
- Le Roux, F., Wegner, K. M., Baker-Austin, C., Vezzulli, L., Osorio, C. R., Amaro, C., Ritchie, J. M., Defroidt, T., Destoumieux-Garzón, D., Blokesch, M., Mazel, D., Jacq, A., Cava, F., Gram, L., Wendling, C. C., Strauch, E., Kirschner, A. and Huehn, S. (2015) The emergence of *Vibrio* pathogenesis in Europe: ecology, evolution, and pathogenesis (Paris, 11-12th March 2015). *Front. Microbiol.* 6:830. doi: 10.3389/fmicb.2015.

00830.

- Le Roux, F. and Blokesch, M. (2018) Eco-evolutionary dynamics linked to horizontal gene transfer in *Vibrios*. *Annu Rev. Microbiol.* 72: 89-110. doi: 10.1146/annurev-micro-090817-062148.
- Lee, S. E., Shin, S.H., Kim, S. Y., Kim, Y. R., Shin, D. H., Chung, S. S., Lee, Z. H., Lee, J. Y., Jeong, K. C., Choi, S. H. and Rhee, J. H. (2000) *Vibrio vulnificus* has the transmembrane transcription activator ToxRS stimulating the expression of the hemolysin gene *vwha*. *J. Bacteriol.* 182(12): 3405-3415. doi: 10.1128/jb.182.12.3405-3415.2000.
- Lemos, M. L., Salinas, P., Toranzo, A. E., Barja, J. L. and Crosa, J. H. (1988) Chromosome-mediated iron uptake system in pathogenic strains of *Vibrio anguillarum*. *J. Bacteriol.* 170(4): 1920-1925. doi: 10.1128/jb.170.4.1920-1925.1988.
- Lemos, M. L., and Osorio, C. R. (2010) *Iron Uptake in Vibrio and Aeromonas*. P. Cornelis & S.C. Andrews (eds.). *Iron Uptake and Homeostasis in Microorganisms*. 117–41. Caister Academic Press, UK .
- Lemos, M. L., Balado, M. and Osorio, C. R. (2010) Anguibactin- versus vanchrobactin-mediated iron uptake in *Vibrio anguillarum*: evolution and ecology of a fish pathogen. *Environ. Microbiol. Rep.* 2(1): 19-26. doi: 10.1111/j.1758-2229.2009.00103.x.
- Lemos, M. L. and Balado, M. (2020) Iron uptake mechanisms as key virulence factors in bacterial fish pathogens. *J. Appl. Microbiol.* 129(1): 104-115. doi: 10.1111/jam.14595.
- Leyn, S. A., Li, X., Zheng, Q., Novichkov, P. S., Reed, S., Romine, M. F., Fredrickson, J. K., Yang, C., Osterman, A. L. and Rodionov, D. A. (2011) Control of proteobacterial central carbon metabolism by the HexR transcriptional regulator: a case study in *Shewanella oneidensis*. *J. Biol. Chem.* 286(41): 35782-35794. doi: 10.1074/jbc.M111.267963.
- Li, G., Mo, Z., Li, J., Xiao, P. and Hao, B. (2013) Complete genome sequence of *Vibrio anguillarum* M3, a serotype O1 strain isolated from Japanese flounder in China. *Genome Announc.* 1(5): e00769-13. doi: 10.1128/genomeA.00769-13.
- Li, K., Chen, W.-H. and Bruner, S. D. (2015) Structure and mechanism of the siderophore-interacting protein from the fuscachelin gene cluster of *Thermobifida fusca*. *Biochem.* 54(25): 3989-4000. doi: 10.1021/acs.biochem.5b00354.

- Li, L., Rock, J. L. and Nelson, D. R. (2008) Identification and characterization of a repeat-in-toxin gene cluster in *Vibrio anguillarum*. *Infect. Immunol.* 76(6): 2620-2632. doi: 10.1128/IAI.01308-07.
- Li, Y. and Ma, Q. (2017) Iron acquisition strategies of *Vibrio anguillarum*. *Front. Cell. Infect. Microbiol.* 7: 342. doi: 10.3389/fcimb.2017.00342.
- Lim, J. G. and Choi, S. H. (2014) IscR is a global regulator essential for pathogenesis of *Vibrio vulnificus* and induced by host cells. *Infect. Immun.* 82(2): 569-578. doi: 10.1128/IAI.01141-13.
- Lindell, K., Fahlgren, A., Hjerde, E., Willassen, N.-P., Fällman, M. and Milton, D. L. (2012) Lipopolysaccharide O-antigen prevents phagocytosis of *Vibrio anguillarum* by rainbow trout (*Oncorhynchus mykiss*) skin epithelial cells. *PLoS One.* 7(5): e37678. doi: 10.1371/journal.pone.0037678.
- Litwin, C. M. and Calderwood, S. B. (1994) Analysis of the complexity of gene regulation by Fur in *Vibrio cholerae*. *J. Bacteriol.* 176(1): 240-248. doi: 10.1128/jb.176.1.240-248.1994.
- Loiseau, L., Gerez, C., Bekker, M., Choudens, S. O., Py, B., Sanakis, Y., de Mattos, J. T., Fontecave, M. and Barras, F. (2007) ErpA, an iron sulfur (Fe S) protein of the A-type essential for respiratory metabolism in *Escherichia coli*. *Proc. Natl. Acad. Sci. USA.* 104(34): 13626-13631. doi: 10.1073/pnas.0705829104.
- López, C. S. and Crosa, J. H. (2007) Characterization of ferric-anguibactin transport in *Vibrio anguillarum*. *Biometals.* 20(3-4): 393-403. doi: 10.1007/s10534-007-9084-9.
- López, C. S., Alice, A. F., Chakraborty, R. and Crosa, J. H. (2007) Identification of amino acid residues required for ferric-anguibactin transport in the outer-membrane receptor FatA of *Vibrio anguillarum*. *Microbiology* 153(2): 570-584. doi: 10.1099/mic.0.2006/001735-0.
- Ma, Y., Wang, Q., Gao, X., and Zhang, Y. (2017). Biosynthesis and uptake of glycine betaine as cold-stress response to low temperature in fish pathogen *Vibrio anguillarum*. *J. Microbiol.* 55: 44–55. doi: 10.1007/s12275-017-6370-2.
- Martinez-García, E., Goñi-Moreno, A., Bartley, B., McLaughlin, J., Sánchez-Sampedro, L., del Pozo, H. P., Hernández, C. P., Marletta, A. S., De Lucrezia, D., Sánchez-Fernández, G., Fraile, S. and de Lorenzo, V.

- (2020) SEVA 3.0: an update of the Standard European Vector Architecture for enabling portability of genetic constructs among diverse bacterial hosts. *Nucleic Acids Res.* 48(D1): D1164-D1170. doi: 10.1093/nar/gkz1024.
- Mazoy, R., Osorio, C. R., Toranzo, A. E. and Lemos, M. L. (2003) Isolation of mutants of *Vibrio anguillarum* defective in haeme utilisation and cloning of *huvA*, a gene coding for an outer membrane protein involved in the use of haeme as iron source. *Arch. Microbiol.* 179(5): 329-338. doi: 10.1007/s00203-003-0529-4.
- McGee, K., Hörstedt, P. and Milton, D. L. (1996) Identification and characterization of additional flagellin genes from *Vibrio anguillarum*. *J. Bacteriol.* 178(17): 5188-5198. doi: 10.1128/jb.178.17.5188-5198.1996.
- McRose, D. L., Seyedsayamdost, M. R. and Morel, F. M. M. (2018) Multiple siderophores: bug or feature? *J. Biol. Inorg. Chem.* 23(7): 983-993. doi: 10.1007/s00775-018-1617-x.
- Mettert, E. L. and Kiley, P. J. (2015) Fe-S proteins that regulate gene expression. *Biochem. Biophys. Acta.* 1853(6):1284-1293. doi: 10.1016/j.bbamcr.2014.11.018.
- Mey, A. R., Wyckoff, E. E., Kanukurthy, V., Fisher, C. R. and Payne, S. M. (2005) Iron and Fur regulation in *Vibrio cholerae* and the role of Fur in virulence. *Infect. Immun.* 73(12): 8167-8178. doi: 10.1128/IAI.73.12.8167-8178.2005.
- Michel, L., González, N., Jagdeep, S., Nguyen-Ngoc, T and Reimann, C. (2005) PchR-box recognition by the AraC-type regulator PchR of *Pseudomonas aeruginosa* requires the siderophore pyochelin as an effector. *Mol. Microbiol.* 58(2): 495-509. doi: 10.1111/j.1365-2958.2005.04837.x.
- Miethke, M., Hou, J. and Marahiel, M. A. (2011) The siderophore-interacting protein YqjH acts as a ferric reductase in different iron assimilation pathways of *Escherichia coli*. *Biochemistry* 50(50): 10951-10964. doi: 10.1021/bi201517h.
- Miethke, M. (2013) Molecular strategies of microbial iron assimilation: from high-affinity complexes to cofactor assembly systems. *Metallomics* 5(1): 15–28. doi: 10.1039/c2mt20193c.
- Mikkelsen, H., Lund, V., Martinsen, L.-C., Gravningen, K. and Schröder, M. B. (2007) Variability among *Vibrio anguillarum* O2 isolates from

- Atlantic cod (*Gadus morhua* L.): characterisation and vaccination studies. *Aquaculture*. 266(1-4): 16-25. doi: 10.1016/j.aquaculture.2007.02.041.
- Miller, J. H. (1992) *A Short Course in Bacterial Genetics*. Plainview, N.Y.: Cold Spring Harbor Laboratory Press.
- Miller, D. A. and Walsh, C. T. (2001) Yersiniabactin synthetase: probing the recognition of carrier protein domains by the catalytic heterocyclization domains, Cy1 and Cy2, in the chain-initiating HMWP2 subunit. *Biochemistry* 40(17): 5313-5321. doi: 10.1021/bi002905v.
- Miller, D. A., Luo, L., Hillson, N., Keating, T. A and Walsh, C. T. (2002) Yersiniabactin synthetase: a four-protein assembly line producing the nonribosomal peptide/polyketide hybrid siderophore of *Yersinia pestis*. *Chem. Biol.* 9(3): 333-344. doi: 10.1016/s1074-5521(02)00115-1.
- Milton, D. L., O'Toole, R, Hörstedt, P. and Wolf-Watz, H. (1996) Flagellin A is essential for the virulence of *Vibrio anguillarum*. *J. Bacteriol.* 178(5): 1310-1319. doi: 10.1128/jb.178.5.1310-1319.1996.
- Mohamad, N., Amal, M. N. A., Salwany, I., Yasin, M., Saad, M. Z., Nasruddin, N. S., Al-saari, N., Mino, S. and Sawabe, T. (2019) Vibriosis in cultured marine fishes: a review. *Aquaculture* 512: 734289. doi: 10.1016/j.aquaculture.2019.734289.
- Moravec, A. R., Siv, A. W., Hobby, C. R., Lindsay, E. N., Norbash, L. V., Shults, D. J., Symes, S. J. K. and Gibes, D. K. (2017) Exogenous polyunsaturated fatty acids impact membrane remodeling and affect virulence phenotypes among pathogenic *Vibrio* species. *Appl. Environ. Microbiol.* 83(22): e01415-1417. doi: 10.1128/AEM.01415-17.
- Mouriño , S., Osorio, C. R. and Lemos, M. L. (2004) Characterization of heme uptake cluster genes in the fish pathogen *Vibrio anguillarum*. *J. Bacteriol.* 186(18): 6159–6167. doi: 10.1128/JB.186.6159-6167.2004.
- Morris, J. G. (2003) Cholera and other types of vibriosis: a story of human pandemics and oysters on the half shell. *Clin. Infect. Dis.* 37(2): 272-280. doi: 10.1086/375600.
- Mou, X., Spinard, E. J., Driscoll, M. V., Zhao, W. and Nelson, D. R. (2013) H-NS is a negative regulator of the two hemolysin/cytotoxin gene clusters in *Vibrio anguillarum*. *Infect. Immun.* 81(10): 3566-3576. doi: 10.1128/IAI.00506-13.

- Naikare, H., Butcher, J., Flint, A., Xu, J., Raymond, K. N. and Stintzi, A. (2013) *Campylobacter jejuni* ferric-enterobactin receptor CfrA is TonB3 dependent and mediates iron acquisition from structurally different catechol siderophores. *Metallomics* 5(8): 988–996. doi: 10.1039/c3mt20254b.
- Naka, H., López, C. S. and Crosa, J. H. (2008) Reactivation of the vanchrobactin siderophore system of *Vibrio anguillarum* by removal of a chromosomal insertion sequence originated in the plasmid pJM1 encoding the anguibactin siderophore system. *Environ. Microbiol.* 10(1): 265–277. doi: 10.1111/j.1462-2920.2007.01450.x.
- Naka, H., Dias, G. M., Thompson, C. C., Dubay, C., Thompson, F. L. and Crosa, J. H. (2011) Complete genome sequence of the marine fish pathogen *Vibrio anguillarum* harboring the pJM1 virulence plasmid and genomic comparison with other virulent strains of *V. anguillarum* and *V. ordalii*. *Infect. Immun.* 79(7): 2889–2900. doi: 10.1128/IAI.05138-11.
- Naka, H. and Crosa, J. H. (2012) Identification and characterization of a novel outer membrane protein receptor FetA for ferric enterobactin transport in *Vibrio anguillarum* 775 (pJM1). *Biometals* 25(1): 125–133. doi: 10.1007/s10534-011-9488-4.
- Naka, H., Liu, M., Crosa, J. H. (2013) Two ABC transporter systems participate in siderophore transport in the marine pathogen *Vibrio anguillarum* 775 (pJM1). *FEMS Microbiol. Lett.* 341(2): 79–86. doi: 10.1111/1574-6968.12092.
- Noinaj, N., Guillier, M., Bernard, T. J. and Buchanan, S. K. (2010) TonB-dependent transporters: regulation, structure, and function. *Annu. Rev. Microbiol.* 64: 43–60. doi: 10.1146/annurev.micro.112408.134247.
- Ochman, H., Lawrence, J. G. and Groisman, E. A. (2000) Lateral gene transfer and the nature of bacterial innovation. *Nature* 405: 299–304. doi: 10.1038/35012500.
- Ohlemacher, S. I., Xu, Y., Kober, D. L., Malik, M., Nix, J. C., Brett, T. J., Henderson, J. P. (2018) YbtT is a low-specificity type II thioesterase that maintains production of the metallophore yersiniabactin in pathogenic enterobacteria. *J. Biol. Chem.* 293(51): 19572–19585. doi: 10.1074/jbc.RA118.005752.
- Okuda, J., Nakai, T., Chang, P. S., Oh, T., Nishino, T., Koitabashi, T. and Nishibuchi, M. (2001) The *toxR* gene of *Vibrio (Listonella) anguillarum*

- controls expression of the major outer membrane proteins but not virulence in a natural host model. *Infect. Immun.* 69(10): 6091-6101. doi: 10.1128/IAI.69.10.6091-6101.2001.
- Olafsen, J. A., Christie, M. and Raa, J. (1981) Biochemical ecology of psychrotrophic strains of *Vibrio anguillarum* isolated from outbreaks of vibriosis at low temperature. *Zentralblatt für Bakteriologie, Mikrobiologie, Hygiene, I. Abteilung, Originale, Allgemeine Angewandte Ökologische Mikrobiologie*. 2: 339-348. doi: 10.1016/S0721-9571(81)80027-80020.
- Ormonde, P., Hörstedt, P., O'Toole, R., and Milton, D. L. (2000) Role of motility in adherence to and invasion of a fish cell line by *Vibrio anguillarum*. *J. Bacteriol.* 182(8): 2326-2328. doi: 10.1128/jb.182.8.2326-2328.2000.
- Osorio, C. R., Juiz-Río, S and Lemos, M. L. (2006) A siderophore biosynthesis gene cluster from the fish pathogen *Photobacterium damsela* subsp. *piscicida* is structurally and functionally related to the *Yersinia* high-pathogenicity island. *Microbiology* 152(11): 3327-3341. doi: 10.1099/mic.0.29190-0.
- Osorio, C. R., Rivas, A. J., Balado, M., Fuentes-Monteverde, J. C., Rodríguez, J. Jiménez, C., Lemos, M. L. and Waldor, M. K. (2015) A transmissible plasmid-borne pathogenicity island confers piscibactin biosynthesis in the fish pathogen *Photobacterium damsela* subsp. *piscicida*. *Appl. Environ. Microbiol.* 81(17): 5867-5879. doi: 10.1128/AEM.01580-15.
- O'Toole, R., Milton, D. L. and Wolf-Watz, H. (1996) Chemotactic motility is required for invasion of the host by the fish pathogen *Vibrio anguillarum*. *Mol. Microbiol.* 19(3): 625-637. doi: 10.1046/j.1365-2958.1996.412927.x.
- O'Toole, R., Lundberg, S., Fredriksson, S. A., Jansson, A., Nilsson, B. and Wolf-Wartz, H. (1999) The chemotactic response of *Vibrio anguillarum* to fish intestinal mucus is mediated by a combination of multiple mucus components. *J. Bacteriol.* 181(14): 4308-4317. doi: 10.1128/JB.181.14.4308-4317.1999.
- Parales, R. E. and Harwood, C. S. (1993) Construction and use of a new broad-host-range *lacZ* transcriptional fusion vector, pHRP309, for Gram-bacteria. *Gene* 133(1): 23-30. doi: 10.1016/0378-1119(93)90220-w.
- Park, C. and Zhang, J. (2012) High expression hampers horizontal gene transfer. *Genome Biol. Evol.* 4(4): 523-532. doi: 10.1093/gbe/evs030.

- Payne, S. M., Mey, A. R. and Wyckoff, E. E. (2016) *Vibrio* iron transport: evolutionary adaptation to life in multiple environments. *Microbiol. Mol. Biol. Rev.* 80(1): 69-90. doi: 10.1128/MMBR.00046-15.
- Pedersen, K., Grisez, L., van Houdt, R., Tiainen, T., Ollevier, F. and Larsen, J. L. (1999) Extended serotyping scheme for *Vibrio anguillarum* with the definition and characterization of seven provisional O-serogroups. *Curr. Microbiol.* 38(3): 183-189. doi: 10.1007/pl00006784.
- Pelludat, C., Rakin, A., Jacobi, C. A., Schubert, S. and Heesemann, J. (1998) The yersiniabactin biosynthetic gene cluster of *Yersinia enterocolitica*: organization and siderophore-dependent regulation. *J. Bacteriol.* 180(3): 538-546. doi: 10.1128/JB.180.3.538-546.1998.
- Peterson, K. M. and Mekalanos, J. J. (1988) Characterization of the *Vibrio cholerae* ToxR regulon: identification of novel genes involved in intestinal colonization. *Infect. Immun.* 56(11): 2822-2829. doi: 10.1128/iai.56.11.2822-2829.1988.
- Pfau, J. D. and Taylor, R. K. (1998) Mutations in *toxR* and *toxS* that separate transcriptional activation from DNA binding at the cholera toxin gene promoter. *J. Bacteriol.* 180(17): 4724-4733. doi: 10.1128/JB.180.17.4724-4733.1998.
- Prajapat, M. K. and Saini, S. (2012) Interplay between Fur and HNS in controlling virulence gene expression in *Salmonella typhimurium*. *Comput. Biol. Med.* 42(11): 1133-1140. doi: 10.1016/j.combiomed.2012.09.005.
- Price, N. M., and Morel, F. M. M. (1998) Biological cycling of iron in the ocean. *Metal Ions Biol. Sys.* 35: 1-36.
- Prouty, M. G., Osorio, C. R. and Klose, K. E. (2005) Characterization of functional domains of the *Vibrio cholerae* virulence regulator ToxT. *Mol. Microbiol.* 58(4): 1143-1156. doi: 10.1111/j.1365-2958.2005.04897.x.
- Pukatzki, S., Ma, A. T., Sturtevant, D., Krastins, B., Sarracino, D., Nelson, W. C., Heidelberg, J. F. and Mekalanos, J. F. (2006) Identification of a conserved bacterial protein secretion system in *Vibrio cholerae* using the *Dictyostelium* host model system. *Proc. Natl. Acad. Sci. USA.* 103(5): 1528-1533. doi: 10.1073/pnas.0510322103.
- Ratledge, C., and Dover, L. G. (2000) Iron metabolism in pathogenic bacteria. *Annu. Rev. Microbiol.* 54: 881-941. doi: 10.1146/annurev.micro.54.1.881.

- Rey-Varela, D., Cisneros-Sureda, J., Balado, M., Rodríguez, J., Lemos, M. L. and Jiménez, C. (2019) The outer membrane protein FstC of *Aeromonas salmonicida* subsp. *salmonicida* acts as receptor for amonabactin siderophores and displays a wide ligand plasticity. Structure-activity relationships of synthetic amonabactin analogues. *ACS Infect Dis.* 5(11): 1936-1951. doi: 10.1021/acsinfecdis.9b00274.
- Rodkhum, C., Hirono, I., Crosa, J. H. and Aoki, T. (2005) Four novel hemolysin genes of *Vibrio anguillarum* and their virulence to rainbow trout. *Microb. Pathog.* 39(4): 109-119. doi: 10.1016/j.micpath.2005.06.004.
- Romalde, J. L. (2002) *Photobacterium damsela* subsp. *piscicida*: an integrated view of a bacterial fish pathogen. *Int. Microbiol.* 5(1): 3-9. doi: 10.1007/s10123-002-0051-6.
- Rønneseth, A., Castillo, D., D'Alvise, P., Tønnesen, Ø., Haugland, G., Grotkjær, T., Engell-Sørensen, K., Nørremark, L., Bergh, Ø., Wergeland, H. I. and Gram, L. (2017) Comparative assessment of *Vibrio* virulence in marine fish larvae. *J. Fish Dis.* 40(10): 1373-1385. doi: 10.1111/jfd.12612.
- Russo, T. A., McFadden, C. D., Carlino-MacDonald, U. B., Beanan, J. M., Olson, R. and Wilding, G. E. (2003) The siderophore receptor IroN of extraintestinal pathogenic *Escherichia coli* is a potential vaccine candidate. *Infect. Immun.* 71(12): 7164–7169. doi: 10.1128/IAI.71.12.7164-7169.
- Sambrook, J., and Russell, D. W. (2006) *Molecular cloning: a laboratory manual*. J. Sambrook, E.F. Fritsch and T. Maniatis, *Cold Spring Harbor Laboratory Press, New York*. 3^a Ed. pp 201-215. Spring Harbor Laboratory Press, New York.
- Santos, J. A., Pereira, P. J. B. and Macedo-Ribeiro, S. (2015) What a difference a cluster makes: the multifaceted roles of IscR in gene regulation and DNA recognition. *Biochem. Biophys. Acta.* 1854(9): 1101-1112. doi: 10.1016/j.bbapap.2015.01.010.
- Savioz, A., Jeenes, D. J., Kocher, H. P. and Haas, D. (1990) Comparison of *proC* and other housekeeping genes of *Pseudomonas aeruginosa* with their counterparts in *Escherichia coli*. *Gene.* 86(1): 107–111. doi:10.1016/0378-1119(90)90121-7.
- Schmidt, H. and Hensel, M. (2004) Pathogenicity islands in bacterial

- pathogenesis. *Clin. Microbiol. Rev.* 17(1): 14-56. doi: 10.1128/CMR.17.1.14-56.2004.
- Schmidt, J. G., Korbut, R., Ohtani, M., Jørgensen, L. v. G. (2017) Zebrafish (*Danio rerio*) as a model to visualize infection dynamics of *Vibrio anguillarum* following intraperitoneal injection and bath exposure. *Fish Shellfish Immunol.* 67: 692-697. doi: 10.1016/j.fsi.2017.06.052.
- Schwarz, S., West, T. E., Boyer, F., Chiang, W.-C., Carl, M. A., Hood, R. D., Rohmer, L., Tolker-Nielsen, T., Skerrett, S. J. and Mougous, J. D. (2010) *Burkholderia* type VI secretion system have distinct roles in eukaryotic and bacterial cell interactions. *PLoS Pathog.* 6:e1001068. doi: 10.1371/journal.ppat.1001068.
- Schwarzer, D., Finking, R. and Marahiel, M. A. (2003) Nonribosomal peptides: from genes to products. *Nat. Prod. Rep.* 20(3): 275-287. doi: 10.1039/b111145k.
- Schwyn, B., and Neilands, J. B. (1987) Universal chemical assay for the detection and determination of siderophores. *Anal. Biochem.* 160 (1): 47-56. doi: 10.1016/0003-2697(87)90612-9.
- Seeger, M. A. and van Veen, H. W. (2009) Molecular basis of multidrug transport by ABC transporters. *Biochim. Biophys. Acta.* 1794(5): 725-737. doi: 10.1016/j.bbapap.2008.12.004.
- Sekine, Y., Tanzawa, T., Tanaka, Y., Ishimori, K. and Uchida, T. (2016) Cytoplasmic heme-binding protein (HutX) from *Vibrio cholerae* is an intracellular heme transport protein for the heme-degrading enzyme, HutZ. *Biochemistry.* 55(6): 884-893. doi: 10.1021/acs.biochem.5b01273.
- Shin, M., Mey, A. R. and Payne, S. M. (2019) *Vibrio cholerae* FeoB contains a dual nucleotide-specific NTPase domain essential for ferrous iron uptake. *Proc. Natl. Acad. Sci. USA.* 116(10): 4599-4604. doi: 10.1073/pnas.1817964116.
- Skaar, E. P. (2010) The battle for iron between bacterial pathogens and their vertebrate hosts. *PLoS Pathog.* 6(8): e1000949. doi : 10.1371/journal.ppat.1000949.
- Skorupski, K. and Taylor, R. K. (1997) Control of the ToxR virulence regulon in *Vibrio cholerae* by environmental stimuli. *Mol. Microbiol.* 25(6): 1003-1009. doi: 10.1046/j.1365-2958.1997.5481909.x.
- Skov, M. N., Pedersen, K. and Larsen, J. L. (1995) Comparison of pulsed-

- field gel electrophoresis, ribotyping, and plasmid profiling for typing of *Vibrio anguillarum* serovar O1. *Appl. Environ. Microbiol.* 61(4):1540-1545. doi: 10.1128/aem.61.4.1540-1545.1995.
- Smati, M., Magistro, G., Adiba, S., Wieser, A., Picard, B., Schubert, S. and Denamur, E. (2017) Strain-specific impact of the high-pathogenicity island on virulence in extra-intestinal pathogenic *Escherichia coli*. *Int. J. Med. Microbiol.* 307(1):44-56. doi: 10.1016/j.ijmm.2016.11.004.
- Soengas, R. G., Anta, C., Espada, A., Paz, V., Ares, I. R., Balado, M., Rodríguez, J., Lemos, M. L. and Jiménez, C. (2006) Structural characterization of vanchrobactin, a new catechol siderophore produced by the fish pathogen *Vibrio anguillarum* serotype O2. *Tetrahedron Lett.* 47(39): 7113–7116. doi: 10.1016/j.tetlet.2006.07.104.
- Sommerset, I., Krossøy, B., Biering, E. and Frost, P. (2005) Vaccines for fish in aquaculture. *Expert Rev. Vaccines.* 4(1): 89-101. doi: 10.1586/14760584.4.1.89.
- Sørensen, U. B. and Larsen, J. L. (1986) Serotyping of *Vibrio anguillarum*. *Appl. Environ. Microbiol.* 51(3): 593-597. doi: 10.1128/aem.51.3.593-597.1986.
- Souto, A., Montaos, M. A., Rivas, A. J., Balado, M., Osorio, C. R., Rodríguez, J., Lemos, M. L. and Jiménez, C. (2012) Structure and biosynthetic assembly of piscibactin, a siderophore from *Photobacterium damsela* subsp. *piscicida*, predicted from genome assembly. *European J. Org. Chem.* 2012(29): 5693-5700. doi: 10.1002/ejoc.201200818.
- Stentiford, G. D., Sritunyalucksana, K., Flegel, T. W., Williams, B. A. P., Withyachumnarnkul, B., Itsathitphaisarn, O. and Bass, D. (2017) New paradigms to help solve the global aquaculture disease crisis. *PLoS Pathog.* 13(2): e1006160. doi: 10.1371/journal.ppat.1006160.
- Stevenson, G., Leavesley, D. I., Lagnado, C. A., Heuzenroeder, M. W. and Manning, P. A. (1985) Purification of the 25-kDa *Vibrio cholerae* major outer-membrane protein and the molecular cloning of its gene: *ompV*. *Eur. J. Biochem.* 148(2): 385-390. doi: 10.1111/j.1432-1033.1985.tb08850.x.
- Stoebel, D. M., Free, A. and Dorman, C. J. (2008) Anti-silencing: overcoming H-NS-mediated repression of transcription in Gram-negative enteric bacteria. *Microbiology* 154(9): 2533-2545. doi: 10.1099/mic.0.2008/020693-0.

- Stork, M., Di Lorenzo, M., Welch, T. J., Crosa, L. M. and Crosa, J. H. (2002) Plasmid-mediated iron uptake and virulence in *Vibrio anguillarum*. *Plasmid* 48(3): 222-228. doi: 10.1016/s0147-619x(02)00111-7.
- Stork, M., Di Lorenzo, M., Mouriño, S., Osorio, C. R., Lemos, M. L. and Crosa, J. H. (2004) Two TonB systems function in iron transport in *Vibrio anguillarum*, but only one is essential for virulence. *Infect. Immun.* 72(12): 7326-7329. doi: 10.1128/IAI.72.12.7326-7329.2004.
- Stork, M., Otto, B. R. and Crosa, J. H. (2007) A novel protein, TtpC, is a required component of the TonB2 complex for specific iron transport in the pathogens *Vibrio anguillarum* and *Vibrio cholerae*. *J. Bacteriol.* 189(5): 1803-1815. doi: 10.1128/JB00451-06.
- Svendsen, Y. S. and Bogwald, J. (1997) Influence of artificial wound and non-intact mucus layer on mortality of Atlantic salmon (*Salmo salar* L.) following a bath challenge with *Vibrio anguillarum* and *Aeromonas salmonicida*. *Fish Shellfish Immunol.* 7(5): 317-325. doi: 10.1006/fsim.1997.0087.
- Tamura, K., Stecher, G., Peterson, D., Filipski, A. and Kumar, S. (2013) MEGA6: Molecular Evolutionary Genetics Analysis version 6.0. *Mol. Biol. Evol.* 30(12): 2725-2729. doi: 10.1093/molbev/mst197.
- Tanabe, T., Takata, N., Naka, A., Moon, Y.-H., Nakao, H., Inoue, Y., Narimatsu, S. and Yamamoto, S. (2005) Identification of an AraC-like regulator gene required for induction of the 78-kDa ferrioxamine B receptor in *Vibrio vulnificus*. *FEMS Microbiol. Lett.* 249(2): 309-314. doi: 10.1016/j.femsle.2005.06.025.
- Tang, L., Yue, S., Li, G.-Y., Li, J., Wang, X.-R., Li, S.-F. and Mo, Z.-L. (2016) Expression, secretion and bactericidal activity of type VI secretion system in *Vibrio anguillarum*. *Arch. Microbiol.* 198(8): 751-760. doi: 10.1007/s00203-016-1236-2.
- Thode, S. K., Rojek, E., Kozłowski, M., Ahmad, R. and Haugen, P. (2018) Distribution of siderophore gene systems on a *Vibrionaceae* phylogeny: database searches, phylogenetic analyses and evolutionary perspectives. *PLoS One.* 13(2): e0191860. doi: 10.1371/journal.pone.0191860.
- Tolmasky, M. E., Wertheimer, A. M., Actis, L. A. and Crosa, J. H. (1994) Characterization of the *Vibrio anguillarum fur* gene: role in regulation of expression of the FatA outer membrane protein and catechols. *J. Bacteriol.* 176(1): 213-220. doi: 10.1128/jb.176.1.213-200.1994.

- Toranzo, A. E., Santos, Y., Lemos, M. L., Ledo, A., Bolinches, J. (1987) Homology of *Vibrio anguillarum* strains causing epizootics in turbot, salmon and trout reared on the Atlantic coast of Spain. *Aquaculture*. 67(1-2) : 41-52. doi: 10.1016/0044-8486(87)90006-8.
- Toranzo, A. E., Barreiro, S., Csal, J. F., Figueras, A., Magariños, B. and Barja, J. L. (1991) Pasteurellosis in cultured gilthead seabream (*Sparus aurata*): first report in Spain. *Aquaculture*. 99(1-2): 1-15. doi: 10.1016/0044-8486(91)90284-E.
- Toranzo, A. E., Magariños, B. and Romalde, J. L. (2005) A review of the main bacterial fish diseases in mariculture systems. *Aquaculture*. 246(1-4): 37-61. doi: 10.1016/j.aquaculture.2005.01.002.
- Toranzo, A. E., Romalde, J. L., Magariños, B. and Barja, J. L. (2009) Present and future of aquaculture vaccines against fish bacterial diseases. *Options Méditerranéennes: Série A* 86: 155-176.
- Toranzo, A. E., Magariños, B. and Avendaño-Herrera, R. (2017) *Vibriosis: Vibrio anguillarum, V. ordalii and Aliivibrio salmonicida*, in *Fish Viruses and Bacteria: Pathobiology and Protection*, eds P. T. K. Woo, and R. C. Cipriano, (Wallingford: CABI), 314-333. doi: 10.1079/9781780647784.0314.
- Touati, D. (2000) Iron and oxidative stress in bacteria. *Arch. Biochem. Biophys.* 373(1): 1-6. doi: 10.1006/abbi.1999.1518.
- Troxell, B., and Hassan, H. M. (2013) Transcriptional regulation by ferric uptake regulator (Fur) in pathogenic bacteria. *Front. Cell. Infect Microbiol.* 3: 59. doi: 10.3389/fcimb.2013.00059.
- Valderrama, K., Balado, M., Rey-Varela, D., Rodríguez, J., Vila-Sanjurjo, A., Jiménez, C. and Lemos, M. L. (2019) Outer membrane protein FrpA, the siderophore piscibactin receptor of *Photobacterium damsela* subsp. *piscicida*, as a subunit vaccine against photobacteriosis in sole (*Solea senegalensis*). *Fish Shellfish Immunol.* 94: 723-729. doi: 10.1016/j.fsi.2019.09.066.
- van Oirschot, J.T. (1997) *Classical inactivated vaccines*. P.P. Pastoret (Ed.) *Veterinary Vaccinology*, 258-60. Elsevier Press, Amsterdam, The Netherlands.
- Varina, M., Denkin, S. M., Staroscik, A. M. and Nelson, D. R. (2008) Identification and characterization of EPP, the secreted processing protease for the *Vibrio anguillarum* EmpA metalloprotease. *J. Bacteriol.*

190(20): 6589-6597. doi: 10.1128/JB.00535-08.

- Wandersman, C., and Delepelaire, P. (2004) Bacterial iron sources: from siderophores to hemophores. *Annu. Rev. Microbiol.* 58: 611–647. doi: 10.1146/annurev.micro.58.030603.123811.
- Wang, F. R. and Kushner, S. R. (1991) Construction of versatile low-copy-number vectors for cloning, sequencing and gene expression in *Escherichia coli*. *Gene.* 100: 195-199. doi: 10.1016/0378-1119(91)90366-J.
- Wang, S.-Y., Lauritz, J., Jass, J. and Milton, D.L. (2002) A ToxR homolog from *Vibrio anguillarum* serotype O1 regulates its own production, bile resistance, and biofilm formation. *J. Bacteriol.* 184(6): 1630–1639. doi: 10.1128/JB.184.6.1630-1632.2002.
- Wang, S.-Y., Lauritz, J., Jass, J. and Milton, D.L. (2003) Role for the major outer-membrane protein from *Vibrio anguillarum* in bile resistance and biofilm formation. *Microbiology* 149(4): 1061–1071. doi: 10.1099/mic.0.26032-0.
- Weber, B., Hasic, M., Chen, C., Wai, S. N. and Milton, D. L. (2009) Type VI secretion modulates quorum sensing and stress response in *Vibrio anguillarum*. *Environ. Microbiol.* 11(12): 3018-3028. doi: 10.1111/j.1462-2920.2009.02005.x.
- Weber, B., Chen, C. and Milton, D. L. (2010) Colonization of fish skin is vital for *Vibrio anguillarum* to cause disease. *Environ. Microbiol. Rep.* 2(1): 133-139. doi: 10.1111/j.1758-2229.2009.00120.x.
- Welch, T. J. and Crosa, J. H. (2005) Novel role of the lipopolysaccharide O1 side chain in ferric siderophore transport and virulence of *Vibrio anguillarum*. *Infect. Immun.* 73(9): 5864-5872. doi: 10.1128/IAI.73.9.5864-5872.2005.
- Whitaker, W. B., Parent, M. A., Boyd, A., Richards, G. P. and Boyd, E. F. (2012) The *Vibrio parahaemolyticus* ToxRS regulator is required for stress tolerance and colonization in a novel orogastric streptomycin-induced adult murine model. *Infect. Immun.* 80(5): 1834-1845. doi: 10.1128/IAI.06284-11.
- Wugeditsch, T., Paiment, A., Hocking, J., Drummelsmith, J., Forrester, C. and Whitfield, C. (2001) Phosphorylation of Wzc, a tyrosine autokinase, is essential for assembly of group 1 capsular polysaccharides in *Escherichia coli*. *J. Biol. Chem.* 276(4): 2361-2371. doi: 10.1074/jbc.M009092200.

- Wyckoff, E. E., Schmitt, M., Wilks, A. and Payne, S. M. (2004) HutZ is required for efficient heme utilization in *Vibrio cholerae*. *J. Bacteriol.* 186(13): 4142–4151. doi: 10.1128/JB.186.13.4142-4151.2004.
- Wyckoff, E. E., Allred, B. E., Raymond, K. N. and Payne, S. M. (2015) Catechol siderophore transport by *Vibrio cholerae*. *J. Bacteriol.* 197(17): 2840–2849. doi: 10.1128/JB.00417-15.
- Yang, H., Chen, J., Yang, G., Zhang, X.-H., Liu, R. and Xue, X. (2009) Protection of Japanese flounder (*Paralichthys olivaceus*) against *Vibrio anguillarum* with a DNA vaccine containing the mutated zinc-metalloprotease gene. *Vaccine* 27(15): 2150-2155. doi: 10.1016/j.vaccine.2009.01.101.
- Yu, N. Y., Wagner, J. R., Laird, M. R., Melli, G., Rey, S., Lo, R., Dao, P., Sahinalp, S. C., Ester, M., Foster, M. and Brinkman, F. S. (2010) PSORTb 3.0: improved protein subcellular localization prediction with refined localization subcategories and predictive capabilities for all prokaryotes. *Bioinformatics* 26(13): 1608-1615. doi: 10.1093/bioinformatics/btq249.
- Zhang, Y., Hu, L., Osei-adjei, G., Zhang, Y., Yang, W., Yin, Z., Lu, R., Sheng, X., Yang, R., Huang, X. and Zhou, D. (2018) Autoregulation of ToxR and its regulatory actions on major virulence gene loci in *Vibrio parahaemolyticus*. *Front. Cell. Infect. Microbiol.* 8: 291. doi: 10.3389/fcimb.2018.00291.

VII. APPENDIX

VII. APPENDIX 1

Asunto:R: PhD Thesis

Fecha:Fri, 8 Jul 2021 07:40:21 +0000

De:Copyright <Copyright@fao.org>

Para:Marta<marta0lages@gmail.com>

Dear Marta,

Permission for this request to reproduce FAO copyright material is granted at no charge, including the right to publish, reproduce, publicly display and distribute the whole or any part of the material in this and all revisions and any subsequent editions of your work; in any ancillary aids that may be prepared to accompany your work, including promotion and publicity uses; and in all forms of media now known or later developed.

Please note that:

- FAO remains the copyright holder of the material, and retains the right to reproduce, translate, publish, and disseminate the whole or any part of it in print and electronic formats, and to grant others the right to do the same, as well as to incorporate material derived from the material in any subsequent work.
- The use of the official emblem or other logos of FAO is prohibited without express and prior written approval by FAO.
- The material must not be used in any way that implies FAO's endorsement of any companies, services or products.

Due acknowledgement shall be made to FAO, with the source document cited and Web URL provided if applicable as follows:

Source: Food and Agriculture Organization of the United Nations, [year], [title], [URL]. Reproduced with permission

Kind regards,
Radhika



VII. APPENDIX 2

----- Forwarded message -----

De: **Editorial Office** <editorial.office@frontiersin.org>

Date: quinta, 23/12/2021 à(s) 16:21

Subject: RE: Fwd: Figures for PhD thesis

To: marta0lages@gmail.com <marta0lages@gmail.com>

Dear Dr Lages

Many thanks for your email. Reproduction of figures with citation is perfectly fine.

Best wishes

Ryan Begley (he/him)

Research Integrity Senior Specialist

Frontiers | Research Integrity Team

www.frontiersin.org

12 Moorgate

EC2R 6DA

London, UK

Office T +41 215 101 797

For technical issues, please contact our Application Support team

In light of the COVID-19 pandemic, making science open has never been more essential to global well-being. Frontiers is responding rapidly and continuing to support researchers with our publishing services. Visit our Coronavirus Knowledge Hub for initiatives and resources.

VII. APPENDIX 3

The figures of chapter Results and Discussion are included in open access papers. It is not required permission to reproduce these figures (see below).

Balado, M., **Lages, M. A.**, Fuentes-Monteverde, J. C., Martínez-Matamoros, D., Rodríguez, J., Jiménez, C., et al. (2018). The siderophore piscibactin is a relevant virulence factor for *Vibrio anguillarum* favored at low temperatures. *Front. Microbiol.* 9: 1766.

Lages, M. A., Balado, M., and Lemos, M. L. (2019). The expression of virulence factors in *Vibrio anguillarum* is dually regulated by iron levels and temperature. *Front. Microbiol.* 10: 2335.

Lages, M. A., Balado, M., and Lemos, M. L. (2021). The Temperature-Dependent Expression of the High-Pathogenicity Island Encoding Piscibactin in *Vibrionaceae* Results From the Combined Effect of the AraC-Like Transcriptional Activator PbtA and Regulatory Factors From the Recipient Genome. *Front. Microbiol.* 12: 748147.

Lages, M. A., de la Fuente, M. C., Ageitos, L., Martínez-Matamoros, D., Rodríguez, J., Balado, M., Jiménez, C., Lemos, M. L. (2022). FrpA is the outer membrane piscibactin transporter in *Vibrio anguillarum*: structural elements in synthetic piscibactin analogues required for transport. *J. Biol. Inorg. Chem.* 27(1): 133-142.

----- Forwarded message -----

De: **Journalpermissions** <journalpermissions@springernature.com>

Date: terça, 14/12/2021 à(s) 13:15

Subject: AW: Figures for PhD thesis

To: Marta Lages <marta0lages@gmail.com>

Hello Ms. Lages,

This is an open access article distributed under the terms of the Creative Commons CC BY license <http://creativecommons.org/licenses/by/4.0/>, which permits unrestricted use, distribution, and reproduction in any medium, provided the original work is properly cited.

You are not required to obtain permission to reuse this article.

To request permission for a type of use not listed, please contact journalpermissions@springernature.com directly.

Thank you.

Alice Essenpreis

Rights and Permissions

Springer Nature

Tiergartenstrasse 17, 69121 Heidelberg, Germany

Regularly in Mondays, Tuesdays, Thursdays and Fridays

bookpermissions@springernature.com

www.springernature.com

Branch of Springer-Verlag GmbH, Heidelberger Platz 3, 14197 Berlin, Germany

Registered Office: Berlin / Amtsgericht Berlin-Charlottenburg, HRB 91881 B

Directors: Martin Mos, Dr. Ulrich Vest, Dr. Niels Peter Thomas, Volker Böing



Von: Marta Lages <marta0lages@gmail.com>

Gesendet: Dienstag, 14. Dezember 2021 13:08

An: Journalpermissions <journalpermissions@springernature.com>

Betreff: Fwd: Figures for PhD thesis

[External - Use Caution]

Dear Sir/Madam,

My name is Marta Lages and I am PhD student at the University of Santiago de Compostela, Spain. For my final report I would like to add figures from the following research papers where I am a co-author:

FrpA is the outer membrane piscibactin transporter in *Vibrio anguillarum*: structural elements in synthetic piscibactin analogues required for transport

<https://link.springer.com/article/10.1007%2Fs00775-021-01916-1>

I would like to request the authorisation to add it to my thesis.

Kind regards,

Marta Lages

----- Forwarded message -----

De: **Editorial Office** <editorial.office@frontiersin.org>

Date: quinta, 23/12/2021 à(s) 16:21

Subject: RE: Fwd: Figures for PhD thesis

To: marta0lages@gmail.com <marta0lages@gmail.com>

Dear Dr Lages

Many thanks for your email. Reproduction of figures with citation is perfectly fine.

Best wishes

Ryan Begley (he/him)
Research Integrity Senior Specialist

Frontiers | Research Integrity Team

www.frontiersin.org

12 Moorgate

EC2R 6DA

London, UK

Office T +41 215 101 797

For technical issues, please contact our Application Support team

In light of the COVID-19 pandemic, making science open has never been more essential to global well-being. Frontiers is responding rapidly and continuing to support researchers with our publishing services. Visit our Coronavirus Knowledge Hub for initiatives and resources.



----- Original Message -----

From: Marta Lages [marta0lages@gmail.com]

Sent: 14.12.2021 12:04

To: editorial.office@frontiersin.org

Subject: Fwd: Figures for PhD thesis

Dear Sir/Madam,

My name is Marta Lages and I am PhD student at the University of Santiago de Compostela, Spain. For my final report I would like to add figures from the following research papers where I am a co-author:

- The Siderophore Piscibactin Is a Relevant Virulence Factor for *Vibrio anguillarum* Favored at Low Temperatures
<https://www.frontiersin.org/articles/10.3389/fmicb.2018.01766/full>
- The expression of virulence factors in *vibrio anguillarum* is dually regulated by iron levels and temperature
<https://www.frontiersin.org/articles/10.3389/fmicb.2019.02335/full>
- The Temperature-Dependent Expression of the High-Pathogenicity Island Encoding Piscibactin in Vibrionaceae Results From the Combined Effect of the AraC-Like Transcriptional Activator PbtA and Regulatory Factors From the Recipient Genome
<https://www.frontiersin.org/articles/10.3389/fmicb.2021.748147/full>

I would like to request the authorisation to add it to my thesis.

Kind regards,

Marta Lages

ref:_00D58JetR._5004KDSRJ4:ref



Vibrio anguillarum is a marine pathogen that can infect diverse fish species with economic importance in aquaculture worldwide. In this thesis, it was demonstrated that *V. anguillarum* expresses a specific set of virulence factors in response to the environmental temperature, which enables the pathogen to infect cold and warm-water adapted fish species. Moreover, the High-Pathogenicity Island *irp*-HPI present in strain RV22 was fully characterized as a genomic island that encodes the synthesis, transport, and regulation of the siderophore piscibactin. Thus, *V. anguillarum* produces simultaneously two siderophores, vanchrobactin and piscibactin and this work demonstrates that the latter is a key virulence factor, whose expression is dually regulated by iron levels and low temperatures.